

Universidade do Minho
Escola de Engenharia

Dynamic Structural Identification using Wireless Sensor Networks

A thesis submitted for the degree of Doctor of Philosophy in Civil
Engineering at the Engineering School of the University of Minho

by

Rafael Aguilar Velez

Supervisor

Prof. Paulo José Brandão Barbosa Lourenço
University of Minho

Co-Supervisor

Dr. José Luís Ferreira da Silva Ramos
University of Minho

August 2010

... to my parents and sisters

*Imagination is more important than knowledge.
Knowledge is limited. Imagination encircles the world
(Albert Einstein)*

Acknowledgments

I am greatly indebted to many people for whose support, encouragement and friendship made this thesis possible. Among all of them, I would like to express my gratitude to:

- My supervisor Prof. Paulo B. Lourenço for all the support during these years. Furthermore I would like to thank for the great opportunity to work in the Masonry and Historical Constructions research group headed by him.
- Dr. Luís F. Ramos for being more than my co-supervisor a friend who guided me in the most difficult moments of this thesis.
- The Cister/Hurray research group at the School of Engineering (ISEP) of the Polytechnic Institute of Porto (IPP): Prof. Eduardo Tovar, Mario Alves, Paulo Gandra and colleagues Ricardo Severino and Ricardo Gomes, for their help when developing the new wireless platform and their kindness during the period of preparation that I spent with them.
- To my mentor at the Catholic University of Peru, Prof. Marcial Blondet for giving me the opportunity of starting this challenge and to whom I will be eternally in debt.
- My gratitude to my former and present colleagues at the University of Minho for the academic interactions: Miguel Azenha, Murat Alaboz, and Michele Luong.
- Mr. Antonio Matos and Alberto Araujo for their tremendous help and support in the laboratory and field works.
- My friends in random order: Pedro Medeiros, Fernando Ribeiro, Ignacio Castelluci and João Leite with whom I spent long time of fruitful discussions and from who I learned day by day.
- My dear partner and life complement Suyeon; she brought happiness, quietness and wisdom to my life.

And finally, I would like to make a special acknowledgment to my family:

- My parents Danton and Carmen as well as my sisters Claudia and Maki; with their love and unconditional support they made short this long journey. They taught me the value of the life and they are models for my personal and professional life. For them, I will always try to be a better person.



The PhD Studies of the author were supported by Alban, European Union Programme of High Level Scholarships for Latin America, with the scholarship number E07D400374PE

Abstract

Structural dynamic monitoring is currently used in several areas of engineering such as the mechanical, aeronautical, and civil communities. While in the most of these areas, dynamic monitoring tests started to be used in the 1970s, in the civil engineering field these tools have been used mostly since the 1980s for studying high flexible structures such as bridges and tall buildings.

The use of these tools for monitoring cultural heritage buildings started to be studied at the University of Minho only in the last decade due to the interest in using non destructive methodologies for assessing the global response of these structures. The present work explores the possible inclusion of Wireless Sensor Networks (WSN) in the Operational Modal Analysis (OMA) schemes of existent structures. Since a complete solution of dynamic monitoring would also contemplate the improvement of feature extraction algorithms, the development of a new methodology for performing automatic and remote processes is addressed in this work.

With this purpose, the possibilities of the commercial off-the-shelf solutions on WSN platforms were first explored. Laboratory and field OMA tests were carried out using these platforms and the results showed that this technology, as it is provided, has no direct application in this type of studies. The main reasons are the low resolution of the accelerometers and the ADCs embedded and the lack of communication protocols that assure not only a proper synchronization among nodes but also reliability in the communication processes. Once the limitations of the ready to use WSN solutions were identified a joint team involving electronic and communication engineers developed a prototype WSN system aiming at fulfilling the demanding requirements of OMA tests in existent structures. Despite the need of some improvements in this prototype system, the results of several rounds of validation tests demonstrated their excellent performance, which is comparable to conventional wired based systems, in scenarios with vibrations amplitudes higher than 0.1 mg.

The last part of this work was dedicated to the improvement of the data processing stage of the dynamic monitoring processes. Due to the huge amount of collected data, the feasibility of continuous monitoring studies relies on the use of automatic feature extraction techniques. With this respect, a new algorithm was proposed for performing remote and automatic processes based on the interpretation of the information resulting from the parametric modal identification methods using a combination of the clustering techniques and the rule-based approach. The results of numerical and laboratory validation tests demonstrated the reliability of this algorithm since highly accurate estimations were obtained, with a high success rate. When the algorithm was tested in a field test using a 19th century church, the results demonstrated not only the efficacy of the algorithm but also the difficulties on performing OMA tests in these structures, due to the fact that the environmental noise was, particularly during critical night hours, not enough to excite such heavy buildings.

Resumo

A monitorização dinâmica de estruturas é usada actualmente em diferentes áreas da engenharia, como por exemplo a mecânica, aeronáutica e civil. Enquanto na maioria destas áreas estes ensaios começaram a ser usados na década dos 70s, na engenharia civil a sua aplicação foi feita a partir dos anos 80, com o intuito principal de estudar estruturas altamente flexíveis como pontes e edifícios altos.

O uso deste tipo de técnicas de monitorização em edifícios de carácter histórico começou a ser estudada na Universidade do Minho só na última década devido ao interesse na exploração de ferramentas não destrutivas que permitiriam ajudar a compreender o comportamento global destas estruturas. O presente trabalho explora a possível inclusão dos sistemas de sensores sem fios na Análise Modal Operacional de estruturas existentes. Uma vez que uma solução de monitorização completa contempla também a melhoria dos algoritmos de extracção das propriedades dinâmicas, a procura desta solução, mediante o desenvolvimento de uma nova metodologia remota e automática para o processo dos dados, faz também parte desta tese.

Neste sentido, foram inicialmente exploradas as possibilidades reais das plataformas comerciais sem fios. Os resultados dos ensaios realizados mostraram que estas plataformas, como são vendidas, não têm aplicação directa neste tipo de estudos. Os principais motivos são à baixa resolução dos acelerómetros e conversores analógicos - digitais (ADC_s) disponíveis, além da falta de implementação de um protocolo de comunicação, o qual garantiria não só a sincronização entre nós, mas também um processo fiável de comunicação entre eles. Uma vez identificadas as limitações destas plataformas comerciais, uma equipa conjunta envolvendo engenheiros electrónicos e de comunicações desenvolveu um novo sistema de monitorização sem fios visando cumprir os exigentes requisitos dos ensaios Modais Operacionais em estruturas existentes. Sendo ainda preciso fazer melhorias no protótipo desenvolvido, os resultados dos numerosos ensaios de validação provaram o excelente desempenho deste, comparável com o dos sistemas convencionais com fios, em situações com vibrações superiores a 0.10 mg.

A parte final deste trabalho foi dedicada à melhoria da etapa do processamento de dados nos processos de monitorização dinâmica. Devido a grande quantidade de informação recolhida nestes processos, a sua falibilidade está sujeita ao uso de ferramentas automáticas para o seu tratamento. Neste sentido, no presente trabalho propõe-se um novo algoritmo de identificação remota e automática baseado na interpretação dos resultados dos métodos de identificação paramétrica usando uma combinação das técnicas de agrupamento (clustering) e das baseadas na experiência (ruled-based). Os resultados dos ensaios numéricos e laboratoriais demonstraram a eficácia do algoritmo desenvolvido com estimações altamente precisas e confiáveis. Quando o algoritmo foi testado numa experiência de campo no estudo duma igreja do século XIX, os resultados confirmaram não só a eficácia do algoritmo mas também a dificuldade de aplicação das técnicas de Análise Operacional nestas estruturas. Isto, devido ao facto de o ruído ambiente ser, em algumas horas críticas, insuficiente para excitar estes edifícios altamente rígidos.

Content

Acknowledgments	i
Abstract	iii
Resumo	v
Content	vii
Glossary	xi
List of Figures	xv
List of Tables	xxiii
CHAPTER 1: Introduction	1
1.1 Motivation for Studying Existent Structures using Dynamic Monitoring Systems	2
1.2 Background of the Experimental Modal Analysis	3
1.3 Aim of the Work.....	5
1.4 Outline of the Thesis	5
CHAPTER 2: Dynamic Monitoring Systems for Civil Engineering Structures	7
2.1 Introduction	8
2.2 Wired Based Monitoring Systems.....	9
2.2.1 Measurements Sensors	9
2.2.2 Data Acquisition Systems.....	12
2.2.3 Remote Connections.....	15
2.3 Wireless Based Monitoring Systems.....	16
2.3.1 Measurement Units.....	19
2.3.2 Base Station	26
2.3.3 Mote's Operating System	27
2.4 Applications to Civil Engineering Structures	28
2.5 Conclusions	29

CHAPTER 3: Operational Modal Analysis for Civil Engineering Structures..... 31

3.1 Introduction 32

3.2 Modal Identification using Output-Only Methods 33

 3.2.1 Frequency Domain Identification Methods 35

 3.2.2 Time domain Identification Methods 39

3.3 Automatic Modal Identification 43

 3.3.1 Cluster Analysis..... 44

 3.3.2 Rule-Based Approach..... 45

3.4 Correlation Analysis of Modal Identification Results..... 46

 3.4.1 Comparison of Modal Properties..... 46

 3.4.2 Comparison of Response Properties..... 49

3.5 Conclusions 51

CHAPTER 4: Operational Modal Analysis using Commercial WSN Platforms 53

4.1 Introduction 54

4.2 Description of the Measurement Sensors and Data Acquisition Systems..... 55

4.3 Experimental Modal Identification Tests: Laboratory Specimens 59

 4.3.1 Description of the Studied Specimen and Analytical Solution 59

 4.3.2 Time Domain Analysis..... 61

 4.3.3 Frequency Domain Analysis 65

 4.3.4 Experimental Modal Identification using Parametric Methods..... 68

4.4 Experimental Modal Identification Tests: Field Case Applications..... 75

 4.4.1 Description of the Building and Analytical Solution for the Chimney75

 4.4.2 Time and Frequency Domain Analysis 77

 4.4.3 Experimental Modal Identification Using Parametric Methods..... 79

4.5 Conclusions 81

CHAPTER 5: New WSN Platform for Operational Modal Analysis of Civil Structures..... 83

5.1	Introduction	84
5.2	Description of the Developed Prototype of WSN Platform	85
5.3	Prototype Validation Tests in the Inverted Wooden Pendulum	90
5.3.1	Description of the Monitoring System and Testing Specimen.....	90
5.3.2	Time Domain Analysis.....	91
5.3.3	Frequency Domain Analysis	94
5.3.4	Experimental Modal Identification using Parametric Methods.....	99
5.3.5	Discussion of the Results.....	105
5.4	Application of the Developed Platforms in Tie-Rods	107
5.4.1	Motivation of the Study and Analytical Solution.....	107
5.4.2	Experimental Tests and Dynamic Monitoring System Deployment .	110
5.4.3	Modal Identification Results	112
5.5	Proposed Approach for Improving the Data Transmission Process.....	117
5.5.1	Conceptual Formulation	117
5.5.2	Validation with Numerical Data.....	118
5.5.3	Validation with Field Collected Information.....	120
5.6	Conclusions	124

CHAPTER 6: Automatic System Identification Procedures for Operational Modal Analysis..... 127

6.1	Introduction	128
6.2	Automatic Feature Extraction Algorithm for Operational Modal Analysis Data	129
6.3	Numerical Validation Tests	133
6.4	Structural Health Monitoring of Concrete Specimens since Casting	141
6.4.1	Description of the Testing Specimens	142
6.4.2	Numerical Modal Analysis.....	144
6.4.3	Dynamic Monitoring System Description.....	145
6.4.4	Automatic Modal Identification Results	146
6.5	Dynamic Monitoring of the St. Torcato Church.....	153

6.5.1	Description of the Church.....	153
6.5.2	Preliminary Monitoring System and Numerical Simulation	154
6.5.3	Continuous Dynamic Monitoring System Description	155
6.5.4	Automatic Modal Identification Results	158
6.6	Conclusions	163
CHAPTER 7: Conclusions and Future Work.....		165
7.1	Conclusions	166
7.2	Future Work.....	169
References		171
Annex A.....		185
Annex B		189
Annex C.....		191
Annex D.....		193

Glossary

List of Symbols

f	Natural Frequency of the system
f_s	Sampling Frequency
f_M	Nyquist Frequency
ξ	Damping coefficient
ω_k	Process noise
v_k	Measured noise
x_k	Discrete-time space state vector
y_k	Observation vector
X^T	Transpose of matrix X
X^H	Complex Conjugate Transpose of X
Y_f	Future information of the Hankel matrix
Y_f^{ref}	Past information of the Hankel matrix
A	Discrete-time state matrix
B	Discrete-time input matrix
C	Discrete-time output matrix
D	Discrete-time direct transmission matrix
E	Elasticity Modulus
H	Frequency response function
I	Inertia moment
L,Q	Factors from a LQ factorization
M	Mass Matrix
T	Tension Force
h	Hankel matrix
j	Number of columns in the Hankel Matrix
k	Stiffness
m	Mass
Λ	Eigenvalues matrix
S	Observability matrix

Ψ	Complex modes shape matrix
Φ	Eigenvectors matrix
ϕ	Modal vector
λ	Real eigenvalues or real eigen frequencies
ρ	Material's specific weight

List of Abbreviations

ADC	Analog to Digital Converter
ANPSD	Average Normalized Power-Spectral Density
CCF	Complex Correlation Coefficient
CDMA	Code Division Multiple Access
CMOS	Complementary Metal-Oxide Semiconductor
COMAC	Coordinate Modal Assurance Criterion
DAQ	Data Acquisition
ECOMAC	Enhanced Coordinate Modal Assurance Criterion
EDGE	Enhanced Data Rates for GSM Evolution
EFDD	Enhanced Frequency Domain Decomposition Method
FAC	Frequency Assurance Criterion
FDAC	Frequency Domain Assurance Criterion
FDD	Frequency Domain Decomposition
FFT	Fast Fourier Transform
FMAC	Modal Assurance Criterion with Frequency Scales
FRAC	Frequency Response Assurance Criterion
FRF	Frequency Response Function
GPRS	General Packet Radio Service
GPS	Global Positioning System
GSM	Global System for Mobile communication
IC	Integrated Circuits
IMAC	Inverse Modal Assurance Criterion
LVDT	Linear Variable Differential Transformer
MAC	Modal Assurance Criterion
MACRV	Modal Assurance Criterion using Reciprocal Modal Vectors
MACSR	Modal Assurance Criterion Square Root

MCC	Modal Correlation Coefficient
MEMS	Micro Electro Mechanical Systems
MFAC	Modal FRF Assurance Criterion
OMA	Operational Modal Analysis
PP	Peak Picking Method
PMAC	Partial Modal Assurance Criterion
RAM	Random Access Memory
RMS	Root Mean Square
SDOF	Single-Degree of Freedom
SHM	Structural Health Monitoring
SMAC	Scaled Modal Assurance Criterion
SSI	Stochastic Subspace Identification method
SSI-data	DATA driven stochastic subspace identification
SVD	Singular Value Decomposition
USB	Universal Serial Bus
VI	Virtual Instrument
WSN	Wireless Sensors Networks
WMAC	Weighted Modal Assurance Criterion

List of Figures

Figure 1.1 – Applications of MEMS	4
Figure 1.2 – Stages of the statistical pattern recognition paradigm.....	5
Figure 1.3 – Schematic outline of the thesis.....	6
Figure 2.1 – Structural monitoring systems.....	8
Figure 2.2 – Monitoring system with wired based equipments.....	9
Figure 2.3 – SDOF representation of an accelerometer	10
Figure 2.4 – Typical FRF of an accelerometer	10
Figure 2.5 – Sensing Range versus Resolution for accelerometers.....	11
Figure 2.6 – Sensing Range vs. Sensing Frequency for accelerometers	11
Figure 2.7 – Most common types of filters	13
Figure 2.8 – Analog-Digital Conversion process	14
Figure 2.9 – Original signal acquired with different sampling rates	14
Figure 2.10 – DAQ equipments used for dynamic identification.....	15
Figure 2.11 – Overview of the State of the art of wireless technology for structural monitoring purposes	17
Figure 2.12 – Monitoring system with wireless with embedded MEMS equipments	18
Figure 2.13 – Global MEMS market 2006–2011	19
Figure 2.14 – Schematics of the microaccelerometer ADXL50	20
Figure 2.15 – Examples of commercial MEMS accelerometers	21
Figure 2.16 – MEMS based humidity and temperature sensors.....	22
Figure 2.17 – Schematics illustration of a pressure microsensors with piezoresistive sense elements	22
Figure 2.18 – Wireless Device and Networking Standards.....	25
Figure 2.19 – Different options of network topologies	25
Figure 2.20 – Commercial interface boards for wireless systems.....	26
Figure 3.1 – Equipments used to perform Input-Output tests	33
Figure 3.2 – Schematic representation of the output-only modal identification methods...	34
Figure 3.3 – General views of the Lourosa church.....	35

Figure 3.4 – Setup of the dynamic tests performed in the Lourosa church.....	36
Figure 3.5 – Time series collected in the first setup.....	36
Figure 3.6 – Modal Identification of the Lourosa church using the PP method	37
Figure 3.7 – Flow chart of the FDD method	38
Figure 3.8 – Modal Identification of the Lourosa church using the FDD and EFDD methods.....	39
Figure 3.9 – Flow chart of the SSI-DATA method	40
Figure 3.10 – Modal Identification of the Lourosa church using the SSI-data method	41
Figure 3.11 – Estimated modal shapes for the Lourosa church using the SSI-data method.....	42
Figure 3.12 – Example of the application of the FMAC method	48
Figure 4.1 – Conventional wired based equipments used in the tests	55
Figure 4.2 – Crossbow base station unit.....	56
Figure 4.3 – Crossbow sensors’ platform.....	56
Figure 4.4 – Front panel of the VI program developed to acquire the data from the WSN	58
Figure 4.5 – DAQ systems arrangement for the experimental tests using commercial WSN platforms.....	58
Figure 4.6 – Specimen description	59
Figure 4.7 – Pendulum configurations for the experimental modal identification tests.....	60
Figure 4.8 – Dynamic response of the inverted pendulum calculated using analytical expressions	61
Figure 4.9 – First round of time domain evaluation tests using commercial WSN platforms	62
Figure 4.10 – Time series record of the response of the inverted pendulum under an impact force test	62
Figure 4.11 – Measurement errors comparison for the impact force test.....	63
Figure 4.12 – Second round of time domain evaluation tests using commercial WSN platforms.....	63
Figure 4.13 – Time series collected by mote # 3 and accelerometer # 3 in the time domain evaluation considering two setups of measurements.....	64
Figure 4.14 – Frequency domain evaluation tests	65
Figure 4.15 – Frequency domain validation tests carried out in the inverted pendulum	66
Figure 4.16 – Results of the frequency domain repeatability analysis	68

Figure 4.17 – Modal identification tests in the Pendulum - 1st Configuration considering two setups of measurements	69
Figure 4.18 – Stabilization diagrams of the modal identification tests considering random excitation in the Pendulum – 1 st Configuration	69
Figure 4.19 – Stabilization diagrams of the modal identification tests considering ambient noise in the Pendulum – 1 st Configuration	70
Figure 4.20 – Modal identification tests in the pendulum – 2 nd Configuration.....	71
Figure 4.21 – Stabilization diagrams of the modal identification tests in the Pendulum – 2 nd Configuration.....	72
Figure 4.22 – Modal identification tests in the pendulum – 3 rd Test Configuration	73
Figure 4.23 – Stabilization diagrams of the modal identification tests in the Pendulum – 3 rd Configuration.....	74
Figure 4.24 – Paço dos Duques Building	75
Figure 4.25 – Chimneys at Paço dos Duques building.....	76
Figure 4.26 – Modal identification tests in the Chimneys at Paço dos Duques building....	76
Figure 4.27 – Analytical modal identification of the Chimneys at Paço dos Duques building.....	77
Figure 4.28 – Time domain series and resultant frequency domain spectrums from the modal identification of the Chimney at Paço dos Duques building – Random excited tests	78
Figure 4.29 – Time domain series and resultant frequency domain spectrums from the modal identification of the Chimney at Paço dos Duques building – Environmental noise tests	79
Figure 4.30 – Stabilization diagrams of the analysis of the tests performed under random excitation and ambient noise in the chimney at Paço dos Duques building.....	80
Figure 5.1 – Overview of the system architecture of the developed WSN platform.....	85
Figure 5.2 – Measurement unit.....	86
Figure 5.3 – Scheme of the network’s management	88
Figure 5.4 – Final appearance of the developed WSN solution	89
Figure 5.5 – DAQ systems arrangement for the experimental tests – Validation Tests New WSN Platforms.....	90
Figure 5.6 – Description of the arrangement of sensors for the time domain evaluation tests.	91

Figure 5.7 – Time series recordings of the response of the inverted pendulum under an impact force test – Validation Tests for New WSN Platforms 92

Figure 5.8 – Measurement errors comparison of the impulse force tests – Validation Tests for New WSN Platforms. 93

Figure 5.9 – Time series collected by the evaluated systems – Validation Tests for New WSN Platforms..... 94

Figure 5.10 – Frequency domain results of the tests with light random excitation – Validation Tests for New WSN Platforms 95

Figure 5.11 – Frequency domain results of the tests with ambient noise – Validation Tests for New WSN Platforms 96

Figure 5.12 – Results of the frequency domain repeatability analysis of the evaluated platforms in moderate noise environments – Validation Tests for New WSN Platforms... 98

Figure 5.13 – Results of the frequency domain repeatability analysis of the evaluated platforms in low noise environments – Validation Tests for New WSN Platforms..... 98

Figure 5.14 – Pendulum first modal analysis tests – Validation Tests for New WSN Platforms..... 100

Figure 5.15 – Stabilization diagrams of the pendulum first modal analysis tests – Validation Tests for New WSN Platforms 100

Figure 5.16 – First three mode shapes estimated from the experimental modal analysis tests in the pendulum first configuration – Validation Tests for New WSN Platforms 101

Figure 5.17 – Pendulum second modal analysis tests – Validation Tests for New WSN Platforms..... 102

Figure 5.18 – Stabilization diagrams of the pendulum second modal analysis tests – Validation Tests for New WSN Platforms 102

Figure 5.19 – First three mode shapes estimated from the experimental modal analysis tests in the pendulum second configuration (added mass at the top) – Validation Tests for New WSN Platforms..... 103

Figure 5.20 – Pendulum third modal analysis tests – Validation Tests for New WSN Platforms..... 104

Figure 5.21 – Stabilization diagrams of the pendulum third modal analysis tests – Validation Tests for New WSN Platforms 104

Figure 5.22 – First three mode shapes estimated from the experimental modal analysis tests in the pendulum third configuration (stiffer support element) – Validation Tests for New WSN Platforms.....	105
Figure 5.23 – Relation between sampling time and transmission time for the case of the new WSN platforms	106
Figure 5.24 – Examples of tie-rods in existent masonry structures.....	108
Figure 5.25 – Illustration of how the boundary conditions can affect the accuracy of the estimations of the tensile stress	109
Figure 5.26 – Experimental tests in the tie-rods.....	110
Figure 5.27 – Considered tensile stages during the experimental tests – Case study of tensile tests in tie-rods	111
Figure 5.28 – Deployment of sensors in the tie-rods’ experimental tests	112
Figure 5.29 – Time domain recordings with the developed WSN platforms – Case study of tensile tests in tie-rods	112
Figure 5.30 – Frequency domain results from the data recorded with the developed prototype of WSN platforms – Case study of tensile tests in tie-rods.....	113
Figure 5.31 – Results of the experimentally estimated modal shaped with the new WSN platforms and comparison with their counterparts obtained from the conventional wired based systems (equal to the theoretical modal shapes) – Case study of tensile tests in tie-rods	115
Figure 5.32 – Comparisson of the experimentally results of the first three natural frequencies and the theoretical results corresponding to the extreme conditions of pinned-pinned and fixed-fixed boundary conditions – Case study of tensile tests in tie-rods	116
Figure 5.33 – Scheme of the proposed approach for improving the data transmission process	118
Figure 5.34 – Summary of time domain series and results of the real and imaginary plots for the present case study.....	119
Figure 5.35 – Location of the sensors that will be processed using the proposed approach	121
Figure 5.36 – Summary of time domain series and results of the real and imaginary plots for the case of the tie rods tests	122

Figure 6.1 – Summary of the proposed automatic modal identification algorithm..... 131

Figure 6.2 – Dataflow of the remote dynamic monitoring system developed in this work 132

Figure 6.3 – Front Panel of the developed Automatic Modal Analyzer tool AMA V1.0. 132

Figure 6.4 – Time domain signals “registered” with the first measurement sensor – Numerical validation tests 133

Figure 6.5 – First measurement sensor’s frequency domain spectrums – Numerical validation tests 134

Figure 6.6 – Results of the estimated frequencies – AMA V1.0 Tool 135

Figure 6.7 – Results of the estimated 1st mode shapes amplitudes – AMA V1.0 Tool..... 136

Figure 6.8 – Results of the estimated frequencies – AMA V2.0 Tool 139

Figure 6.9 – Results of the estimated 1st mode shapes amplitudes – AMA V2.0 Tool..... 140

Figure 6.10 – Concrete E-modulus tracking methodology proposed by Azenha (2009).. 142

Figure 6.11 – Details of the steel formwork used for the tests of the CB-01 and CB-02 and the concrete casting process 143

Figure 6.12 – Uniaxial tensile tests of the steel formwork’s plate 143

Figure 6.13 – Setup of the dynamic monitoring system used to study the hardening process of concrete specimens..... 145

Figure 6.14 – Results of the natural frequencies calculated with the tool AMA V1.0..... 147

Figure 6.15 – Results of the natural frequencies calculated with the tool AMA V2.0..... 147

Figure 6.16 – Summary of the results of the automatic modal identification process for the case study CB-01 using the two versions of the developed tool 149

Figure 6.17 – Summary of the results of the automatic modal identification process for the case study CB-02 using the two versions of the developed tool 149

Figure 6.18 – Analysis of the variation of the first modal shape along the experimental tests 150

Figure 6.19 – Comparison of the data processing time and the selected model order level where the estimations were performed in both versions of the developed tools: Case study CB-01 151

Figure 6.20 – Comparison of the data processing time and the selected model order level where the estimations were performed in both versions of the developed tools: Case study CB-02 152

Figure 6.21 – Experimental E-modulus evolution curve..... 152

Figure 6.22 – Construction stages of the St. Torcato Church located in Guimarães, Portugal	153
Figure 6.23 – Sensors location; St. Torcato Church case study	154
Figure 6.24 – Experimental and numerical modal analysis results; St. Torcato church case study	155
Figure 6.25 – Dynamic monitoring system setup - St. Torcato church case study	156
Figure 6.26 – RMS of the time series collected by accelerometer A 04 (node 02) – St. Torcato church case study	159
Figure 6.27 – Evolution of the natural frequencies – St. Torcato church case study	159
Figure 6.28 – Evolution of the damping coefficients – St. Torcato church case study	160
Figure 6.29 – Median values of the absolute modal amplitudes automatically estimated along the dynamic monitoring study	161
Figure 6.30 – Results of the automatically selected model orders – St. Torcato church case of study	162

List of Tables

Table 2.1 – Operating Systems for resource constrained devices	27
Table 3.1 – PP results of the Lourosa church.	37
Table 3.2 – FDD and EFDD results of the Lourosa church.	39
Table 3.3 – Experimental results of the dynamic tests performed in the Lourosa church. .	42
Table 4.1 – Technical comparison of the MEMS microaccelerometer ADXL202JE and the conventional piezoelectric accelerometer PCB 393B12.	57
Table 4.2 – Example of the content of one message sent by the mote.....	57
Table 4.3 – Time series results of the tests under random excitation considering two setups of measurements.....	64
Table 4.4 – Time series results of the tests under ambient noise considering two setups of measurements.	65
Table 4.5 – Frequency domain results from the modal analysis tests in the inverted pendulum.	67
Table 4.6 – Experimental results of the dynamic response of the Pendulum – 1 st Configuration.....	71
Table 4.7 – Experimental results of the dynamic response of the Pendulum – 2 nd Configuration.....	72
Table 4.8 – Experimental results of the dynamic response of the Pendulum – 3 rd Configuration.....	74
Table 4.9 – Dynamic response of the studied Chimney at Paço dos Duques building.	80
Table 5.1 – Technical specifications of the MEMS accelerometers implemented in the developed WSN platforms.	87
Table 5.2 – Statistical evaluation of the time series results – Validation Tests for New WSN Platforms.....	94
Table 5.3 – Results of the repeatability tests in moderate noise environments – Validation Tests for New WSN Platforms.	97

Table 5.4 – Results of the repeatability tests in low noise environments – Validation Tests for New WSN Platforms.	97
Table 5.5 – Results of pendulum first modal analysis tests – Validation Tests for New WSN Platforms.....	101
Table 5.6 – Results of pendulum second modal analysis tests – Validation Tests for New WSN Platforms.....	103
Table 5.7 – Results of pendulum third modal analysis tests – Validation Tests for New WSN Platforms.....	105
Table 5.8 – Characteristics of the tie-rods tested in laboratory.	110
Table 5.9 – Summary of the time domain indicators resultant from the collected information of the developed WSN platforms – Case study of tensile tests in tie-rods....	113
Table 5.10 – Comparison of the frequency estimations resultant from the data recorded with the conventional and developed systems – Case study of tensile tests in tie-rods....	114
Table 5.11 – Theoretical frequencies and mode shapes of the generated signals.	118
Table 5.12 – Results of frequencies and mode shapes after the application proposed approach.....	120
Table 5.13 – Required transmission times in each of the considered approaches per sensing node.	120
Table 5.14 – Results of frequencies and mode shapes after the application proposed approach to the collected information in the tie bars tests in 0 MPa of tension state.....	123
Table 5.15 – Results of frequencies and mode shapes after the application proposed approach to the collected information in the tie bars tests in 73 MPa of tension state.....	123
Table 6.1 – Variables considered for the signals’ generation stage of the numerical validation tests.	133
Table 6.2 – Peak Values and RMS of the time series generated – Numerical validation tests.	134
Table 6.3 – Processing parameters AMA V1.0 – Numerical validation tests.	135
Table 6.4 – Estimated frequencies AMA v1.0 – Numerical validation tests.	136
Table 6.5 – Estimated Mode Shapes AMA v1.0 – Numerical validation tests.	137
Table 6.6 – Processing parameters AMA v2.0 – Numerical validation tests.....	138
Table 6.7 – Estimated frequencies AMA v2.0 – Numerical validation tests.	139
Table 6.8 – Estimated Mode Shapes AMA v2.0 – Numerical validation tests.	140

Table 6.9 – Results of the analytical analysis of the dynamic response of the concrete beams at the beginning and the end of the performed tests.	144
Table 6.10 – Acquisition and processing parameters – Concrete hardening tracking case study.	146
Table 6.11 – Comparison of the results of the proposed algorithms and commercial modal analysis software: Case Study CB-01.....	148
Table 6.12 – Comparison of the results of the proposed algorithms and commercial modal analysis software: Case Study CB-02.....	148
Table 6.13 – Data collection campaigns – St. Torcato church case study.	157
Table 6.14 – Acquisition and processing parameters AMA V2.0 – St. Torcato church case study.	158
Table 6.15 – Peak Values and RMS of the time series recordings – St. Torcato church case study.	158
Table 6.16 – Automatic modal identification results – St. Torcato church case study.	161
Table A.1 – Summary of academic wireless sensing unit prototypes (1998-2003).	185
Table A.2 – Summary of academic wireless sensing unit prototypes (2003-2004).	186
Table A.3 – Summary of academic wireless sensing unit prototypes (2005-2008).	187
Table A.4– Summary of commercial wireless sensing unit prototypes	188
Table B.1 – Technical Specifications of the Mica2 platforms.....	189
Table B.2 – Characteristics of the Humidity and Temperature Sensor	189
Table B.3 – Characteristics of the Barometric Pressure and Temperature Sensor.....	189
Table B.4 – Characteristics of the Light Sensor	190
Table B.5 – Characteristics of the Accelerometer Sensor	190

CHAPTER 1

INTRODUCTION

1.1 Motivation for Studying Existent Structures using Dynamic Monitoring Systems

Given the current social and economical demands, conservation of cultural heritage buildings, which provide identity to a region or country, is a key aspect to modern communities. In the experimental tests carried out by civil engineers for the preservation of these buildings, continuous static and dynamic monitoring offer significant possibilities. These techniques fit into the modern conservation principles of minimum repair and the use of non intrusive methodologies. Moreover, they can also be used as control therapy in the framework of model updating and damage detection processes.

In a broader aspect, structural monitoring also represents the present and the future of civil engineering, since structural diagnosis works in new and existent structures were performed with few resources of experimental techniques until a few years ago. Dynamic monitoring systems are currently used for assessing the operational conditions of the structures and these systems can also be used as powerful near real-time tools for assisting decisions required immediately after the occurrence of extreme events, such as earthquakes or unanticipated blast loadings (Farrar and Worden, 2007). It should be noticed that these possible applications gain much more interest when applied to cultural heritage buildings.

The few tests reported in the literature regarding the use of dynamic monitoring systems in existent structures have evidenced serious difficulties for applying traditional monitoring techniques. These difficulties can be summarized as: a) architectural limitations for the deployment of conventional wired based equipments; and b) high costs of these equipments due to the necessity of high sensitive transducers for measuring the low amplitude vibrations of these thick walls' buildings.

A large progress in the field of preservation of cultural heritage would be possible from the practical implementation of new monitoring systems considering cheap and reliable measurement sensors, combined with wireless communication solutions, which is the focus of this thesis.

1.2 Background of the Experimental Modal Analysis

The beginning of the studies related to vibrations probably starts at the sixth century B.C. with Pythagoras [572-512 B.C.] and his experiments of vibrating strings. After him, Galileo [1564-1642], Newton [1643-1727], Euler [1707-1783], Lagrange [1736-1813], Rayleigh [1842-1919], Timoshenko [1878-1972] and Den Hartog [1901-1989] continue the preceding studies formulating the principles of the classical vibration theory (Braun et al., 2002).

A milestone in the development of the vibration theory was the proposal of the Fast Fourier Transform (FFT) by Cooley and Tuckey (1965). Soon after in the 1970s, digital analyzers capable of performing signal acquisition and signal processing using the FFT started to be commercialized (Braun et al., 2002). Since the proposal of the FFT, the methods for processing the data obtained in the experimental modal analysis campaigns have evolved significantly. Currently the available methodologies can be divided in two groups according to the domain in which they were developed: frequency or time domain (Rodrigues, 2004).

Not only have the methods for data processing experienced a large evolution over the time but also the experimental techniques for carrying out the tests followed a similar track. According to Cunha et al. (2006), the available experimental modal analysis techniques can be classified in function of the excitation source as Input-Output and Output-Only (also called as Operational Modal Analysis – OMA) techniques. For the first case both excitations, the input and the output, are experimentally measured while, for the second case, only the response of the structural system (output) is recorded.

According to the Moore's law (Moore, 1968), the measurement sensors and data acquisition equipments is without any doubt the area where the technology is growing faster. Conventional sensors are mainly heavy, big sized, expensive and wired based while currently new technologies, like the ones based on wireless communications and Micro-Electro-Mechanical-Systems – MEMS (combination known as Wireless System Networks – WSN), are exactly the opposite and thus are being explored as alternatives for replacing conventional systems. MEMS are low cost, low size, and low energy consumption sensors that can properly fulfill most of the traditional requirements of the monitoring systems. As shown in Figure 1.1, these systems are mostly used in the

automotive industry even if they also have a broad spectrum of applications that can include civil engineering applications (Stiharu, 2002a).

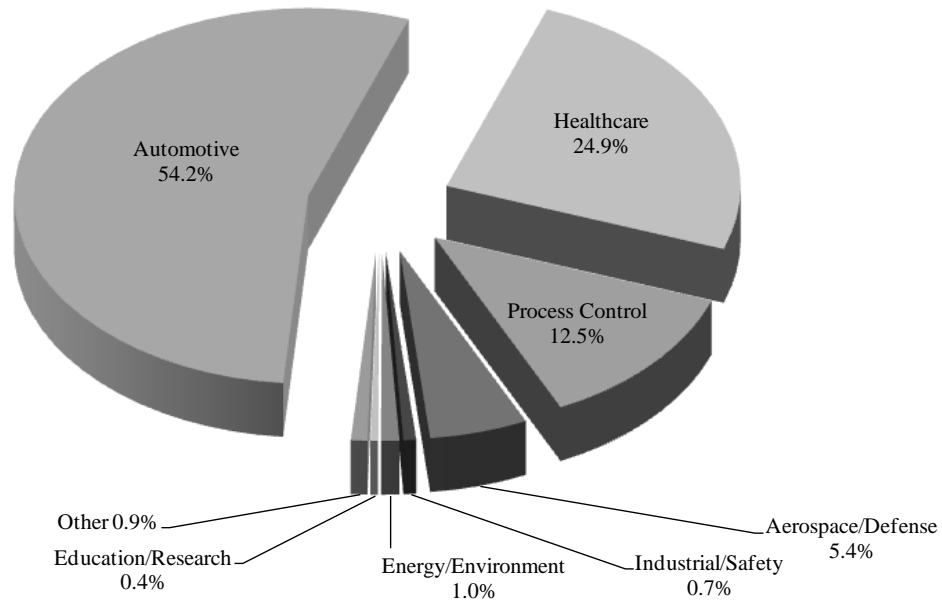


Figure 1.1 – Applications of MEMS (adapted from Stiharu, 2002a)

With respect to experimental modal analysis applications, the first tests were initially carried out in the 1970s for performing damage identification of offshore platforms and aerospace structures. For civil engineering purposes, the dynamic monitoring started to be used in the early 1980s for the detection of changes in the structural behavior along the time, process referred to as Structural Health Monitoring - SHM (Farrar and Worden, 2007).

So far, the studies of SHM for civil engineering structures are mainly based on OMA procedures using conventional wired based sensors in bridges with few applications in buildings and historical constructions. One of the first applications related to this last type of structures was presented by Ramos (2007). The present work focuses now in the use of up to date measurement sensors as well as the improvement of data processing algorithms for carrying out OMA studies in existent structures.

1.3 Aim of the Work

The general objectives of this thesis are to: a) increase the knowledge on ancient buildings by developing tools to improve their monitoring processes; and b) contribute for the development of SHM for civil engineering structures by presenting new alternatives of sensors and feature extraction techniques.

The two specific objectives of the thesis are to:

1. Test off-the-shelf solutions and develop new alternative of WSN platforms to use in dynamic monitoring works of existent masonry structures.
2. Develop an automatic feature extraction algorithm to process the large quantities of data collected in continuous dynamic monitoring campaigns.

To clarify how the present work contributes to the overall progress of SHM, the division of the statistical pattern recognition paradigm presented by Farrar and Worden (2007) is used. According to them, the SHM process is a sequence of four steps which are summarized in Figure 1.2. The present work fits in the 2nd and 3rd stages of the proposed division.

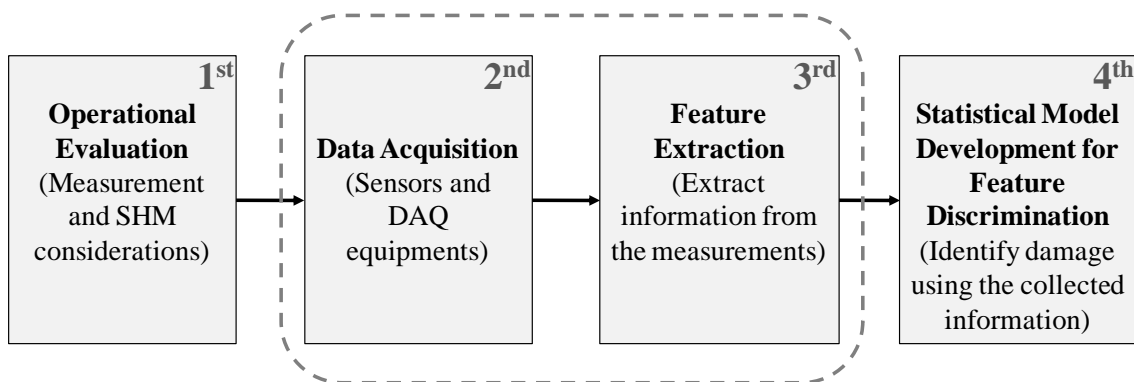


Figure 1.2 – Stages of the statistical pattern recognition paradigm (adapted from Farrar and Worden, 2007)

1.4 Outline of the Thesis

This thesis is organized in three main parts. The first part of the thesis (Chapters 1, 2 and 3) is dedicated to the general considerations, the state of the art of the monitoring systems, and the theory of Operational Modal Analysis. The second part (Chapters 4, 5 and 6) introduces new developments and presents a discussion of the obtained results. Finally, the last part (Chapter 7) presents the main conclusions and recommendations for future work. The detailed content of the thesis is detailed next.

Chapter 1, the current chapter, presents the introduction of the work referring the motivation, the general background of the experimental modal identification topics as well as the objectives of this research.

Chapter 2 reviews the available technologies on measurement sensors and data acquisition equipments for performing dynamic monitoring. Special emphasis is given to the wireless based systems presenting their state of the art and their current and past applications for monitoring civil engineering structures.

Chapter 3 presents the theoretical basis of the Operational Modal Analysis. Here, topics related to the automation of the modal identification process are also stated, as well as the existing indicators to compare modal identification results.

Chapter 4 is dedicated to evaluate the possible application of the commercial off-the-shelf wireless platforms for Operational Modal Analysis of civil engineering structures. Here, the discussion of the attained results of laboratory and field tests is also presented.

Chapter 5 presents the new prototype of WSN platform developed in this work. Details and results of numerous validation tests are also shown.

Chapter 6 is related to the proposal of a new automatic feature extraction algorithm for processing the information collected in continuous dynamic monitoring studies. The results of numerical and field monitoring test performed using this new tool are also presented.

Chapter 7 presents the conclusions of the work as well as the proposal of future developments.

A schematic outline of the thesis is shown in Figure 1.3.

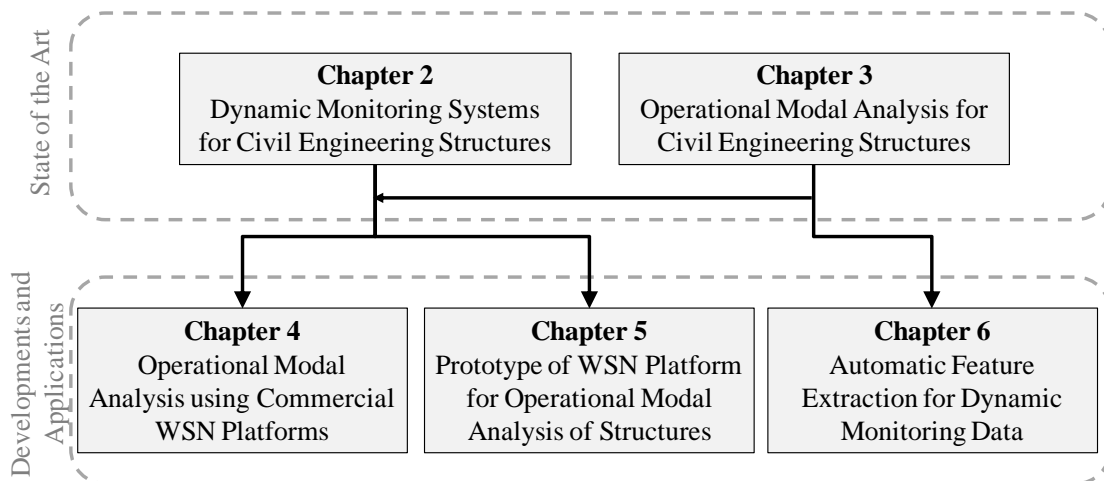


Figure 1.3 – Schematic outline of the thesis

CHAPTER 2

Dynamic Monitoring Systems for Civil Engineering Structures

Abstract

In this chapter the review of the equipments used for performing dynamic monitoring works of civil engineering structures is addressed. The chapter starts by presenting a general introduction of the equipments. According to the types of instruments involved, the systems are classified in two groups: conventional wired based systems and wireless based systems. The chapter continues by presenting the measurement sensors and data acquisition platforms related to conventional monitoring systems. Important considerations with respect to remote data transmission are also stated. Subsequently, the wireless based systems are presented. These types of systems use MEMS and wireless technology for monitoring issues. The main aspects considered here are related to microsensors, microcontrollers, wireless communication modules and software. The new technology based on wireless systems with embedded MEMS sensors offers great advantages with respect to economy, time saving and simplicity of the monitoring systems. However, the characteristics of the software, hardware and communication protocols, available or implemented in the commercial platforms, show that the systems are not yet fully suitable for carrying out structural dynamic monitoring works.

2.1 Introduction

In the recent years, numerous applications of modal analysis covering wide areas of engineering have been reported in the literature. In the civil engineering field, this tool is used to calibrate analytical models, to provide a better understanding of the behavior of the structures, to control the quality of execution or to perform damage detection.

Currently, significant hardware developments have also occurred for structural monitoring purposes. Conventional monitoring sensors used for these applications, see Figure 2.1a, involve significant wiring (fiber-optic cables or other physical transmission medium) and centralized data acquisition systems with remote connections.

The fact that conventional sensors work with wires might lead to high costs, problems in maintenance and difficulties in placing the sensors in given locations in the structures. Therefore, the recent years have witnessed an increasing interest in a new technology, see Figure 2.1b, based on Wireless Systems Networks (WSN) with embedded Micro-Electro-Mechanical Systems (MEMS) as a low-cost alternative for the monitoring studies performed in civil engineering structures (Ruiz-Sandoval, 2004).

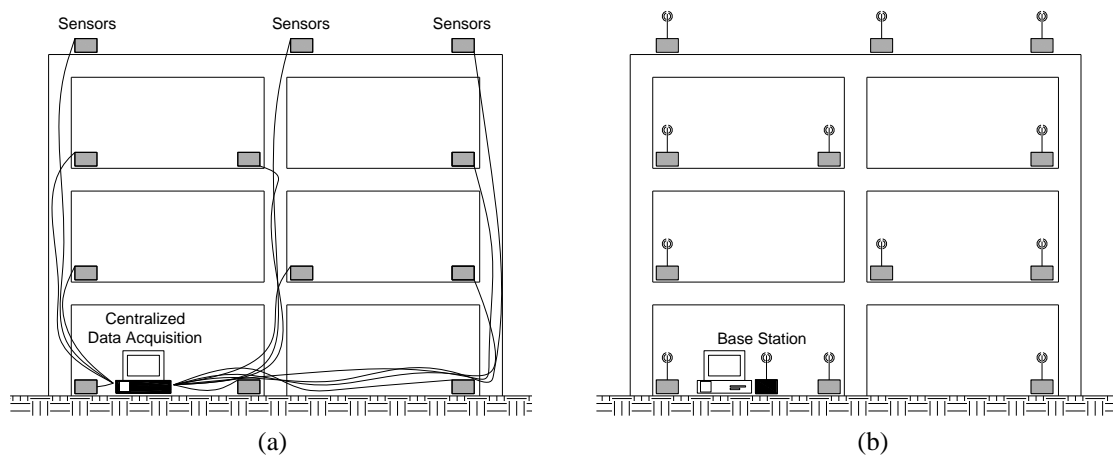


Figure 2.1 – Structural monitoring systems: (a) wired based systems; and (b) wireless based systems (adapted from Ruiz-Sandoval, 2004)

Conventional systems are still widely used by the civil engineering community mainly for three reasons: 1) there are plenty of commercial solutions that need just to be placed in the field; 2) there are several available solutions for measurement sensors and data acquisition platforms with high sensitivity and high resolution; and 3) there are well known commercial software available, usually, with high programming flexibility.

In spite of the advantages of conventional systems, the future of structural monitoring is obviously based on the development of wireless and MEMS technology. In the following sections conventional and WSN monitoring systems are detailed with the aim to present an overview of the state-of-the-art of dynamic monitoring systems focused on civil engineering applications.

2.2 Wired Based Monitoring Systems

The wired based systems (also called in this work “conventional systems”) used for monitoring are composed by three parts: 1) measurement sensors; 2) data acquisition equipments; and in some cases 3) remote connection systems. The measurement sensors are connected with cables to the data acquisition system that can be also remotely connected to a central station. The Figure 2.2 gives a general perspective of a wired based monitoring system.

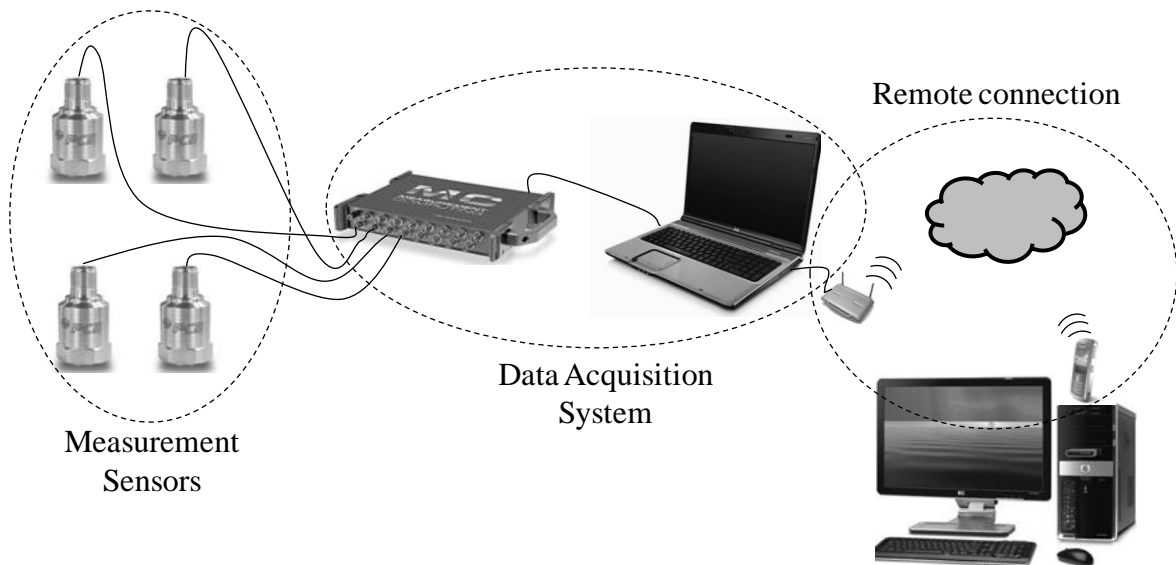


Figure 2.2 – Monitoring system with wired based equipments

2.2.1 Measurements Sensors

The dynamic response of a structure is usually measured by equipments able to transform physical quantities such as displacements, velocities or accelerations in electric signals. In what concerns civil engineering structures, the accelerometers are the most used measurement sensors due to their relatively low cost and high sensitivity. However, there are cases when other response transducers, such as velocity meters (Weng et al., 2008), displacement meters, LVDT's or GPS can be used (Rodrigues, 2004). In the rest of this

section, only accelerometers will be detailed as they are used for the experimental tests carried out in this work.

As it is shown in Figure 2.3, an accelerometer can be understood as a SDOF system with an inertial mass that moves proportionally to the acceleration amplitude of a moving body. This amplitude of motion is detected and converted into an electrical signal in the form of voltage (He and Fu, 2001).

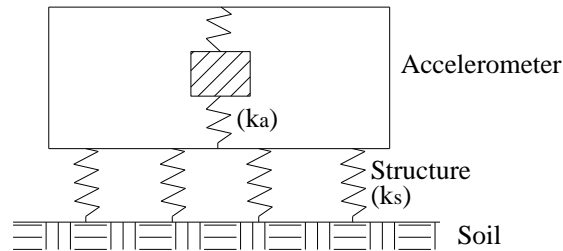


Figure 2.3 – SDOF representation of an accelerometer

An ideal accelerometer should have a linear input and output relationship, in order to ensure that the amplitude content of the acceleration signal at different frequencies is truthfully recorded. For this reason, the Frequency Response Function (FRF) of the accelerometer should be uniformly flat in the frequency range of interest (considered as $1/5$ to $1/2$ of the accelerometer resonance frequency) so that no amplitude of any frequency is distorted. The accelerometer should also impose zero phase shift to the measured signal (He and Fu, 2001). A typical accelerometer FRF is shown in Figure 2.4.

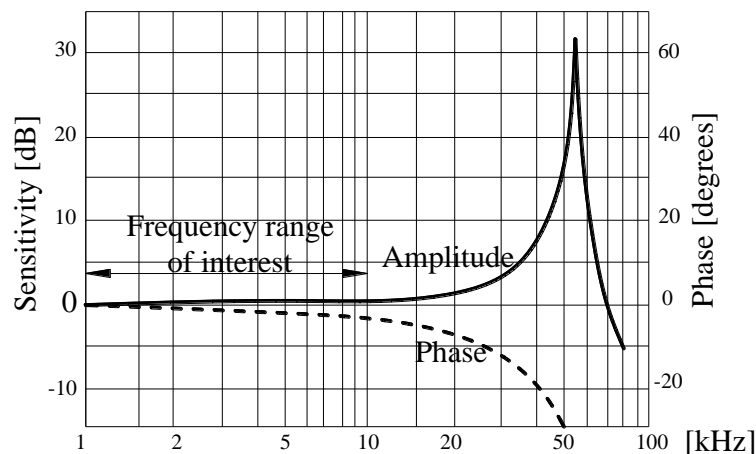


Figure 2.4 – Typical FRF of an accelerometer (adapted from He and Fu, 2001)

There are five main types of accelerometers that, depending on their characteristics, are used for different applications. These five types are the: piezoelectric, piezoresistive, capacitive, force balanced (also known as servo) and the strain gauge based.

In order to compare the performance of the different types of accelerometers the relations Resolution δ vs. Sensing Range R and Sensing Frequency f vs. Range R are presented in Figure 2.5 and Figure 2.6 respectively.

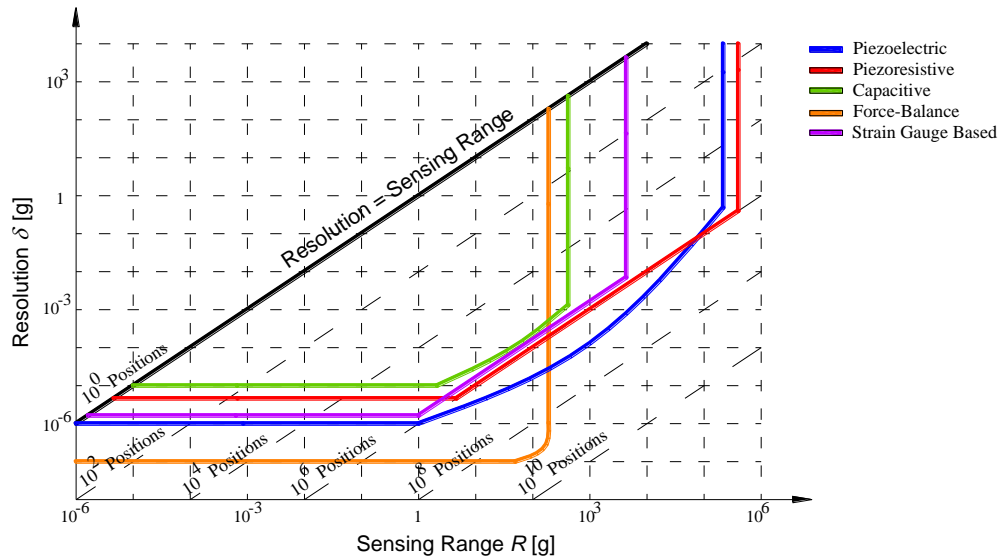


Figure 2.5 – Sensing Range versus Resolution for accelerometers (adapted from Shieh et al., 2001)

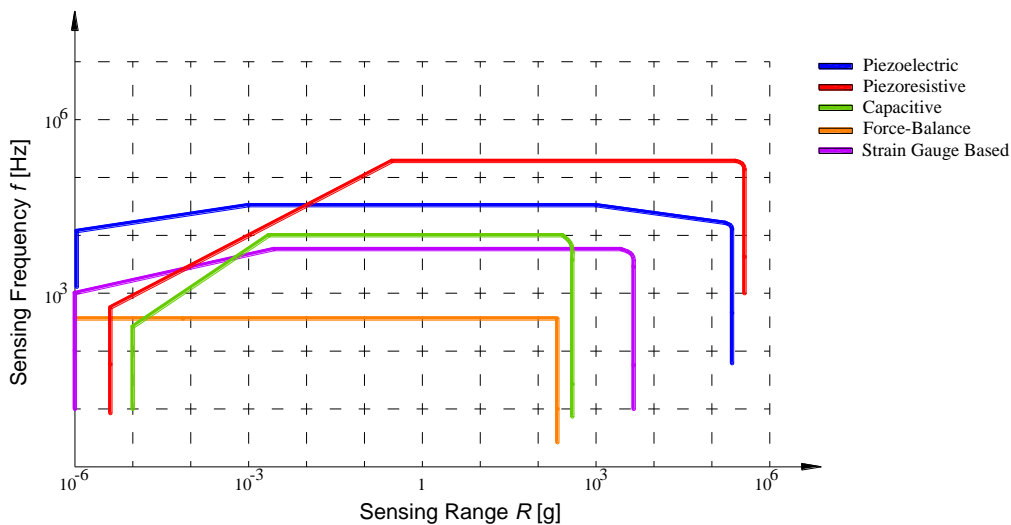


Figure 2.6 – Sensing Range vs. Sensing Frequency for accelerometers (adapted from Shieh et al., 2001)

In Figure 2.5, the operating regime for each sensor has the upper limit $R = \delta$. A relation R/δ (lines with slope of 45°) was used to define the number of distinct measurable positions for the accelerometers. As seen, four of the five types of sensors have a resolving power of about 10^6 positions while just one (the force-balanced) is able to measure more than 10^8 discrete positions. Piezoresistive accelerometers have the highest output range (up to $\pm 200\,000$ g) while the force balanced accelerometers have the smaller sensing range (approximately ± 100 g). Piezoelectric accelerometers are rugged (high shock limit),

versatile (light) and cover the widest span in operating range, from μg to high impact measurement, at fine resolution (Shieh et al., 2001).

In Figure 2.6 it is possible to observe that the piezoresistive and piezoelectric accelerometers have the higher sensing frequency f (exceeding 10 kHz) which makes them suitable for high frequency measurements. However, it is important to understand that high sensing frequency requires also high ratio of stiffness to mass and therefore comes with the penalty of sensitivity, resolution, size and weight (Shieh et al., 2001).

All the accelerometers with the exception of those of piezoelectric type are supplied by energy and are DC-coupled devices with lower measurement frequency limit of zero.

2.2.2 Data Acquisition Systems

A Data Acquisition (DAQ) system is an electronic device designed to collect the information that is acquired by the measurement sensors. The information that comes from the sensors need to be properly adjusted using signal modification processes. The main tasks that signal modification processes comprise are signal condition (amplification and filtering) and signal conversion (analog to digital, digital to analog or, frequency to voltage). Next, the main processes and concepts involved in the DAQ process will be detailed.

2.2.2.1 *Signal Amplification*

The level of an electrical signal can be represented by variables such as voltage, current, and power. A signal should maintain its level above some threshold during transmission, so that errors due to signal weakening will not be excessive. Many types of sensors produce weak signals that have to be upgraded before they can be fed into a monitoring system, data processor, controller, or data logger. Signal amplification concerns the proper adjustment of a signal level for performing a specific task. Amplifiers are active devices that need an external power source to operate, which are used to accomplish signal amplification processes. For more details see De Silva (2007).

2.2.2.2 *Filtering*

Unwanted signals can seriously degrade the performance of a vibration monitoring and analysis system. External disturbances, error components in excitations, and noise generated internally within system components are common spurious signals. A filter is a

device that allows only the desirable part of a signal to pass through, rejecting the unwanted part. It is possible to identify four categories of filters: low-pass, high-pass, band-pass and band-reject filters (De Silva, 2007). In Figure 2.7 the ideal FRFs of each of these four types of filters are shown.

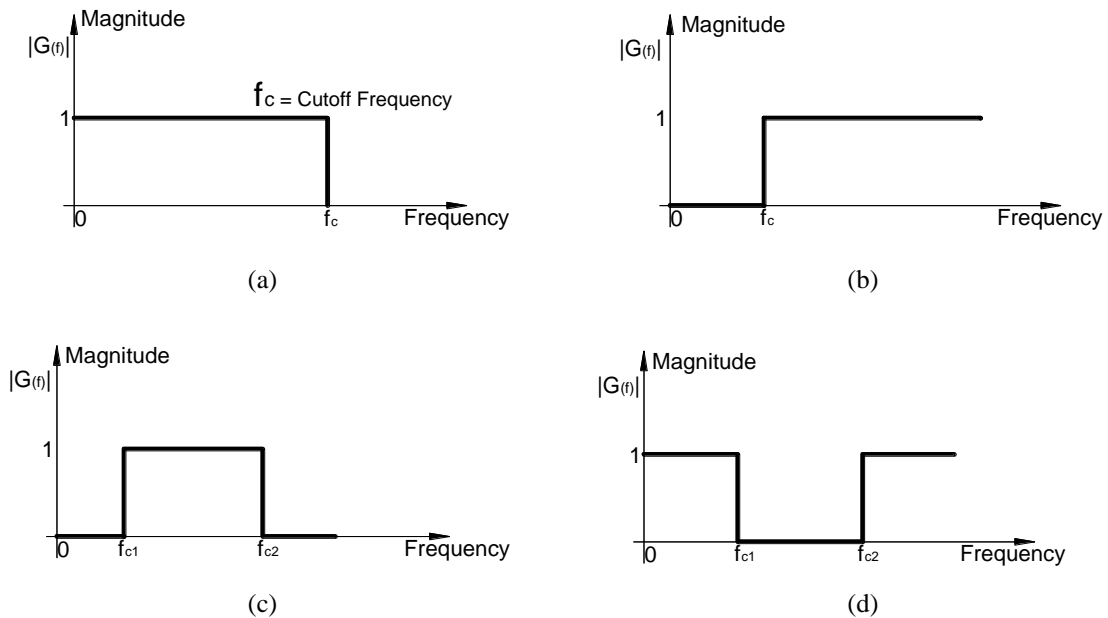


Figure 2.7 – Most common types of filters: (a) low-pass filter; (b) high-pass filter; (c) band-pass filter; and (d) band-reject filter

2.2.2.3 Analog-Digital Conversion

Typically, the measured response of a system is available in an analog form. Analog signals, which are continuously defined with respect to time, have to be sampled at discrete time points (sampling frequency) and the sample values have to be represented in the digital form to be read into a digital system such as a computer (De Silva, 2007). Therefore the Analog-Digital Conversion (ADC) is an electronic process in which an analog signal is changed, without altering its essential content, into a digital signal. The ADC process is shown in Figure 2.8.

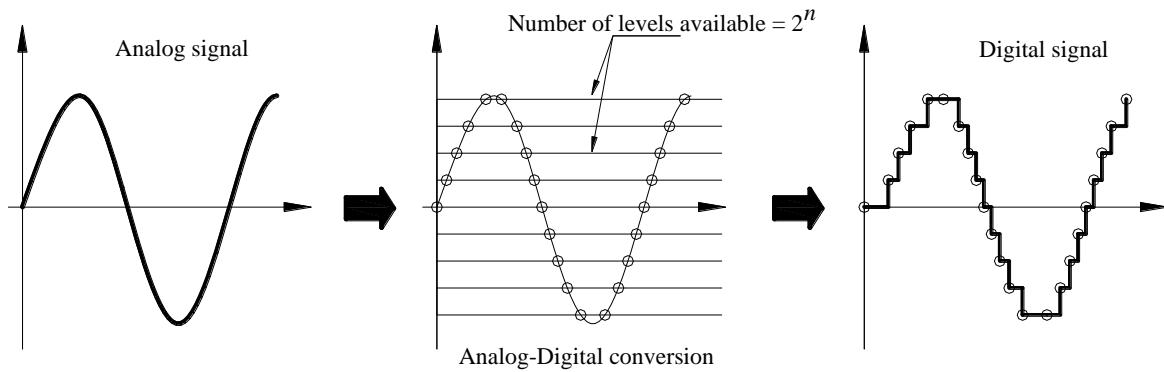


Figure 2.8 – Analog-Digital Conversion process

In the ADC process, the resolution depends on the available number of bits used to digitalize the signal. For an n -bit ADC the number of levels available is 2^n ; e.g. it is possible to get an accuracy of $1.2\mu\text{V}$ in a digitalize process of a signal by using a voltage range of $\pm 10\text{V}$ and an ADC with 24 bits resolution.

2.2.2.4 Sampling Rate and Aliasing Problem

Sampling consists of the time discretization of a continuous signal. If an adequate sampling frequency f_s is used for data acquisition, the sampled signal would be a faithful representation of the continuous signal with no information lost in the process, since the original waveform can be readily recovered by interpolating the sampled values. The higher f_s is, the more the sampled waveform resembles the continuum signal. Conversely, if f_s are low, the sampled waveform will no longer represent the original signal (see Figure 2.9). The spurious waveform resulting from undersampling is called an “alias” and the phenomenon is named “aliasing” (Gatti and Ferrari, 2003).

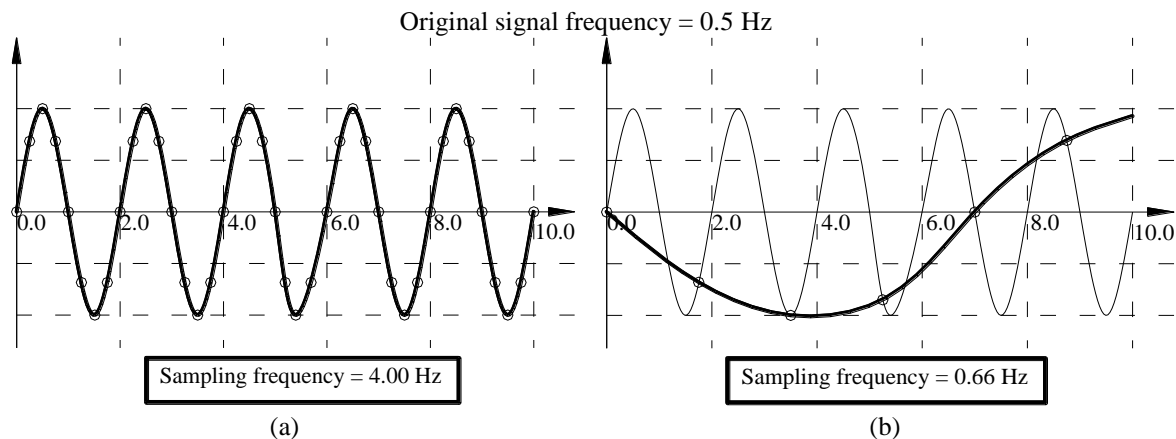


Figure 2.9 – Original signal acquired with different sampling rates: (a) adequate sampling rate; and (b) insufficient sampling rate which carries the problem of aliasing

The theorem of Shannon (previously implicitly formulated by Nyquist) gives a solution for the aliasing problem (Shannon, 1949). The theorem states that to reconstruct a continuous signal having its highest frequency component at f_M from its sampled version, the sampling frequency f_s must be, at least, two times f_M , ($f_s \geq 2f_M$). The frequency f_M is called Nyquist frequency of the signal and the maximum sampling rate is called Nyquist rate.

2.2.2.5 Commercial Equipments

The information coming from dynamic monitoring systems of civil engineering structures are typically acquired with DAQ platforms with capabilities of moderate sampling rates (up to 2000 Hz) and ADCs with resolutions over 16 bits. Figure 2.10 shows different DAQ equipments used for structural dynamic monitoring.

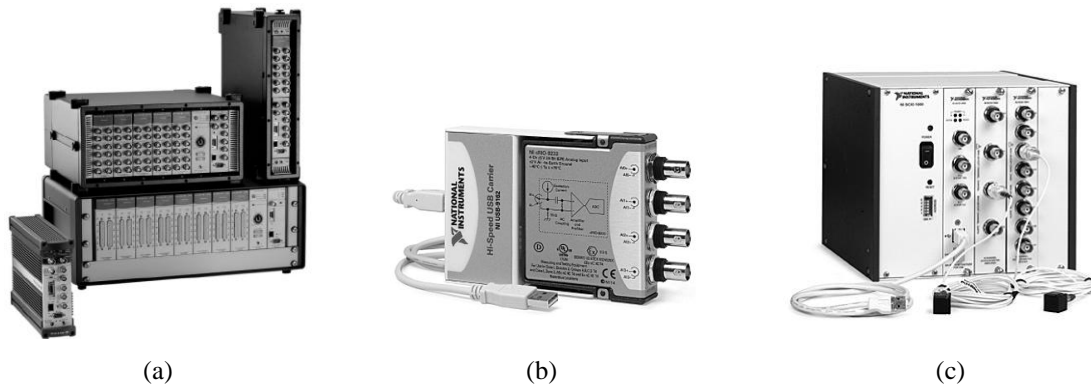


Figure 2.10 – DAQ equipments used for dynamic identification: (a) Lan-XI DAQ model 3560 with 24 bits (Brüel and Kjaer, 2009); (b) USB DAQ model NI USB-9233 with 24 bits (NI, 2009b); and (c) NI SCXI-1531 with 16 bits (NI, 2009b)

2.2.3 Remote Connections

Depending on the duration of data acquisition, structural monitoring is classified as continuous monitoring or portable testing. The continuous monitoring, also called Structural Health Monitoring (SHM), is performed in engineering structures by collecting data over an extended period of time (months, years or even permanently). On the other hand, portable testing is related to discrete measurements in time, performed to assess the existing condition of the structure. Quick and easy setups as well as connectivity with a laptop are important attributes for structural monitoring.

In the case of continuous monitoring systems, as they are supposed to work over long periods in unattended and often remote locations, their optimization is important, which can be achieved by considering aspects related to reliability and remote operation.

With this respect, there are some important considerations to be taken into account. The first one is to set up notifications while the works are performed. These notifications may include alarms to report the existence of possible damages or the achievement of a specified threshold level. The second aspect to consider is the remote data accessibility that can be used for data transferring and system adjusting purposes or as a tool to inform the condition of the system (Kullaa, 2008).

For remote communication with the monitoring systems, the most popular approaches include the use of the IEEE 802.11a, b, and g standards or cellular (such as CDMA, GSM/GPRS or EDGE). Other options include proprietary long-range radios and satellite communications (NI, 2009a).

2.3 Wireless Based Monitoring Systems

The research efforts in many scientific areas, like physics, microelectronics, control, material science etc., are oriented to the creation of smaller, autonomous and easier to handle mechanisms for sensing purposes. In the area of physical parameter measurements these goals were successfully achieved via the integration of Micro-Electro-Mechanical Systems (MEMS) with low power and high frequency transceivers, joined in silicon chips. Sensor prototypes, called “motes”, were developed to reach four attributes that a desirable sensor should have: sensing, processing, communication and actuation.

A *mote* is an autonomous, compact device, a sensor unit that has the capability of processing and communicating wirelessly. One of the biggest strengths of *motes* is that they can form networks, known as wireless sensor networks (WSN), and co-operate between each other. This technology is a product of considerable research efforts that had been carried out in the areas of communications, electronics and control engineering (Arampatzis et al., 2005).

Wireless technology is being used for a wide range of applications such as military, environmental monitoring (indoor and emergency services or, outdoor for ecology and agriculture applications), support for logistics (considering even the use of wearable motes

in firemen), human centric (motes for health science and health care) and robotics. For more detail see Arampatzis et al. (2005).

The use of wireless technology with embedded MEMS for structural monitoring was first proposed by Straser and Kiremidjian (1996), Kiremidjian et al. (1997), Straser and Kiremidjian (1998), and Straser et al. (1998). In those works the researchers proposed the integration of wireless communications with sensors to develop a near real time monitoring system. After those works a lot of efforts to improve the technology have been made.

The first commercial wireless with MEMS platform was developed by the University of California-Berkeley (Lynch and Loh, 2006) and subsequently commercialized by Crossbow (2009) since 1999. From that moment on, the commercial technology is growing constantly.

Lynch and Loh (2006), presented an exhaustive compilation that highlights the state of the art of this type of sensors up to March 2005. In Figure 2.11, updated information is presented. Detailed information can be found in Annex A.

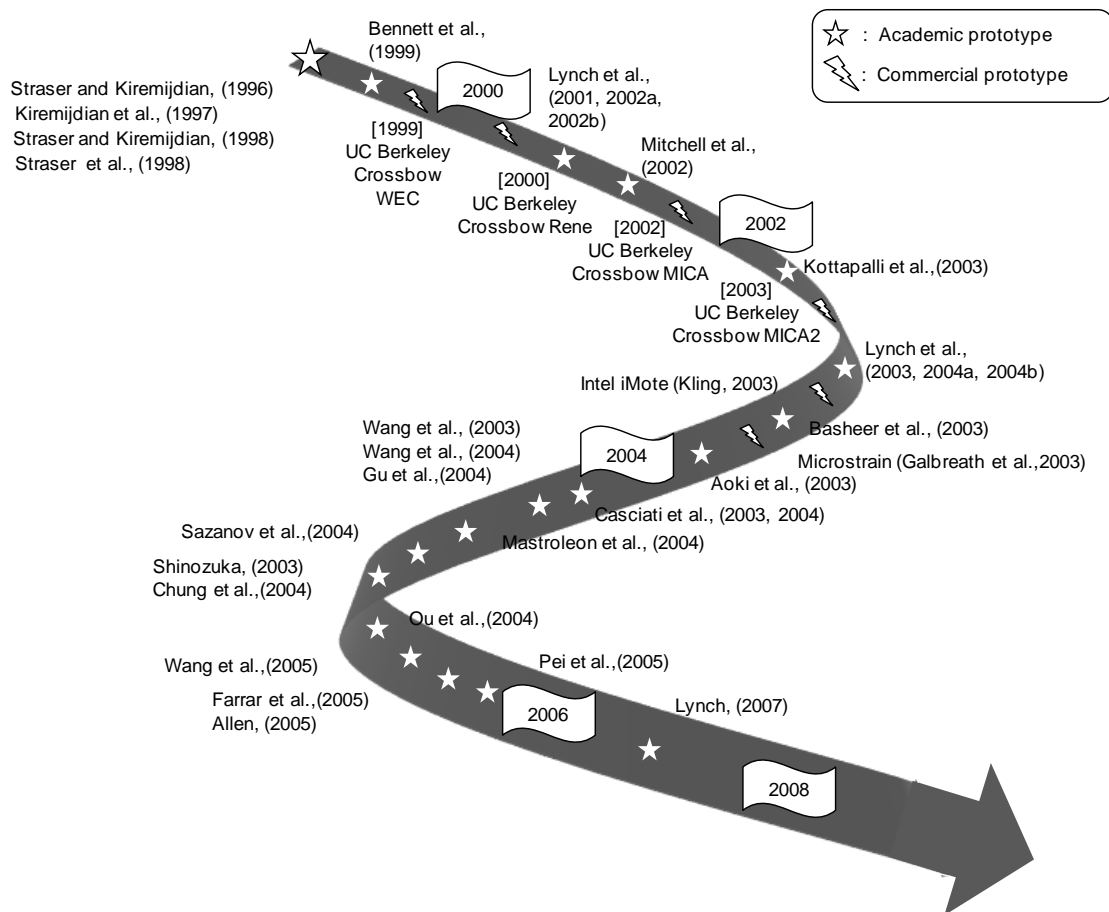


Figure 2.11 – Overview of the State of the art of wireless technology for structural monitoring purposes

Figure 2.11 shows the most relevant works related to the use of the wireless technology for structural monitoring applications. As it observed, until 2006 the number of works were increasing exponentially, which reflects the interest of the scientific and the professional community in this field. Nowadays the works are mainly oriented to the application of the available technology to real monitoring studies, to improve the current limited behavior in terms of energy and to implement other data transmission protocols available for wireless communication.

A monitoring system based on wireless with embedded MEMS equipments can be understood as composed by three parts: 1) measurement units; 2) base station; and 3) in some cases remote connection system. The measurement units are formed by MEMS, as measurement sensors, and autonomous DAQ platforms that collect the data and send them wirelessly to a base station. The base station is formed by a DAQ platform coupled with an interface board in charge on data transferring to a local computer. The third part of the system is a remote connection system in charge on data transferring from the local computer to a central “brain” station. Figure 2.12 gives a general vision of a wireless based monitoring system.

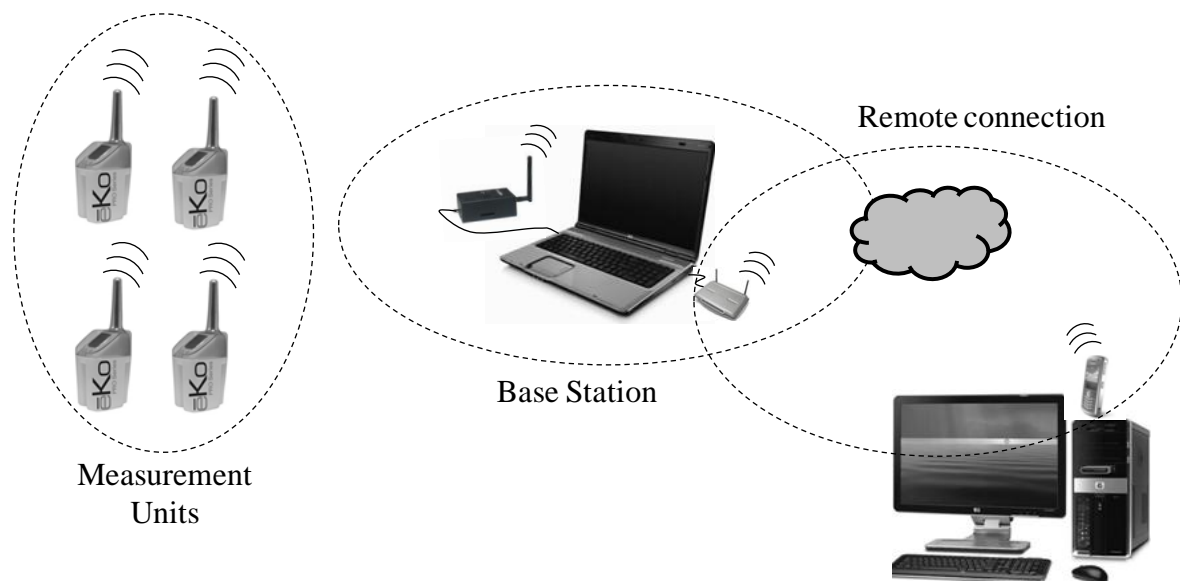


Figure 2.12 – Monitoring system with wireless with embedded MEMS equipments

The technology and the considerations related to the third part of the system (remote connection) are the same as the ones related to conventional systems (wired based). For this reason, only the two first parts of the wireless based systems are going to be further detailed here. Some important remarks with respect to the operating systems used to control the equipments will also be presented.

2.3.1 Measurement Units

A wireless measurement unit can be understood as three functional subsystems working in parallel: 1) sensing interface (MEMS as sensors and DAQ subsystem); 2) computational core (microcontrollers and memory); and 3) wireless communication module (wireless radio to transmit or receive data).

2.3.1.1 Sensing Interface

a) MEMS as Sensors

MEMS is an emerging technology through which miniature mechanical systems are built making use of the standard Integrated Circuits (IC) technologies on the same chip as the electronic circuitry. The main advantage of MEMS is that, because of the high effectiveness used in their fabrication process, can perform measurements at relatively low cost and low power consumption. The field of MEMS has been acknowledged at the end of the 1980s while the silicon-based sensors and actuators goes back to the 1970s (Stiharu, 2002b).

As shown in Figure 2.13, MEMS markets reached almost US\$ 6000 M in 2006 and for 2011 it is estimated that MEMS markets will reach over US\$ 10000 M (Eloy, 2007).

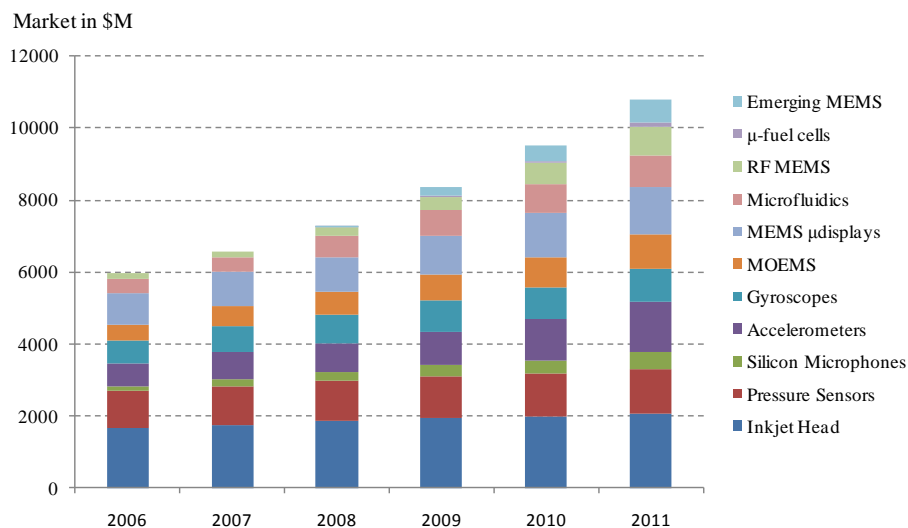


Figure 2.13 – Global MEMS market 2006–2011 (adapted from Eloy, 2007)

MEMS are classified into two large functional classes: microsensors and microactuators. Microsensors are conceived as fully signal-conditioned transducers that provide the same function as the classic sensors, while microactuators are conceived to convey energy to their surrounding environment.

Currently, the MEMS are used for diverse applications such as communications (mobile phones), finding industrial, automotive industrial, medical and security purposes. For dynamic monitoring of civil engineering structures the mechanical microsensors (microaccelerometers) are the most appropriate.

In the following not only microsensors for dynamic monitoring but also microsensors for static and environment monitoring purposes will be presented as their inclusion in the monitoring scheme offer interesting possibilities.

Microaccelerometers

Microaccelerometers are miniature inertial mass elastically suspended on inertial frames that are rigidly connected to the body on which the acceleration should be measured. The amplitude of motion is detected and converted into an electric signal. Figure 2.14 shows the working principle of ADXL50 micro machined accelerometer (Stiharu, 2002a).

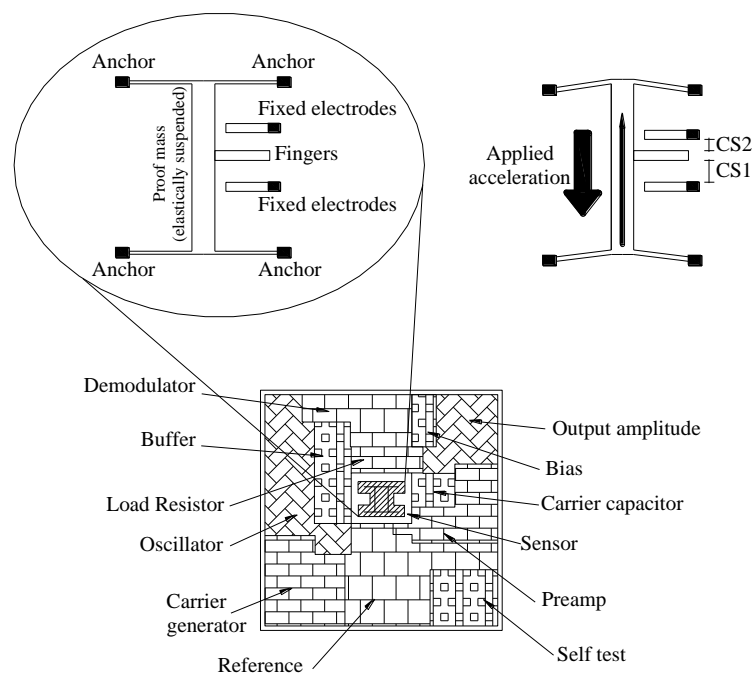


Figure 2.14 – Schematics of the microaccelerometer ADXL50 (adapted from Stiharu, 2002a)

Microaccelerometers are built on a variety of principles like capacitance, strain and piezoelectricity. Commercial accelerometers are primarily based on the capacitive principle and are able to perform measurements in 1, 2 or 3 axis. The measurement range of these sensors is between ± 2 g to ± 400 g and the sensitivity range varies from 150 mV/g

to 2000 mV/g. Due to the fact that in dynamic structural monitoring small vibrations are measured, microaccelerometers with a low range and high sensitivity should be chosen.

Figure 2.15 shows an example of commercial MEMS based accelerometers.

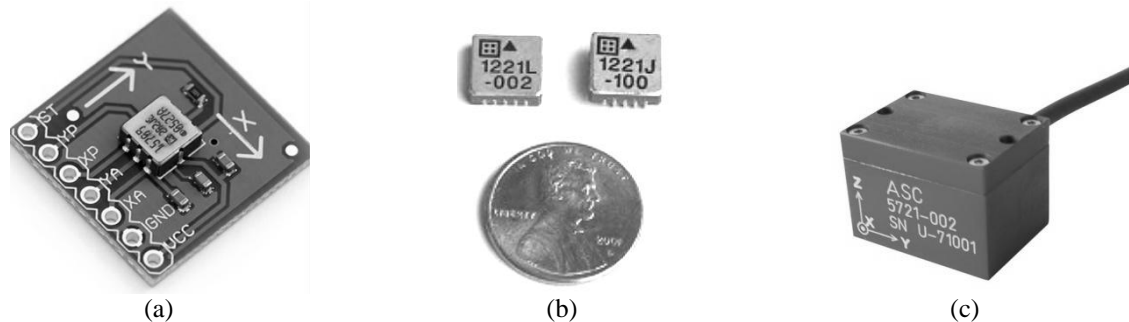


Figure 2.15 – Examples of commercial MEMS accelerometers: (a) dual axes accelerometer model ADXL202 (Analog, 2009); (b) one axis accelerometer model SD1221 (SD, 2009); and (c) tri axes accelerometer model ASC5721 (ASC, 2009)

Humidity and Temperature Microsensors

Humidity microsensors determine relative ambient humidity using capacitive measurement technology. For this principle, the sensor element is built out of a film capacitor on different substrates (glass, ceramic, etc.). The dielectric is a polymer that absorbs or releases water proportionally to the relative environmental humidity, and thus changes the capacitance of the capacitor, which is measured by an onboard electronic circuit.

Temperature readings are carried out using resistance measuring technology. The resistance of most metals is approximately a linear function of temperature. Therefore, by measuring the change in resistance of a metal meander deposited on an insulated silicon substrate, it is possible to detect temperature changes.

Because the microsensors have to be integrated on a platform where their response will be processed, simple circuitry is designed to convert changes in resistance and capacitance into a change in voltage, without loss of sensitivity. For this purpose, CMOS-MEMS technology is used. For more details see Hautefeuille et al. (2007).

Commercial available humidity and temperature microsensors have a range of 0% to 100% for relative humidity measurements and -40°C to 125°C for temperature measurements. Figure 2.16a and Figure 2.16b show a typical graph of maximal accuracy limits for relative humidity and temperature measurements of these type of sensors.

Figure 2.16c shows an example of a commercial humidity-temperature microsensor (Sensirion, 2009).

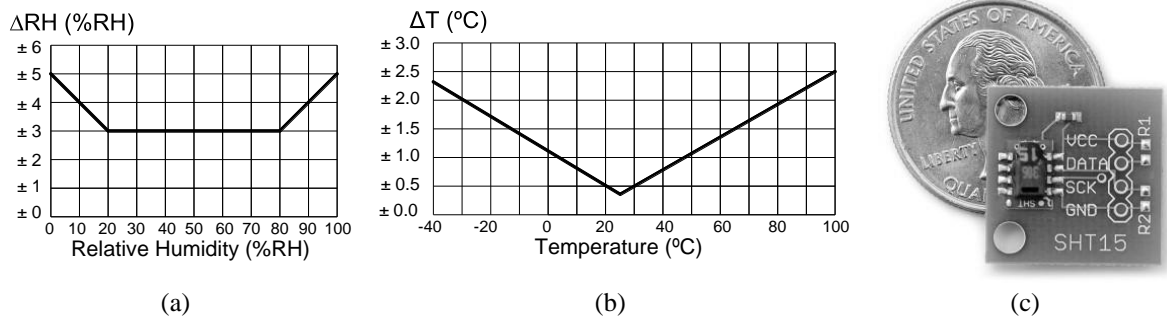


Figure 2.16 – MEMS based humidity and temperature sensors (Sensirion, 2009): (a) typical graph of maximal accuracy limit for humidity measurements; (b) typical graph of maximal accuracy limit for temperature measurements; and (c) commercial humidity-temperature sensor model SHT15

Pressure Microsensors

The vast majority of pressure microsensors use piezoresistive sense elements and a thin silicon diaphragm to detect responses to a pressure load. The basic structure of a piezoresistive pressure microsensor is shown in Figure 2.17 and consists of four sense elements in a Wheatstone bridge configuration that measure stress within a thin crystalline silicon membrane.

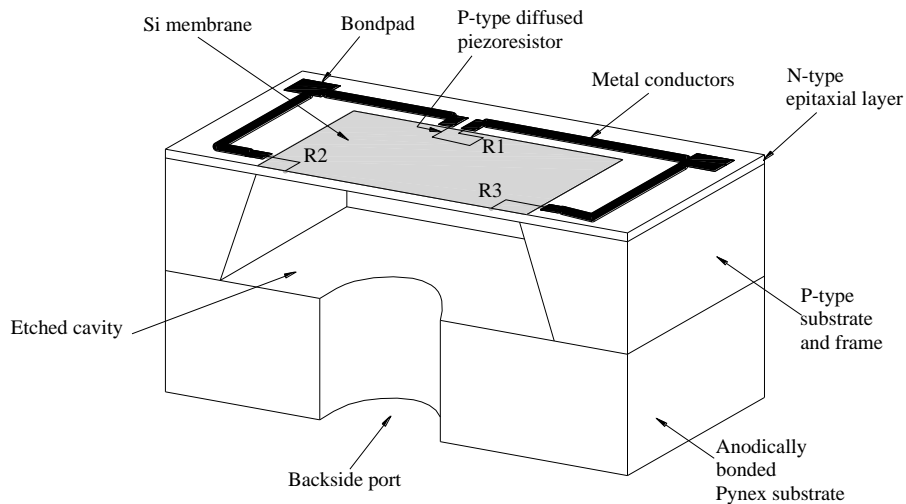


Figure 2.17 – Schematics illustration of a pressure microsensor with piezoresistive sense elements (Maluf and Williams, 2004)

The stress is a direct consequence (thus linearly proportional) of the membrane deflecting in response to an applied pressure differential across the front and back sides of the sensor.

The membrane deflection in this type of microsensors is typically less than one micrometer. The thickness and geometrical dimensions of the membrane affect the sensitivity and, consequently, the pressure range of the sensor. Devices rated for very low pressures (less than 10 kPa) usually incorporate complex membrane structures, such as central bosses, to concentrate the stresses near the piezoresistive sensors and improve both sensitivity and linearity. For more details see Maluf and Williams (2004).

Currently there are several commercial solutions for pressure microsensors which can perform absolute, gauge or differential measurements. Depending on the specific requirements, it is possible to find pressure sensors able to perform oceanographic measurements in the range of 0 MPa to 200 MPa or to perform works in a smaller range such as from 0 MPa to 0.0002 MPa (GlobalSpec, 2009).

b) DAQ Subsystem

If the wireless based monitoring platforms try to be considered as an alternative to the conventional systems, the DAQ systems embedded in the platforms should be able to collect sensor data with equivalent accuracy. For dynamic structural monitoring purposes, the sensing interface should therefore be capable of recording at moderate sample rates (up to 200 Hz) and the ADCs should have resolutions over 16 bits. As it is shown in Lynch and Loh (2006), commercial platforms are only equipped with low resolutions ADCs which varies from 10 bits (Mica platforms) to 12 bits (Imote2 platforms), see below.

2.3.1.2 Computational Core

The computational core is responsible for the operation of the wireless sensing unit, including collection of data from the sensor interface, implementation of algorithms for damage detection, modal analysis or structural control and managing the flow of data through the wireless communication channel (Lynch et al., 2004b).

The computational core is microcontrollers assembled with on-chip computing resources to support the embedded algorithms that interrogate the measurement data collected. For support, the computational core also requires memory where both measurement data and embedded computing software can be stored. To accommodate the storage of measurement data, rewritable random access memory (RAM) will be needed. Similarly, flash memory is needed for the storage of software written for operation of the unit and for the processing of response data (Lynch, 2007).

A major classifier for microcontrollers is the size of their internal data bus with most microcontrollers classified as 8, 16, or 32 bits. Larger data buses suggest higher processing throughput but also imply higher costs and power consumption (Gadre, 2001). Another internal element of the microcontrollers is the clock. The speed of the clock is a direct measure of how fast embedded programs will be executed by the microcontroller. Again, as the speed of the microcontroller increases, the power consumption increase (Lynch and Loh, 2006).

A broad assortment of microcontrollers is commercially available such as the ATmega103L (mica platforms), Atmel ATmega128L (mica2 platforms) and the ARM7TDMI (iMote2 platforms). The range of memory available in the platforms varies from 4 kB to 64 kB for the RAM memory and from 128 kB to 512 kB for the flash memory. The size of the bus varies from 8 bits to 32 bits and the speed of the clock also varies from 4 MHz to 12 MHz.

2.3.1.3 Wireless Communication Module

The wireless communication module provides an interface for the exchange of data with other wireless units or with the base station. Important considerations are such as communication reliability, range, data transfer rate and frequency allocation allowed by the country where the works are carried out (aspects related to the communication standard that is being used). Due to the fact that the wireless modules are the most power consuming components in the measurement unit, the power consumption is another important aspect to take into account (Wang, 2007).

Figure 2.18 shows the power consumption and data rate for several wireless communications standards. The IEEE 802.11x standards were developed for mobile computing applications, and are at the high end of both data rate and power consumption. While these standards have proven very popular for mobile web browsing, they are not yet suitable for structural monitoring applications because of the high power consumption, limitations on the number of devices in a network, and the cost and complexity of the radio chipsets. On the other hand, the ZigBee standard (Kinney, 2003) was built upon specification of the IEEE 802.15.4 standard and offer the advantage of supporting diverse topologies, low data rates, low power consumption, security, and reliability. These considerations make this communication standard suitable for being used in structural monitoring systems (Kintner-Meyer and Conant, 2004).

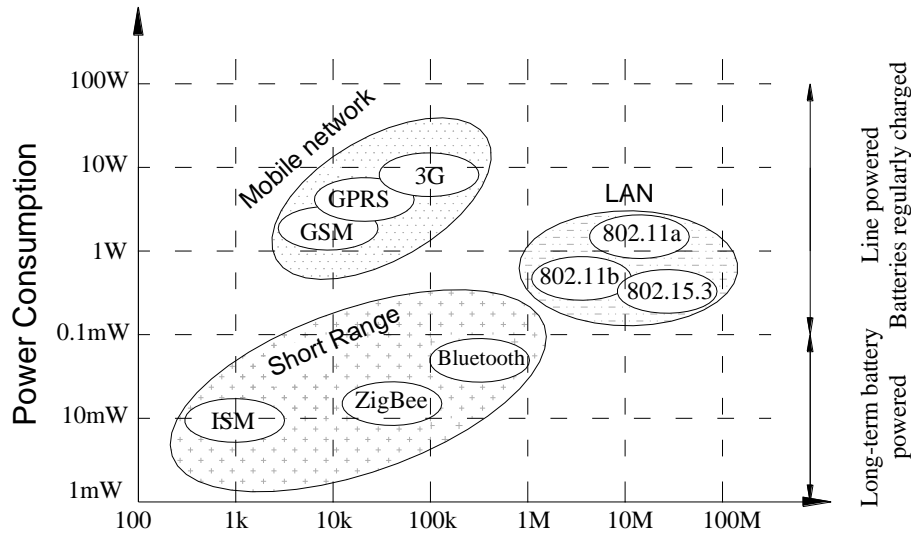


Figure 2.18 – Wireless Device and Networking Standards (adapted from Kintner-Meyer and Conant, 2004)

The data transfer between nodes can be performed according to different communication topologies. The simplest network topology is the single-hop star (Figure 2.19a) where the whole nodes communicate directly to a central node. The main drawback of this topology is its poor scalability and robustness. In the case of measurements performed in larger areas, multi-hop routing is necessary which, depending on the sensors arrangement, can be performed using different meshes (see Figure 2.19b and Figure 2.19c). Figure 2.19d shows a third option of network topology where multiple cluster of nodes report to local nodes, which in turn send the information to a central node. The advantage of this last network topology is the possibility of decomposition of a large network into separate zones within which data processing and storage can be performed locally (Krishnamachari, 2005).

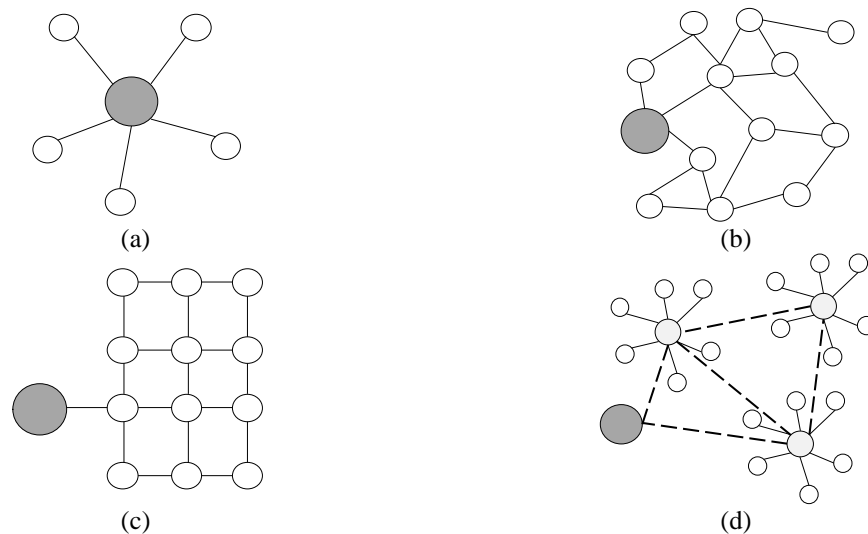


Figure 2.19 – Different options of network topologies: (a) single-hop topology; (b) flat multi-hop mesh; (c) structured grid; and (d) two-tier hierarchical cluster topology (adapted from Krishnamachari, 2005)

At the moment, commercial platforms are not yet implemented with the ZigBee communication standard. The platforms available have data transmission rates varying from 40 kb/s (micas platforms) to 250 kb/s (imote2 platform). Security in the data transmission process is another aspect that is not yet addressed in these platforms.

2.3.2 Base Station

A base station (also known as gateway) is a receiver/transmitter unit serves as the connection point between the wireless network and the computer where the data is collected. The base station is composed by a wireless communication module coupled with an interface board in charge of data collecting and *mote* programming.

The characteristics of the wireless communication module are the same of the modules used in the measurements units. Similar considerations with respect to the communication reliability, range, data transfer rate and the frequency allocation allowed by the country where the *notes* are operated should also be considered. The power consuming aspect, as the wireless module is directly connected to the computer, is not a critical issue.

The interface board is mainly connected to a computer through a serial port RS-232. Other physical mediums, like the USB port or the JTAG interface, can also be used with the same purpose. In the case of the serial port RS-232, the transmission rates vary from 20 kb/s to 115.2 kb/s. With the use of USB ports, faster data transmission rates like 1.5 Mb/s (USB 1.0), 480 Mb/s (USB 2.0) or 5 Gb/s (USB 3.0) can be achievable. Figure 2.20 shows examples of interface boards available in the market for different wireless communication modules.

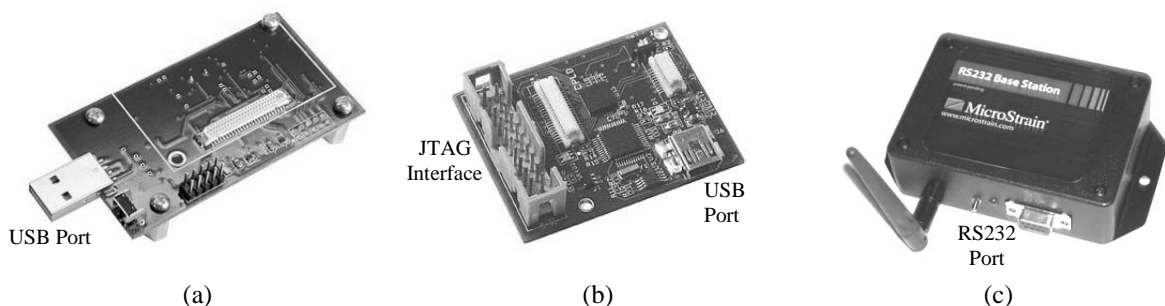


Figure 2.20 – Commercial interface boards for wireless systems: (a) Mica2/MicaZ USB interface board (Crossbow, 2009); (b) Imote2 USB/JTAG interface board (Crossbow, 2009); and (c) MicroStrain RS232 interface board (MicroStrain, 2009)

2.3.3 Mote's Operating System

The Operating System provides an abstraction of the machine hardware and is in charge of reacting to events and handling access to memory, CPU, and hardware peripherals.

In memory constrained hardware devices like those of sensor boards, the effectiveness in the operating system largely affects the response in the target application. The most well-known operating systems used for resourced constrained devices are shown in the Table 2.1 (Severino, 2008).

Table 2.1 – Operating Systems for resource constrained devices (adapted from Severino, 2008).

Operating System	Origin	Open Source	Real Time	Link
TinyOS	UCB, Intel (USA)	Yes	No	http://www.tinyos.net
Contiki	SICS (Sweden)	Yes	No	http://www.sics.se/contiki
Nano-RK	CMU (USA)	Yes	Yes	http://www.nanork.org
ERIKA	SSSUP (Italy)	Yes	Yes	http://erika.sssup.it
MANTIS	UC Boulder (USA)	Yes	No	http://mantis.cs.colorado.edu
SOS	UCLA (USA)	Yes	No	https://projects.nesl.ucla.edu/public/sos-2x/doc

The wireless based commercial platforms available at the market use TinyOS as operating system. TinyOS is a free and open source component-based operating system developed by the University of California at Berkeley in co-operation with Intel that, in its first release, was presented on 1999 (TinyOS, 2009).

TinyOS utilizes a unique software architecture specifically designed for the severe constraints of the sensor network nodes (Olusola, 2007). The components in TinyOS are written in a “Network Embedded Systems C” nesC, a dialect of C, that adds some new features to support the structure and execution model (Gay et al., 2003). The supplemental tools that the system uses come mainly in the form of Java and shell script front-ends and, because it was originally designed for Linux, under Windows environment, it runs with an emulator called Cygwin.

The programming of the *notes* is a challenging issue with serious difficulties for new users due to the fact that, even if TinyOS has almost 10 years of existence, it is still new software with only a few programmers involved and with limited expertise in its use.

2.4 Applications to Civil Engineering Structures

According to Farrar and Worden (2007), dynamic wired based monitoring systems are being widely applied to study civil engineering structures since the early 1980s. Most of those studies are related to large structures by means of bridges and tall buildings. In the case of existent masonry structures, there are also several applications such as the study of temples (Jaishi et al., 2003), and masonry towers (Gentile and Saisi, 2004; Ivorra and Pallarés, 2007; Rebelo et al., 2007; Schmidt, 2007). These systems were also used to study other types of masonry structures like arch bridges (Costa et al., 2004), churches (Baptista et al., 2004; Casarin and Modena, 2007; Ramos et al., 2010a) and minarets (Ramos et al., 2006).

In the case of dynamic wireless based monitoring systems, the first case of study was the Alamosa Canyon Bridge in 1998 (Straser and Kiremijdian, 1998). Afterwards, more case studies related with bridges were considered. These are the experiences in the Tokyo Rainbow Bridge in Japan (Aoki et al., 2003), again the Alamosa Canyon Bridge in USA (Lynch et al., 2003), a pedestrian bridge in the University of California-Irvine in USA (Chung et al., 2004), the Geumdang Bridge in Korea (Lynch et al., 2005), the Gi-Lu cable-stayed bridge in Taiwan (Weng et al., 2008) and the Golden Gate Bridge in USA (Pakzad et al., 2008). However, the only task reported in the literature related to large buildings is the dynamic monitoring of the 79 stories Di Wang Tower, located in Guangdong, China (Ou et al., 2005).

As masonry structures are difficult to excite and commercial MEMS have currently low resolution capabilities, only one case of dynamic wireless monitoring systems applications in existent masonry structures were reported. This study is the modal analysis of the Aquila Tower in Italy (Ceriotti et al., 2009). A novel contribution is given in Chapters 4 and 5 of this thesis, regarding the application of wireless based monitoring systems to other structures.

2.5 Conclusions

Structural monitoring is a topic gaining considerable importance in the civil engineering field due to the variety of its applications. With this respect, there is a specific area called dynamic structural monitoring that determines the dynamic response of the structures by performing experimental tests.

Depending on the equipments involved, the systems for dynamic monitoring can be divided in two groups. The first group, called in this work as wired based systems, uses sensors linked to DAQ platforms with wires. The second group, called in this work as wireless based systems, use a new technology based on wireless platforms with embedded MEMS as an alternative for monitoring purposes.

The wired based systems require expensive sensors and DAQ platforms as well as much cabling. Under some specific circumstances, such as studies in churches, cathedrals, monuments or other structures, the use of these conventional systems might be severely constrained. The new, small and cheap, MEMS sensors, the development of faster and more powerful computer platforms and the new communications protocols available offer great possibilities for monitoring purposes.

A wired based system can be understood as composed of three parts: the measurement sensors, the data acquisition system and, in some cases, a remote transmission unit. The accelerometers are commonly used as measurement sensors for dynamic monitoring due to the fact that they offer enough resolution, sensing range and sensing frequency for civil engineering purposes. In the case of the DAQ systems, high resolution ADCs (over 16 bits) embedded are usually employed. As the natural frequencies of the structures are low (the first natural frequencies of a conventional structure are normally less than 100 Hz), only moderate sampling rates are normally required. The process of remote transmission is common for both systems (conventional and wireless) and is used when long-term monitoring works are carried out. For this purpose internet, 802.11x standards or cellular technologies are normally employed.

Wireless systems with embedded MEMS can also be understood as three parts: the measurement unit, the base station and the remote transmission unit. The measurement unit is composed by MEMS as measurement sensors, a core unit as the heart of the system and a wireless communication module. Capacitive microaccelerometers are normally commercialized for dynamic monitoring purposes while for static monitoring there are also

temperature, humidity and pressure microsensors available. For the core unit, aspects like RAM and flash memory available, bus size and speed of the microcontroller clock should be considered in the moment of choosing the appropriate platform. The communication standard and the power consumption should be considered when the appropriate wireless communication module is implemented. The base station is in charge of data collecting and is composed by a wireless communication module and an interface board. In the moment of choosing the appropriate wireless communication module the aspects previously considered for the measurement unit should be taken into account. In the case of the interface board, only the physical medium for data transferring between the gateway and the local computer is important.

The commercial wireless based platforms have specific hardware, software and, communication characteristics that makes their application for dynamic monitoring of civil engineering structures difficult. Problems identified are the following: low resolution of MEMS accelerometers and ADCs (up to 12 bits of resolution), data acquisition constraints, imprecise synchronization schemes, core unit with limited RAM and flash memory, low clock speed of the core unit, limited bandwidth for transmission (case of micas platforms), limited energy and, finally, security and software issues.

CHAPTER 3

Operational Modal Analysis for Civil Engineering Structures

Abstract

In this chapter the most important aspects related to structural dynamic monitoring of civil structures when Operational Modal Analysis is performed are addressed. The chapter starts by presenting the mathematical techniques utilized to identify dynamic properties of the structures, a process also known as modal identification. Dynamic monitoring of structures deals not only with the problem related to the large quantity of recorded data but also with the requirements of remote data processing and of accurate analysis of the experimental results. For remote data processing, the implementation of an algorithm for automatic modal identification is desirable. For this reason the most used techniques to develop an efficient automatic modal identification algorithm are presented here. The accuracy analysis of experimental results consists of their comparison with data produced by analytical models or by previously calibrated experimental results. The most important techniques related to this topic are also shown at final part of the chapter.

3.1 Introduction

The design and construction of complex structures and the new trend of predicting damage in existing structures stimulate structural engineers to develop appropriate experimental tools to evaluate the structural behavior over time using monitoring techniques (process called Structural Health Monitoring). In the short, medium or long term monitoring processes, static and dynamic data are collected, which can then be used for numerical analysis, such as in a process of model updating or damage identification.

The aim of static monitoring is to observe phenomena with small variations on time, such as displacement variations during construction, a crack or tilt progress, or monitor environmental conditions. On the other hand, the aim of dynamic monitoring is to observe fast time-dependant phenomena. Dynamic monitoring systems also allow modal identification in terms of identifying resonance frequencies, damping and mode shapes. Static monitoring is beyond the scope of this work and only dynamic monitoring will be addressed next.

For structural dynamic monitoring, depending on the excitation source, two different groups of techniques are currently used, namely, Input-Output and Output-Only techniques.

Input-Output techniques are based on the estimation of a set of Frequency Response Functions (FRF_s) relating an applied force to the corresponding response at several points along the structure. The most common equipment used to excite small and medium size structures is an impulse hammer (Figure 3.1a). The main drawback of these equipments is the relatively low resolution for the spectral frequency estimates and the lack of energy to excite some relevant modes of vibration. In order to excite more vibration modes, other impulse excitation devices (Figure 3.1b) and electro dynamic shakers are used. In the case of bigger structures, eccentric mass vibrator and servo-hydraulic shakers (Figure 3.1c) are often used (Cunha et al., 2006).

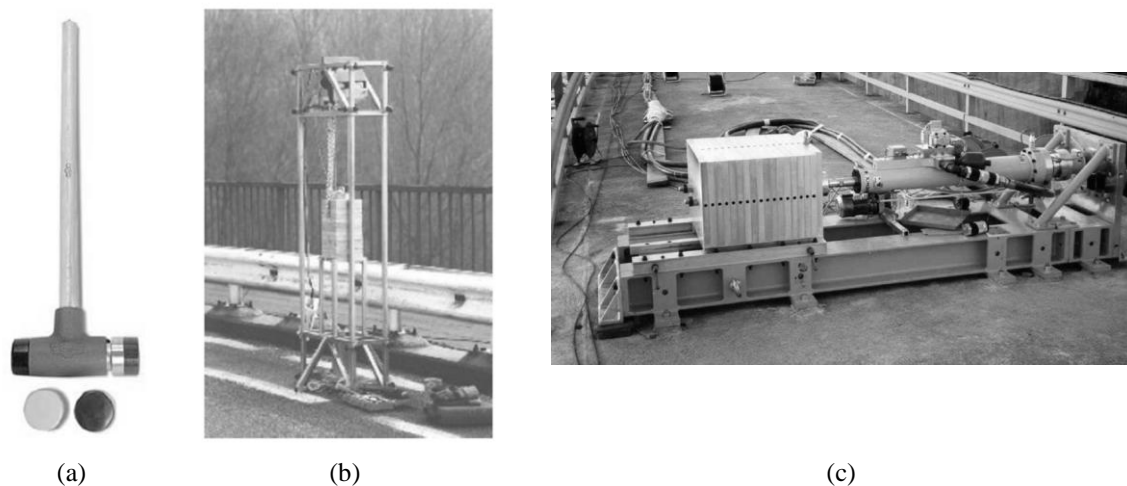


Figure 3.1 – Equipments used to perform Input-Output tests. (a) impulse hammer; (b) impulse excitation device for bridges (Cunha et al., 2006); and (c) servo-hydraulic shakers to laterally excite dams (Cantieni, 2004)

The methods for performing modal identification using Input-Output techniques are classified by Cunha et al. (2006) according the following four criteria: a) domain of application (time or frequency); b) type of formulation (indirect or modal and direct); c) number of modes analyzed (SDOF or MDOF); and d) number of inputs and type of estimates (SISO, SIMO, MIMO, MISO). For more detail about Input-Output techniques, see Maia and Silva (1997).

Testing civil engineering structures with forced vibration generally requires a large amount of specialized equipment and trained personnel, making the tests difficult and expensive. Additionally, when automated health monitoring systems are implemented, force vibration tests are not a suitable alternative. For these reasons, simpler tests in which the structures are excited just by ambient vibration, called Output-Only techniques, are desirable and often used (Doebbling et al., 1997).

3.2 Modal Identification using Output-Only Methods

During the last years, the technological developments in the field of sensors made feasible the accurate measurement of low levels of dynamic responses strongly stimulating the development of the Output-Only identifications methods, also called Operational Modal Analysis (OMA).

Output-Only methods are based on the premise that wind, traffic and human activities can adequately excite structures. The main assumption of the Output-Only identification

methods is that the ambient excitation input is a Gaussian white noise stochastic process in a frequency range of interest. Due to the nature of the excitation, the response includes not only the modal contributions of the ambient forces and the structural system, but also the contribution of the noise signals from undesired sources. In this way the measurements reflect the response from the structural system and also from the ambient forces, meaning that the identification techniques must have the ability to separate them.

As it is summarized in Cunha et al. (2006), Output-Only modal identification methods are divided in two groups, namely, nonparametric methods, essentially developed in frequency domain, (Group G1 in Figure 3.2), and parametric methods, developed in time domain (Group G2 in Figure 3.2).

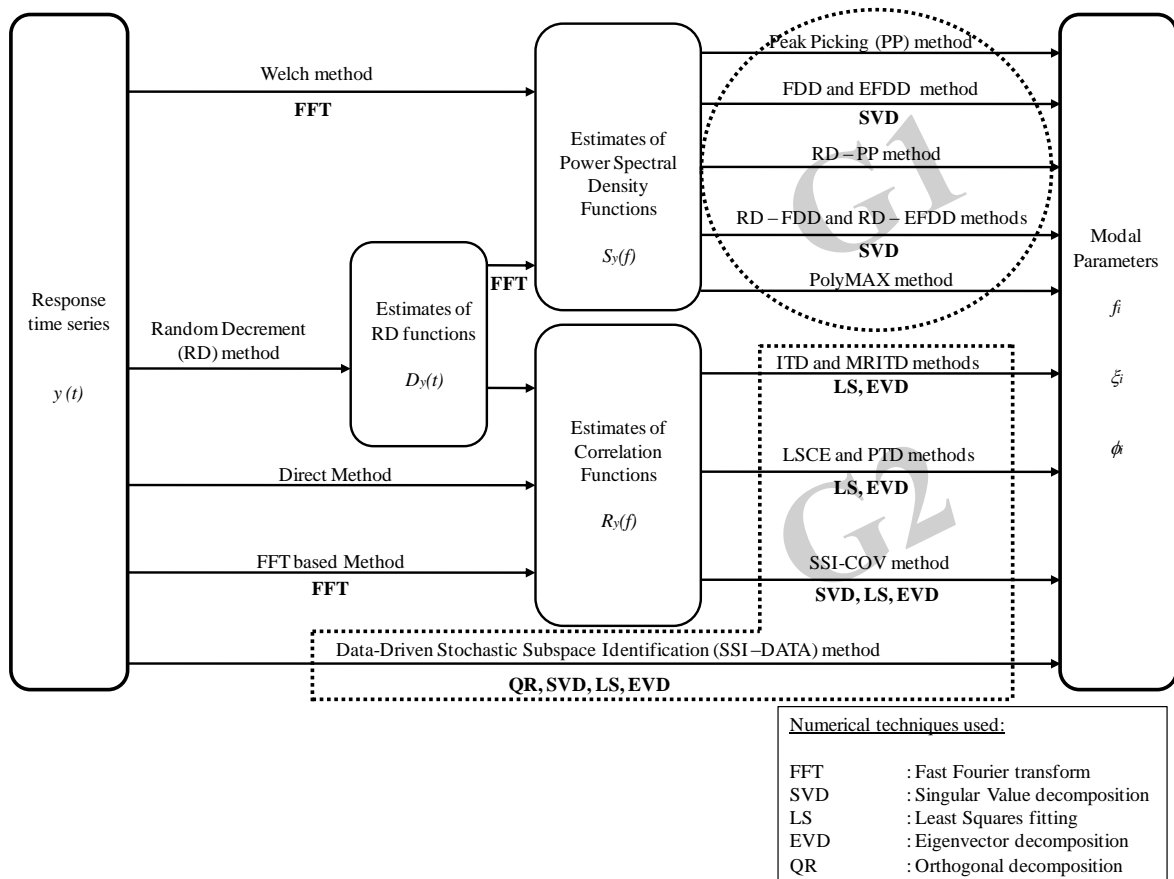


Figure 3.2 – Schematic representation of the output-only modal identification methods (adapted from Rodrigues, 2004)

Next, the main methods used for modal identification of structural systems are briefly presented.

3.2.1 Frequency Domain Identification Methods

3.2.1.1 *Peak-Picking*

The peak-picking method (PP) is the simpler and more practical method for modal identification. In spite of some drawbacks, the PP method gives very fast results and is useful as a pre-process tool when dynamic monitoring is performed.

The PP method was systematized by Felber (1993). In this method the natural frequencies of the structures are determined as the peaks of the Average Normalized Power-Spectral Densities (ANPSDs), see Braun (2002), the damping factors are determined using the Half Power Bandwidth Method, see Chopra (1995), and the components of the mode shapes are determined by the values of the transfer functions at the natural frequencies, see Peeters et al. (1999).

The main limitations of the PP method, is that picking the peaks is often a subjective task, identifying close frequencies is difficult, spurious modes can be confused as real ones, operational deflection shapes are obtained instead of mode shapes and the damping estimates are unreliable (Peeters et al., 1999).

To illustrate the procedure of modal identification using the PP method, the dynamic response of an existent building was studied in this work. The referred building is a 19th century church located in the village of Lourosa, in the south of the city of Porto, Portugal. The plant dimensions of the church are 10 m width and 35 m length and the walls are stone masonry with 1.0 m thick. The Figure 3.3 shows an aerial and a front view of the church.



Figure 3.3 – General views of the Lourosa church

In the experimental modal analysis tests of the Lourosa church, seven high sensitive piezoelectric accelerometers model PCB 393B12 (PCB, 2009) and one 16-bit DAQ system

model NI SCXI-1531 (NI, 2009b) were used. As it is shown in Figure 3.4a, 13 measurement nodes (two sensors in node P04 and P09 respectively) were considered. Due to the available number of transducers, the measurement sensors were displayed in two setups maintaining as references the two sensors at node P09. The Figure 3.4b shows the central data acquisition station.

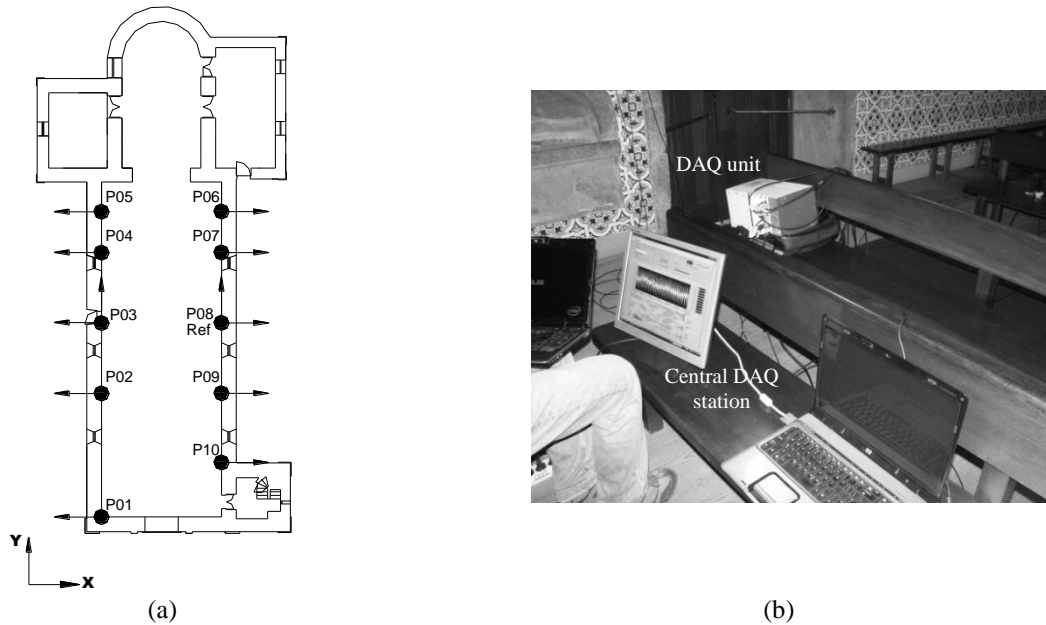


Figure 3.4 – Setup of the dynamic tests performed in the Lourosa church: (a) plant view with the location of the measurement nodes central acquisition station; and (b) central DAQ station

The dynamic acquisition was performed at 200 Hz of sampling rate and the measurement time considered was 10 min. Figure 3.5 presents the collected time series for the first setup.

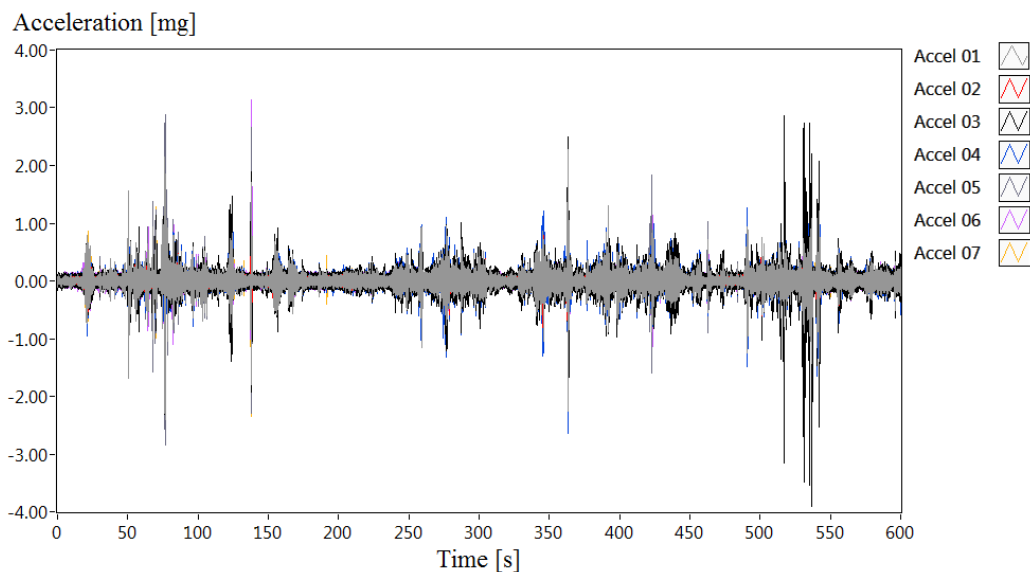


Figure 3.5 – Time series collected in the first setup

The PP method was used to perform the modal identification. Figure 3.6 shows the modified periodogram spectral estimation, known as Welch Spectrum (Welch, 1967), of the acquired signal and Table 3.1 shows the obtained frequencies. Damping coefficients and mode shapes estimations are not shown due to the low reliability of this method.

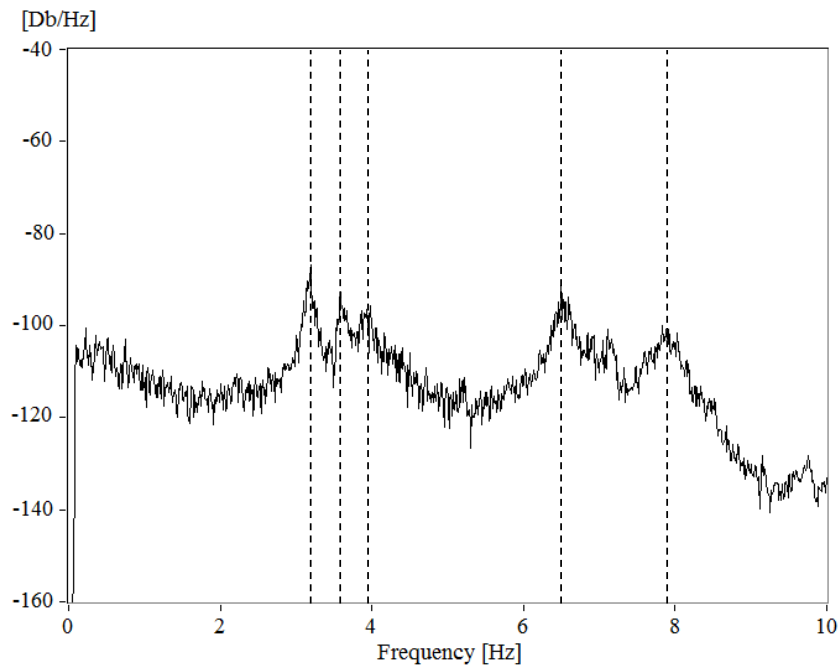


Figure 3.6 – Modal Identification of the Lourosa church using the PP method

Table 3.1 – PP results of the Lourosa church.

	Frequency [Hz]
Mode 1	3.18
Mode 2	3.59
Mode 3	3.93
Mode 4	6.53
Mode 5	7.93

3.2.1.2 Frequency Domain Decomposition

In the Frequency Domain Decomposition method (FDD) presented by Brincker et al. (2000b), the spectral density functions matrix is, at each discrete frequency, decomposed in singular values and vectors using the Singular Value Decomposition (SVD) algorithm. By doing so, the spectral densities functions are decomposed in the contributions of different modes of a system that, at each frequency, contribute to its response. From the analysis of the singular values it is possible to identify the auto power spectral density functions corresponding to each mode of a system. In the FDD method, the mode shapes are estimated as the singular vectors at the peak of each auto power spectral density function corresponding to each mode. A flow chart in Figure 3.7 summarizes the FDD method.

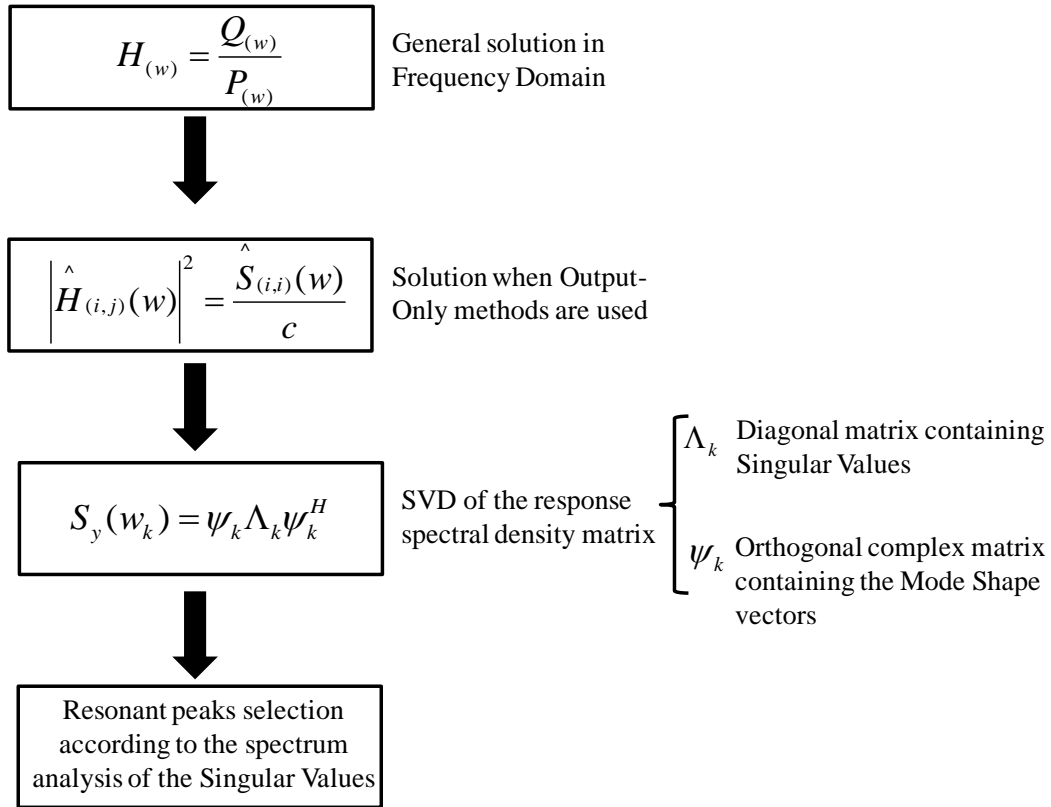


Figure 3.7 – Flow chart of the FDD method

Brincker et al. (2001) improved the FDD method by presenting the Enhanced Frequency Domain Decomposition method (EFDD), which is closely related with the previous FDD method but includes additional procedures to evaluate the damping and to get enhanced estimates of the frequencies and mode shapes of a system.

According to the EFDD method, the selection of the autospectra corresponding to each mode of a system is performed based on the values of the MAC coefficient (see section 3.4.1.2) between the singular vectors at the resonance peaks at their neighboring frequency lines. Those SDOF auto-spectral density functions are then transformed into the time domain using the Inverse Fast Fourier Transform (IFFT), resulting in autocorrelation functions for each mode of a system. Based on those autocorrelation functions, frequencies and dampings are estimated from the zero crossing times and the logarithmic decrement respectively. The estimate of the mode shapes is also enhanced, considering all the singular vectors within each SDOF autospectral density function, weighted with the corresponding singular values (Rodrigues et al., 2004).

The same example of the experimental modal identification of the Lourosa church previously presented is now used to illustrate the procedure of modal identification using the FDD and the EFDD methods. Figure 3.8 presents the average of the normalized

singular values of spectral density matrices for all setups and Table 3.2 gives the identified natural frequencies and damping factors. The differences found in the measured frequencies between the two methods are negligible presenting both high similarities with their counterparts estimated with the PP.

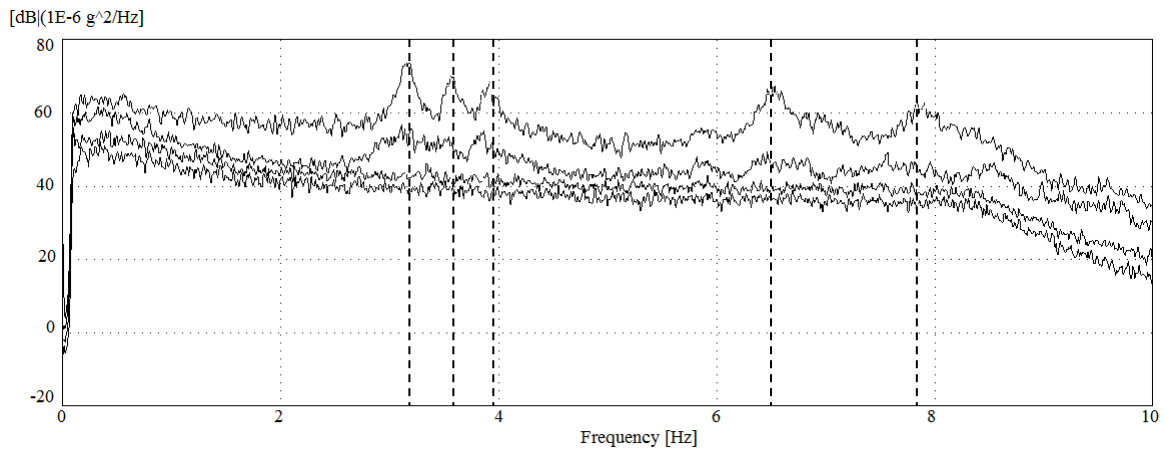


Figure 3.8 – Modal Identification of the Lourosa church using the FDD and EFDD methods

Table 3.2 – FDD and EFDD results of the Lourosa church.

	FDD		EFDD	
	Frequency [Hz]	Damping (%)	Frequency [Hz]	Damping (%)
Mode 1	3.15	----	3.16	1.12
Mode 2	3.56	----	3.55	1.02
Mode 3	3.93	----	3.89	0.69
Mode 4	6.49	----	6.50	0.63
Mode 5	7.83	----	7.85	0.65

3.2.2 Time domain Identification Methods

3.2.2.1 Stochastic Subspace Identification

The Stochastic Subspace Identification (SSI) method was originally proposed by Van Overschee and De Moor (1991) and then modified (SSI-Data method) by Peeters and De Roeck (1999).

The Data-Driven Stochastic Subspace Identification method (SSI-Data) is based on the stochastic space model theory from output-only measurements and so is focused in the identification of the state matrix A and the output matrix C that contains the modal information of the studied system. The SSI method uses robust numerical techniques such as QR-factorization, and singular value decomposition (SVD). The QR-factorization results in a significant data reduction whereas the SVD is used to reject system noise. A summary of the method is presented in Figure 3.9.

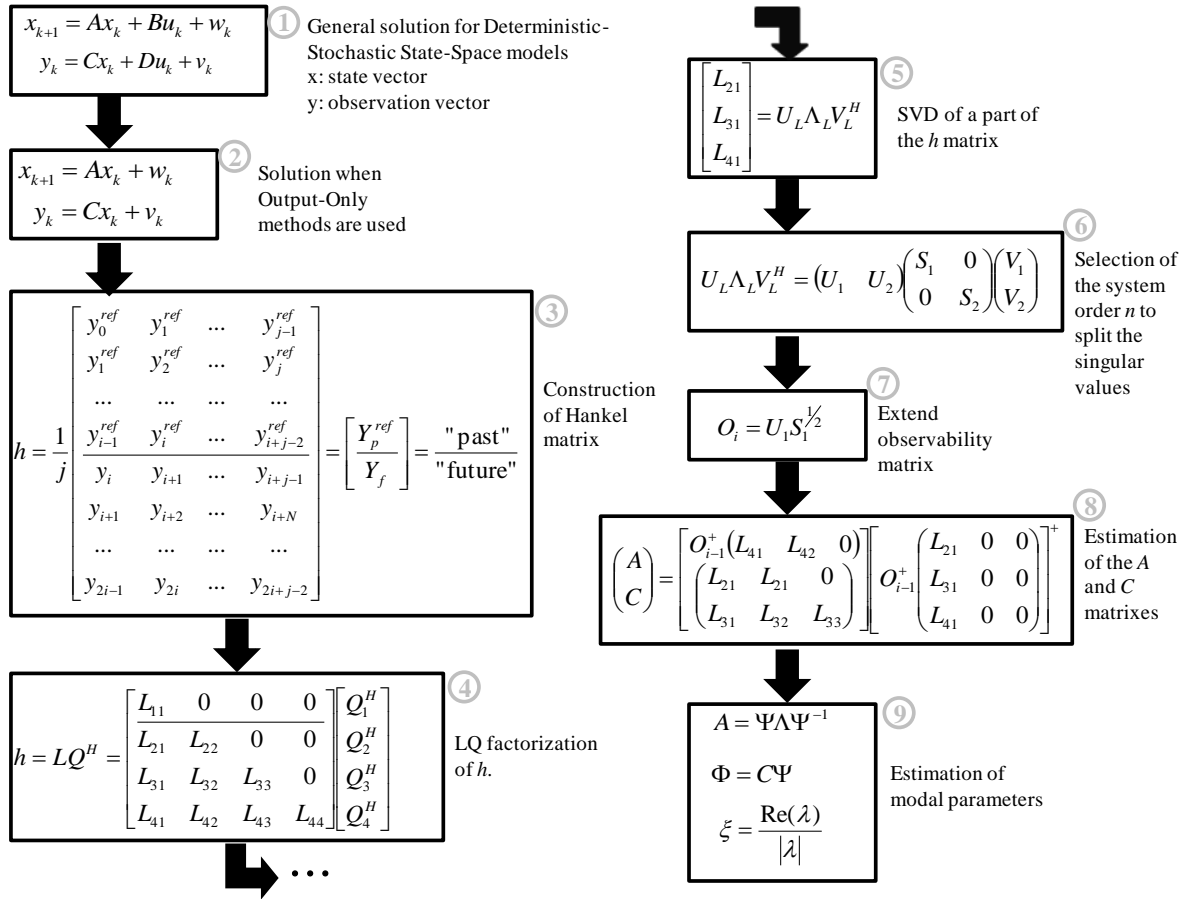


Figure 3.9 – Flow chart of the SSI-DATA method

The choice of an appropriate order n for the system is the most important issue when the SSI method is implemented. A selection of an unwarranted large system order will increase the number of the identified modes but will also result in the identification of many unreliable numerical modes (also called spurious or noise modes). Thus, the modal identification is performed by constructing stabilization diagrams and selecting the stable poles in a certain system order.

The idea of the stabilization diagram is that several runs of the complete pole identification process are made, by using models of increasing order. Experience shows that in such analysis, the pole values of the “physical” eigenmodes always appear at a nearly identical frequency, while mathematical poles tend to scatter around the frequency range. The pole value from all the analyses using different orders can be combined in one single diagram, using the pole frequency as horizontal axis and the solution order as vertical axis. Physical poles are readily visible in the diagram.

From the stabilization diagram, it is not possible to select the optimal system order, and for this order, the valid system poles, but it is possible to select individual poles from different analysis. For this purpose, several criteria can be used but the most used one is the selection of the lowest order at which the pole becomes “stable”.

Continuing with the example of the Lourosa church, Figure 3.10 illustrates the process of model order selection in the stabilization diagrams. Differently from the previous methods, seven natural frequencies were clearly identified with the SSI-data method (see Figure 3.10c), which indicates the importance of this method for data processing purposes of OMA tests.

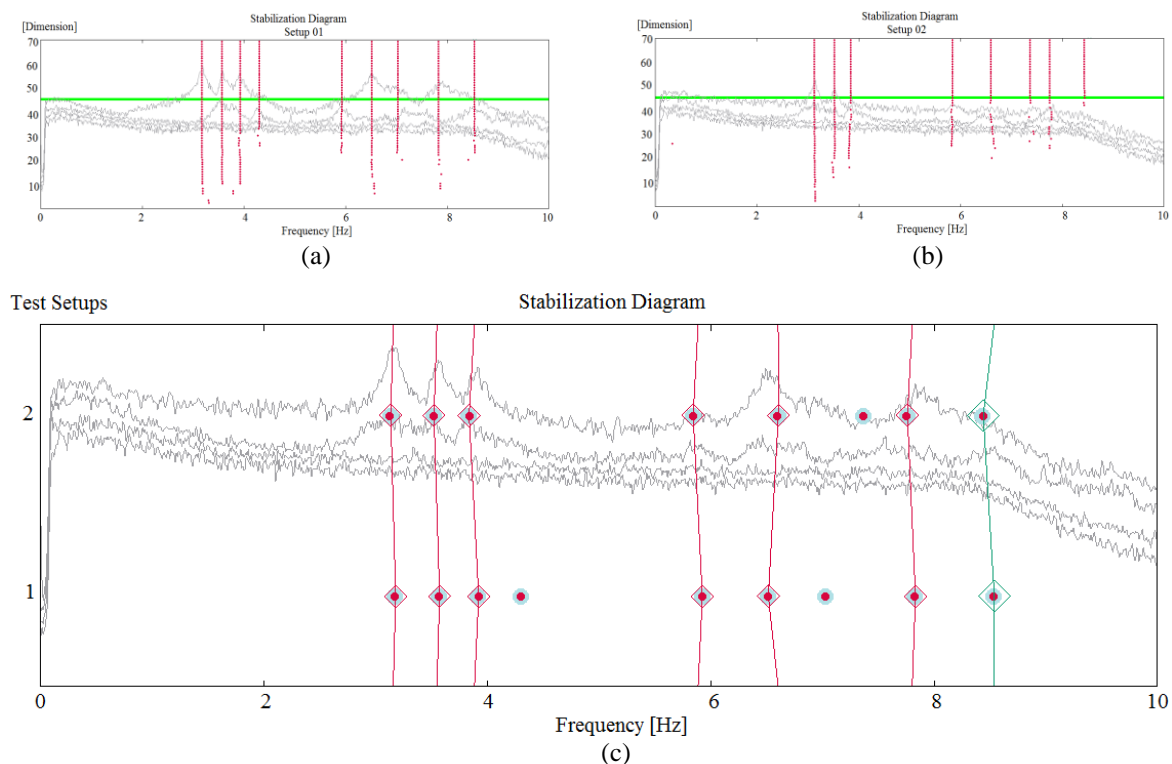


Figure 3.10 – Modal Identification of the Lourosa church using the SSI-data method: (a) stabilization diagram setup 01; (b) stabilization diagram setup 02; and (c) stabilization diagram of the both setups together

Figure 3.11 summarizes the results of the modal identification process for the present case study. Table 3.3 presents the detailed results of the identified frequencies and damping coefficients using the SSI-data method, as well as a comparison, in terms of the percent error, with the results of identified dynamic properties using the previous PP, FDD and EFDD methods. As shown, similar natural frequencies and mode shape estimations were obtained in the whole cases. On the other hand, even if the results of damping coefficients were reasonable, the observed higher scatter indicate a drawback of the OMA

techniques for the proper estimation of this factor and therefore other procedures such as free vibration tests should be considered for improved results.

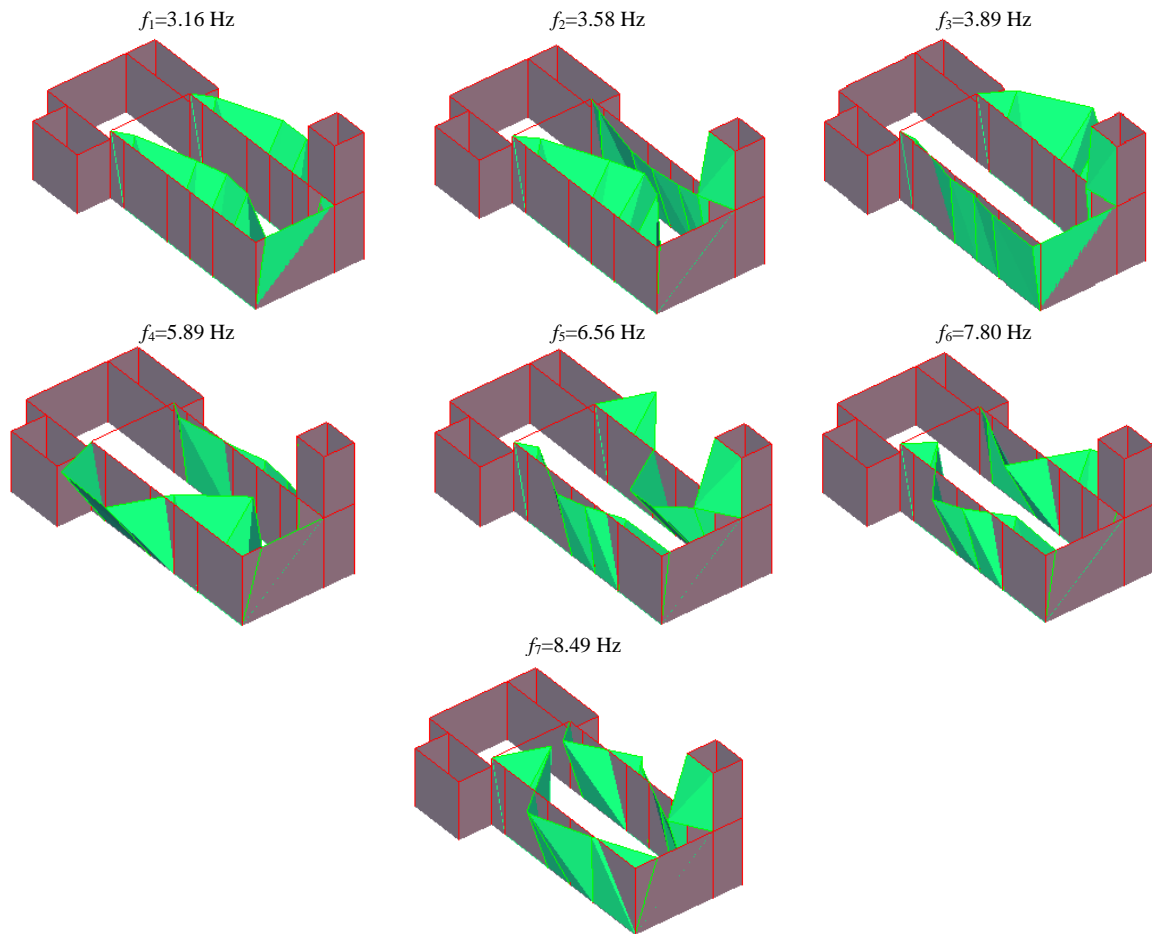


Figure 3.11 – Estimated modal shapes for the Lourosa church using the SSI-data method

Table 3.3 – Experimental results of the dynamic tests performed in the Lourosa church.

Mode	SSI-Data		Frequency Comparison			Damping Comparison	Mode Shape Comparison	
	Freq [Hz]	Damp [%]	SSI/PP [%]	SSI/FDD [%]	SSI/EFDD [%]	SSI/EFDD [%]	MAC (*) SSI/FDD	MAC(*) SSI/EFDD
1	3.16	1.15	0.6	0.3	< 0.01	2.6	0.99	0.99
2	3.58	0.80	0.3	0.6	0.8	27.5	0.96	0.97
3	3.89	1.80	1.0	1.0	< 0.01	61.7	0.95	0.96
4	5.89	1.45	----	----	----	----	----	----
5	6.56	2.26	0.5	1.1	0.9	72.1	0.80	0.85
6	7.80	1.45	1.7	0.4	0.6	55.2	0.67	0.76
7	8.49	2.60	----	----	----	----	----	----

(*)MAC is a coefficient that correlates two mode shapes estimations and is defined in section 3.4.1.2

3.3 Automatic Modal Identification

If an effective use of modal identification is intended in the context of Structural Health Monitoring (SHM), it is necessary to avoid constant user interaction in the modal extraction process. As it was presented in Andersen et al. (2007), three problematic issues are related to the process of modal identification of civil engineering structures. The first one is the excitation source, as variations on the source during tests and variations on the excitation levels are commonly found throughout the experimental tests. The second aspect is the huge quantity of data recorded, encompassing many measurement channels, many setups and/or long sample periods. The third issue is related to the modal identification process itself, as there may be cases where manual extraction of modes might not be possible, or cases where the modes are weakly excited or highly damped.

When continuous monitoring systems are conceived, the implementation of an automatic modal identification process is desirable. This automatic process has to deal with the above mentioned problems and also with extracting accurate physical features that are useful in post processing stages.

Current research efforts to automate the identification of structural modal parameters are focused on (Magalhães et al., 2009):

- a) conception of identification algorithms using parametric methods in order to obtain clearer stabilization diagrams;
- b) definition of additional parameters or signal processing techniques (such as filtering or SVD) that can result in more accurate estimations of the dynamic parameters of the studied systems; and
- c) development of methodologies for automatically interpreting the information obtained from the application of the data processing methods.

Rainieri and Fabroccino (2009) present the state of the art of the methodologies related to the automation of OMA, including the work of several research groups which combined the aspects mentioned above in order to obtain strategies for data processing routines. Existing proposals can be classified according to the domain in which they were developed. There are works using frequency domain automatic processes such as the ones presented by Verboven et al. (2001), Verboven et al. (2002), Verboven et al. (2003b), Guan et al. (2005), Brincker et al. (2007), Magalhães et al. (2008), and Rainieri and

Fabroccino (2009). On the other hand, there are works focused on time domain processes such as the ones presented by Peeters and De Roeck (2001), Scionti et al. (2003), Andersen et al. (2007), Deraemaeker et al. (2008), and Magalhães et al. (2009).

There are known limitations related to the frequency domain methods, because the quality of the estimations is dependent on the spectrums resolution, which are particularly difficult to obtain in noisy environments or in structures that are difficult to excite. For this reason, this work was focused on exploring the possibilities for the implementation of an automatic identification algorithm of time domain methods. With this respect, the best way for automatic interpretation of stabilization diagrams is to develop algorithms to mimic the decisions that an experienced modal analyst takes during the examination of a stabilization diagram. The clustering and the ruled-based techniques are two approaches used for overcoming these considerations and will be detailed next.

3.3.1 Cluster Analysis

Clustering is a classic technique of unsupervised learning (all the observations are taken as variables) which is used for grouping data with similar characteristics. In the context of experimental modal identification, clustering techniques can be also applied. The stabilization diagrams are basically a product of a clustering process since each of the estimated groups (clusters or columns of poles) represents physical modes which share values of frequencies, damping and mode shapes.

The available techniques for performing cluster analysis can be classified as parametric or non hierarchical techniques (probability based models, Gaussian mixture models, C-means fuzzy clustering, K-means and K-median algorithms) and non parametric or hierarchical techniques (agglomerative and divisive algorithms), Fung (2001). In recent years both types of clustering techniques have been used for processing the results from modal analysis tests such as the works presented by Goethals et al. (2004) and Verboven et al. (2002) which used C-means fuzzy clustering techniques, as well as the works presented by Verboven et al. (2003a) and Magalhães et al. (2009) where hierarchical techniques were used.

3.3.2 Rule-Based Approach

The rule base approach is another classical technique for data processing that carries out a same logical process similar to human beings. If this technique is applied to the interpretation of stabilization diagrams, it is first important to understand what happens when this process is performed manually. In stabilization diagrams, the visual information that is presented to the engineer consists of symbols that represent the similarity of frequencies, damping ratios and/or mode vectors between poles belonging to subsequent model orders. The manual procedure for interpretation of stabilization diagrams includes the following tasks: a) selection of vertical columns of stable poles in frequency, damping and mode shapes, and b) selection of the lower model order where stable poles appear for the whole frequencies of interest.

The ruled-based approach was used by Scionti et al. (2003) for improving the modal identification process of in-flight flutter data. In the referred work, the process was performed by initially selecting columns in the stabilization diagrams (obtained by applying the SSI method) and then performing pole picking of the stable poles. For this final pole picking stage, not only stable frequency poles were considered but also the comparison of the damping ratios and, when applicable, the information of mode shapes.

3.4 Correlation Analysis of Modal Identification Results

Efforts have been done since the late 1970s for finding quality indicators of the information obtained from experimental modal tests. At that point, the standard methodology considered the orthogonality check of the modal vectors as the main tool for comparison purposes (Allemang, 2003). Currently, the available approaches aim at comparing two aspects: the correlation of modal properties and response properties (Ewins, 2000).

3.4.1 Comparison of Modal Properties

The comparison of modal properties can be carried out using different techniques that goes from simple graphic comparisons to more complex numerical procedures. When using graphic procedures, the degree of correlation of two sets of results is visually assessed looking at the plots of frequencies and corresponding modes. On the other hand, numerical correlation techniques are based on the comparison of modal estimations (frequencies and mode shapes) using global or individual indicators of similitude by means of vector and Degrees of Freedom (DOF) correlations.

The most important modes shape's vector correlation criteria are the: Modal Vector Orthogonality, Modal Assurance Criterion (MAC), Weighted Modal Assurance Criterion (WMAC), Partial Modal Assurance Criterion (PMAC), Modal Assurance Criterion Square Root (MACSR), Scaled Modal Assurance Criterion (SMAC), Inverse Modal Assurance Criterion (IMAC), Modal Assurance Criterion Using Reciprocal Modal Vectors (MACRV), Modal Assurance Criterion with Frequency Scales (FMAC), and the Modal Correlation Coefficient (MCC). With respect to the verification of the correlation of the mode shape's degrees of freedom, the most important techniques are the Coordinate Modal Assurance Criterion (COMAC) and the Enhanced Coordinate Modal Assurance Criterion (ECOMAC). A brief summary of the most used criteria follow below.

3.4.1.1 *Modal Vector Orthogonality*

The primary method that has historically been used to validate an experimental modal model is the weighted orthogonality check, which compares the measured modal vectors and an appropriately sized analytical mass matrix (usually obtained from a finite element model).

Theoretically, for proportional damping, each modal vector of a system will be orthogonal to all other modal vectors of that system when weighted by the mass, stiffness or damping matrix. In practice, the mass matrix is considered to be the most accurate. As a result, the orthogonality relations can be stated as follows (Clough and Penzien, 2003):

$$\text{For } a \neq e: \quad \{\phi^{(a)}\}^T [M] \phi^{(e)} = 0 \quad \text{Equation 3.1}$$

$$\text{For } a = e: \quad \{\phi^{(a)}\}^T [M] \phi^{(e)} = M^{(a)} \quad \text{Equation 3.2}$$

where ϕ is the modal vector for mode i , M is the mass matrix, $\{\phi\}^T$ is the transpose of the modal vector ϕ , and the super indexes a and e denotes the analytical and experimental results respectively.

Experimentally, the result of zero for the orthogonality calculations are difficult to achieve (when $a \neq e$). In real case studies, values up to one tenth of the magnitude of the generalized mass of each mode are considerate to be acceptable (Allemang, 2003).

The orthogonality verification, however, gathers errors in the analytical model development, the reduction of the analytical model and the estimated modal vectors into a single indicator and, therefore, not always represent the best accuracy indicator.

3.4.1.2 Modal Assurance Criterion

The Modal Assurance Criterion method (MAC) was first proposed by Allemang and Brown (1982) with the aim to provide a measure of consistency between estimates of a modal vector.

The modal assurance criterion is defined as a scalar constant relating the degree of consistency between two modal vectors (e respect to a) as follows:

$$\text{For } \phi \text{ a non-real vector:} \quad MAC_{(a,e)} = \frac{|\phi_a^H \phi_e|^2}{(\phi_a^H \phi_a)(\phi_e^H \phi_e)} \quad \text{Equation 3.3}$$

$$\text{For } \phi \text{ a real vector:} \quad MAC_{(a,e)} = \frac{|\phi_a^T \phi_e|^2}{(\phi_a^T \phi_a)(\phi_e^T \phi_e)} \quad \text{Equation 3.4}$$

where H denotes the Complex conjugate transpose (Hermitian) of ϕ , and T denotes the transpose.

The MAC assumes values between zero and one. Values close to one indicate consistent correspondence, whereas values close to zero indicate poor resemblance of the two shapes.

3.4.1.3 Weighted Modal Analysis Criterion

The purpose of the Weighted Modal Analysis Criterion (WMAC) is to increase the performance of the MAC method recognizing that the MAC is not sensitive to mass or stiffness distribution. The WMAC becomes a unity normalized orthogonality or pseudo-orthogonality check in which the desirable result for a set of modal vectors would be ones along the diagonal (same modal vectors) and zeros off-diagonal (different modal vectors) regardless of the scaling of the individual modal vectors.

The WMAC is defined as:

$$WMAC_{(a,e)} = \frac{|\phi_a^H W \phi_e|^2}{(\phi_a^H W \phi_a)(\phi_e^H W \phi_e)} \quad \text{Equation 3.5}$$

where W is the weighting matrix that can be either the mass or the stiffness matrix.

3.4.1.4 Modal Assurance Criterion with Frequency Scales

The Modal Assurance Criterion with Frequencies Scales method (FMAC) was proposed by Fotsch and Ewins (2000). The method considers that displaying simultaneously the mode shape correlation, the degree of spatial aliasing and the frequency comparison in a single plot is more useful for correlation applications. This method is used mainly in studies related to model updating and assessment of parameters variation. Figure 3.12 shows an example of the application of this methodology.

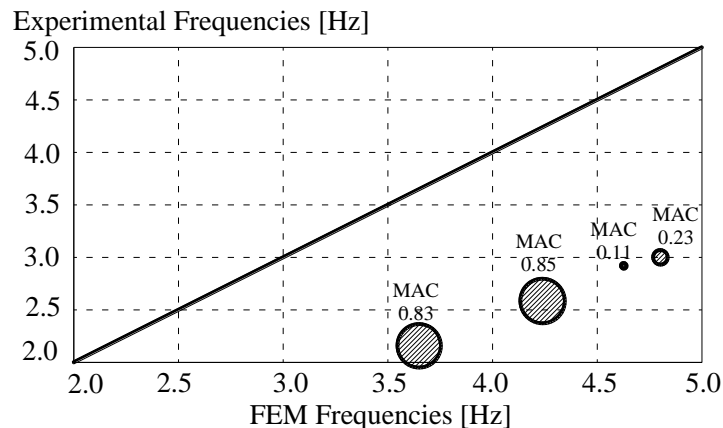


Figure 3.12 – Example of the application of the FMAC method (Ramos et al., 2010a)

3.4.1.5 *Coordinate Modal Assurance Criterion*

The Coordinate Modal Assurance Criterion (COMAC) was proposed by Lieven and Ewins (1988) as an extension of the previously proposed MAC method. The COMAC is used to detect differences at the DOF level between two modal vectors and is basically a row-wise correlation of two sets of compatible vectors, which in MAC is done column-wise. The COMAC is calculated using the following approach, once the mode pairs have been identified with MAC or some other approach:

$$COMAC_{(i,a,e)} = \frac{\left[\sum_{j=1}^m |\phi_{i,j}^{(a)} \cdot \phi_{i,j}^{(e)}| \right]^2}{\sum_{j=1}^m (\phi_{i,j}^{(a)})^2 \cdot \sum_{j=1}^m (\phi_{i,j}^{(e)})^2} \quad \text{Equation 3.6}$$

where i is the index of the correlated mode pairs, $\phi_{i,j}$ is the j^{th} element of the i^{th} paired modal vector and m the number of estimated mode shapes.

3.4.1.6 *Enhanced Coordinate Modal Assurance Criterion*

The Enhanced Coordinate Modal Assurance Criterion (ECOMAC) was proposed by Hunt (1992) and was developed to extend the COMAC computation to be more aware of typical experimental errors that occur in defining modal vectors, such as sensor scaling mistakes and sensor orientation errors. The ECOMAC is given by:

$$ECOMAC_{(i,a,e)} = \left[\frac{\sum_{j=1}^m |\phi_{i,j}^{(a)}| - |\phi_{i,j}^{(e)}|}{2m} \right] \quad \text{Equation 3.7}$$

3.4.2 *Comparison of Response Properties*

The next type of correlation analysis considers the verification of the correspondence of the response functions obtained from experimental modal tests and their analytically predicted counterpart. With this respect, the most important criteria are the: Frequency Response Assurance Criterion (FRAC), Complex Correlation Coefficient (CCF), Frequency Domain Assurance Criterion (FDAC), and the Modal FRF Assurance Criterion (MFAC).

3.4.2.1 Frequency Response Assurance Criterion

The Frequency Response Assurance Criterion (FRAC) was proposed by Heylen and Lammens (1996) and uses as comparison factor any of two Frequency Response Functions (FRFs) representing the same input-output relationship (one synthesized from the model and the other measured in the field). The FRAC is stated according to Equation 3.9.

$$FRAC(j)_k = \frac{\sum_{i=1}^L \left| \left({}_e H_{jk}(\omega_i) \right) \left({}_a H_{jk}^*(\omega_i) \right) \right|^2}{\sum_{i=1}^L \left| {}_e H_{jk}(\omega_i) \right|^2 \cdot \sum_{i=1}^L \left| {}_a H_{jk}(\omega_i) \right|^2} \quad \text{Equation 3.8}$$

where $H_e(\omega)$ is the measured FRF, $H_a(\omega)$ is the synthesized FRF, $i=1, L$ represents individual frequencies for both tests and analysis data exists and the suffix k indicates that the relevant FRFs have DOF k as reference.

3.4.2.2 Frequency Domain Assurance Criterion

The Frequency Domain Assurance Criterion (FDAC) was proposed by Pascual et al. (1997) which is a FRAC-type of calculation evaluated with different frequency shifts. The FDAC is given by:

$$FDAC_{(j,a,e)} = \frac{\left| \{H_e(\omega_i)\}_k^T \cdot \{H_a(\omega_j)\}_k \right|^2}{\left| \{H_e(\omega_i)\}_k^T \cdot \{H_e(\omega_i)\}_k \right| \cdot \left| \{H_a(\omega_j)\}_k^T \cdot \{H_a(\omega_j)\}_k \right|} \quad \text{Equation 3.9}$$

3.5 Conclusions

For the civil engineering community, especially for those working in the area related to preservation of historical monuments, Structural Health Monitoring (SHM) is a very attractive tool to detect damage in early stages as well as to observe the behavior of the structures over time. Several field tests are carried out with the aim of performing SHM and it is possible to classify them as static or dynamic monitoring tests.

In the case of dynamic monitoring, the techniques are based on the record of the dynamic response of the structure under artificial or ambient excitation. The artificial excitation involves usually large and expensive equipments which are sometimes not easy to handle in conventional monitoring studies. Recently, the studies are mostly carried out considering ambient noise as source of excitation (process called Operational Modal Analysis).

The mathematical methods for processing the Operational Modal Analysis data are classified according to the domain in which they are performed: the frequency or the time domain. Depending on the simplicity and the feasibility of the application in the field, the methods can be used in one of two phases of the data processing. The first phase, considered as a pre-processing, consists on the verification of the acquired data by means of checking the frequency content. The most used method for the first stage is the Peak Picking method (PP). The second phase, considered as a post-process, is frequently carried out in the office, when more reliable results are required and more time can be devoted to the task. In the second phase, the most used methods are the Frequency Domain Decomposition (FDD), the Enhanced Frequency Domain Decomposition (EFDD) and the Stochastic Subspace Identification method (SSI-data).

An important aspect, related to the application of the methodologies mentioned above, is the requirement of user interaction. When large quantities of data are analyzed or the data is required to be remotely processed, the manual process is difficult and tedious, meaning that automatic modal identification is desirable. Several automatic modal identification algorithms are proposed in the literature considering that the manual process can be replayed in a computer algorithm. When the SSI-data method is used as a processing tool, the automatic process consists on the analysis of the stabilization diagrams by means of the comparison of similar results from consequent model orders.

Another aspect to be taken into account when data processing is performed is the possibility to check the accuracy of the results. Numerous techniques are currently available and the process consists in the comparison of the experimental results with some previously defined training data.

CHAPTER 4

Operational Modal Analysis using Commercial WSN Platforms

Abstract

In this chapter, the commercial off-the-shelf technology of Wireless and MEMS (combination known as Wireless Sensor Networks-WSN) was explored for application in the Operational Modal Analyses of civil engineering structures.

With this purpose, wireless and conventional wired based systems were used together for performing experimental modal analysis tests in laboratory and field experiments. In the laboratory, detailed time and frequency domain studies, as well as modal identification procedures, were carried out considering a wooden pendulum specially built for this purpose. Aiming at observing the performance of the wireless systems in real field cases, similar studies were performed in one chimney of a 15th Century building located in the North of Portugal.

The results of the experimental tests evidenced the poor performance of the commercial WSN platforms for recording low amplitude accelerations due to the low resolution of the microaccelerometers and the low number of bits of the Analog Digital Convertors (ADC_s) embedded. The modal shape information extracted from the records of these systems was also of low reliability since no communication protocols are implemented in the platforms. In spite of these facts, it should be noticed that acceptable accuracy in the frequency content of the recorded signals can be expectable when structural systems under high amplitude excitations are studied.

4.1 Introduction

The previous chapters presented in this work provided a detailed review of the available equipments and data processing tools used in dynamic monitoring works. As it was shown, dynamic monitoring of structures can be used for a wide range of applications. However, there are considerations related to the equipments and the huge quantity of recorded data that difficult their broad applicability in real situations. In the present chapter, alternatives for the Data Acquisition (DAQ) equipments and measurement sensors will be explored.

It was shown in Chapter 3 that, based on the source of excitation, there are two testing options for carrying out experimental modal identification of structures: 1) Input-Output tests in which external devices are used to excite the structures; or 2) Operational Modal Analysis tests (OMA) in which it is assumed that the environmental noise (wind, cars, people, etc) is enough to excite the structures in their natural frequencies.

With respect to the measurement sensors and DAQ equipments for structural monitoring, Chapter 2 classified these systems according to the linking facilities as conventional or wired based, and wireless based. In the last type of systems, a new technology based on Wireless Sensor Networks-WSN (platforms that use Wireless technology with embedded MEMS) results very attractive for improving the overall efficiency of the monitoring systems. However, few case studies were reported related to the application of this technology in field monitoring studies of civil engineering structures.

The present work represents a first attempt of a thorough exploration of the advantages and restrictions of the commercial off-the-shelf technology of WSN to perform OMA tests in historical masonry buildings. To accomplish this objective, experimental laboratory and field modal analysis tests were carried out using wired and wireless based equipments. The detailed explanation of the sensors, DAQ equipments, DAQ software, testing procedures, as well as the discussion of the results will be presented in the following sections.

4.2 Description of the Measurement Sensors and Data Acquisition Systems

Since 2003, conventional wired based equipments have been used by the Civil Engineering Department of the University of Minho to perform OMA tests on historical masonry structures. Due to the gained experience and the reliability of the obtained results, in this work these equipments were considered as a reference for assessing the performance of the WSN platforms. The conventional wired based measurement sensors selected were the high sensitivity piezoelectric accelerometers, model PCB 393B12 (PCB, 2009) with a measurement range of ± 0.5 g, 10 V/g of sensitivity, and 0.1 to 2000 Hz of dynamic frequency response range. For DAQ purposes, the NI-USB9233 (NI, 2009b) board with an ADC resolution of 24 bits was selected. Figure 4.1 shows the accelerometer and the DAQ board used in the experimental tests.

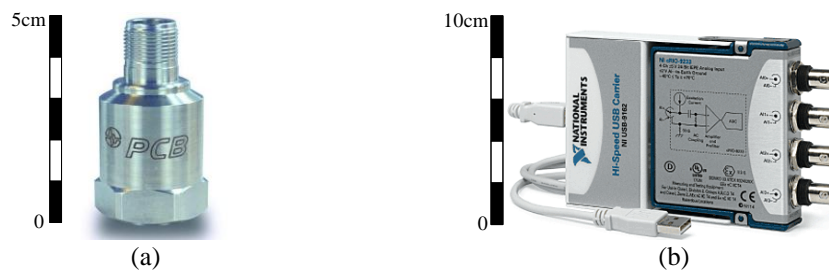


Figure 4.1 – Conventional wired based equipments used in the tests: (a) accelerometer 393B12 (PCB, 2009); and (b) DAQ equipment model NI-9233 (NI, 2009b)

Regarding the wireless based equipments, the Crossbow technology (Crossbow, 2009) was chosen as it offers economical solutions including low powering boards and measurement platforms with microaccelerometers embedded. The selected Crossbow product (WSN professional kit) uses as gateway a Mica2 board (Figure 4.2a) in charge of the communication over the network in the radio frequency range of 868/916 MHz. To provide in-system programming and to supply energy to the devices, the system uses an interface board model MIB520 (Figure 4.2b) connected to a central computer trough an USB bus. The components of the gateway and the mounting process of the boards are shown in Figure 4.2c.

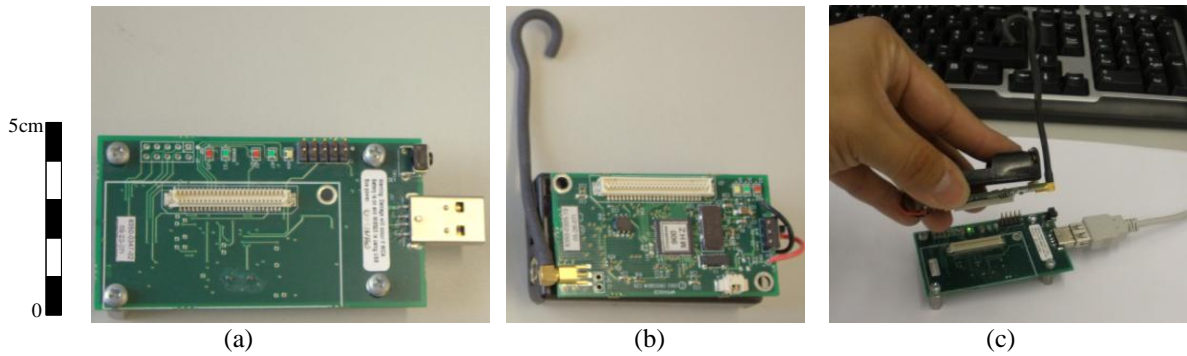


Figure 4.2 – Crossbow base station unit: (a) MIB520 board, (b) Mica2 board; and (c) unit's mounting process

The sensors' platform supplied by Crossbow is composed by a measurement board that works mounted on a Mica2 board. In this unit, the Mica2 board is not only in charge of the network communication but also in charge on supplying energy to the measurement board (using two AA batteries), as well as acquiring and converting the analog measurements with an ADC resolution of 10 bits. There are several options of measurements boards available in the market, however; the one suitable for dynamic monitoring works is the MTS400. This measurement board has embedded four microsensors: biaxial microaccelerometer; light; pressure-temperature; and humidity-temperature. The technical specifications of the referred sensors are found in Annex B of the present work. The location of the sensors in the MTS400 board and a view of the mounted unit are shown in Figure 4.3.

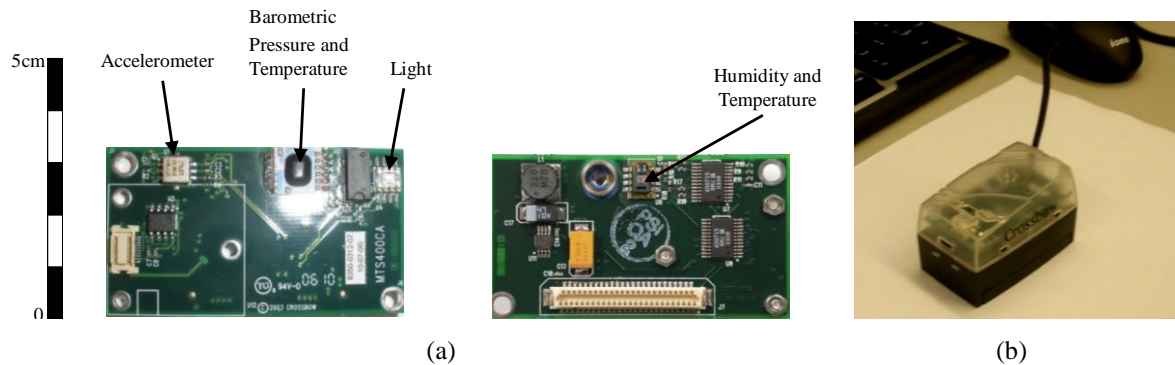


Figure 4.3 – Crossbow sensors' platform: (a) front and back of the MTS400 sensors' board; and (b) mounted unit

For comparison purposes, Table 4.1 presents the characteristics of the biaxial microaccelerometer ADXL202 embedded in the MTS400 board and the characteristics of the conventional wired based piezoelectric accelerometer PCB 393B12.

Table 4.1 – Technical comparison of the MEMS microaccelerometer ADXL202JE and the conventional piezoelectric accelerometer PCB 393B12.

	MEMS Microaccelerometer	Piezoelectric Accelerometer
Sensor Type	ADXL202JE	PCB 393B12
Channels	X, Y	X
Frequency Response (Hz)	0 - 50	0.1 - 2000
Range (g)	±2.0	±0.5
Sensitivity (mV/g)	167 ±17%	10000
Resolution (g rms)	0.002	0.000008
Size (mm)	5.0 x 5.0 x 2.0	30.2 (diam.) x 55.6 (height)
Weight (gram)	1.6	210
Noise Density ($\mu\text{g}/\sqrt{\text{Hz}}$)	500	0.32 (at 10 Hz)
Cost (€)	10	1000

Since the aim of this work was the evaluation of the performance of the commercial WSN platforms in dynamic monitoring tests, only the microaccelerometers were activated in the mote programming stage, and set to a single axis configuration. With this solution it was intended to avoid data collision issues and to reduce data loss in the measurement process.

The DAQ process of the wireless system consists on receiving and converting into engineering units the data that arrives from the motes at the RS-232 port in hexadecimal format. The data is transmitted in successive messages each one containing 10 ADC data readings (2 bytes each one) in little-endian format. An example of the transmitted message is shown in Table 4.2.

Table 4.2 – Example of the content of one message sent by the mote.

Dest Addr	HandlerID	GroupID	Msg Len	Source Addr	Counter	Channel	Readings
7e 00	0a	7d	1a	01 00	14 00	01 00	96 03 97 03 97 03 98 03 97 03 96 03 97 03 96 03 96 03 96 03

For the DAQ process of the wireless system, a Virtual Instrument (VI) routine was developed using the Labview programming environment (Labview, 2006). In this VI, a subroutine was also included to pre-process the recorded data by calculating the Welch Spectrum (Welch, 1967) of the acquired time domain series. A screenshot of the front panel of the developed program is shown in Figure 4.4. The detailed Block diagram can be found in Annex C.

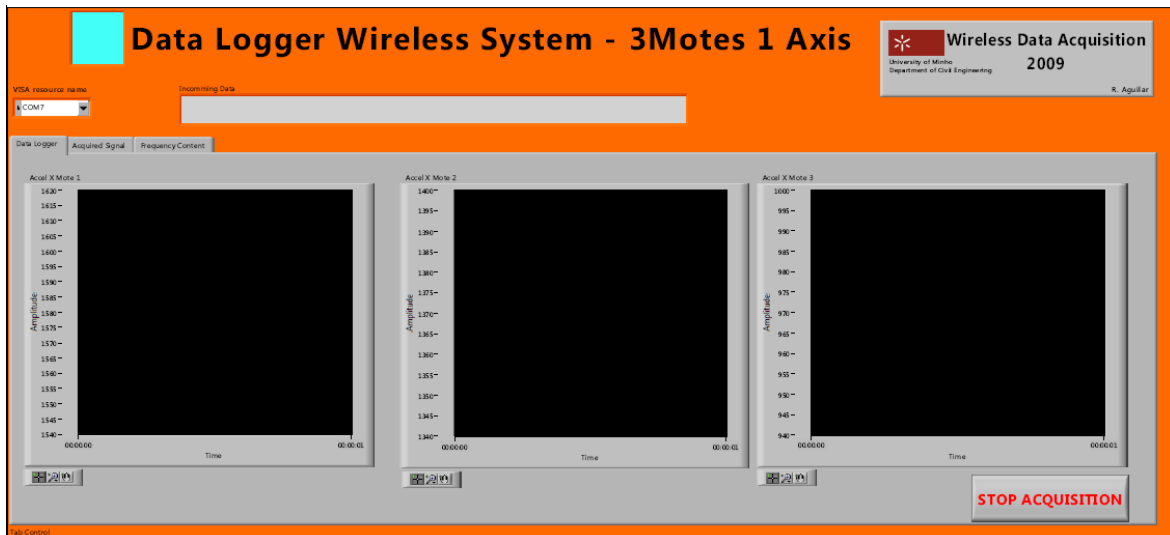


Figure 4.4 – Front panel of the VI program developed to acquire the data from the WSN

The experimental tests carried out in this work were divided in two types. The first one was related to the laboratory tests where, under controlled environment, the calibration of the studied systems could be carried out. Aiming at evaluating the performance of the WSN platforms in real field studies, a second round of tests was performed in a structural element of a historical construction. For comparison purposes, in the laboratory experiments the data from the conventional and WSN platforms were collected at the same instant of time using parallel DAQ stations (Figure 4.5). Due to the difficulties on carrying two DAQ systems for the field tests, this process was performed considering independent tests using only one station. For the DAQ processes carried out in the laboratory and field tests, a sampling rate of 128 Hz was adopted for acquiring the data from the conventional and the wireless systems.

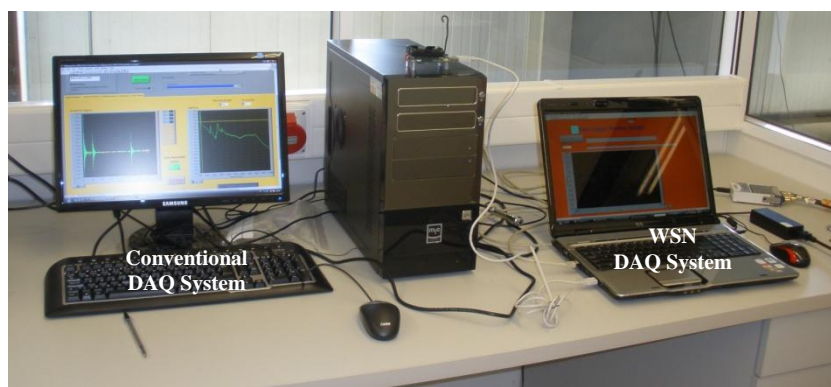


Figure 4.5 – DAQ systems arrangement for the experimental tests using commercial WSN platforms

4.3 Experimental Modal Identification Tests: Laboratory Specimens

4.3.1 Description of the Studied Specimen and Analytical Solution

A Single Degree of Freedom (SDOF) structure given by an inverted pendulum is one of the simplest examples used by civil engineers to explain the fundamentals of the dynamics of structures. In this work, this structure was also used as a tool to evaluate and understand the performance of the WSN platforms and its utility for engineering works.

The pendulum built in laboratory was 1.70 m height and consisted in a wooden beam with 39 mm x 42 mm of cross section with a heavy steel plate at the base to assure adequate support conditions. A second, lighter, steel plate was placed at the top of the pendulum to replicate the effect of a concentrated mass. Figure 4.6 shows the characteristics of the specimen.

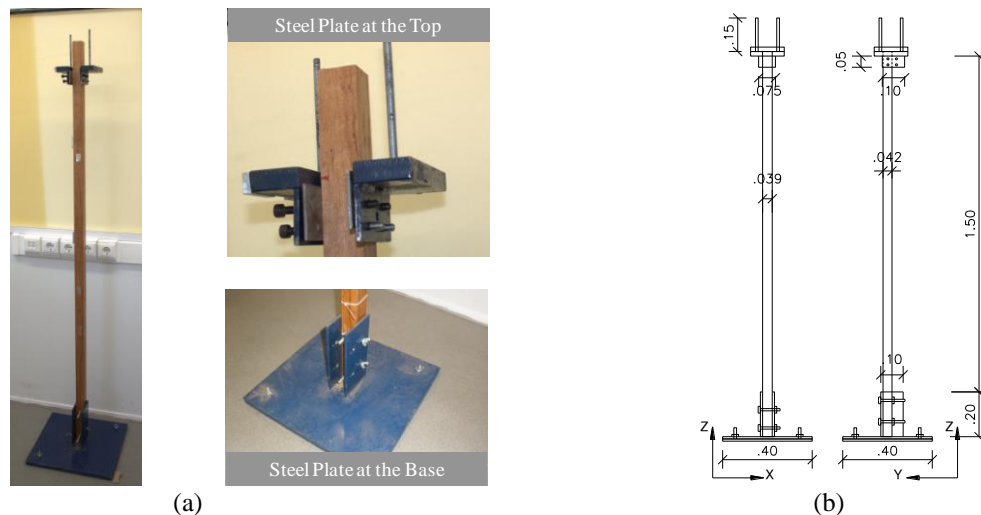


Figure 4.6 – Specimen description: (a) pendulum in the laboratory; and (b) geometric details (units: meters)

This pendulum was designed in such a way that its dynamic properties could be controlled by changing the position and the quantity of mass located at the top, or by varying the cross section of the supporting structure. The analytical dynamic response of this structure was determined considering a SDOF system with a fixed end under free vibration. The natural frequency of the system is calculated according to Equation 4.1, as given by Chopra (1995):

$$f = \frac{1}{2\pi} \sqrt{\frac{k}{m}} = \frac{1}{2\pi} \sqrt{\frac{3EI}{mh^3}} \quad \text{Equation 4.1}$$

where f denotes the frequency in [Hz], k the stiffness in [N/m^2], m the mass in [kg], E the elasticity modulus in [Pa], I the inertia moment in [m^4], and h the system's height in [m].

Using the inverted pendulum, three different configurations were considered for the experimental modal identification tests. The first one considers the system in its original condition; hereafter referred to as “Pendulum - 1st Configuration”. The second corresponds to the system with additional masses at the top, referred to as “Pendulum - 2nd Configuration”. Finally, the last configuration concerns the system with stiffer supporting element referred to as “Pendulum - 3rd Configuration”. The different considerations related to each case of study are shown in Figure 4.7.

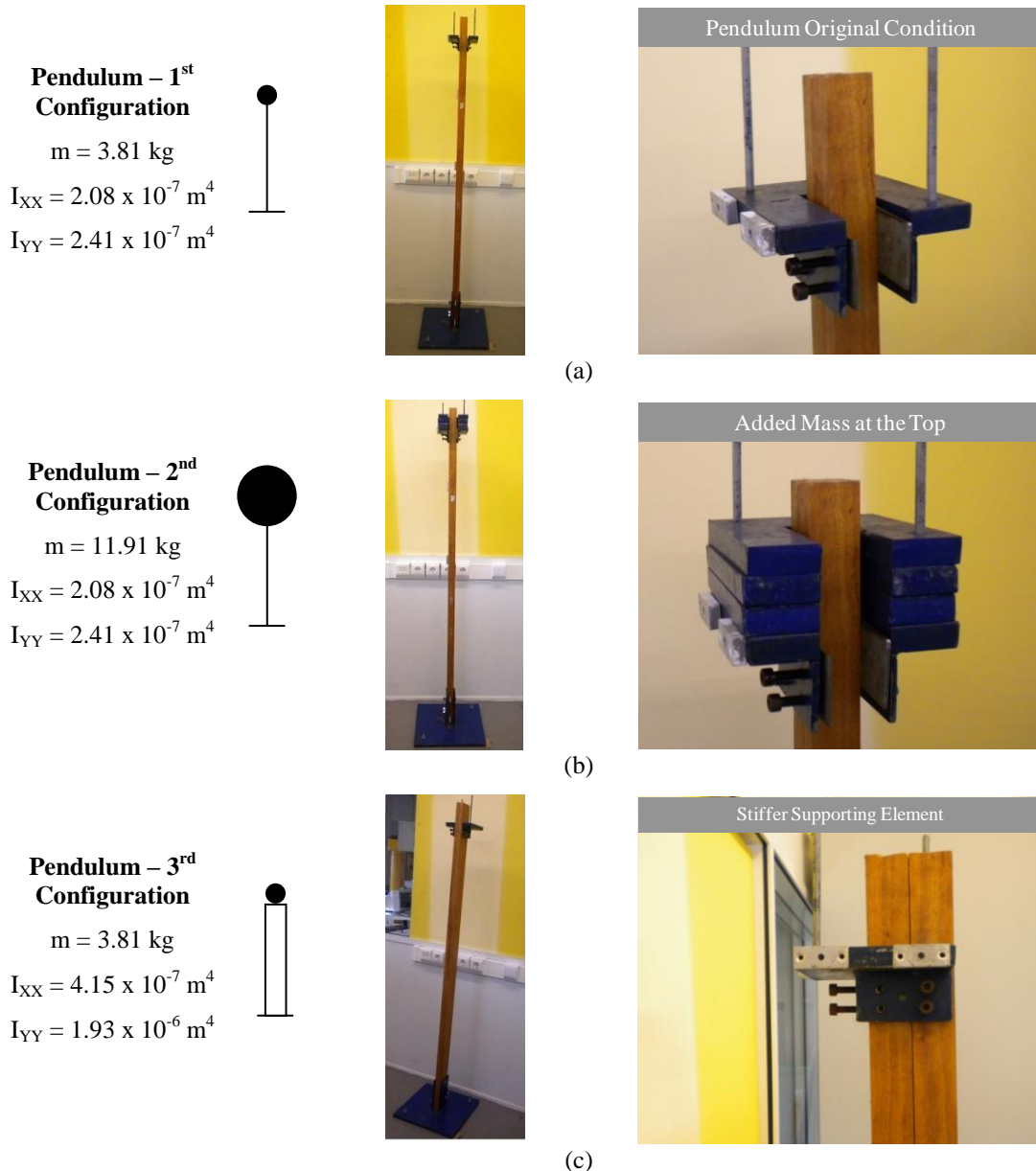


Figure 4.7 – Pendulum configurations for the experimental modal identification tests: (a) 1st configuration considering the pendulum in its original condition; (b) 2nd configuration considering the case of an added mass at the top; and (c) 3rd configuration considering a stiffer supporting element

Using Equation 4.1 and considering the variation of the mass and the variation on the major and minor moment of inertia of the supporting structure, the dynamic response of the pendulum in its different configurations were calculated. The analytical results corresponding to the first two translational modes are shown in Figure 4.8.

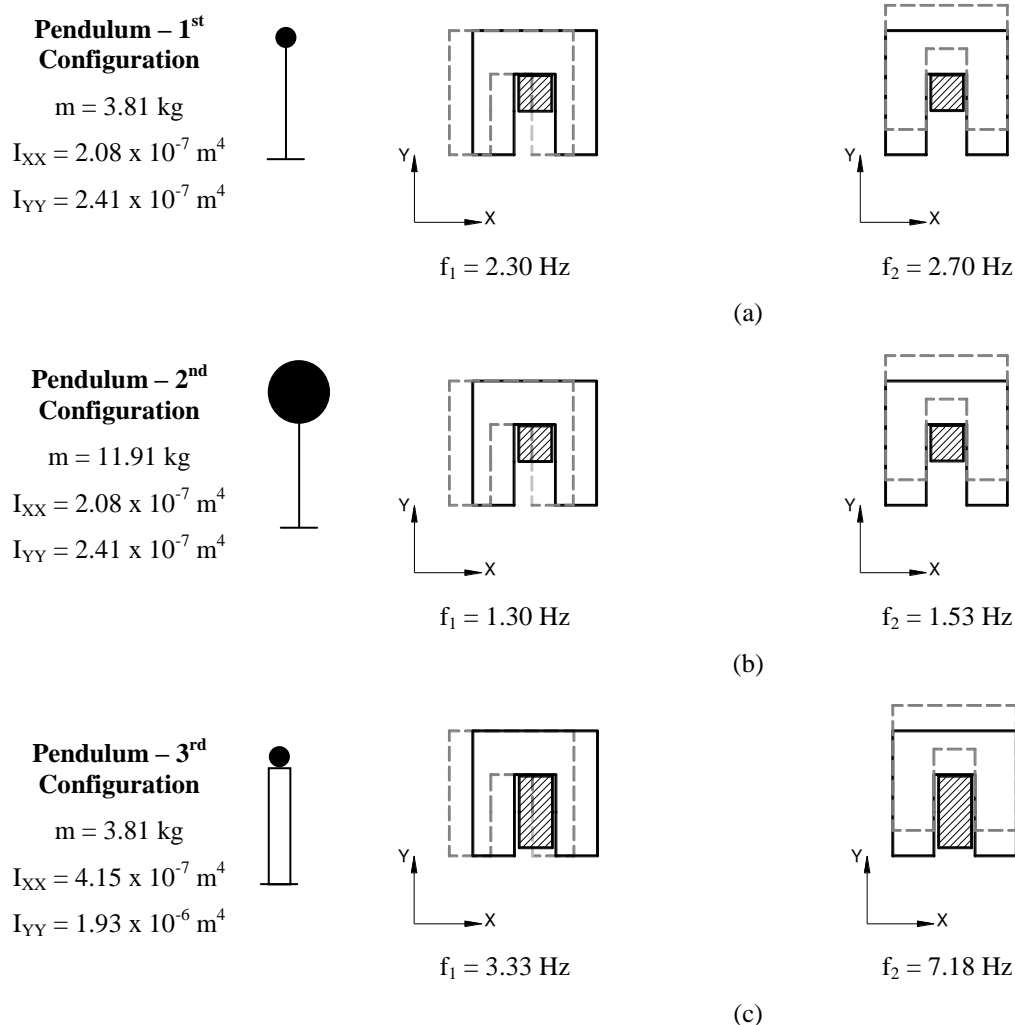


Figure 4.8 – Dynamic response of the inverted pendulum calculated using analytical expressions: (a) 1st Configuration considering the pendulum in its original condition; (b) 2nd Configuration considering an added mass at the top; and (c) 3rd Configuration considering a stiffer supporting element

4.3.2 Time Domain Analysis

The initial time domain analysis was meant to validate the performance of the wireless based platforms in terms of accuracy of their time series record. With this purpose, one conventional accelerometer and one mote were placed at the top of the Pendulum - 1st Configuration to register its response when subjected to an externally applied impulsive force.

As shown in Figure 4.9, the sensors were fixed in the same measurement point recording the response of the pendulum in the X-X direction. For this test, a sampling time of 10 seconds was considered.

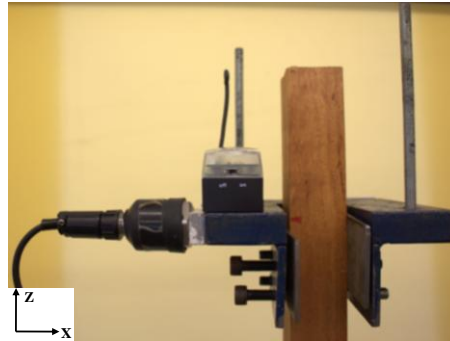


Figure 4.9 – First round of time domain evaluation tests using commercial WSN platforms

An impulsive force was applied to the pendulum five seconds after having started the acquisition process. In Figure 4.10, the time series recordings were split in two zoom windows to observe the effect of the applied force in the response of the evaluated measurement systems. The results of this first test indicate the good performance of the commercial WSN platforms for measuring high amplitude vibrations. However as expected, for signals with amplitudes below 20 mg the WSN platforms recorded only noise due to the low resolution of the microaccelerometers and ADC_s embedded. Note that in this last scenario, it was even possible to observe the digitization lines (see bottom left Figure).

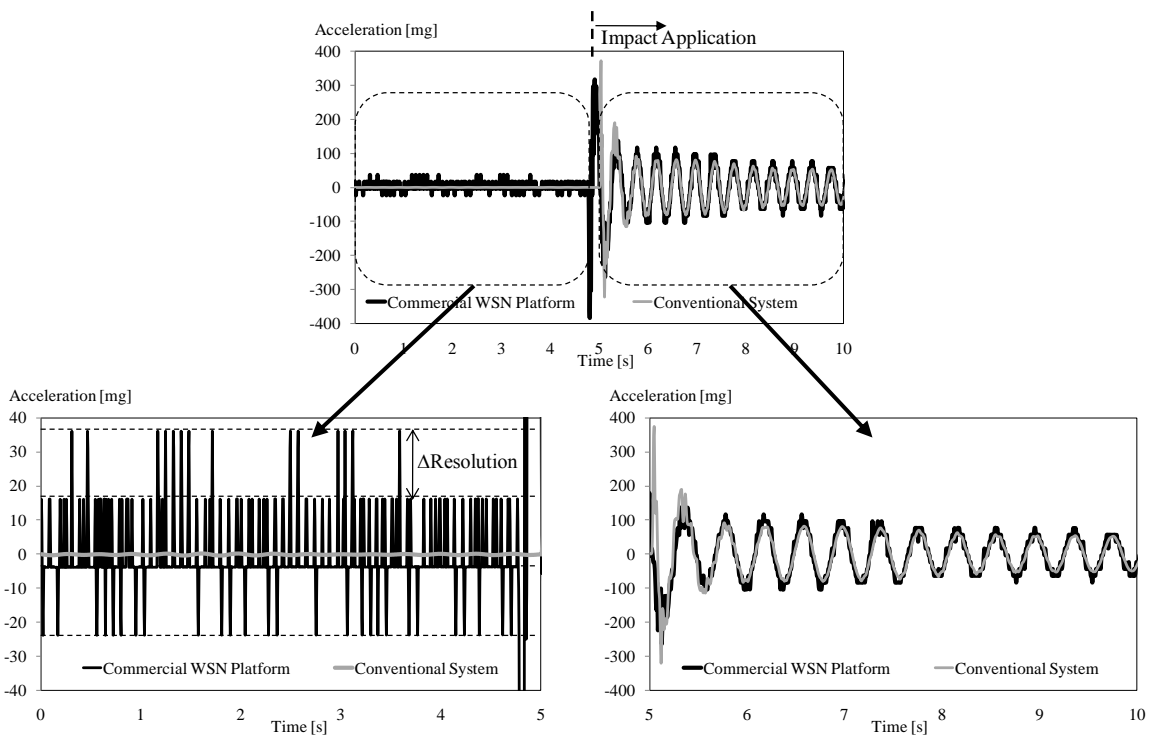


Figure 4.10 – Time series record of the response of the inverted pendulum under an impact force test

The relative errors, defined as the differences between the measurements of the wireless system and the conventional system taking these last as references, were calculated and are presented in Figure 4.11. As it is possible to observe, the effect of the impulsive force in the measurements is clearly evidenced since a sudden decrease of the calculated errors was registered immediately after the application of the force.

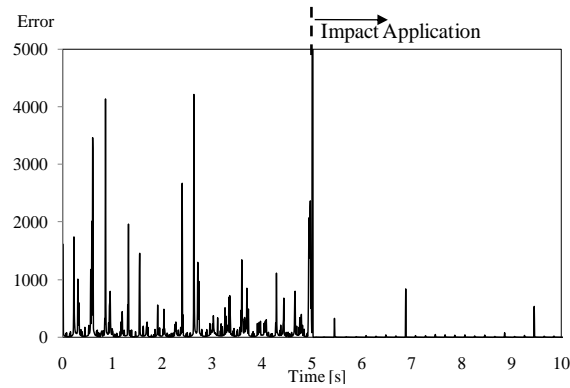


Figure 4.11 – Measurement errors comparison for the impact force test

A second round of time domain evaluation tests were performed to study the accuracy of the wireless systems in longer sampling periods considering again the Pendulum - 1st Configuration. With this purpose, two setups of measurements were carried out considering three conventional wired based accelerometers and three motes. The arrangement of sensors in their respective setup is shown in Figure 4.12. Tests were performed under random impact excitation and under ambient noise. Figure 4.13 shows an example of the recorded signal by mote #3 and by accelerometer #3 in Setup 01 and 02 for each of the considered excitation scenarios.

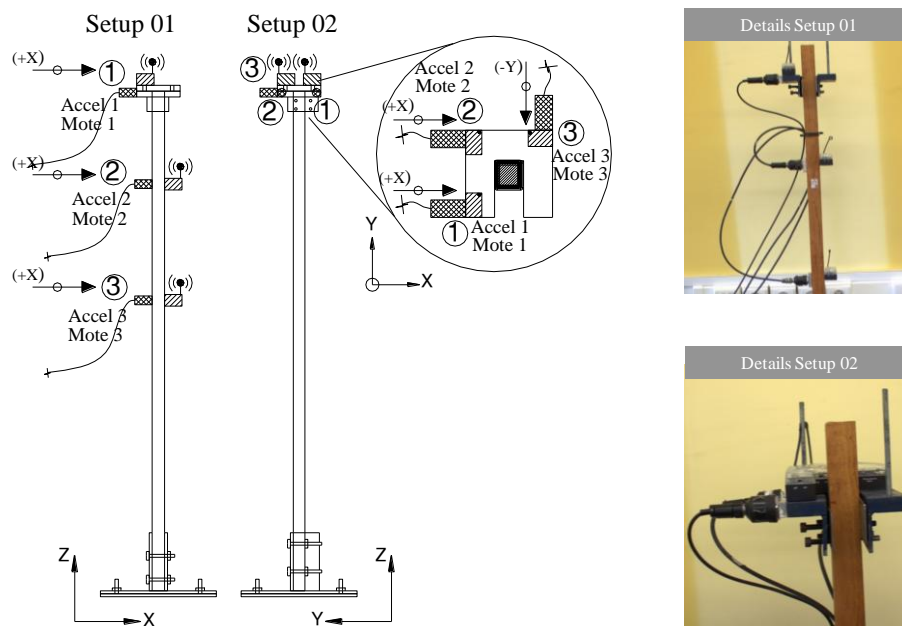


Figure 4.12 – Second round of time domain evaluation tests using commercial WSN platforms

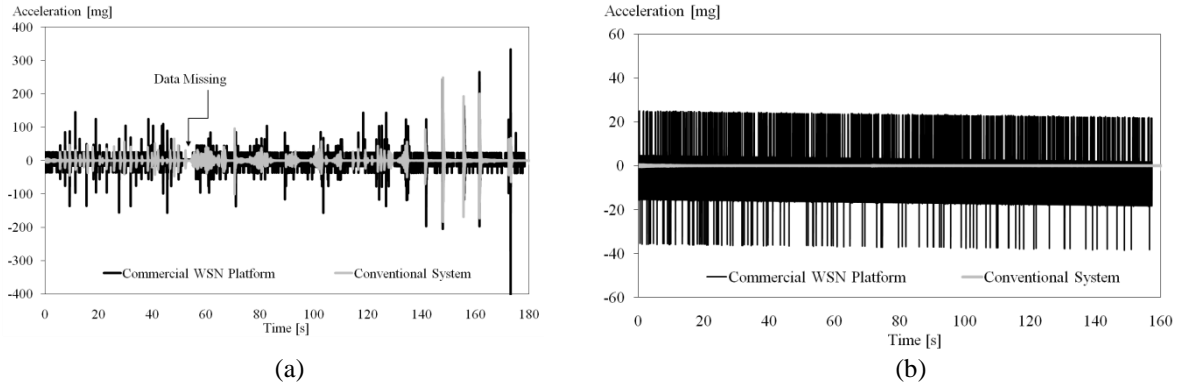


Figure 4.13 – Time series collected by mote # 3 and accelerometer # 3 in the time domain evaluation considering two setups of measurements: (a) response under random excitation in Setup 01 and, (b) response under ambient noise in Setup 02

Table 4.3 and Table 4.4 summarize the statistical results’ comparison of the time series recordings by means of the peak values detected (Max) and Root Mean Squares (RMS). The results of the ambient noise tests evidence again the poor performance of the wireless systems for measuring low amplitude vibrations. In this scenario, in comparison to the values recorded with the conventional platforms, the maximum values and the RMS registered with the wireless platforms had inaccuracies over 1000%. In random excited tests, the maximums and RMS values presented in Table 4.3 confirm the similar response of the conventional and wireless systems which was also evident in Figure 4.13a. As shown in the referred Figure, due to the lack of implementation of communication protocols in the wireless systems, some data was lost in the recorded time series. This fact might influence the subsequent modal analysis process.

Table 4.3 – Time series results of the tests under random excitation considering two setups of measurements.

		Conventional Accelerometer		Wireless Platform		Percent Error Comparison	
		Max (g)	RMS (g)	Max (g)	RMS (g)	Max (%)	RMS (%)
Setup 01	Ch 01	62.50	3.29	199.90	10.23	220	211
	Ch 02	136.10	5.38	353.40	13.53	160	152
	Ch 03	248.50	8.52	456.70	15.26	84	79
Setup 02	Ch 01	36.10	2.20	243.20	13.06	574	494
	Ch 02	15.80	1.35	147.10	12.53	831	828
	Ch 03	27.90	2.20	154.20	13.29	453	504

Table 4.4 – Time series results of the tests under ambient noise considering two setups of measurements.

		Conventional Accelerometer		Wireless Platform		Percent Error Comparison	
		Max (g)	RMS (g)	Max (g)	RMS (g)	Max (%)	RMS (%)
Setup 01	Ch 01	1.30	0.05	39.50	8.50	> 1000	> 1000
	Ch 02	4.50	0.11	35.90	9.40	698	> 1000
	Ch 03	5.60	0.17	36.50	10.50	552	> 1000
Setup 02	Ch 01	0.20	0.02	37.70	8.76	> 1000	> 1000
	Ch 02	0.17	0.02	38.20	8.57	> 1000	> 1000
	Ch 03	0.22	0.02	37.70	8.74	> 1000	> 1000

4.3.3 Frequency Domain Analysis

Considering the Pendulum - 1st Configuration, two analyses were carried out for determining the accuracy of the frequency content of the data recorded with the WSN platforms. As shown in Figure 4.14a, for the first analysis three accelerometers and three motes were placed at the top of the pendulum aiming at evaluating the quality of the resultant spectrums of both systems. For the second analysis, repeatability studies were carried out using only one accelerometer and one mote placed at the top of the pendulum (Figure 4.14b).

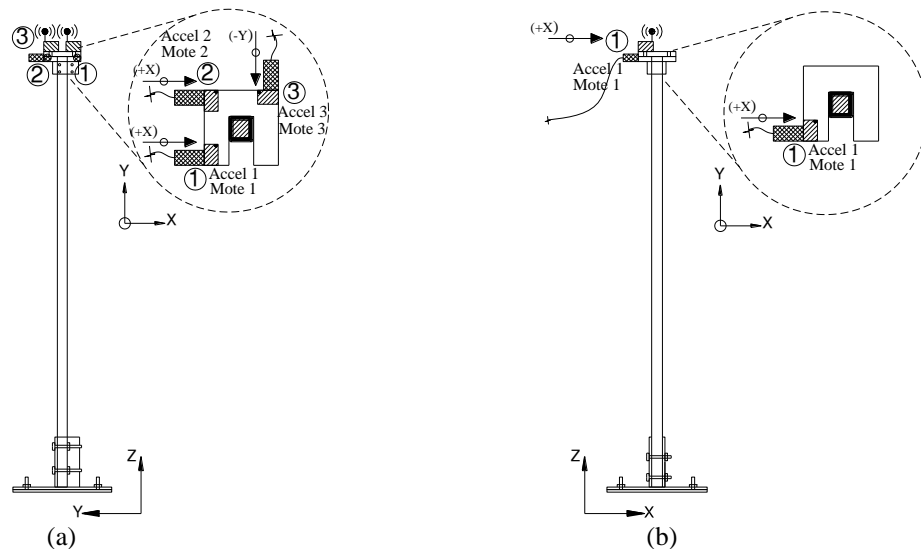


Figure 4.14 – Frequency domain evaluation tests: (a) sensors' deployment for evaluating the quality of the resultant spectrums; and b) sensors' deployment for performing repeatability evaluation tests

In the first analysis, random impact and ambient noise tests with 180 seconds of sampling time were carried out. Figure 4.15 present the resultant Welch spectrums of the data recorded with the evaluated systems, for each of the considered excitation scenarios. Despite the expectable higher noise level of the data recorded with the wireless systems, similar frequency contents were found in both systems in the excited tests. In this scenario,

the presence of two peaks, the first one in the band of 0 Hz-10 Hz and the second one close to the band of 30 Hz, were clearly identified (Figure 4.15a). On the other hand, for ambient noise tests, no peaks could be detected for commercial WSN platforms (Figure 4.15b) since the resultant spectrums showed only noise.

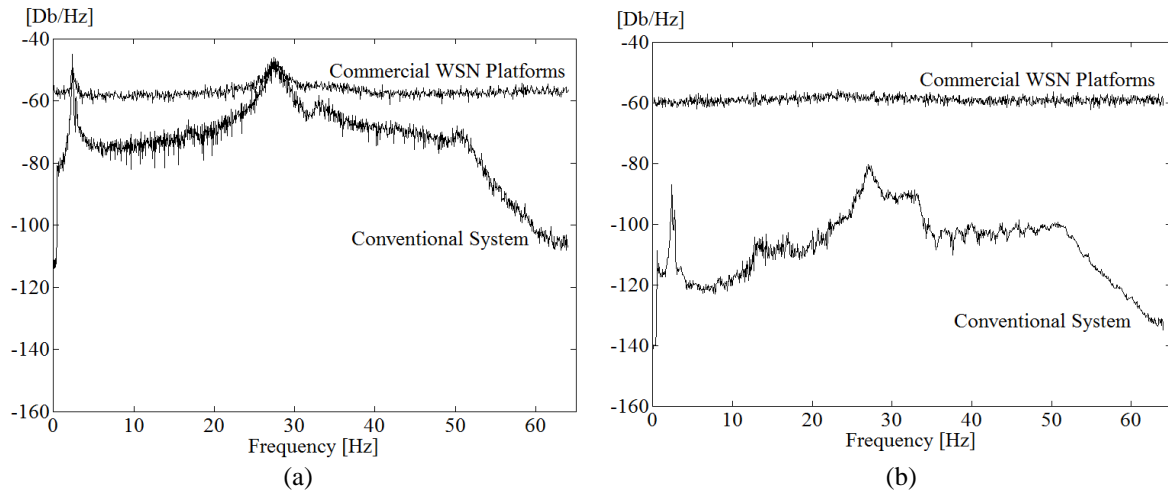


Figure 4.15 – Frequency domain validation tests carried out in the inverted pendulum: (a) random excitation results; and (b) ambient noise results

In this first frequency domain analysis, the data processing stage was performed using the Enhanced Frequency Domain Decomposition method (EFDD) since estimations of frequencies and damping coefficients were of interest. The identified dynamic parameters are shown in Table 4.5. The results of the random excited tests confirmed the high similarity on the estimated frequencies (error of less than 2%) calculated from the measurements of both systems. Moreover, the estimations of the first two mode shapes from the records of the conventional platforms are in accordance with the analytical calculations (2.30 Hz and 2.70 Hz respectively). On the other hand, the limitations of the frequency domain data processing methods were evident in the ambient vibration tests of the wireless systems, since no reliable results could be obtained from the resultant noisy spectrums. With respect to the damping estimations in excited environment, the results of the WSN platform evidenced higher scatter in comparison to the conventional system. Here, note the similarities of the results of the damping coefficients for the conventional systems in both excited and ambient tests, which stress the importance of the sensors' resolution.

Table 4.5 – Frequency domain results from the modal analysis tests in the inverted pendulum.

	Mode	Conventional Sensors		WSN Platforms		Percent Error Comparison	
		f (Hz)	ξ (%)	f (Hz)	ξ (%)	Frequency (%)	Damping (%)
Excited	1	2.36	1.8	2.39	3.5	1.3	94.4
	2	2.74	1.0	----	----	----	----
	3 (**)	16.74	0.7	----	----	----	----
	4 (**)	27.61	2.9	27.58	3.6	0.1	24.1
Ambient	1	2.37	1.8	----	----	----	----
	2	2.76	1.5	----	----	----	----
	3 (**)	16.84	0.7	----	----	----	----
	4 (**)	27.05	2.3	----	----	----	----

* Could not be estimated since the resultant spectrums showed only noise

** Results corresponding to rotational and vertical modes determined only experimentally

The second frequency domain analysis performed was related to the repeatability evaluation of the frequency content of nominally identical 240 seconds sampling time tests performed one immediately after the other. Taking into account the sensors' configuration presented in Figure 4.14b, ten successive experiments were carried out considering again tests under random impacts and environmental noise. In these tests, a modification of the structural configuration was considered by a slight reduction in the effective length of the supporting element. Note that with this modification, the pendulum became stiffer and its theoretical response changed.

Since only the accuracy of the frequency estimations were intended to be evaluated, the data processing stage of the information collected in these tests was performed using the Peak Peaking method. Figure 4.16 presents the average results of the identified frequencies (f) and the standard deviations (σ) of the estimations in each of the excitation scenarios. As it is possible to observe, the results indicate high consistency on the identified first and fourth frequencies from the WSN platforms and conventional accelerometers in excited environments. An important aspect that was noticed in the results of the conventional platforms is that, when ambient vibration tests were carried out, a second frequency that was not notorious in excited condition was identified. This is a clear indicator of the improper application of the excitation in these tests which was unable to excite the pendulum in this frequency. In this excitation scenario, no reliable results from the WSN platforms were obtained since the spectrums showed only noise.

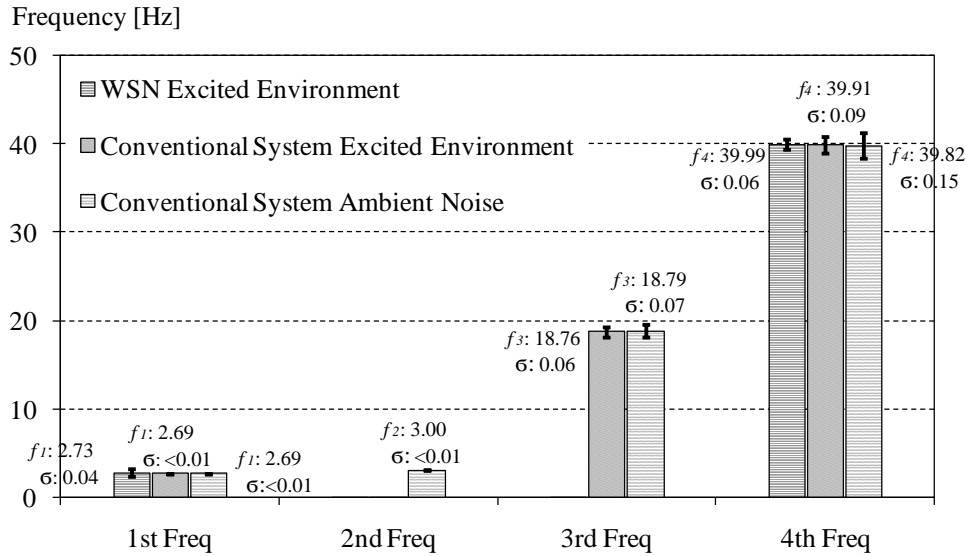


Figure 4.16 – Results of the frequency domain repeatability analysis (Note that the sizes of the bars representing the standard deviation were exaggerated by a factor of 10)

4.3.4 Experimental Modal Identification using Parametric Methods

As shown in the previous analyses, the resultant spectrums from the data recorded with WSN platforms are extremely noisy, which may have direct influence in the accuracy of the results of frequency domain methods. For this reason, a more refined analysis should use parametric modal identification methods since those techniques are independent from the frequency domain resolution.

As mentioned in Chapter 3, the SSI-data method is currently the most used technique for performing experimental modal identification studies and, thus it was the one used in the present work. Using this method, which is implemented in the ARTeMIS extractor software (SVS, 2009), three series of analyses were carried out considering the configurations of the pendulum presented in Figure 4.7. The first modal identification analysis considered a detailed study of the Pendulum - 1st Configuration in two excitation scenarios (random impacts and ambient noise) with 180 seconds sampling time. With this purpose, three accelerometers and three motes were deployed in two setups of measurements (Figure 4.17). The determination of frequencies, damping coefficients and mode shapes was performed by the analysis of the resultant stabilization diagrams shown in Figure 4.18 and Figure 4.19.

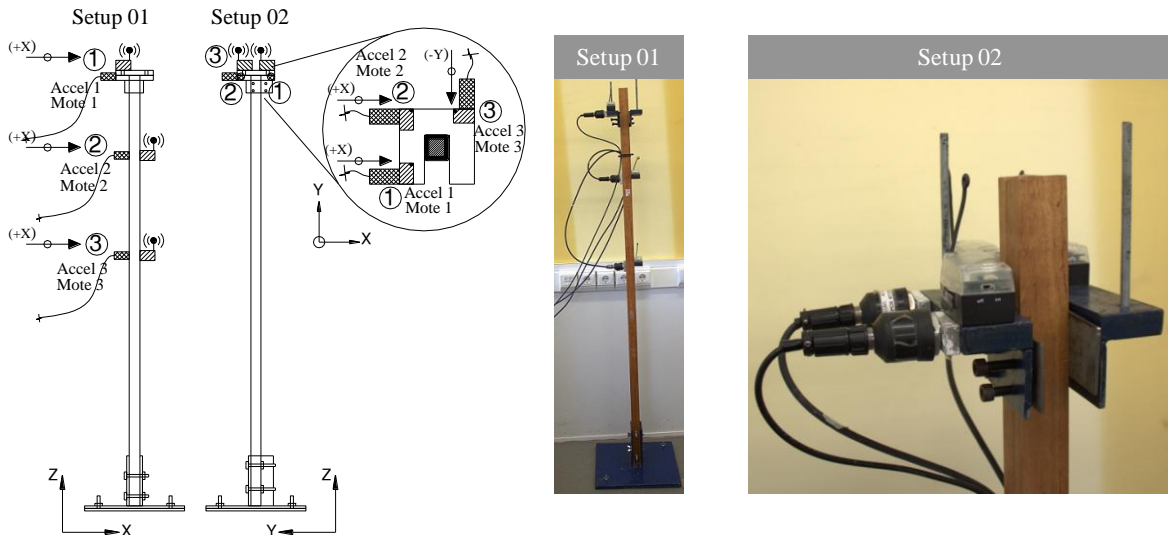


Figure 4.17 – Modal identification tests in the Pendulum - 1st Configuration considering two setups of measurements

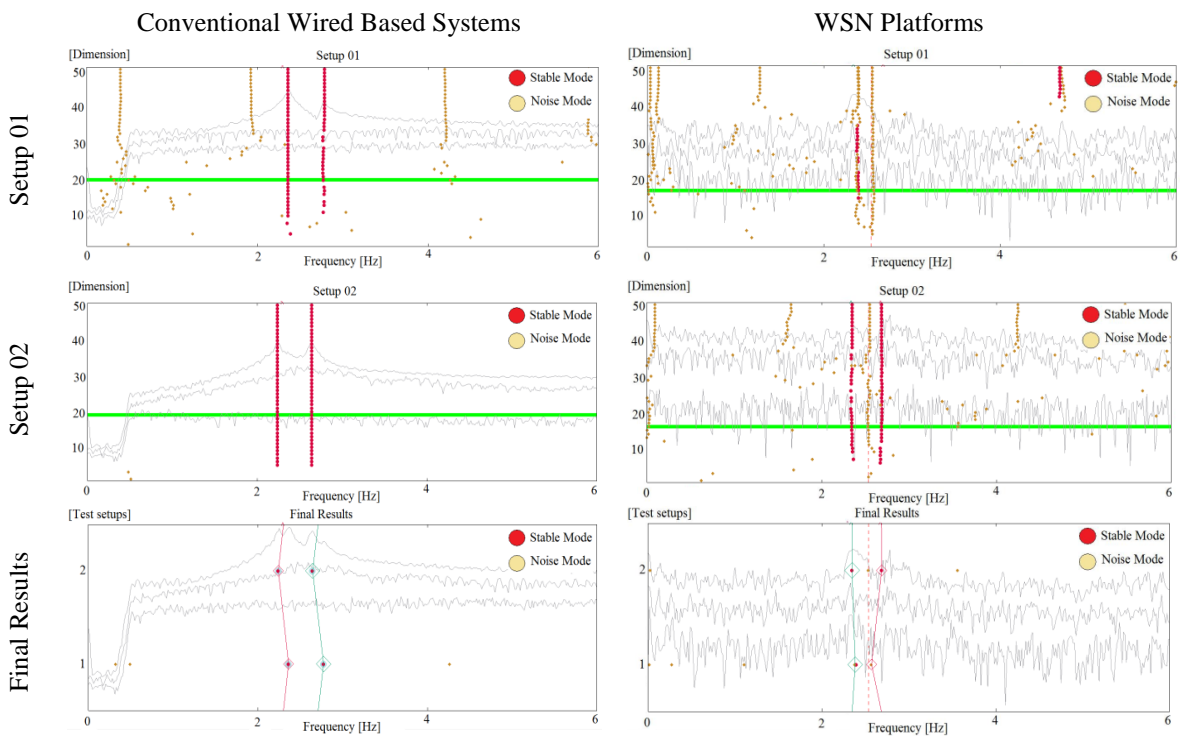


Figure 4.18 – Stabilization diagrams of the modal identification tests considering random excitation in the Pendulum – 1st Configuration

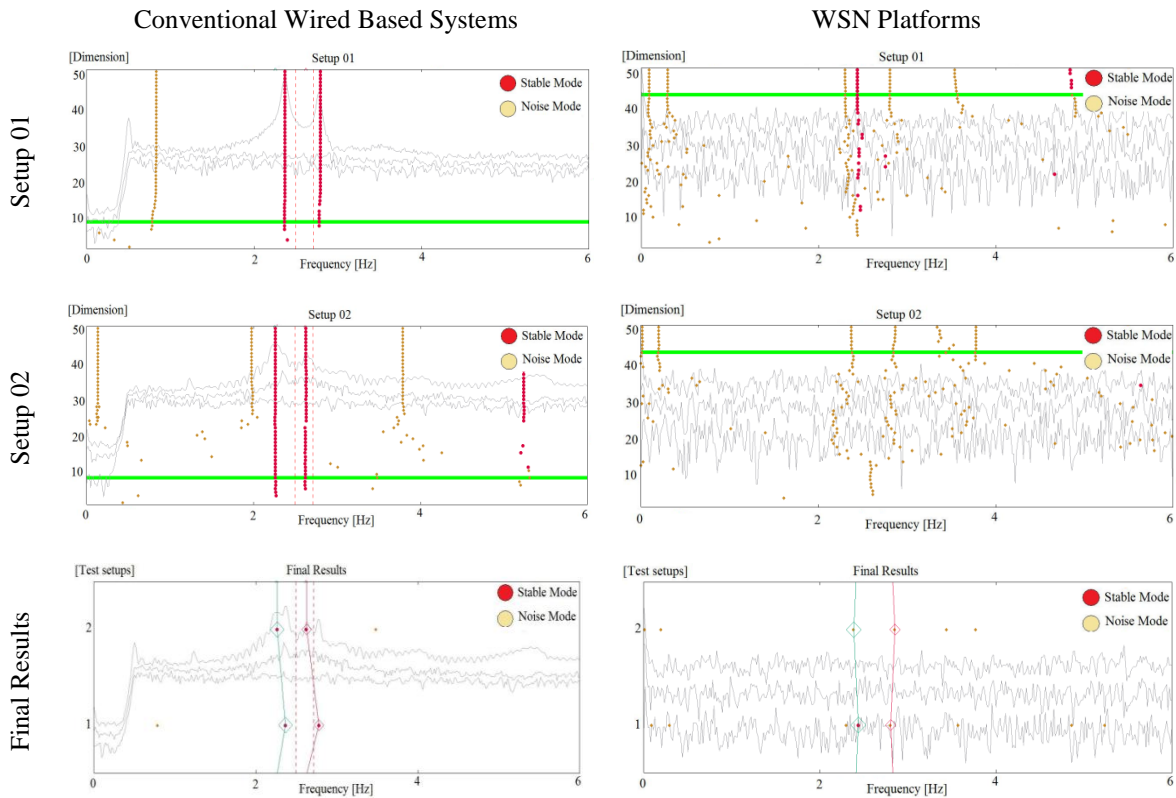


Figure 4.19 – Stabilization diagrams of the modal identification tests considering ambient noise in the Pendulum – 1st Configuration

Hereafter the modal analysis is focused on the identification of the first two translational mode shapes of the pendulum (x - x and y - y) taking into consideration that its theoretical dynamic response was calculated. Table 4.6 summarizes the results of the dynamic response of the studied specimen determined from the data recorded with WSN platforms and conventional accelerometers. The experimental results showed a high degree of similarity in comparison with the theoretical values presented in Figure 4.8a, where the theoretical frequency for the first and second modes read 2.30 Hz and 2.70 Hz, respectively. With respect to the estimated frequencies, the results of both of the evaluated platforms evidenced similarities even for the case of the ambient vibration tests. However, it is important to mention that when the structure was randomly excited, the modal identification task became easier since stables poles appeared aligned in the natural frequencies starting from low model orders. Due to the lack of a synchronization algorithm in the WSN platforms, the results regarding the estimation of mode shapes were not reliable and thus are not shown. The subsequent analyses were performed aiming only at evaluating the accuracy of these platforms for the frequency content.

Table 4.6 – Experimental results of the dynamic response of the Pendulum – 1st Configuration.

Mode	Conv. Accelerometers		Wireless Platforms		Percent Error Comparison		
	f (Hz)	ξ (%)	f (Hz)	ξ (%)	Frequency (%)	Damping (%)	
Excited	1	2.30	1.45	2.35	3.57	2.1	59.4
	2	2.71	1.57	2.68	2.94	1.1	46.6
Ambient	1	2.26	0.82	2.41	9.82	6.2	> 100.0
	2	2.63	2.12	2.83	10.42	7.1	> 100.0

Considering the same excitation scenarios, a second modal identification analysis was carried out for assessing the performance of the WSN platforms in structures with longer period. For this purpose, random excited and ambient noise tests were performed using three conventional accelerometers and three motes displayed along the height of the Pendulum – 2nd Configuration and considering 180 seconds for the sampling time. The details of this analysis are shown in Figure 4.20.

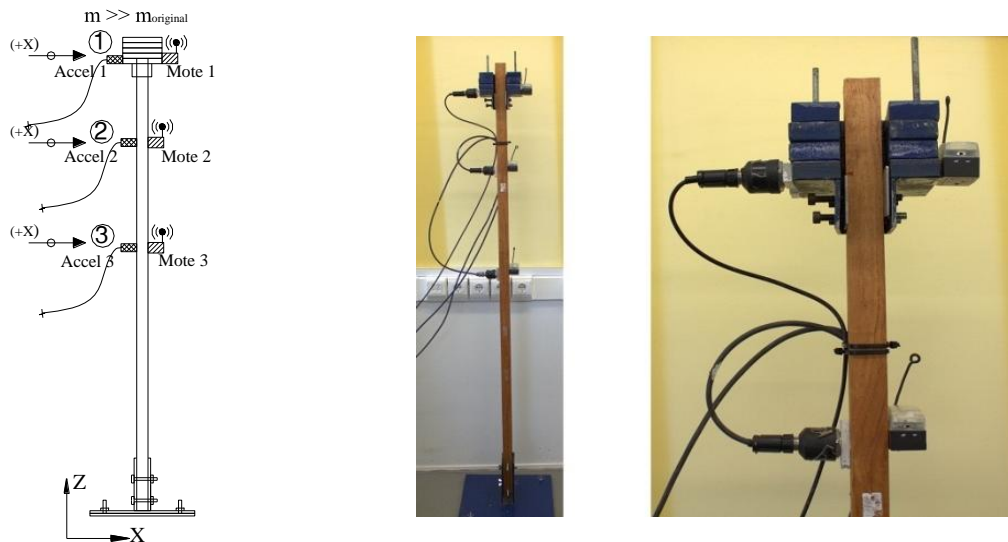
Figure 4.20 – Modal identification tests in the pendulum – 2nd Configuration

Figure 4.21 shows the stabilization diagrams resulting from the time series recorded in this second modal identification analysis under random excitation and under ambient noise while Table 4.7 summarizes the experimental modal identification results. These results confirm that acceptable estimations of frequencies can be obtained using the wireless systems since errors of less than 6% were detected. However, in case of ambient noise environments, the stabilization diagrams were full of spurious modes that complicated the identification task and negatively affected the reliability on the estimations. In this ambient noise scenario, only the second frequency could be identified. It should be noted that the frequencies estimated from the measurements of the conventional and the wireless systems

are in good agreement with the theoretical results of 1.30 Hz and 1.53 Hz for the first two modes.

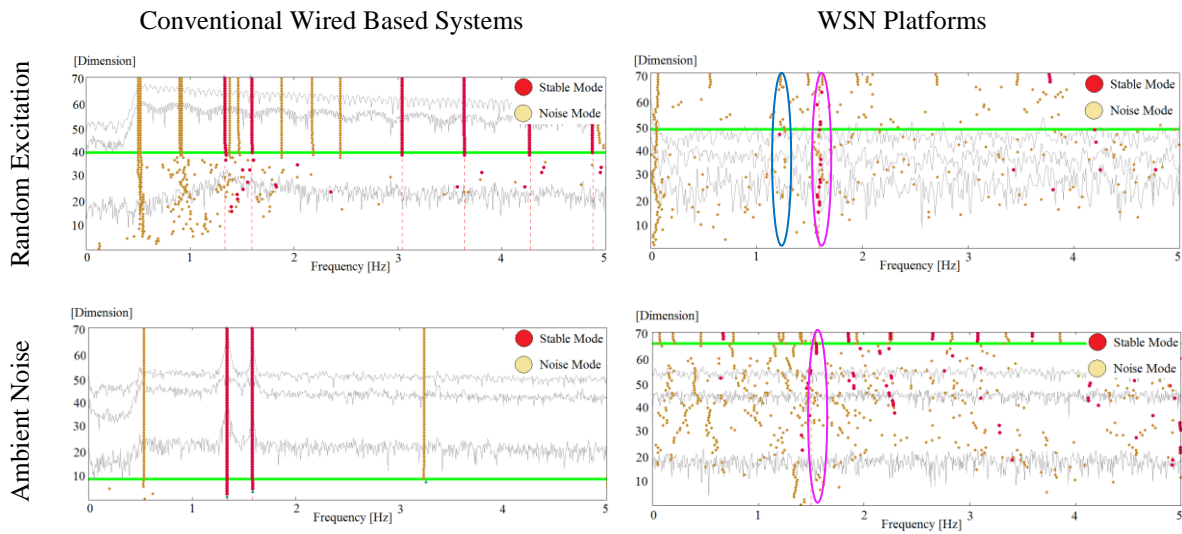


Figure 4.21 – Stabilization diagrams of the modal identification tests in the Pendulum – 2nd Configuration

Table 4.7 – Experimental results of the dynamic response of the Pendulum – 2nd Configuration.

	Mode	Conv. Accelerometers		Wireless Platforms		Percent Error Comparison	
		f (Hz)	ξ (%)	f (Hz)	ξ (%)	Frequency (%)	Damping (%)
Excited	1	1.34	3.74	1.27	6.77	5.5	44.8
	2	1.60	3.05	1.59	4.07	0.6	25.1
Ambient	1	1.34	1.11	----*	----*	----	----
	2	1.58	1.06	1.55	3.03	1.9	65.0

* Could not be reliably estimated since the correspondent stabilization diagram showed only spurious modes

For the third modal identification analysis, the performance of the WSN platforms was verified in stiffer structures. For this purpose, the experimental modal identification of the Pendulum – 3rd Configuration was considered using 180 seconds sampling time tests, under random and ambient excitation scenarios. As shown in Figure 4.22, three conventional accelerometers and three modes were distributed again along the height of the pendulum to record its dynamic response.

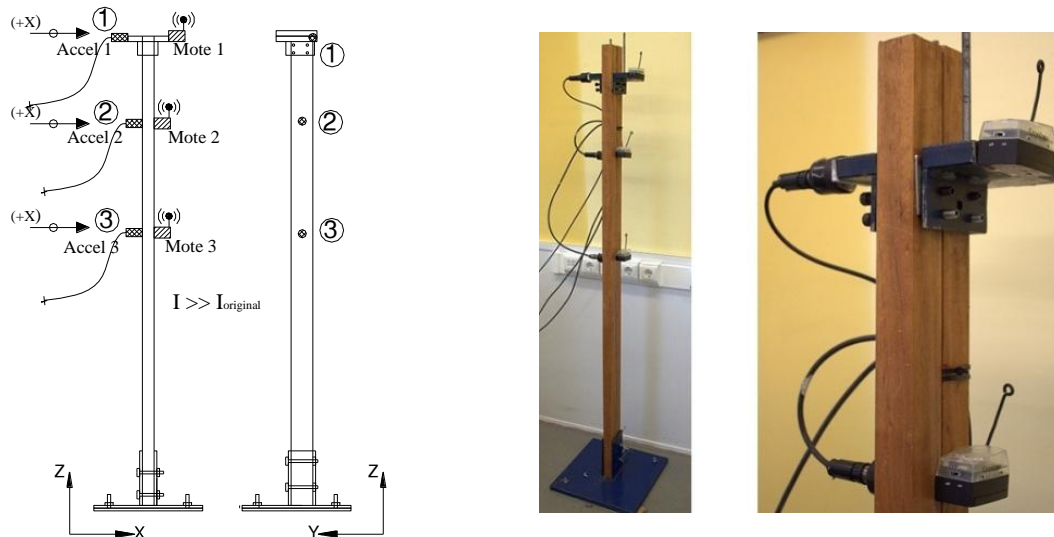


Figure 4.22 – Modal identification tests in the pendulum – 3rd Test Configuration

Figure 4.23 shows the stabilization diagrams and Table 4.8 summarizes the results from both type of monitoring systems in each of the considered excitation scenarios. The results of the WSN platforms present an interesting tendency which directly relates the increase of the stiffness of the structures with the complexity of the modal identification task (this last indicator defined as the quantity of spurious modes in the stabilization diagrams). This relation is surely related to the low resolution of the embedded MEMS microaccelerometers since similar levels of excitation produce smaller amplitude vibrations in shorter period structures which are outside the platform's measurement range. Besides the identified first natural frequencies be in concordance with the analytical results of 3.33 Hz, another relevant aspect was the impossibility to detect the second mode of vibration which, according to the analytical solution (see Figure 4.8c), must be around 7.18 Hz.

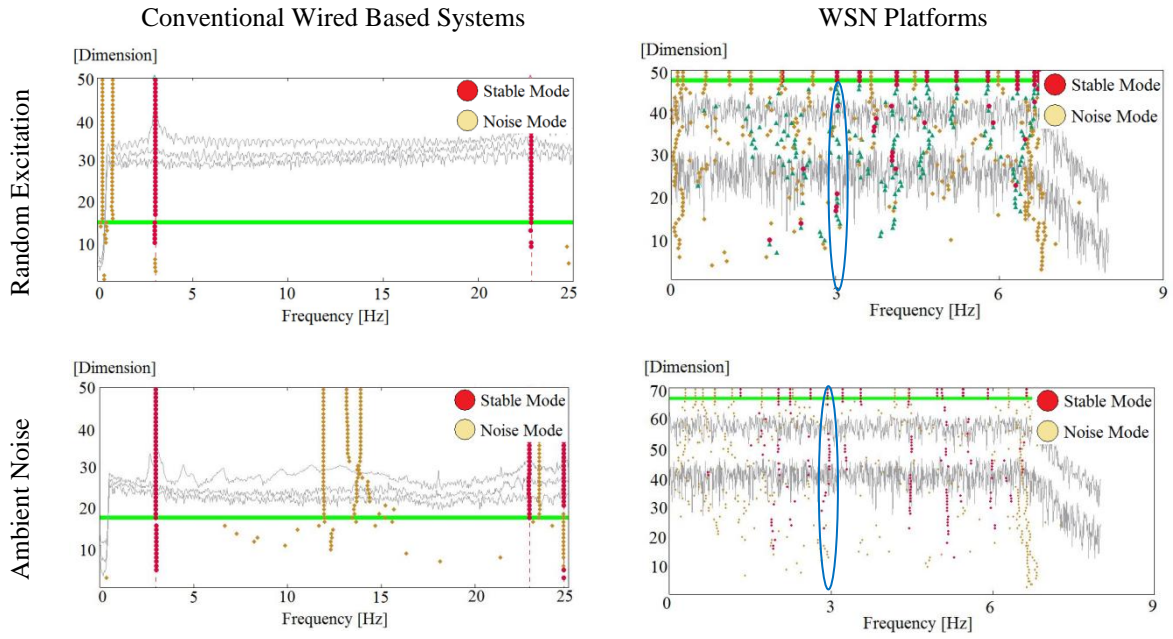


Figure 4.23 – Stabilization diagrams of the modal identification tests in the Pendulum – 3rd Configuration

Table 4.8 – Experimental results of the dynamic response of the Pendulum – 3rd Configuration.

Mode	Conv. Accelerometers		Wireless Platforms		Percent Error Comparison		
	f (Hz)	ξ (%)	f (Hz)	ξ (%)	Frequency (%)	Damping (%)	
Excited	1	3.04	3.11	3.04	2.25	< 0.01	38.2
Ambient	1	3.00	2.74	2.93	2.65	2.4	3.4

4.4 Experimental Modal Identification Tests: Field Case Applications

To evaluate the performance of the commercial off-the-shelf WSN platforms in real field studies, one of the original 15th Century chimneys at the Paço dos Duques Building located in Guimarães, North of Portugal was selected for carrying out experimental modal identification tests.

4.4.1 Description of the Building and Analytical Solution for the Chimney

The Paço dos Duques Palace was built between 1422 and 1433 by D. Afonso (son of the King of Portugal D. João I). At the beginning, the building was used as residence of the “Duques de Bragança” and later, from 1480 to 1807, was inhabited (Azevedo, 1964). In 1807 the building was used as barracks and in 1888 the Architectural and Archeological Portuguese Society catalogued it as a historical monument (Silva, 1974).

The monument was re-built and completed in 1937, when new structural elements were introduced and gave the impressive character to the building. Figure 4.24 shows some views of the original and present condition. As shown in this Figure, one of the most important changes occurred in the intervention of 1937 was the addition of 34 new chimneys on the roof of the building.

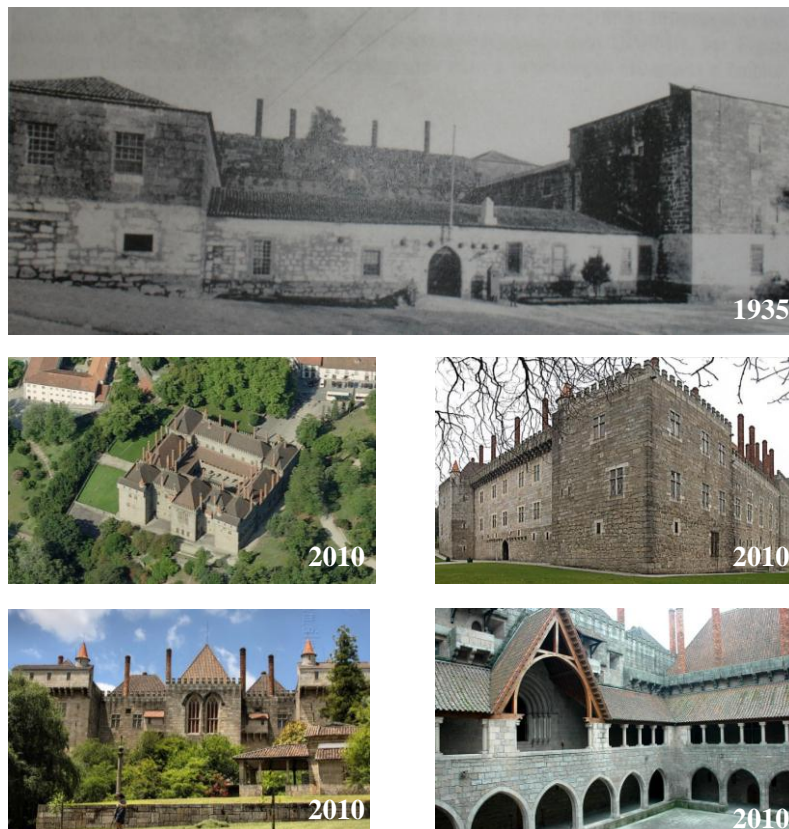


Figure 4.24 – Paço dos Duques Building

From 2002 to 2009, conservation works were carried out due to the damage in the chimneys and the deficient condition of the roof. The present work used commercial WSN platforms for performing experimental modal identification tests in one of the four original chimneys. Figure 4.25 shows a general view of the chimneys on the roof of the building as well as the scaffolding of the conservation works.



Figure 4.25 – Chimneys at Paço dos Duques building: (a) general view; and (b) conservation works

In the modal identification tests carried out, three conventional accelerometers were placed at the top of the chimneys measuring a single node in a triaxial configuration. Due to the feasibility of placing the nodes directly in contact with the structure, two WSN platforms were placed as close as possible to the top of the chimney for measuring perpendicular directions. Figure 4.26 shows the sensors' arrangement in the tests.



Figure 4.26 – Modal identification tests in the Chimneys at Paço dos Duques building: (a) conventional accelerometers' arrangement; and (b) WSN platforms' arrangement

The advantages of using WSN platforms were evident in this case study. In addition to the lower cost, the fact that the wireless platforms are lighter in comparison to the conventional accelerometers allowed an easier placement on the surface of the chimneys. The DAQ process also benefitted from safer and faster works in a difficult zone such as the roof of the building. The analytical dynamic response of this structure was determined considering a cantilever beam with distributed mass along its height. The natural

frequencies of the system are calculated according to Equation 4.2, given by Clough and Penzien (2003).

$$f = \frac{1}{2\pi} (\beta)_n^2 \sqrt{\frac{EI}{\bar{m}h^4}} \quad \text{Equation 4.2}$$

where f denotes the natural frequency in [Hz], β is a constant related to each of the n frequencies of interest, E the elasticity modulus in [Pa], I the inertia moment in [m⁴], \bar{m} the distributed mass per unit length in [kg/m], and h the height of the system in [m].

Using Equation 4.2, the first four analytical frequencies of the chimney were determined. For the calculations, the characteristics of the geometry and materials were adopted from Ramos and Lourenço (2002), while a conservative value of 1.0 GPa was considered for the Elasticity Modulus of the masonry according to the recommendations of Tomazevic (1999). Figure 4.27 show the results of this analytical study and the parameters considered for the calculations.

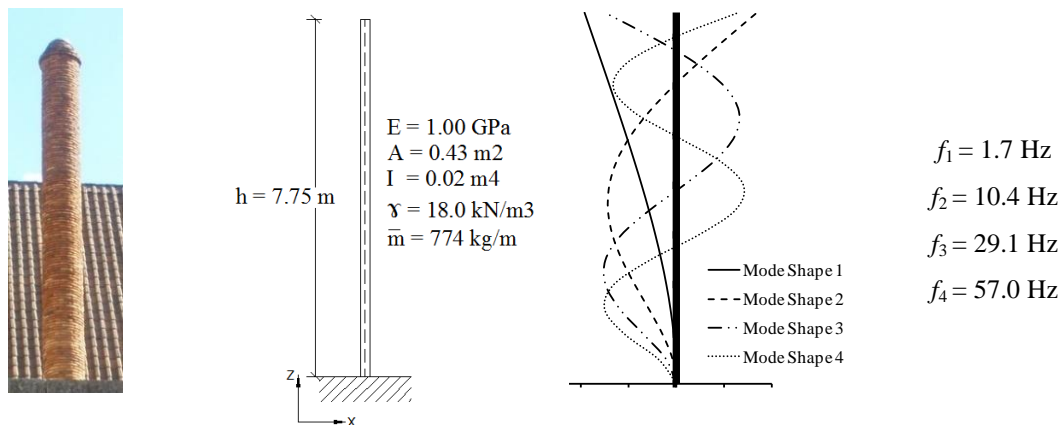


Figure 4.27 – Analytical modal identification of the Chimneys at Paço dos Duques building

4.4.2 Time and Frequency Domain Analysis

For the modal identification tests carried out in the chimney, two excitation scenarios were considered: random impacts and environmental noise. Figure 4.28 and Figure 4.29 show the time series recorded with the conventional and WSN platforms as well as the resultant averaged normalized frequency domain spectrums in each of the excitation scenarios. Note that for gaining resolution at lower frequencies, the data processing of the acquired data was carried out using a decimation factor of 4.0. The results of the time domain series showed high levels of excitation even in the ambient noise tests. This high level of noise was produced by the conservation works that were being performed at the

moment in which the modal identification tests were carried out. However, it is important to stress that even in the random excited case the excitation level was below the resolution limit of the wireless platforms. With respect to the frequency domain analysis, the results showed that the spectrums from the WSN platforms presented similar high levels of noise in both excitation scenarios with a sharp peak, close to the band of 2.0 Hz, in the excited case study. The quantity of noise in the spectrums may have a negative influence in the accuracy of the modal estimations if the frequency domain data processing methods would be used and, thus the modal identification task was only performed using the parametric methods.

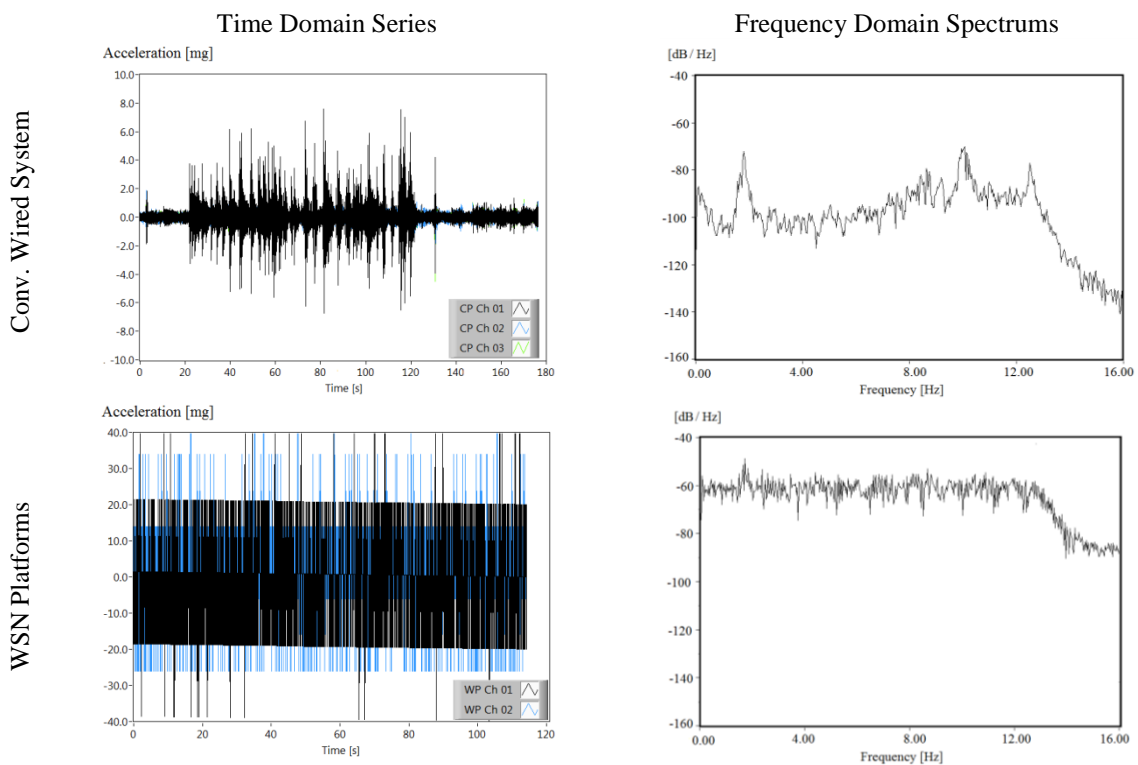


Figure 4.28 – Time domain series and resultant frequency domain spectrums from the modal identification of the Chimney at Paço dos Duques building – Random excited tests

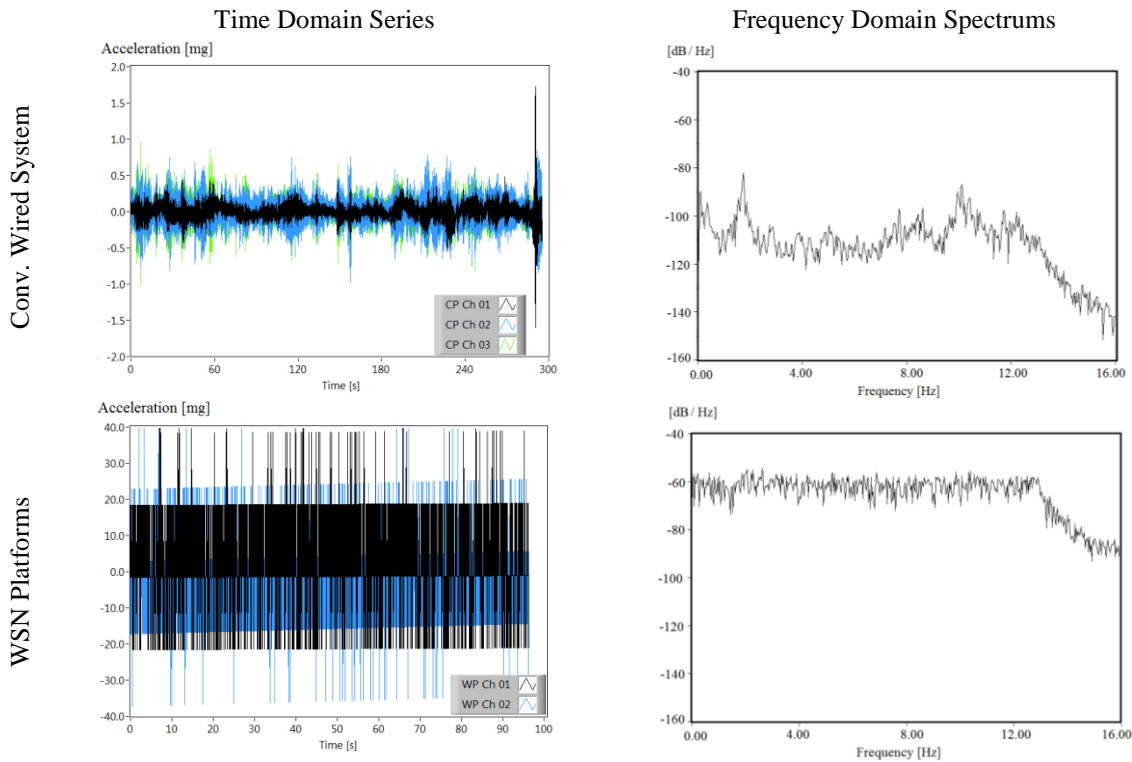


Figure 4.29 – Time domain series and resultant frequency domain spectrums from the modal identification of the Chimney at Paço dos Duques building – Environmental noise tests

4.4.3 Experimental Modal Identification Using Parametric Methods

The SSI-data method was again used for processing the time domain series recorded with both of the studied platforms. The resultant stabilization diagrams of the tests are presented in Figure 4.30. Table 4.9 shows the results of the modal identification process with the estimated frequencies and damping ratios from the data recorded. These results confirm the acceptable performance of the commercial wireless platforms (frequency differences with a maximum of 5%) in high excitation tests such as those performed in this study. As observed, an asymmetry in the cross section of the chimney was detected since two pairs of frequencies corresponding to the first and second modes were identified. Moreover, the results evidenced high correspondence with the first two analytical frequencies (1.7 Hz and 10.4 Hz) calculated using theoretical expressions (Figure 4.27). Due to the large amount of spurious modes in the stabilization diagrams of the wireless systems, only reliable estimations of the first pair of frequencies were obtained from the records of these systems. The results regarding the mode shapes of the chimney were not taken into account since the WSN platforms do not have synchronization possibility.

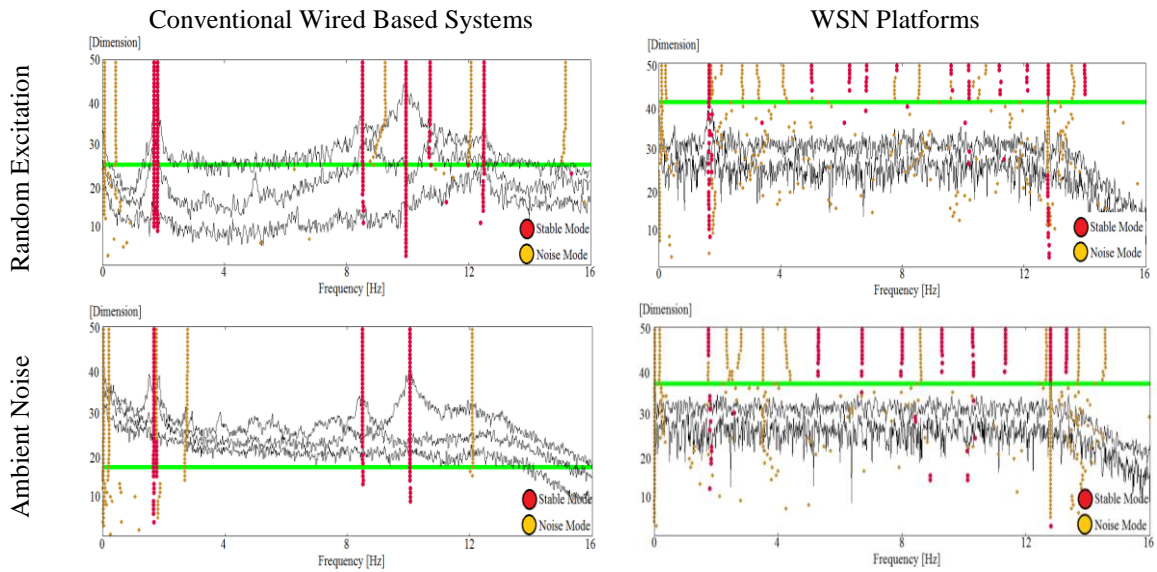


Figure 4.30 – Stabilization diagrams of the analysis of the tests performed under random excitation and ambient noise in the chimney at Paço dos Duques building

Table 4.9 – Dynamic response of the studied Chimney at Paço dos Duques building.

	Mode	Conv. Accelerometers		Wireless Platforms		Percent Error Comparison	
		f (Hz)	ξ (%)	f (Hz)	ξ (%)	Frequency (%)	Damping (%)
Excited	1	1.71	1.16	1.66	2.94	2.9	> 100.0
	1'	1.82	1.45	1.75	2.28	3.9	57.2
	2	8.54	1.95	----*	----*	----	----
	2'	9.95	1.33	----*	----*	----	----
Ambient	1	1.69	1.34	1.77	4.20	4.7	> 100.0
	1'	1.77	4.22	1.84	1.74	4.0	58.8
	2	8.51	1.74	----*	----*	----	----
	2'	10.06	0.81	----*	----*	----	----

* Could not be reliable estimated since the correspondent stabilization diagram showed only spurious modes

4.5 Conclusions

In this chapter, the advantages and limitations of commercial WSN technology for OMA of civil engineering structures were explored. One of the off-the-shelf WSN platform commercialized by Crossbow was selected since it includes not only environmental measurement sensors (humidity, temperature, pressure and light meters) but also microaccelerometers embedded in their measurement boards.

On the other hand, University of Minho has a broad expertise on the use of conventional piezoelectric accelerometers wired to DAQ stations for dynamic monitoring. Due to this reason, these conventional systems were considered as a reference for comparing the performance of the commercial WSN in modal identification tests.

With these considerations, OMA tests were performed in laboratory and field tests using similar DAQ configurations for the two considered monitoring systems. In the tests three aspects were evaluated: accuracy in the time series recordings, accuracy in the frequency domain results and accuracy in the modal identification task. For the case of the time series recordings, the results showed that in environments with high amplitude excitations sources (signals with amplitudes above 20 mg), the use of commercial wireless platforms is possible. However, the lack of synchronization and the data loss during communication between motes represent serious limitations that should be taken into consideration for their application in real studies. With respect to the frequency domain results, it was detected that the resultant spectrums of the data recorded with WSN platforms exhibits higher levels of noise in comparison to what was obtained with the conventional platforms. Despite this, the results of the tests carried out showed that if the systems would be properly excited, the natural frequencies would be feasible to be detected with a small error (lower than 7.5%). Aiming at gaining reliability in the modal identification process, this task was performed using the SSI-data method. Acceptable results were obtained with the use of the commercial wireless platforms in excited environments since clear stabilization diagrams with stable poles properly aligned in the natural frequencies were evidenced.

The advantages of using WSN platforms were also verified specially in the field tests. Faster sensor's deployment times can be achieved in real studies where the problems of the cables itself and their long lengths are evident. Safer placement of the sensors was also verified, reducing the risk in site works.

In conclusion, the results of the performed tests showed that the commercial versions of the WSN platforms are not fully suitable for properly identifying the dynamic properties of civil engineering structures. This fact is mainly due to three reasons: 1) low resolution of the embedded microaccelerometers; 2) low resolution of the embedded ADCs; and 3) lack of adequate communication protocols. Finally, note that the problems related to the energy consumption were not considered since the use of these platforms for long term monitoring was outside the scope of this work.

CHAPTER 5

New WSN Platform for Operational Modal Analysis of Civil Structures

Abstract

This chapter presents a prototype system of Wireless Sensor Network (WSN) platform specially developed for carrying out Operational Modal Analysis of civil engineering structures. This prototype combined up to date MEMS accelerometers and communication technologies, which resulted in an attractive solution when compared with the conventional wired based transducers.

With the developed prototype, numerous validation tests were performed. The estimated frequencies, damping coefficients and mode shapes in these tests showed that reliable measurements can be obtained, evidencing the adequacy of the developed system for practical purposes.

It was also observed that the main drawback of the developed solution is the time consuming data transmission process. The last part of this chapter was precisely dedicated to the exploration of a theoretical approach for overcoming this inconvenient. According to the numerical validation results, a solution might be achievable with a remote and decentralized procedure based on the application of the averaged Fast Fourier Transform (FFT) to the collected data.

5.1 Introduction

One of the main objectives of the present work was to study the recent progresses on wireless technology and Micro-Electro-Mechanical-Systems (MEMS) in order to explore their possible inclusion in the Operational Modal Analysis (OMA) schemes for existent masonry structures. From previous experiences on OMA procedures in this type of structures, a main difficulty was observed related to the low levels of excitation registered in the experimental tests as a consequence of the high stiffness associated to these buildings. Therefore, if OMA tests are planned to be carried out in these structures, the characteristics of the measurement transducers and Data Acquisition (DAQ) equipments should be carefully chosen.

In Chapter 4, several cases studies were presented for assessing the performance of the off-the-shelf technology on WSN platforms in OMA tests of civil engineering structures. Once the limitations of those platforms were identified, the work focused on the development of a new WSN platform considering: a) inclusion of high sensitivity MEMS accelerometers; b) designing of DAQ boards with high resolution Analog Digital Converters (ADCs); c) development of network software which must assure high reliability on the data communication process; d) development of a command and configuration application; and e) development of a data collection and storage software. This chapter presents a prototype WSN system which has been jointly conceived by a team of electronic, computer and civil engineers (joint collaboration project between CISTER/ISEP and ISISE/UM). This system is the product of a combination of the last technology on high resolution MEMS accelerometers and the state of the art of communication technologies that are required to fulfil the demanding requirements of the experimental modal analyses in existent civil engineering structures.

The following sections contain the characteristics and specifications of the developed solution as well as a comprehensive discussion of the results of validation tests that were carried out.

5.2 Description of the Developed Prototype of WSN Platform

Based in the experience gained on performing OMA in civil engineering structures using conventional and commercial off-the-shelf wireless sensors, the minimum requirements that the new WSN platform must fulfill were defined. According to this, the maximum frequency response range of the system was defined to be from 0 Hz to 100 Hz and the maximum sampling frequency to be of 200 Hz. Moreover, the maximum sampling drift must be lower than 5 ms and no samples should be lost during the acquisition and communication process. With respect to the measurement sensors, it was decided that triaxial MEMS accelerometers with a maximum measurement range of $\pm 1g$, typical resolution of 1 mg and maximum resolution of 0.1 mg must be included. In the case of the DAQ board, this must include an ADC with at least 16 bits of resolution.

As explained in Chapter 2, a WSN system can be understood as composed by two parts: the measurement units and the base station (a third part is not considered, the remote connection system, since traditional technology is used for this purpose). The prototype of the WSN platform developed in this work also matches with the mentioned definition following the system architecture presented in Figure 5.1.

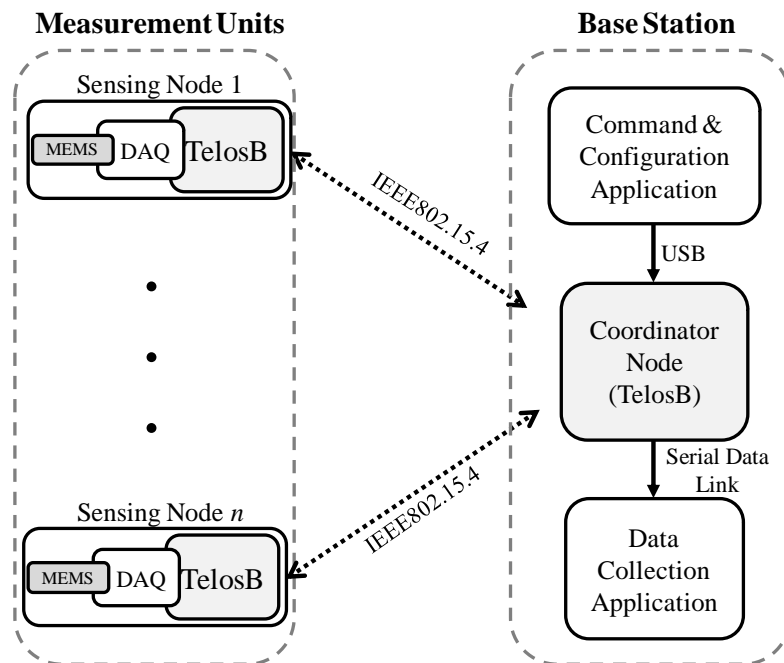


Figure 5.1 – Overview of the system architecture of the developed WSN platform

In the developed WSN, the wireless communication module in the measurement units and the base station was composed by TelosB platforms (Crossbow, 2009) working in the radio frequency range of 2.40/2.48 GHz. These hardware platforms feature an 8MHz TI MSP430 16-bit microcontroller, a CC2420 RF transceiver (IEEE 802.15.4 compliant), 48 kB of Program memory (in-system reprogrammable flash), 16 kB of EEPROM, and UART communication ports. They also include on-board light, temperature and humidity sensors, whose implementation was outside the scope of this work but; which might be useful in future developments for static SHM applications.

As shown in Figure 5.2, each measurement unit was composed by one TelosB platform, one DAQ board and one MEMS accelerometer.

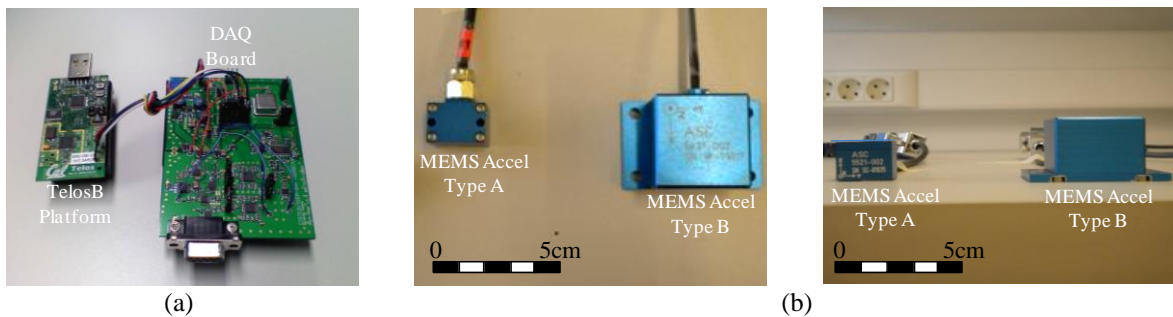


Figure 5.2 – Measurement unit: (a) TelosB communication platform and DAQ board; and (b) two options of MEMS accelerometers considered in this work

The DAQ board was conceived for supporting a high resolution 24 bit ADC and a 32 MB serial flash memory for storing data samples. Both the ADC and the flash memory are managed by an 8 bits microcontroller (which also handles and pre-formats the acquired ADC samples) and accommodated an analogue 8th order Butterworth filter (to avoid undesired aliasing effects). The energy regulation and management circuitry is supplied from a set of four AA size batteries.

From the commercial available solutions of MEMS accelerometers; two different types of capacitive triaxial transducers with a measurement range of $\pm 2g$ were selected. The first one was the model ASC 5521-002 (called in this work as MEMS sensor Type A) and the second one the ASC 5631-002 (called as MEMS sensor Type B). A summary of the technical specifications of the referred MEMS accelerometers are shown in Table 5.1. More technical specifications' details can be found in ASC (2009).

Table 5.1 – Technical specifications of the MEMS accelerometers implemented in the developed WSN platforms.

	MEMS Accelerometer Type A	MEMS Accelerometer Type B
Sensor Type	ASC 5521-002	ASC5631-002
Channels	X, Y, Z	X, Y, Z
Frequency Response (Hz)	0 - 100	0 - 100
Range (g)	± 2.0	± 2.0
Sensitivity (mV/g)	1000	1000
Size (mm)	25 x 15 x 20	35 x 35 x 30
Weight (gram)	22	65
Noise Density ($\mu\text{g}/\sqrt{\text{Hz}}$)	7	Not Defined
Cost (€)	1030	250

As observed, both options of MEMS accelerometers selected have similar characteristics. However, since the noise density level was not defined in the data sheets provided by the manufacturer for the MEMS accelerometers Type B, it was decided to buy three MEMS accelerometer Type A and evaluate the other type of sensors by buying only one unit.

With respect to the base station, and as mentioned before, it was composed by one TelosB platform acting as the system's coordinator in addition to the command & configuration and data collection applications. The role of the coordinator node was to configure and synchronize the whole network using a beacon-based solution contemplated in the IEEE 802.15.4 communication protocol. The coordinator node served also as interface between the network of sensors and the command & configuration application as well as reception point of the forwarded data. The available controls of the command & configuration application enabled full control over the acquisition configuration parameters (i.e. axis selection, sampling rate, sampling period, etc.) and also provided a quick evaluation of the presence of the system nodes.

The network's communication was carried out in this first prototype system in a single-hop configuration. The system operation consists on beacons sent by the coordinator node to the sensing nodes. As soon as the measurement nodes are powered, they enter in an idle state and the coordinator node send a *ready* state beacon. Next, from the command & configuration software is sent a *start* beacon initiating the sampling process which is in turn controlled by periodic *synchronization* beacons. The *stop* beacon is finally sent to end the signal acquisition process and, then, the collected information is saved locally in each sensing node. The communication process starts at this moment and consists on

transmitting the recorded information (*get beacon*) of each sensing node at a time. More specifications about the communication process as well as details of the synchronization solution can be found at Severino et al. (2010). The network management scheme is summarized in Figure 5.3.

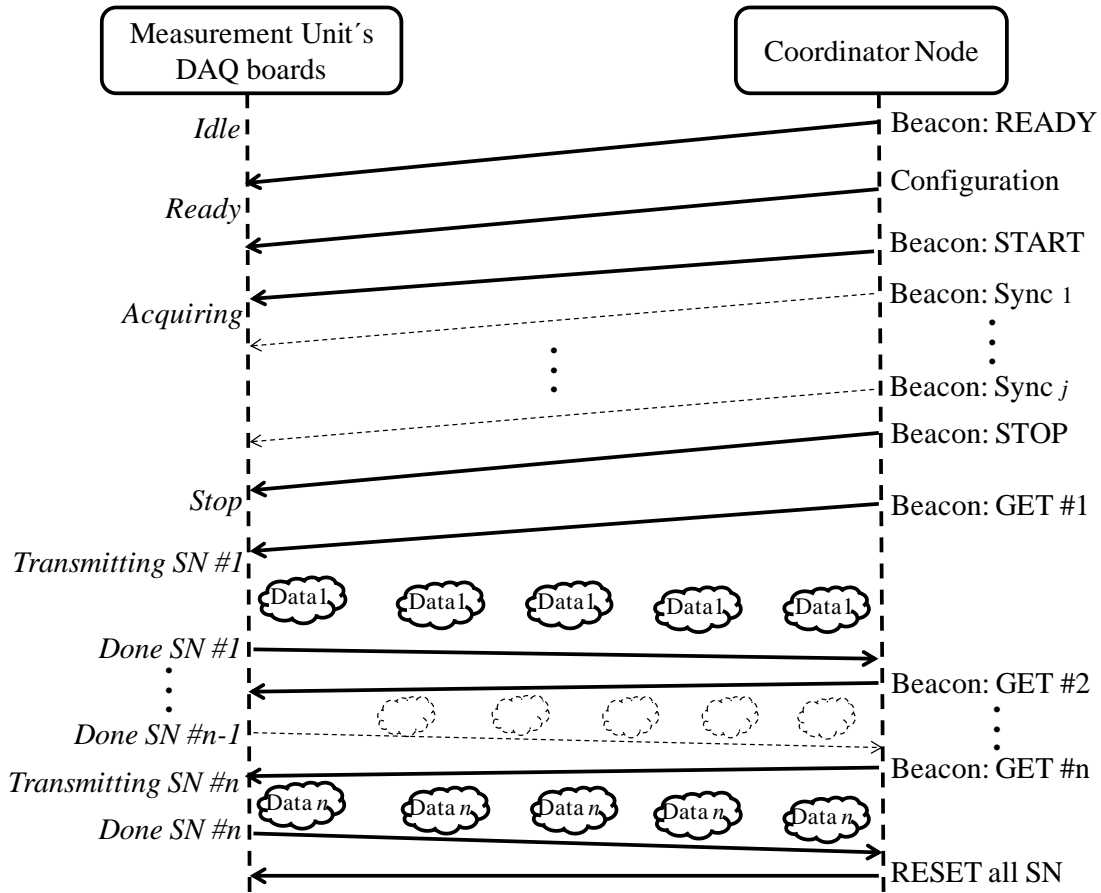


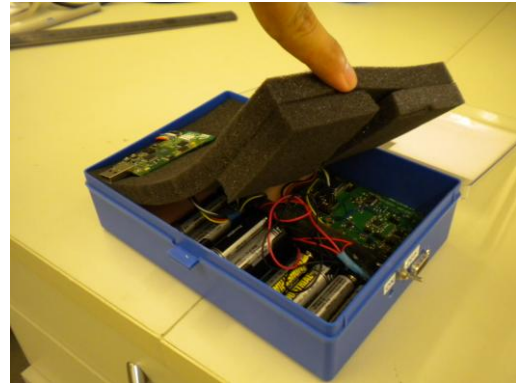
Figure 5.3 – Scheme of the network’s management

To complete the data reception process, a VI routine was developed in Labview (Labview, 2006) for data collection purposes. The data is transmitted from the measurement nodes in successive messages containing 8 measurements (4 bytes each one) in big-endian format. In this case, the developed application was also in charge of the interpretation and conversion into standard units of the received data as well as their local storage in the central station.

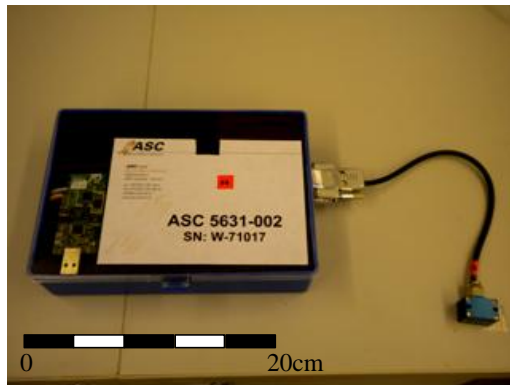
The final appearance of the developed prototype platform is shown in Figure 5.4. In order to ensure the necessary energy resources in case of possible medium and long term monitoring studies, two additional sets of four AA batteries were included.



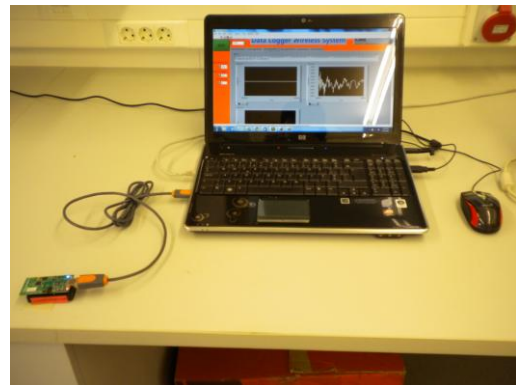
(a)



(b)



(c)



(d)

Figure 5.4 – Final appearance of the developed WSN solution: (a), (b), (c) measurement unit; and (d) base station

5.3 Prototype Validation Tests in the Inverted Wooden Pendulum

5.3.1 Description of the Monitoring System and Testing Specimen

For the laboratory validation tests carried out in this chapter, the case study of the inverted wooden pendulum presented in Chapter 4 was used again, since it offers the possibility of running multiple studies with different configurations.

Aiming at reproducing the measurement conditions considered in the tests of the commercial off-the shelf WSN platforms, the conventional monitoring systems were composed by the same piezoelectric accelerometers 393B12 (PCB, 2009) with a measurement range of ± 0.5 g and sensitivity of 10000 mV/g. In the case of the DAQ board, the NI-USB9233 (NI, 2009b) was considered, which has an embedded ADC of 24 bits of resolution.

Considering the referred conventional monitoring system as reference, numerous validation tests were carried out. In these experiments, the DAQ stations corresponding to both systems (conventional and wireless) were set for running in parallel aiming at performing measurements at the same instant of time using a common sampling rate of 100 Hz. The arrangement of the DAQ systems in the experimental tests is shown in Figure 5.5.

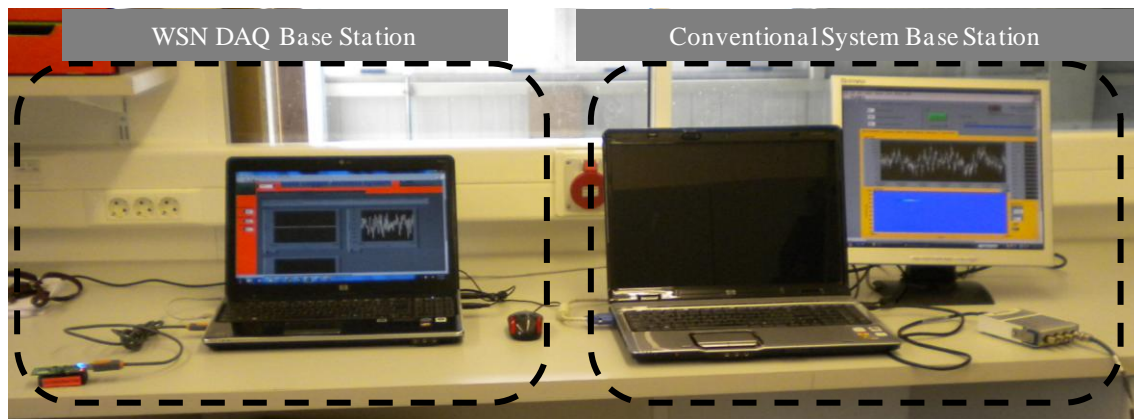


Figure 5.5 – DAQ systems arrangement for the experimental tests – Validation Tests New WSN Platforms

5.3.2 Time Domain Analysis

The initial time domain evaluation tests were carried out considering one measurement point at the top of the pendulum. As shown in Figure 5.6, one of each measurement units was applied (MEMS Accelerometers Type A and B as well as the conventional wired based transducers).

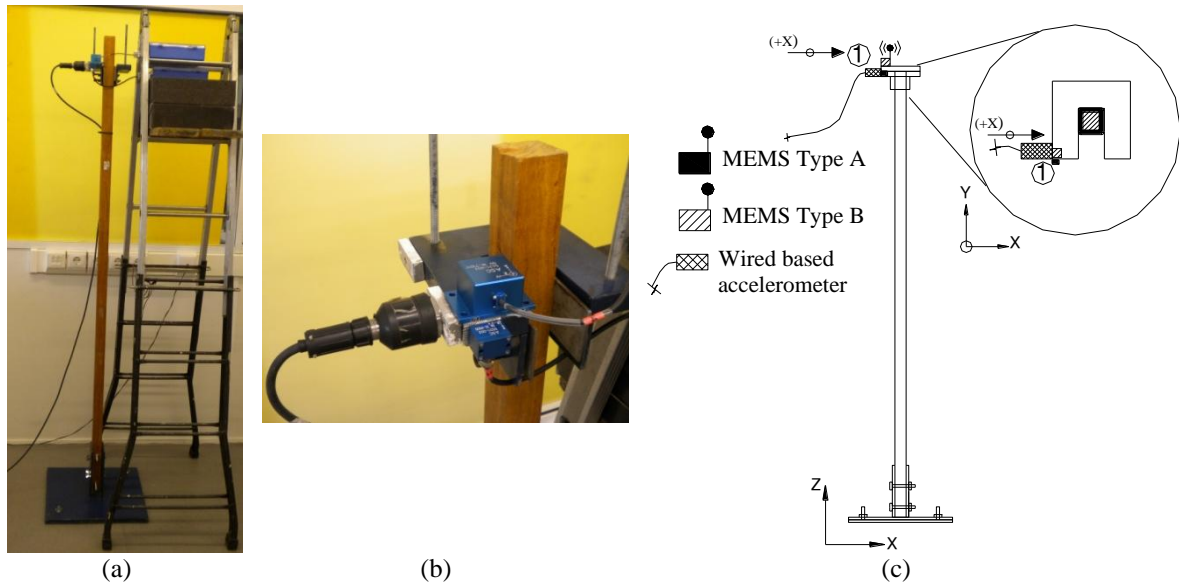


Figure 5.6 – Description of the arrangement of sensors for the time domain evaluation tests. (a) Inverted pendulum in the laboratory; (b) close up of the wired and wireless based sensors arrangement; and (c) scheme of the sensors deployment

For evaluating the performance of the developed platforms in high and low amplitude excitations, the first tests consisted in the application of an impulse force under which the response of the system was studied. For this test, a short sampling period of 10 seconds was considered. The time series recordings of the performed test are presented in Figure 5.7. The results indicated that for moderate amplitude vibrations (above 1 mg) the recordings of the three systems are very similar. However, as shown in the bottom left figure, for signals with amplitudes below this limit, the solution corresponding to the MEMS Accelerometer Type A has limitations. On the contrary, the system with MEMS Accelerometer Type B presents outstanding results maintaining a remarkable similitude with the conventional transducers, even in low noise environments. It is important to state that, even in the case of the MEMS Type A, the considered solutions had at least 20 times better performance in comparison to the commercial WSN studied in Chapter 4. These commercial off-the-shelf WSN platforms can only perform measurements of vibrations above 20 mg (see section 4.3.2).

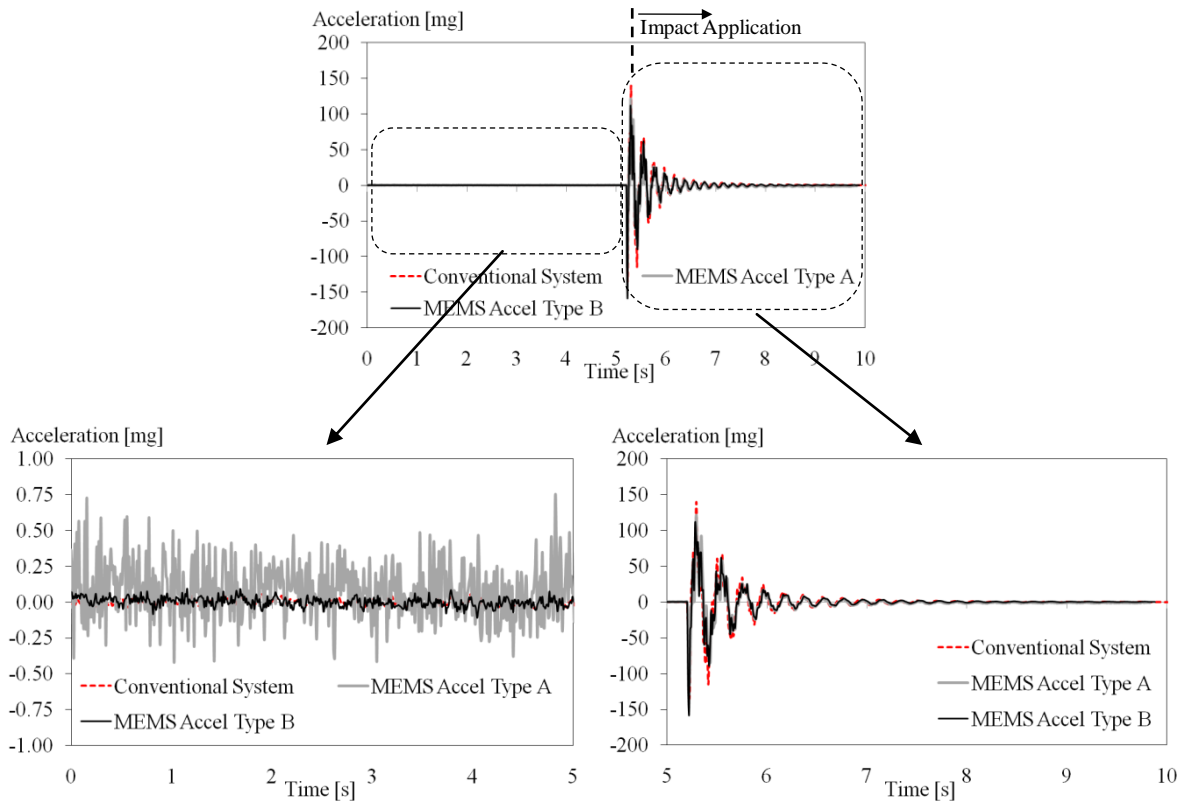


Figure 5.7 – Time series recordings of the response of the inverted pendulum under an impact force test – Validation Tests for New WSN Platforms

For verifying the previous results, the relative errors (discrepancy between the two measurements taking as reference the records of the conventional platforms) of the discrete measurements at each instant of time were calculated. These results are shown in Figure 5.8. The very good performance of the MEMS accelerometers Type B was confirmed in the error comparison tests since, small mean and standard deviation values were registered in the low and high amplitude vibration scenarios (Figure 5.8b). As shown in Figure 5.8a, the MEMS accelerometers Type A has better performance in structures subjected to moderate excitations (above 1 mg). In this case, low values of mean errors and standard deviations were also registered.

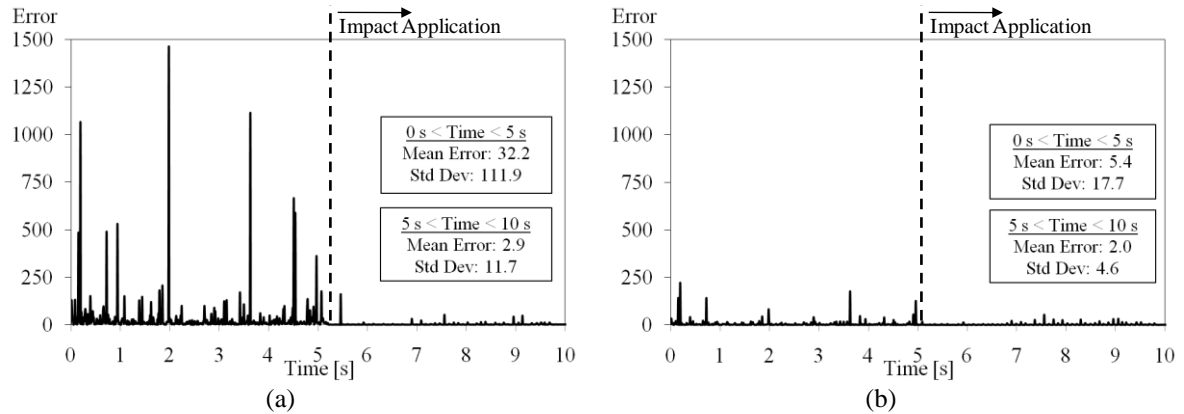


Figure 5.8 – Measurement errors comparison of the impulse force tests – Validation Tests for New WSN Platforms. (a) MEMS Type A vs. Conventional accelerometers; and (b) MEMS Type B vs. Conventional accelerometers

Next, the performance of the developed solution was evaluated considering tests with longer sample periods. Using the same deployment of sensors and 60 seconds for the sampling time, two rounds of tests were carried out: one considering light random impact excitations and the other ambient noise. Note longer sampling periods of 1000-2000 times the structure's first period are recommended for practical recommendations (Ramos, 2007). Hereafter shorter measurement times are considered due to time consuming data transmission process in this first prototype system. Figure 5.9 shows the time series recordings of the systems with MEMS accelerometers Type A and Type B as well as the conventional wired based system in each of the considered noise scenarios. The results showed the good performance of the developed systems for registering time domain responses. In the case of the systems with MEMS accelerometers Type A, these showed a proper concordance with the recordings from conventional wired based systems for scenarios with vibration's amplitudes higher than 1 mg. On the other hand, it was observed that the MEMS accelerometers Type B have higher sensibility and vibrations with amplitudes above 0.1 mg can be acquired.

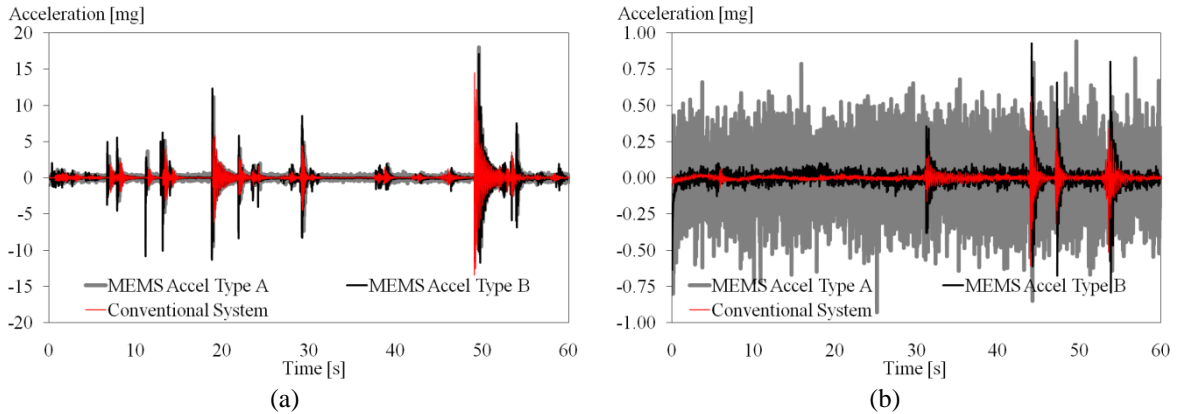


Figure 5.9 – Time series collected by the evaluated systems – Validation Tests for New WSN Platforms. (a) Response of the systems under light random excitation; and (b) response under ambient noise

The statistical comparison of the results of the time series recordings by means of the maximum values registered and RMS of the acquired signals is summarized in Table 5.2. The results confirmed the similarity of the time domain series recorded by the different evaluated systems. In the case of the system with MEMS Accelerometer Type A, small differences were registered especially when these were used for measuring moderate amplitude excitation. In the case of the second system with MEMS Accelerometer Type B, the results showed that high accurate measurements, comparable with the ones registered with conventional wired based systems can be recorded, even in low noise environments.

Table 5.2 – Statistical evaluation of the time series results – Validation Tests for New WSN Platforms.

Noise Condition	Conventional Accelerometer		MEMS Accelerometer Type A		MEMS Accelerometer Type B		Comparison Conv./MEMS Type A		Comparison Conv./MEMS Type B	
	Max (mg)	RMS (mg)	Max (mg)	RMS (mg)	Max (mg)	RMS (mg)	Max Error (%)	RMS Error (%)	Max Error (%)	RMS Error (%)
Excited	14.43	0.90	18.01	0.82	16.90	1.04	24.8	8.9	17.1	15.6
Ambient	0.61	0.04	0.94	0.22	0.93	0.06	54.1	450.0	52.5	50.0

5.3.3 Frequency Domain Analysis

The accuracy of the measurements recorded with the developed prototype of WSN platforms was subsequently evaluated considering the analysis of the resultant frequency domain series. As a first test, the Welch Spectrums of the time series records shown in Figure 5.9 were calculated considering a window length of 512 points and 50% for the overlapping criterion. Figure 5.10 and Figure 5.11 show the resultant spectrums from the records in moderate (Figure 5.9a) and low noise (Figure 5.9b) scenarios respectively. The

location of the peaks in the spectrums corresponding to the data measured with the two MEMS accelerometers solutions in moderate noise scenarios showed high correspondence with the results of the conventional system. In this case, the spectrums presented seven peaks aligned in the same frequencies coordinates (x axis) confirming the very good performance of the development systems. In case of the low noise scenario, the resultant spectrum from the system with MEMS Accelerometers Type A has shown only noise, evidencing the poor performance of these sensors in environments with noise levels below 1 mg. On the contrary, the results from the MEMS Accelerometers Type B have shown a remarkable similitude to what was obtained from the conventional systems. In this case, at least the first two peaks (in the band from 0 Hz to 10 Hz) as well as the last two (close to the band of 40 Hz) were clearly identified.

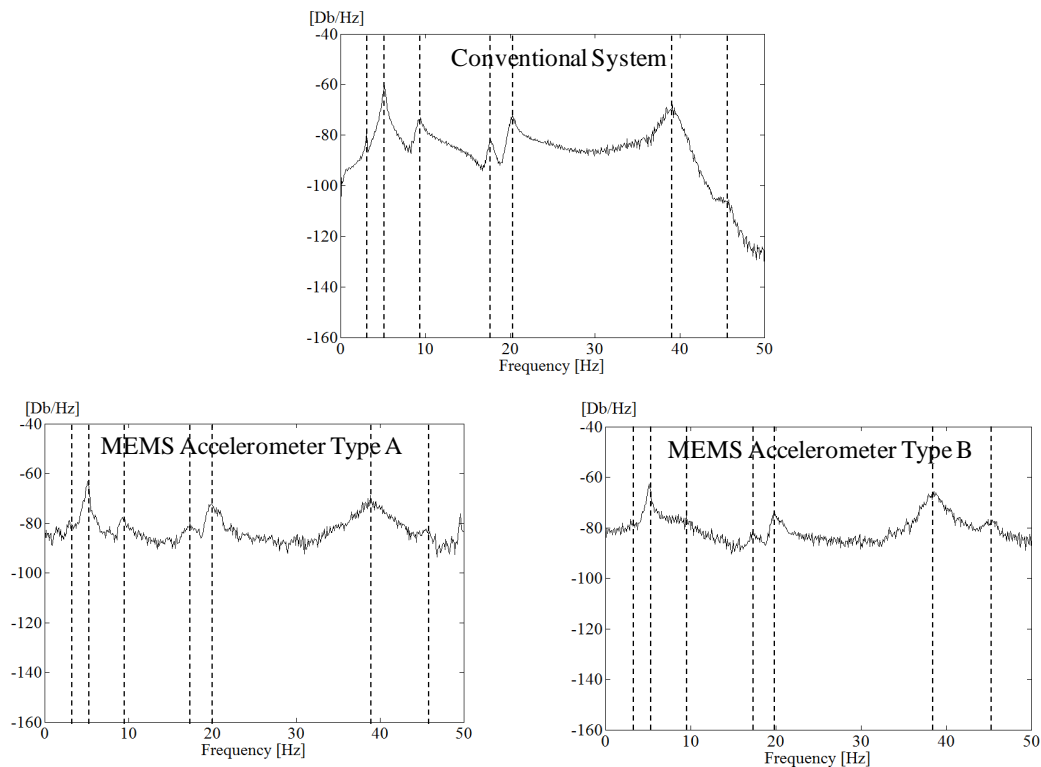


Figure 5.10 – Frequency domain results of the tests with light random excitation – Validation Tests for New WSN Platforms

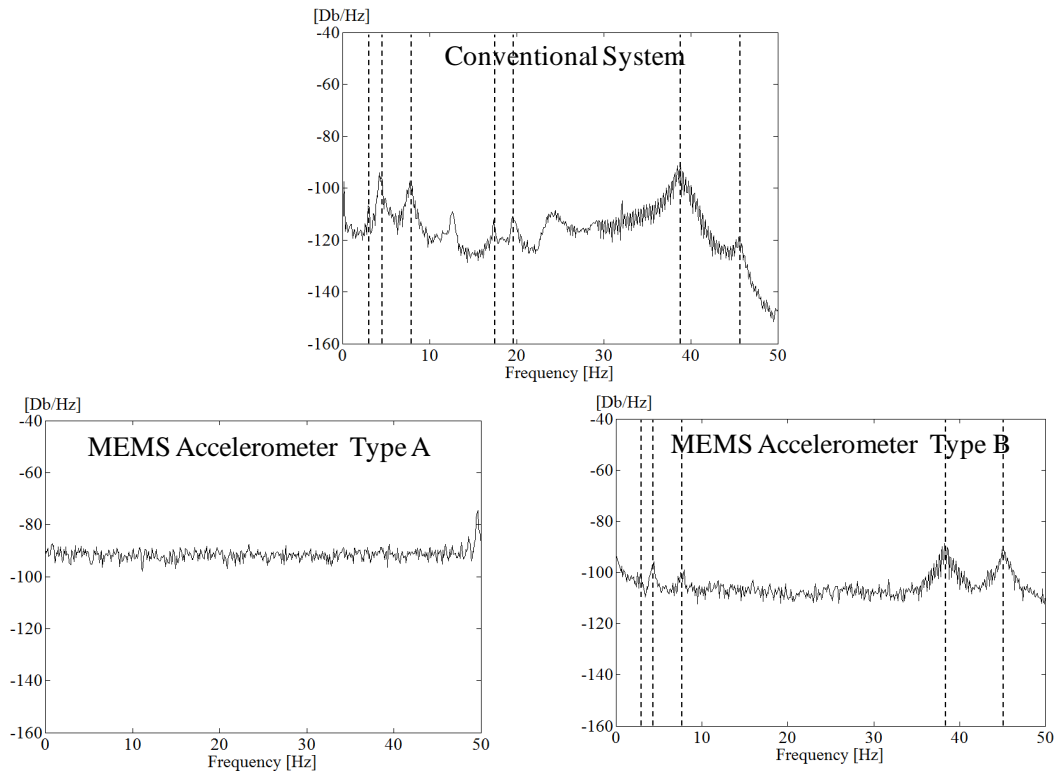


Figure 5.11 – Frequency domain results of the tests with ambient noise – Validation Tests for New WSN Platforms

Aiming at observing if the variation of the frequency content would be significant in successive tests (repeatability of the response), the following stage consisted in performing consecutive modal analysis tests in moderate and low noise scenarios (conditions provided by light random impacts and ambient noise respectively). Considering the same pendulum configuration (all sensors located at node one, see Figure 5.6) and 60 seconds for the sample time, five rounds of frequency validation tests were carried out in each of the considered noise scenarios. Since in these tests only the frequency content was evaluated, the Peak Picking method (PP) was used for performing the frequency detection task. The summary of the detected frequencies in each of the excitation scenarios are shown in Table 5.3 and Table 5.4. The results of the repeatability tests confirmed that high precision can be attained with the use of the developed WSN platforms. It should be noticed that the missing detection of one or more frequencies in some of the tests occurred also when the conventional systems were used indicating that sometimes the applied excitation was not enough for exciting the whole structural modes and the sampling time is insufficient. With respect to the MEMS Accelerometers Type A, the results evidenced again the proper behavior of these systems in moderate excited scenarios. Nevertheless, this system did not allow capturing the existence of a third frequency (which was identified with the other systems). As it was expected from the previous tests in low excitation scenarios, no

frequencies were detected since the spectrums showed only noise. MEMS Accelerometers Type B have shown high accuracy even when they were used in low noise environments. As observed, in the majority of the tests, five frequencies were identified and they coincided with the estimations obtained from the conventional wired based systems.

Table 5.3 – Results of the repeatability tests in moderate noise environments – Validation Tests for New WSN Platforms.

	Conventional Platforms					MEMS Accelerometers Type A					MEMS Accelerometers Type B				
	f_1	f_2	f_3	f_4	f_5	f_1	f_2	f_3	f_4	f_5	f_1	f_2	f_3	f_4	f_5
R1	2.93	4.30	7.62	18.75	38.48	2.93	4.27	---	18.75	38.87	2.93	4.30	7.62	18.36	38.48
R2	2.93	4.49	8.01	18.95	38.87	2.93	4.49	---	18.95	38.48	2.93	4.49	7.23	18.75	38.67
R3	2.93	4.30	7.62	18.75	39.45	2.93	4.30	---	18.75	39.06	2.93	4.30	7.42	18.75	39.06
R4	2.93	4.10	---	18.75	39.65	2.93	4.30	---	18.75	38.87	2.93	4.30	8.00	18.56	39.45
R5	2.93	4.69	7.81	18.95	39.26	---	4.69	---	18.95	39.26	---	4.69	6.84	18.75	38.67

* Could not be estimated since the resultant spectrums showed only noise

Table 5.4 – Results of the repeatability tests in low noise environments – Validation Tests for New WSN Platforms.

	Conventional Platforms					MEMS Accelerometers Type A					MEMS Accelerometers Type B				
	f_1	f_2	f_3	f_4	f_5	f_1	f_2	f_3	f_4	f_5	f_1	f_2	f_3	f_4	f_5
R1	2.93	4.30	7.81	18.95	37.89	---	---	---	---	---	---	4.30	7.62	18.56	37.50
R2	2.93	4.30	7.81	18.75	37.89	---	---	---	---	---	---	4.69	7.81	18.75	37.50
R3	2.93	---	7.03	19.73	38.67	---	---	---	---	---	2.93	3.91	8.60	---	38.48
R4	---	3.71	7.23	18.95	37.89	---	---	---	---	---	2.93	3.71	7.23	18.56	37.50
R5	---	4.46	7.62	19.34	37.70	---	---	---	---	---	---	4.49	7.61	19.14	37.31

* Could not be estimated since the resultant spectrums showed only noise

The statistical information related to the average values of the frequency estimations (f) and their standard deviation (σ) obtained in the repeatability tests are summarized in Figure 5.12 and Figure 5.13. The results of this statistical comparison demonstrated the outstanding precision of the proposed equipments. Despite the limitations of the systems with MEMS Type A in low noise environments, it was possible to observe that for the other cases, the average values as well as the maximum errors obtained from the measurements of the new platforms have comparable values with the ones obtained from the conventional wired based systems.

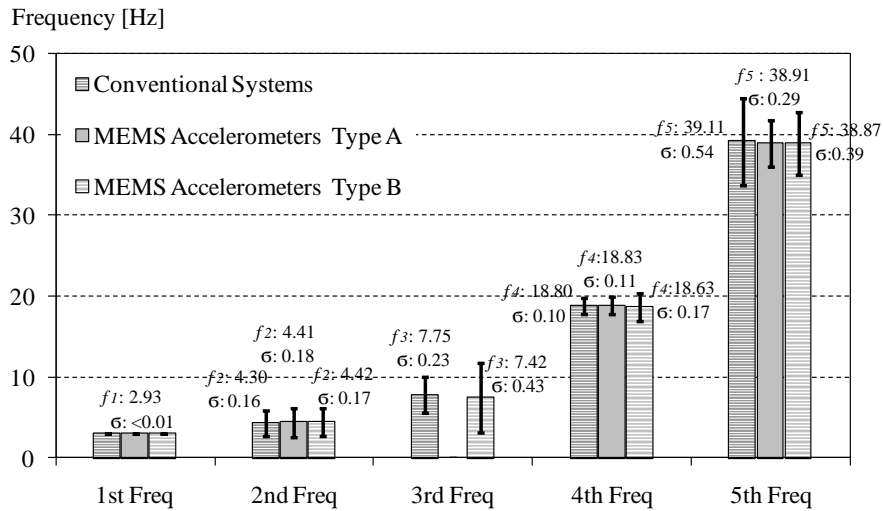


Figure 5.12 – Results of the frequency domain repeatability analysis of the evaluated platforms in moderate noise environments – Validation Tests for New WSN Platforms (Note that the sizes of the bars representing the standard deviation were exaggerated by a factor of 10)

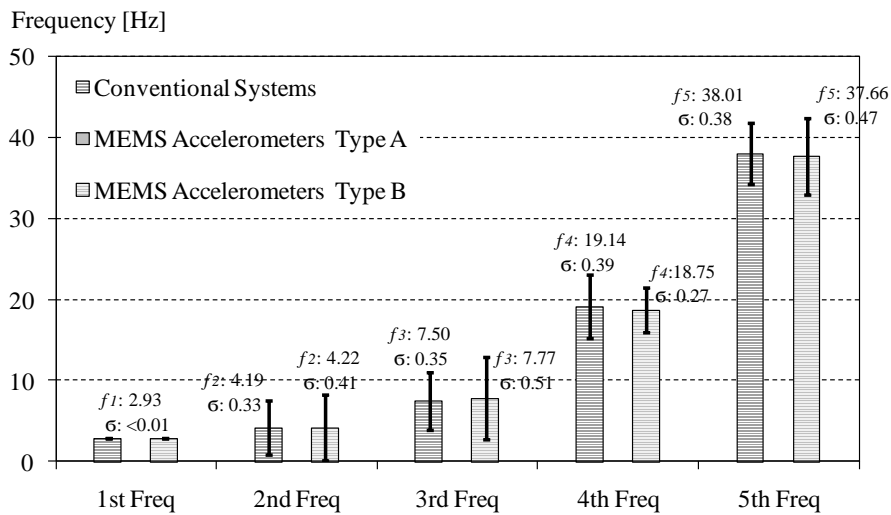


Figure 5.13 – Results of the frequency domain repeatability analysis of the evaluated platforms in low noise environments – Validation Tests for New WSN Platforms (Note that the sizes of the bars representing the standard deviation were exaggerated by a factor of 10)

5.3.4 Experimental Modal Identification using Parametric Methods

The performance of the developed WSN platforms was next assessed using schemes of experimental modal analysis. With this respect, not only the detection of natural frequencies, but also of the damping coefficients and modal shapes was carried out aiming at evaluating the effectiveness of the adopted node's synchronization solution. The data processing stage of the tests carried out in this section was performed using the Stochastic Subspace Identification method – SSI implemented in the ARTeMIS extractor software (SVS, 2009).

As mentioned before, the prototype of WSN platform developed in this work considered four sensing nodes using three MEMS Accelerometers Type A and one MEMS Accelerometer Type B respectively. Since, for the detection of modal shapes at least three measurement nodes are needed, the solution with MEMS Accelerometers Type B was not considered in these modal evaluation tests. Nevertheless, the results that are going to be presented can be extrapolated to these systems taking into consideration that, according to the previous results, better performance in low excited environments should be expectable.

The first tests carried out in this section, considered the study of the pendulum in its original condition using three measurement nodes placed at its top in nodes 1, 2 and 3 (Figure 5.14). As done before, the response of the pendulum was studied considering 60 seconds of sampling time and two excitation scenarios (moderate and low noise environments). In the collected time domain series acceleration peaks of 3.93 mg and 0.35 mg were registered, which corresponded to signals with RMS values of 0.23 mg and 0.03 mg for the medium and low noise environments respectively. The stabilizations diagrams, product of the application of the SSI method to the recorded data in each excitation scenario, are shown in Figure 5.15. As it is possible to observe, the stabilization diagrams corresponding to the measurements of the developed platforms in medium noise environments showed stable poles properly aligned in the same natural frequencies predicted from the recording of the conventional systems. On the contrary, in the case of low level noise environments the stabilization diagrams showed only noise confirming the previous results regarding the limitations of these platforms for performing dynamic monitoring in low vibration environments.

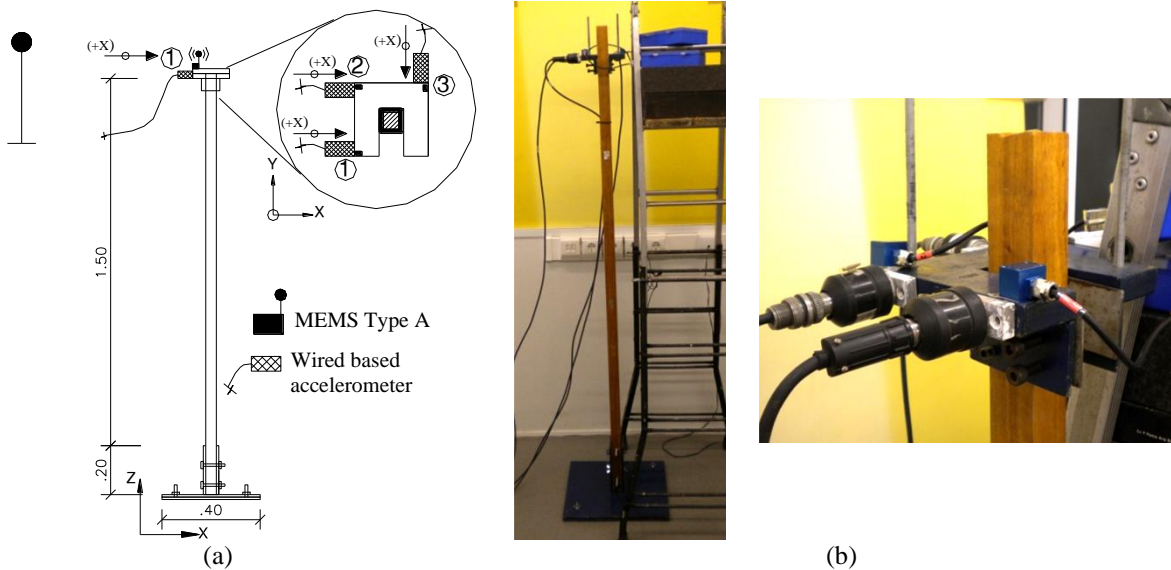


Figure 5.14 – Pendulum first modal analysis tests – Validation Tests for New WSN Platforms: (a) schematic sensors layout; and (b) configuration of the sensors during the experimental tests

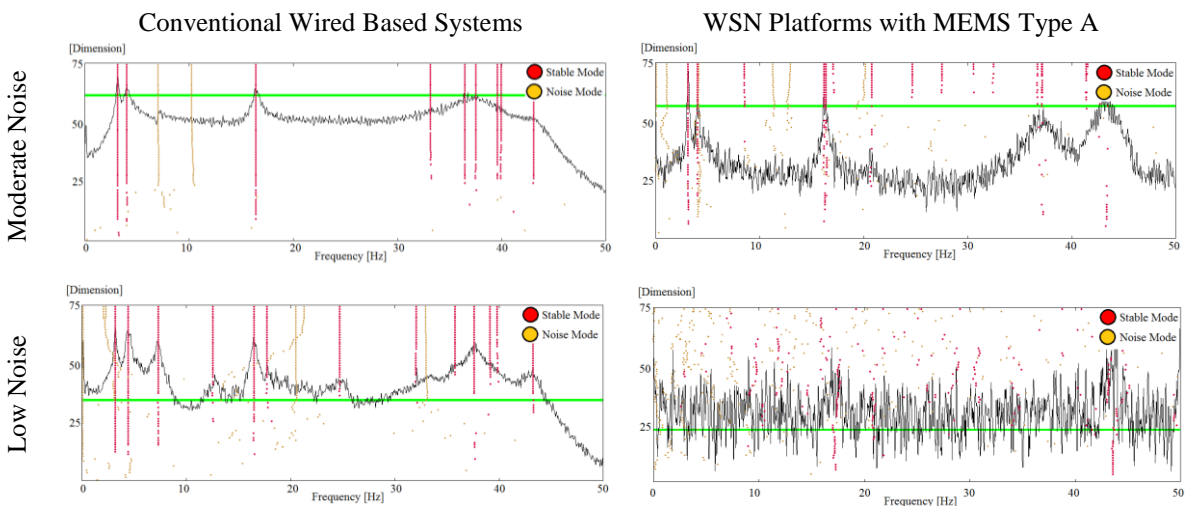


Figure 5.15 – Stabilization diagrams of the pendulum first modal analysis tests – Validation Tests for New WSN Platforms

For the modal identification process, it was considered that the information of interest is related only to the estimation of the first three structural mode shapes (translation in the two principal axes and rotation). In this sense, Table 5.5 summarizes the modal identification process presenting the estimated frequencies and damping coefficients in both excitation scenarios. Since the results of the developed platforms are imprecise in low noise environments, Figure 5.16 presents the results of the identified modal shapes only for the case of medium noise environments. The results of the medium excited environments evidenced the high accuracy that might be expectable from the measurements of the developed platforms. As it is possible to observe, the first two modes of the structure were

identified with no uncertainties (MAC values close to 1) while for the case of the third mode, a slight difference with the results of the conventional systems was registered.

Table 5.5 – Results of pendulum first modal analysis tests – Validation Tests for New WSN Platforms.

	Conventional Systems		MEMS Type A		Percent Error (%)	
	Medium Noise Environment	Low Noise Environment	Medium Noise Environment	Low Noise Environment	Medium Noise Environment	Low Noise Environment
f_1 (Hz)	3.19	3.22	3.16	---*	0.9	---*
f_2 (Hz)	4.07	4.48	4.06	---*	0.3	---*
f_3 (Hz)	16.46	16.53	16.39	---*	0.4	---*
ξ_1 (%)	1.5	1.6	1.4	---*	6.7	---*
ξ_2 (%)	5.4	4.5	8.8	---*	63.0	---*
ξ_3 (%)	1.2	0.9	1.9	---*	58.3	---*

* Could not be estimated since the stabilization diagrams showed only high dispersion poles

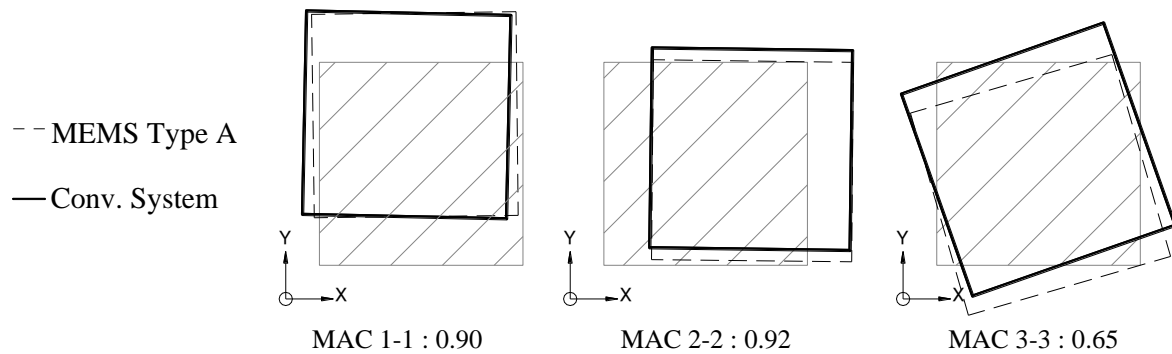


Figure 5.16 – First three mode shapes estimated from the experimental modal analysis tests in the pendulum first configuration – Validation Tests for New WSN Platforms

As a second round of modal validation tests, the study of a new pendulum's arrangement was considered, this time with the inclusion of additional masses in its top (Figure 5.17a). As shown in Figure 5.17b, the deployment of measurement sensors was the same as in the previous study, with all of them located at node 1, 2 and 3. Since the limitations of the platforms in low noise environments was confirmed with the previous tests, in this second round it was decided to study only the response of the structure in medium noise environments with one test with 60 seconds of sampling time. In this experimental test, the maximum value registered was 18.2 mg which corresponded to a signal with RMS of 0.48 mg.

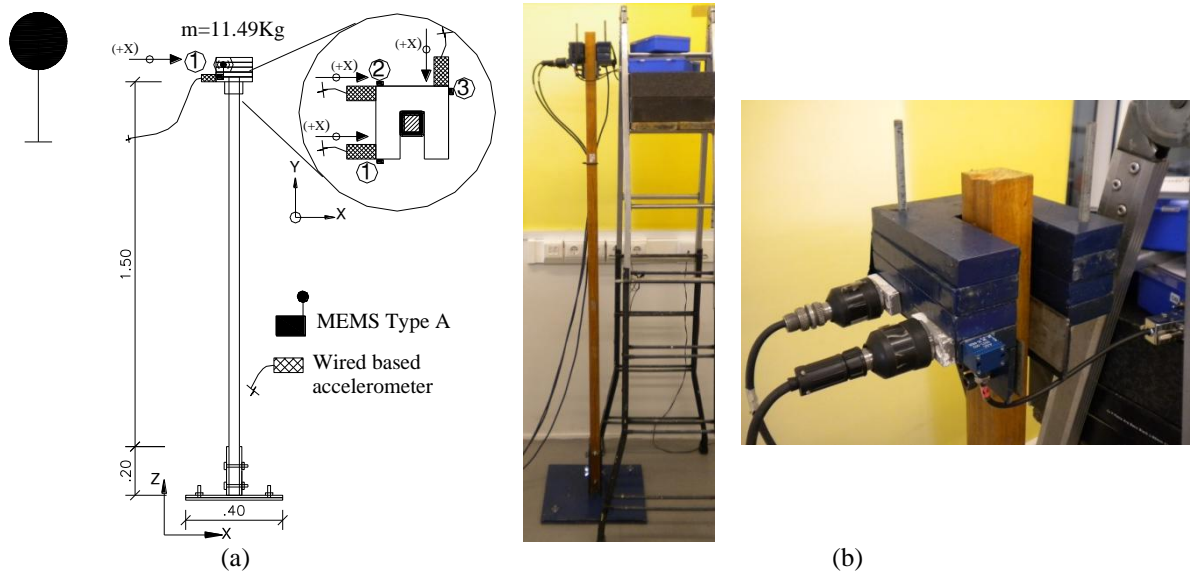


Figure 5.17 – Pendulum second modal analysis tests – Validation Tests for New WSN Platforms: (a) schematic sensors layout; and (b) configuration of the sensors during the experimental tests

The stabilizations diagrams for the collected time domain series are shown in Figure 5.18. As it can be observed in the diagrams from the data recorded by the developed platforms, two clear columns of poles in the band of 1 Hz to 3 Hz (indicating the existence of the first two natural frequencies) were clearly distinguishable. However, the poles around a possible third frequency ($\pm 10\text{ Hz}$) seemed not to become stable even if the SVD spectrum in the background showed a fuzzy peak in this band.

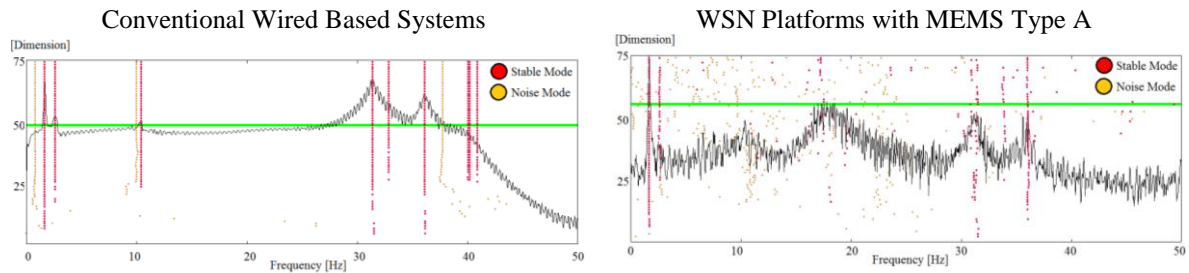


Figure 5.18 – Stabilization diagrams of the pendulum second modal analysis tests – Validation Tests for New WSN Platforms

Table 5.6 presents the estimated frequencies and damping coefficients from the recorded data. The results confirmed that a third frequency corresponding to the rotational mode shape could not be estimated from the measurements of the developed platforms. In spite of this, the estimations of the first and second modes from both systems showed remarkable exactitude with a related maximum error of less than 1.5%. In the case of the estimations of damping coefficients, these presented higher variability evidencing not a limitation of the measurement systems but a drawback in the OMA tests themselves.

Table 5.6 – Results of pendulum second modal analysis tests – Validation Tests for New WSN Platforms.

	Conventional Systems	MEMS Type A	Percent Error (%)
	Medium Noise Environment	Medium Noise Environment	Medium Noise Environment
f_1 (Hz)	1.68	1.70	1.2
f_2 (Hz)	2.64	2.64	< 0.01
f_3 (Hz)	10.42	---*	----
ξ_1 (%)	2.3	2.8	21.7
ξ_2 (%)	6.4	9.2	43.8
ξ_3 (%)	6.5	---*	----

* Could not be estimated since the stabilization diagrams showed only high dispersion poles

For evaluating the precision in the measurements of the developed platforms, the first three mode shapes of the studied structure are presented in Figure 5.19. The results of the estimations of the first modal shape showed a higher MAC value in comparison to the one corresponding to the second mode. However, for both cases it should be noticed that the estimated mode shapes clearly correspond to the translation along the main axes confirming the accuracy of the developed system.

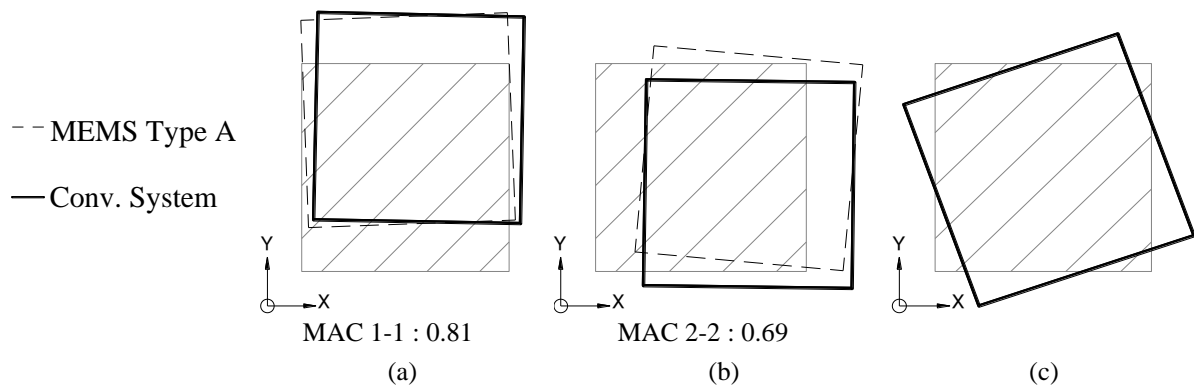


Figure 5.19 – First three mode shapes estimated from the experimental modal analysis tests in the pendulum second configuration (added mass at the top) – Validation Tests for New WSN Platforms

The last round of modal validation tests of the developed platforms was carried out in a stiffer structure. With this purpose, the original condition of the pendulum was modified by increasing the cross section of the supporting element. As shown in Figure 5.20, in this new configuration, three nodes using both, conventional and new platforms were located again at the top of the pendulum for measuring its dynamic response in medium noise environments.

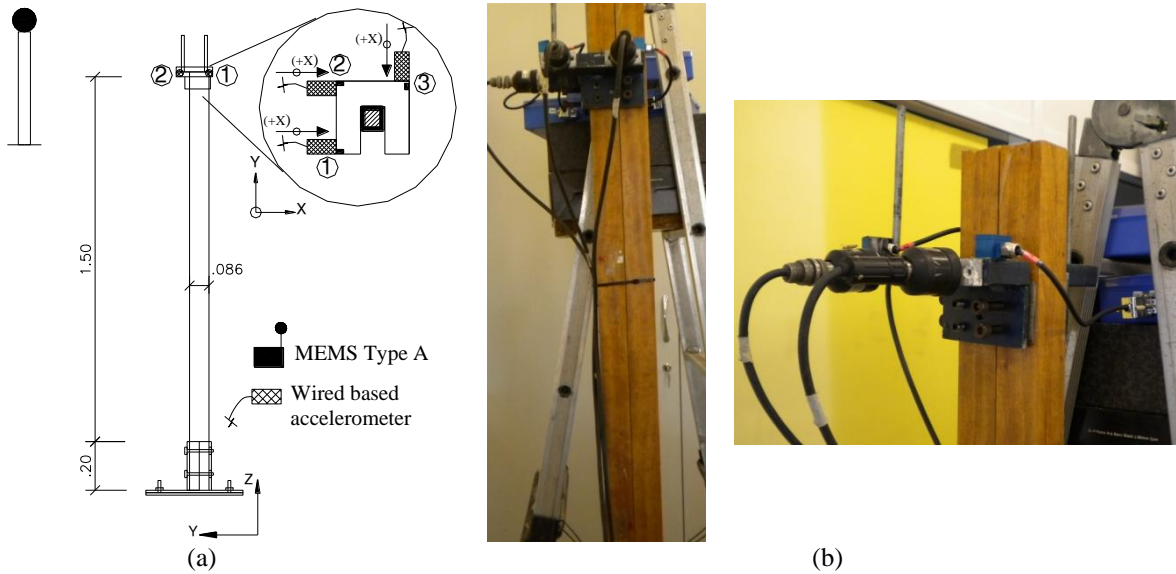


Figure 5.20 – Pendulum third modal analysis tests – Validation Tests for New WSN Platforms: (a) schematic sensors layout; and (b) configuration of the sensors during the experimental tests

The experimental modal analysis test was carried out considering 60 seconds of sampling time. In this test, a maximum acceleration value of 2.78 mg corresponding to signal with RMS of 0.23 mg was registered. The stabilization diagrams of the collected data with the developed platforms and the conventional systems are shown in Figure 5.21. In the presented diagrams it can be observed that the stable poles appeared aligned in the same band of frequencies in both cases corroborating the good performance and accuracy of the developed platforms. From the diagrams, the dynamic properties were estimated and are presented in Table 5.7. Again, the results of the developed platforms indicated that, in medium noise environments (signals with amplitude above 1 mg), the estimations of the dynamic properties can be performed with high precision. In this case, estimations with errors lower than 1.5% were again registered. In respect to the damping coefficients, these values have higher variability; nevertheless the estimations from the developed systems are coherent with the ones obtained with the conventional systems.

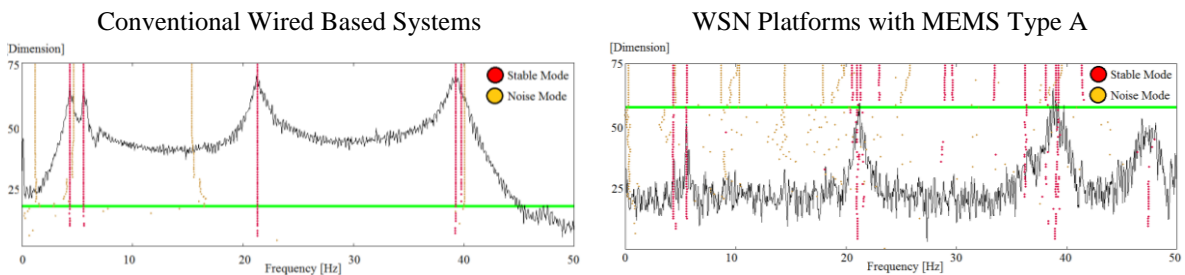


Figure 5.21 – Stabilization diagrams of the pendulum third modal analysis tests – Validation Tests for New WSN Platforms

Table 5.7 – Results of pendulum third modal analysis tests – Validation Tests for New WSN Platforms.

	Conventional Systems	MEMS Type A	Percent Error (%)
	Medium Noise Environment	Medium Noise Environment	Medium Noise Environment
f_1 (Hz)	4.38	4.38	< 0.01
f_2 (Hz)	5.64	5.59	0.9
f_3 (Hz)	21.35	21.04	1.5
ξ_1 (%)	4.89	3.88	20.7
ξ_2 (%)	2.34	1.98	15.4
ξ_3 (%)	1.65	1.34	18.8

The information regarding to the estimated mode shapes is presented in Figure 5.22. The registered MAC values indicated that less accurate estimations were obtained. However, the mode shapes clearly show the proper tendency of translation for the first two modes and rotation for the last third one evidencing, once again, that the developed platforms can be positively considered as alternatives for conventional systems.

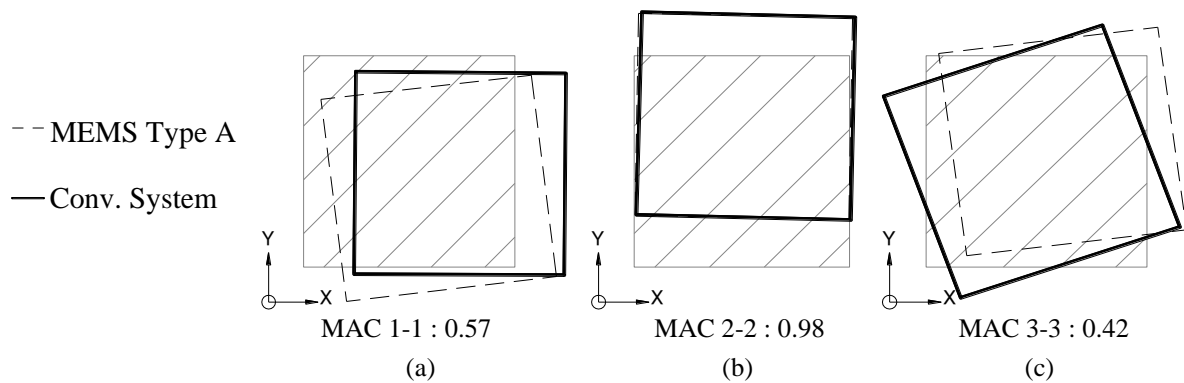


Figure 5.22 – First three mode shapes estimated from the experimental modal analysis tests in the pendulum third configuration (stiffer support element) – Validation Tests for New WSN Platforms

5.3.5 Discussion of the Results

The most significant aspects of the time and frequency domain as well as mode shape results for the inverted pendulum validation tests are summarized next.

Regarding the results of the time domain validations tests, these showed the acceptable performance of the platforms with MEMS accelerometers Type A and Type B for measuring medium and low amplitude vibrations respectively. However, these results also evidenced that there are still some differences when comparing the peak values registered with these platforms and their counterparts with the conventional systems.

On the other hand, the frequency domain results evidenced the outstanding accuracy of the developed system. In this case, comparable results to those obtained with the use of

conventional systems were observed. Even if the estimation of mode shapes of the first two translational modes and the first rotational one were acceptable in most cases, the results evidenced a higher scatter. These results should be carefully considered since in field OMA tests the accurate estimation of modal shapes is important not only for estimating complex modes but also for damage detection schemes.

The reported results allowed identifying the main problems in the platforms that need to be considered in short, medium and long term developments stages. Problems were identified in the signal conditioning process of the units with MEMS Type A. These transducers having similar characteristics to MEMS Type B did not exhibit the expected behavior in low noise environments (at least comparable results between both platforms were expected). The improvement of the ADC capabilities should be also considered since due to multiplexing problems in the ADC implemented in the developed prototype system, the measurement of the three accelerometer axes could not be acquired at the same time.

Finally, it was observed that, probably, the main drawback of the developed solution is the long data transmission times required for performing the synchronization among the sensing nodes. In this first prototype, the way how data are managed involves extended transmission periods (see Figure 5.23) which would represent a serious constraint in future field case applications.

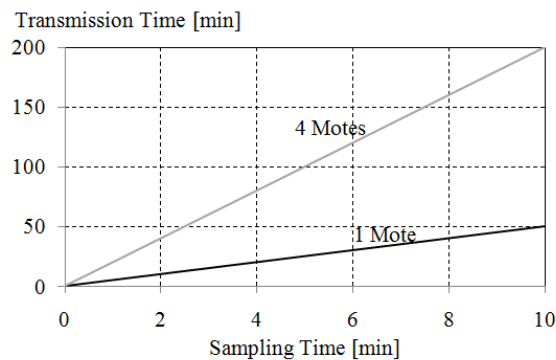


Figure 5.23 – Relation between sampling time and transmission time for the case of the new WSN platforms (signals acquired with 100 Hz of sampling rate)

5.4 Application of the Developed Platforms in Tie-Rods

The possibility of performing modal analysis tests of flexible structures such as tie-rods allowed an interesting opportunity for the application of the developed prototype of WSN platforms. With this respect, laboratory tests were carried out aiming at tracking the change of the dynamic response of tie-rods when different amounts of tension were applied. The experimental program included a large number of tests (over 80) using different types of measurement systems (conventional wired based transducers, laser vibrometers, and WSN platforms).

Since this part of this work was only intended to present the experimental tests carried out using the developed prototype of WSN, the results of the few tests involving these systems are discussed next. More information about the tests as well as the analytical and experimental results can be found at Luong (2010).

5.4.1 Motivation of the Study and Analytical Solution

Ancient tie-rods are different in size and shape and are usually made of iron. The common cross sections are circular or rectangular. However, these elements are often irregular along their length because they were hand wrought. This, in addition to the fact that the mechanical characteristics of iron obtained through non-industrial processes are difficult to determine and that the cross sections may be altered due to corrosion processes, make the problem of studying ancient tie-rods of high complexity (Lagomarsino and Calderini, 2005). Some examples of metallic tie-rods working as strengthening elements of existent masonry structures are presented in Figure 5.24.



Figure 5.24 – Examples of tie-rods in existent masonry structures: (a) circular bars in the Ospedale degli Innocenti, Florence, Italy; (b) circular bars in the Santa Croce, Florence, Italy; (c) rectangular bars in the via Zamboni, Bologna, Italy; (d) circular bars in the cathedral of Porto, Portugal; (e) and (f) rectangular bars in the Jesus' Church, Setúbal, Portugal

In the field of experimental techniques for monitoring the tension state of these elements, the modal analysis offers an attractive option since the stress state of the bars can be assessed by means of non destructive procedures relatively easy to perform.

The simplified structural model used for studying the dynamic response of tie-rods considers these elements as beams, with uniform cross section, subjected to an axial tensile force and spring hinged at both ends (Lagomarsino and Calderini, 2005). The solution of

the referred model for the pinned-pinned condition is given by Equation 5.1 (Clough and Penzien, 2003).

$$f = \frac{n}{2} \sqrt{\frac{n^2 \pi^2 EI}{\bar{m} L^4} + \frac{T}{\bar{m} L^2}} \quad \text{Equation 5.1}$$

where f denotes the natural frequency in [Hz], n the natural frequency of interest at which the formula is evaluated, E the elasticity modulus in [Pa], I the inertia moment in [m^4], \bar{m} the distributed mass per unit length in [kg/m], L the length of the element in [m], and T the tension force in [N].

As it was previously referred, in the case of studying the serviceability conditions of tie-rods in ancient structures, there are numerous variables to take into consideration. The variables affecting the dynamic response of these elements are the applied tensile stresses, boundary conditions, length, cross section, and characteristics of the materials. In this work, as a first stage of a research project, it was decided to neglect the influence of the variations of the cross sections and materials along the length of the bars exploring in this way, numerically and experimentally, the influence of the rest of the variables. Figure 5.25 is presented as an example of the uncertainties and the consequences of an incorrect judgment of the boundary conditions in the estimation of the stress levels in field cases.

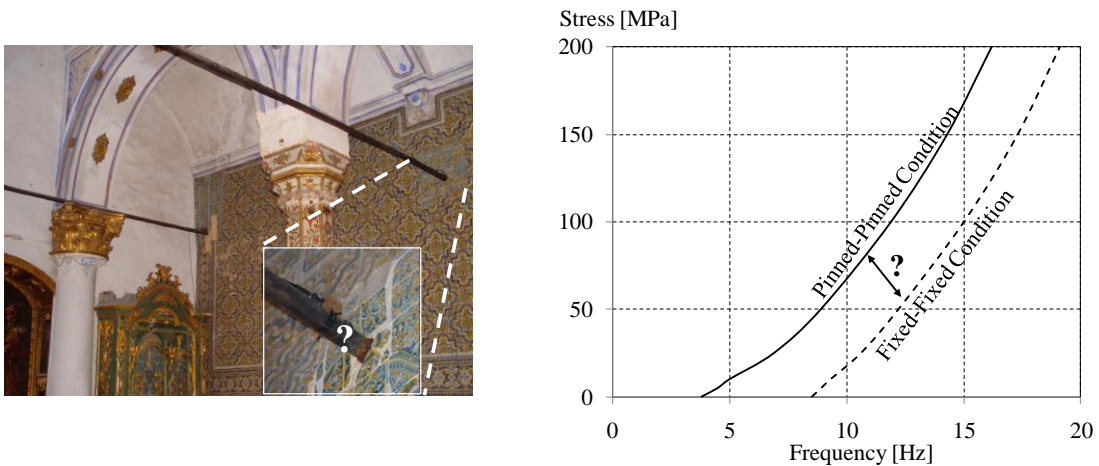


Figure 5.25 – Illustration of how the boundary conditions can affect the accuracy of the estimations of the tensile stress (the figure in the right was built considering the first natural frequency of a tie-rod with length = 5 m and 0.04 m x 0.044 m of cross section)

5.4.2 Experimental Tests and Dynamic Monitoring System Deployment

In the experimental tests carried out, modal analysis was performed considering four types of tie-rods. The characteristics of the studied specimens are summarized in Table 5.8. The possibility of variation in the supports from pinned-pinned to fixed-fixed conditions was considered. Aiming at simulating these conditions in the laboratory and, as shown in Figure 5.26a, different sets of nuts were used. The final specimen corresponding to the longer square tie-rod (S1) mounted in the laboratory is shown in Figure 5.26b. The process of applying the tensile force was manually performed by adjusting and relaxing the nuts, and indirectly measuring the applied force with LVDTs with the arrangement presented in Figure 5.26c.

Table 5.8 – Characteristics of the tie-rods tested in laboratory.

Identification	Length (m)	Cross Section		E (GPa)	Specific Weight (kg/m ³)
		Shape	Size <i>b</i> or Φ (m)		
S1	5.4	Square	0.04	210	7850
S2	2.7	Square	0.04	210	7850
C1	5.4	Circular	0.02	210	7850
C2	2.7	Circular	0.02	210	7850

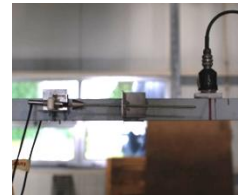
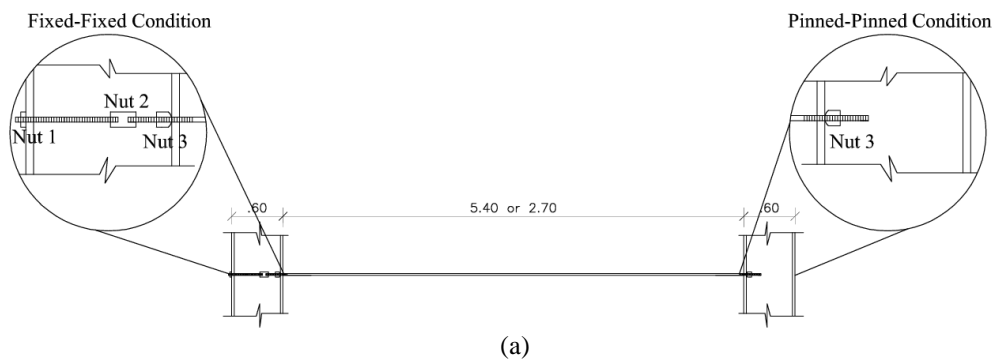


Figure 5.26 – Experimental tests in the tie-rods: (a) scheme of the test; (b) laboratory setup; and (c) LVDTs arrangement and application of the tensile force

Due to the limited measurable band of frequencies with the developed WSN, these platforms were only considered for carrying out the experimental tests of the longer square bars (S1 in Table 5.8) in pinned-pinned condition; see Luong (2010) for other tests. As shown in Figure 5.27, the dynamic response of the tie-rod was studied in five tensile stages considering that the first one corresponds to the original stress condition due to the self weight of the specimen.

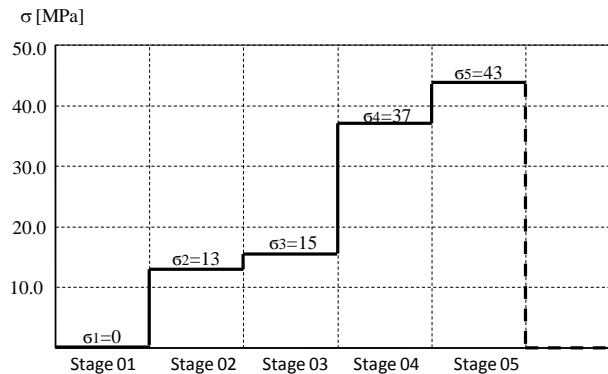


Figure 5.27 – Considered tensile stages during the experimental tests – Case study of tensile tests in tie-rods

As presented in Figure 5.28a, three sensing units with MEMS Accelerometers Type A were symmetrically deployed in the tie-rods. In Figure 5.28b, it can be observed that the base station of the WSN was located around 12 m far away from the sensing nodes. A close up view of how the measurement nodes were fixed to the tie-rods is shown in Figure 5.28c. For the case of the conventional wired based piezoelectric accelerometers, six sensors with the characteristics presented in section 5.3.1 were used. The DAQ equipment used in this case was the NI SCXI-1531 with embedded 16 bits ADC resolution. The acquisition parameters considered for the conventional systems were of 500 Hz and 60 seconds while for the wireless systems were of 100 Hz and 30 seconds for the sampling rate and sampling time respectively. Due to the complexity of the experimental work, it was not possible to run the analyses with the conventional platforms and the wireless systems in parallel. Nevertheless, for determining the accuracy in the frequency content, the results corresponding to the conventional systems are going to be considered as reference values.

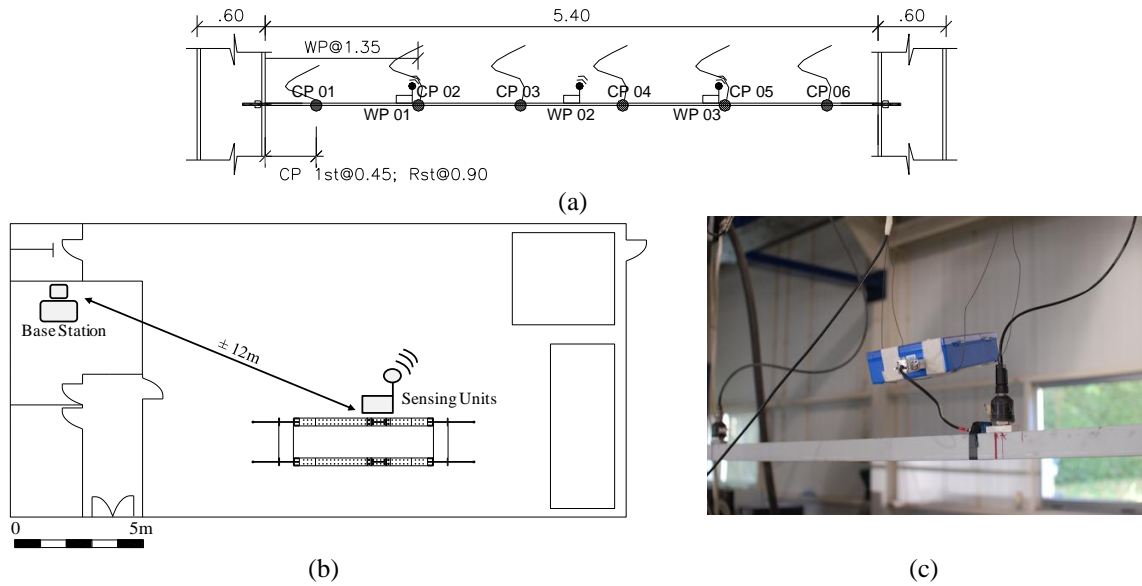


Figure 5.28 – Deployment of sensors in the tie-rods' experimental tests: (a) arrangement of sensors; (b) laboratory plant view with the scheme of the location of the wireless system; and (c) close up view of the sensing nodes

5.4.3 Modal Identification Results

Two examples of the time domain series registered with the developed WSN system corresponding to the original and last tensile states (0 MPa and 43 MPa) are shown in Figure 5.29. The presented time domain registers, for the three accelerometers WP 01, WP 02 and WP 03, clearly show the testing procedure which consisted in the application of random impacts to the tie-rods aiming to get better quality frequency domain spectrums.

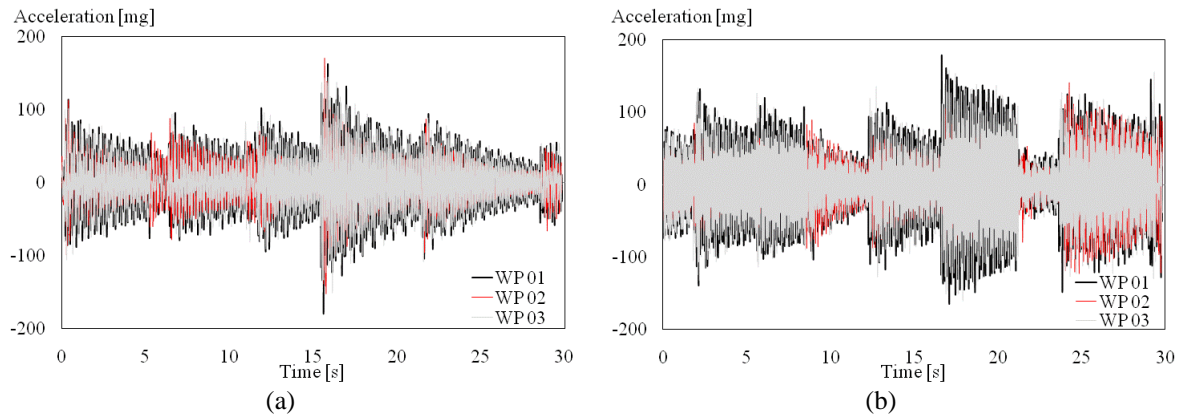


Figure 5.29 – Time domain recordings with the developed WSN platforms – Case study of tensile tests in tie-rods: (a) series corresponding to 0 MPa of tension stress; (b) series corresponding to the maximum tension stress of 43 MPa considered

The maximum values of acceleration registered in the five tensile states tests and the RMS of the acquired signals are summarized in Table 5.9. Figure 5.30 shows the resultant frequency domain spectrums obtained from the measurements of the developed system at each tensile state. As expected, high resolution frequency domain series were obtained in the performed experimental tests. In the resultant spectrums, the evolution of the first three natural frequencies (x axis) accompanying the stress increment can be clearly observed evidencing the reliability of the performed process.

Table 5.9 – Summary of the time domain indicators resultant from the collected information of the developed WSN platforms – Case study of tensile tests in tie-rods.

Stress State (MPa)	Max (mg)			RMS (mg)		
	Node 01	Node 02	Node 03	Node 01	Node 02	Node 03
0.0	179.54	170.77	151.02	37.68	26.73	37.39
13.0	144.86	152.33	151.79	41.10	36.77	40.48
15.0	180.36	138.74	154.71	42.25	28.88	42.22
37.0	95.07	90.33	81.21	26.81	21.17	26.99
43.0	178.74	140.33	160.99	52.35	36.51	52.22

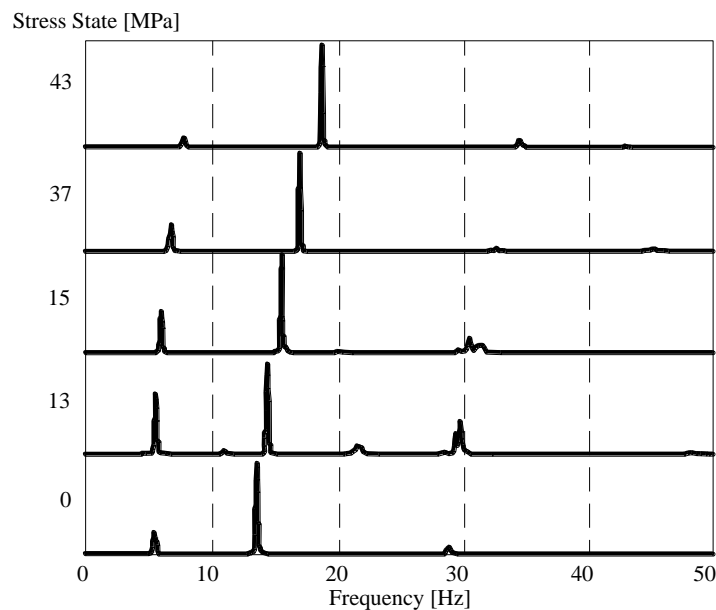


Figure 5.30 – Frequency domain results from the data recorded with the developed prototype of WSN platforms – Case study of tensile tests in tie-rods

Due to the high quality of the frequency domain registers, the feasibility for applying non-parametric data processing method such as the Frequency Domain Decomposition method – FDD (Brincker et al., 2000a) was evidenced. The estimation of the natural frequencies corresponding to the conventional wired based and the developed wireless systems were calculated using the referred FDD method. These results are presented and compared in Table 5.10. The obtained results confirm the excellent performance of the developed systems since estimations with minor variations (less than 1% in most of the cases) were registered.

Table 5.10 – Comparison of the frequency estimations resultant from the data recorded with the conventional and developed systems – Case study of tensile tests in tie-rods.

Stress State (MPa)	Conventional System (Hz)			Developed WSN System (Hz)			Percent Error Comparison (%)		
	f_1	f_2	f_3	f_1	f_2	f_3	$e-f_1$	$e-f_2$	$e-f_3$
0.0	5.49	13.76	29.04	5.50	13.64	29.00	0.2	0.9	0.1
13.0	5.63	14.55	29.98	5.57	14.50	29.86	1.1	0.3	0.4
15.0	6.02	15.67	31.18	6.01	15.62	31.09	0.2	0.3	0.3
37.0	6.83	17.10	32.80	6.76	17.10	32.80	1.0	< 0.01	< 0.01
43.0	7.83	18.89	34.99	7.80	18.82	34.98	0.4	0.4	0.1

The results corresponding to the experimental estimations of modal shapes for the five levels of tensile states considered are presented in Figure 5.31. For validation purposes, the obtained results are compared against their counterparts obtained from the measurements of the conventional sensors (it should be noted that these last values coincide with the theoretical modal shapes). The results of the first and second mode shapes from the information recorded with the developed systems evidence a remarkable similitude with the ones obtained from the measurements of the conventional system. Even if for the first case, the MAC values calculated are not as high as the ones calculated for the second mode, the modal shapes corresponding to the five stress states considered are clearly distinguishable. In case of the estimations of the third mode shape, they show higher uncertainties and thus for their estimation an experienced analyst is needed. Even if these results were not as good as expected, they should be positively considered as contributions that should be taken into account in future adjustments or developments in the prototype system developed. Only for references purposes as this discussion is outside the scope of this thesis, the correlation of the estimated natural frequencies and the theoretical solutions for pinned-pinned and fixed-fixed conditions are presented in Figure 5.32.

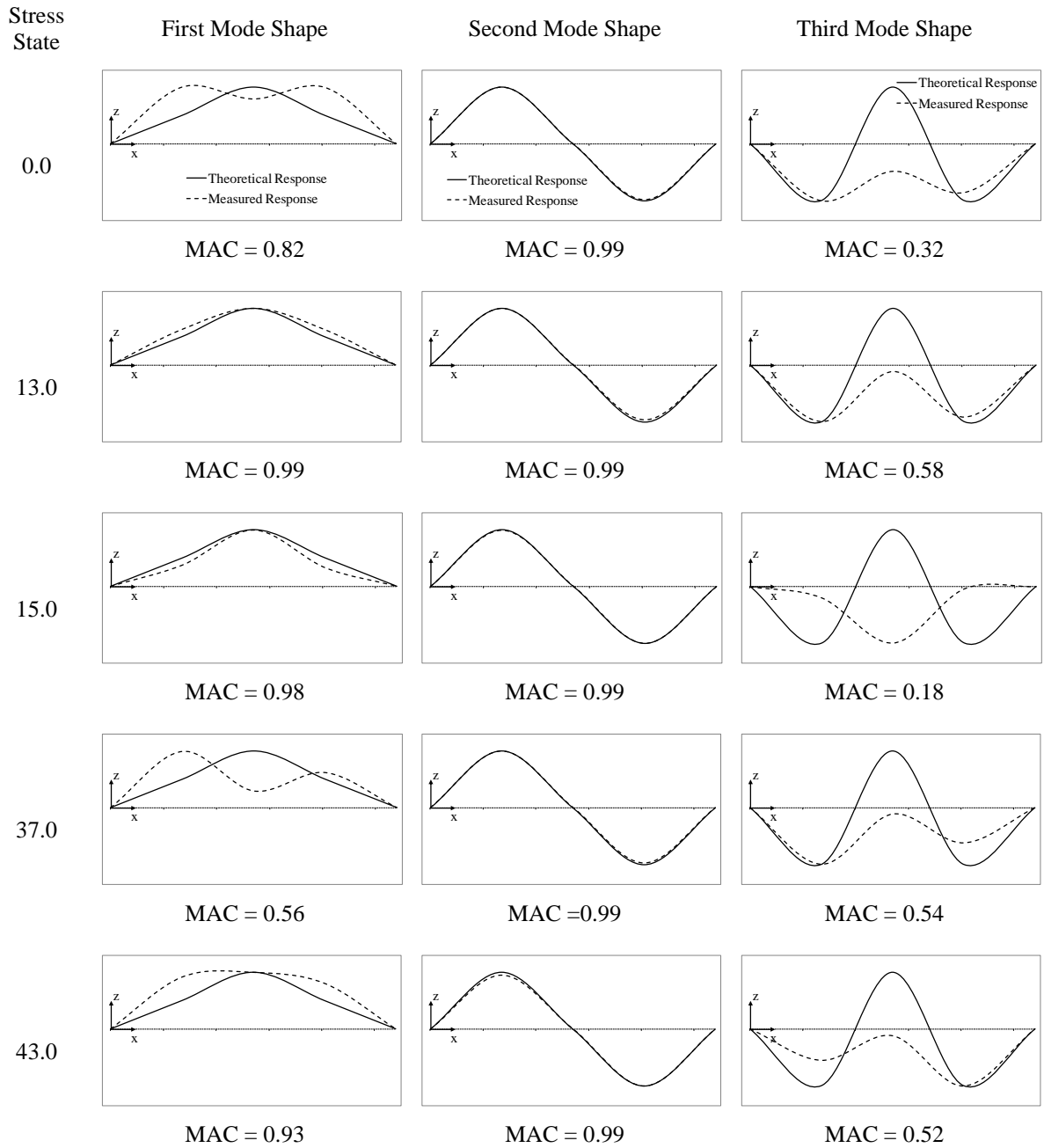


Figure 5.31 – Results of the experimentally estimated modal shaped with the new WSN platforms and comparison with their counterparts obtained from the conventional wired based systems (equal to the theoretical modal shapes) – Case study of tensile tests in tie-rods

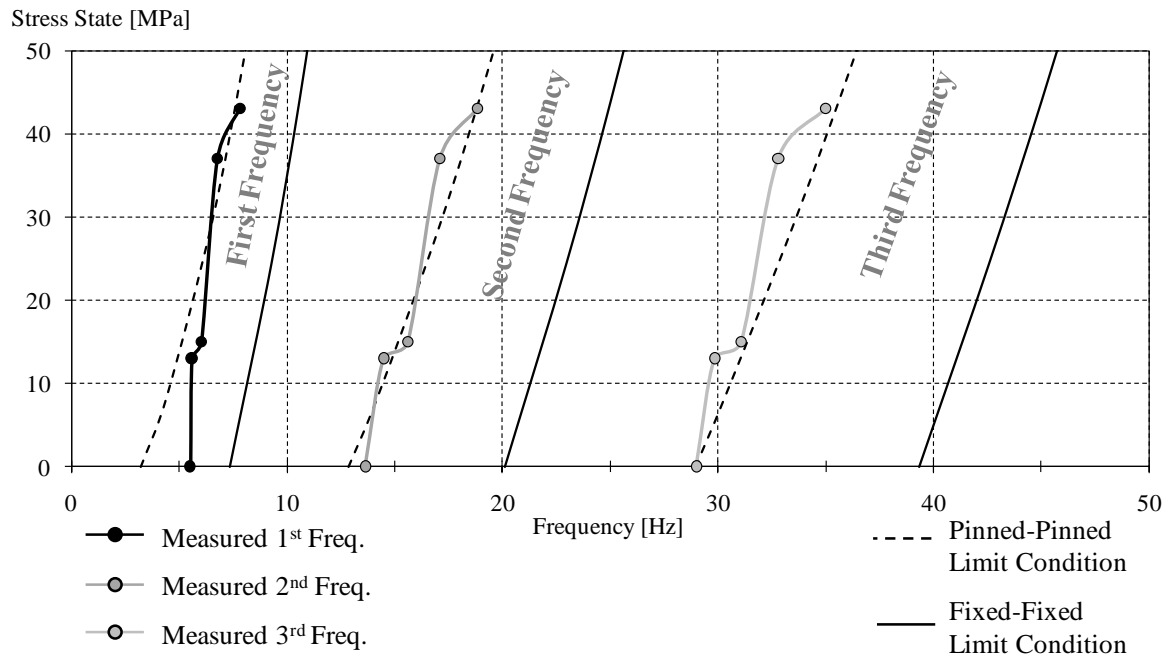


Figure 5.32 – Comparison of the experimentally results of the first three natural frequencies and the theoretical results corresponding to the extreme conditions of pinned-pinned and fixed-fixed boundary conditions – Case study of tensile tests in tie-rods

5.5 Proposed Approach for Improving the Data Transmission Process

As it was stated by Zimmerman et al. (2008), one of the main limitations for the application of WSN_s in dynamic monitoring works is the huge quantities of data usually collected. This single limitation is the origin of several problems, such as; scalability of the networks, possibility of data collisions, high power consumptions, and data losses, which make the practical implementation of these solutions difficult.

It was observed that the main drawback of the developed solution is precisely related to the long data transmission times required for performing the synchronization among the sensing nodes. This section intends to provide a theoretical approach for improving the performance of the developed solution. This approach is based on the basic theory of experimental modal analysis and explores the possibility of transmitting only the information of the averaged Fast Fourier Transform (FFT), known as Welch method (Welch, 1967), of each sensing node without compromising the quality of the results of frequencies and mode shapes.

5.5.1 Conceptual Formulation

The proposed approach states that if the data transmission process only considers the information resultant from the application of the Welch method to the collected data of each sensing node (real and imaginary parts), high data compression rates can be attained. According to this approach, instead of transmitting huge time domain series, only a few frequency domain data (corresponding to the length of the averaging window commonly set as 512, 1024 or 2048 points) would be broadcasted. The summary of the proposed solution is schematically presented in Figure 5.33. The proposed approach was tested in two different tests. Firstly artificially generated data is considered where, under controlled status, the procedure can be clarified. Secondly, the information acquired in a real case study is considered where the proposed procedure can be validated in real field conditions.

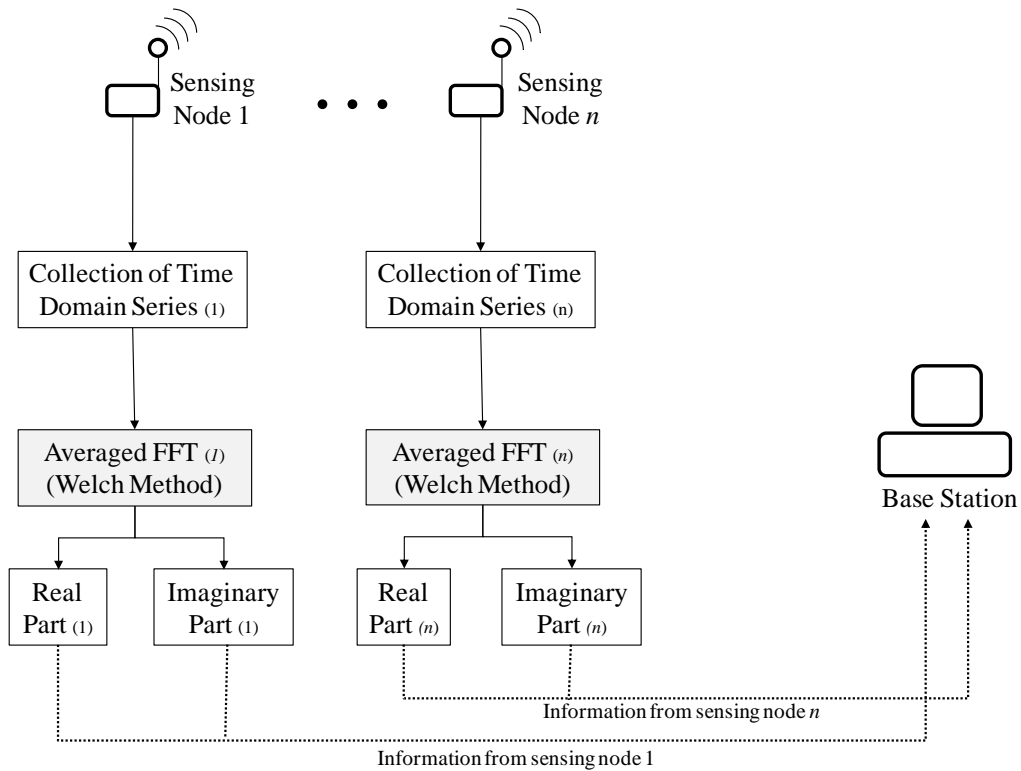


Figure 5.33 – Scheme of the proposed approach for improving the data transmission process

5.5.2 Validation with Numerical Data

The first validation tests were carried out considering the generation of artificial signals in an environment without noise using three fictitious measurement nodes and considering a sampling rate and a sampling time of 100 Hz and 300 seconds respectively. The theoretical frequencies and normalized mode shapes coordinates of these artificial signals are shown in Table 5.11.

Table 5.11 – Theoretical frequencies and mode shapes of the generated signals.

Frequencies (Hz)	Normalized Mode Shapes		
2.50	1.00	-0.50	-0.30
8.50	0.50	1.00	0.20
20.50	0.85	0.65	-1.00

Considering 1024 points (the frequency resolution will be 0.097 Hz) and 50% for the window length and overlapping criteria respectively, the Welch method was applied to the generated signals of each of the measurement nodes separately. The result of this process is one complex vector for each sensing node containing the information of frequencies and mode shapes of the studied system. In the case of the frequencies, these are estimated using the real part of the referred vector, where the peaks with higher amplitude indicate the presence of the natural frequencies. On the other hand, the modal shape information is

extracted from the imaginary part of the obtained complex vector by registering the y coordinates evaluated at each of the values of the natural frequencies of interest (x axis).

The summary of the resultant information from the explained procedure applied to the present case study are presented in Figure 5.34. As it can be observed, due to the use of clean signals without added noise, clear frequency domain spectrums (plots of the real part of the averaged FFT) were obtained. In the case of the plots of the imaginary part of the averaged FFT, these also showed clear peaks around the natural frequencies indicating the feasibility for properly performing the mode shape extraction task.

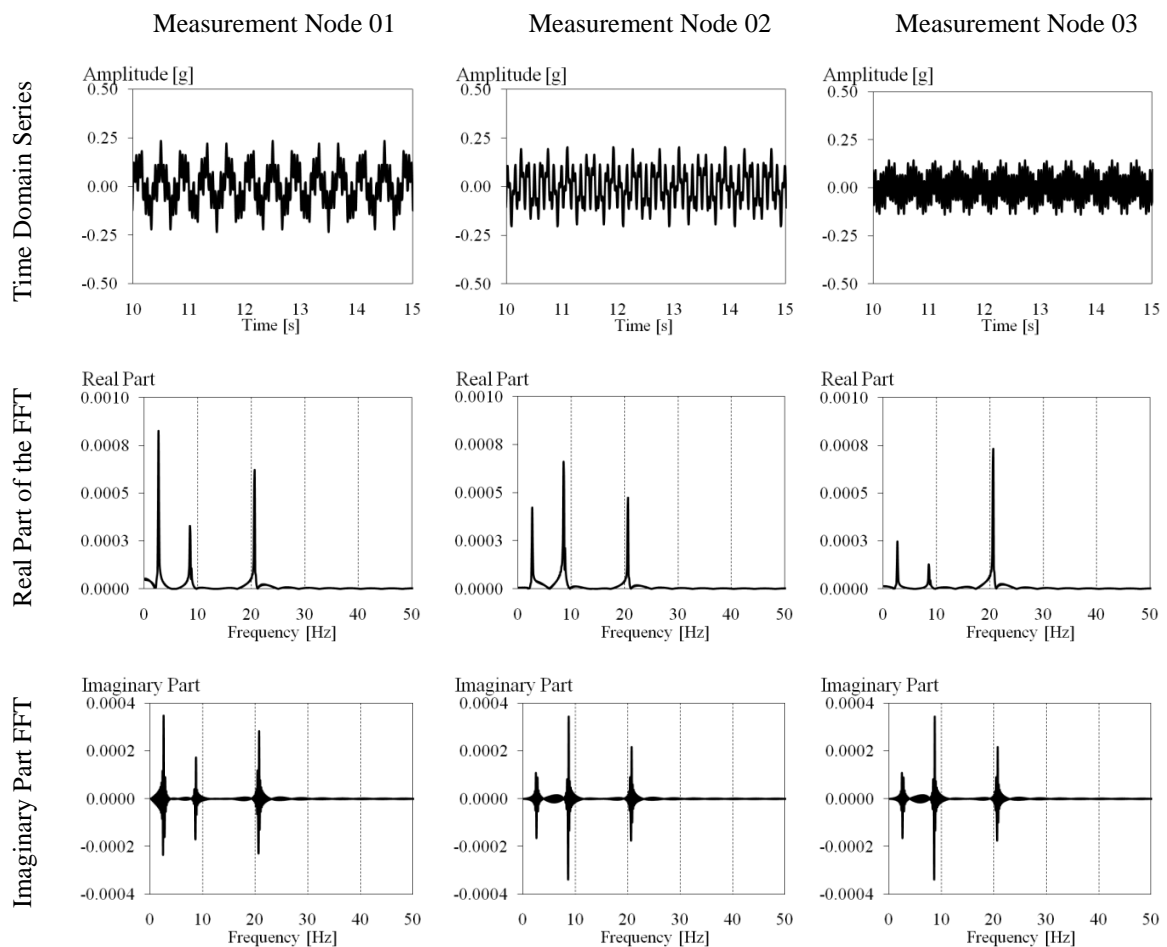


Figure 5.34 – Summary of time domain series and results of the real and imaginary plots for the present case study

The estimations of natural frequencies and mode shapes from the proposed approach, as well as their comparison with the theoretical values (Table 5.11), are summarized in Table 5.12. These results confirmed that if only the information resultant from a specified window length of the FFT (1024 in this case) of each sensing node is transmitted, the content of frequencies and mode shapes maintains high reliability levels.

Table 5.12 – Results of frequencies and mode shapes after the application proposed approach.

Frequencies (Hz)	Percent Error (%)	Normalized Mode Shapes			MAC
2.46	1.6	1.00	-0.46	-0.30	0.99
8.64	1.7	0.50	1.00	0.21	0.99
20.67	0.8	0.85	0.65	-1.00	1.00

The most important contribution of the proposed approach is the data compression rate that can be attained. For the case of the present study, this information is summarized in Table 5.13. Specifically for the present case, the results indicated that if the proposed approach would be remotely performed in the motes, 15 times smaller file sizes and transmission times could be achieved. Since, the proposed approach considers always the broadcasting of one Welch window length; the final transmitted information size would be constant even if higher sampling rates and longer sampling times are considered which is of high interest taking into account that a variation in these variables improves the quality of the results. It should be also taken into account that the proposed algorithm can be enhanced if further compression procedures can be implemented in the mote's communication process.

Table 5.13 – Required transmission times in each of the considered approaches per sensing node (Sampling rate = 100 Hz, Sampling Time = 300 s, Welch Window Length = 1024, Welch Overlap = 50%).

Method	Transmitted Data Type / sensing node	File Size (KB)	Expected Transmission Time (min)
Conventional approach	Time domain series	557	25
	Total	557	
Proposed approach	Real components	19	1.7
	Imaginary components	19	
	Total	38	

5.5.3 Validation with Field Collected Information

The second case study was related to the application of the proposed approach for processing the data acquired during the experimental tests of the tie rods presented in section 5.4. In this case, only the information collected with the conventional wired based sensors will be used since, contrarily to what happened with the wireless platforms, in those tests longer sampling times and wider measurable frequency range were considered (60 seconds for the sampling time and 500 Hz for the sampling frequency). The results and conclusions of the present analysis are also valid if the data acquired with the developed WSN solution would be used since, as it was discussed in the previous sections, similar

results to what can be obtained from the conventional transducers are feasible to achieve. With these considerations, the information collected in the tests of the circular tie rods with 5.4 m length (C1 in Table 5.8), in pinned-pinned condition, and in two tension states (0 MPa and 73 MPa) will be analyzed using the proposed approach. The deployment of sensors (only three measurement nodes will be considered) and the scheme of the experimental layout is shown in Figure 5.35.

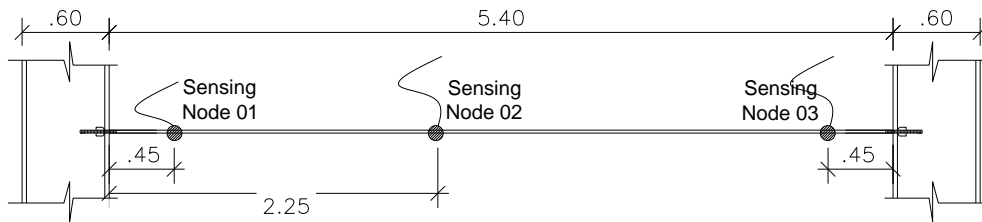


Figure 5.35 – Location of the sensors that will be processed using the proposed approach

The proposed approach was applied to the collected data considering again 1024 points for the window length and 50% for the overlapping criteria. Therefore, the frequency resolution of the results was 0.488 Hz. Figure 5.34 shows the information corresponding to the recorded time domain series as well as the plots of the imaginary and real parts of the averaged FFT which will be next analyzed for extracting the modal information. As shown, due to the fact that the studied structure is flexible and easy to excite, frequency domain signals with good quality were registered. This, as the results indicated, influenced also the quality of the imaginary domain plots where the coordinates of the peaks corresponding to the natural frequencies were easy to detect.

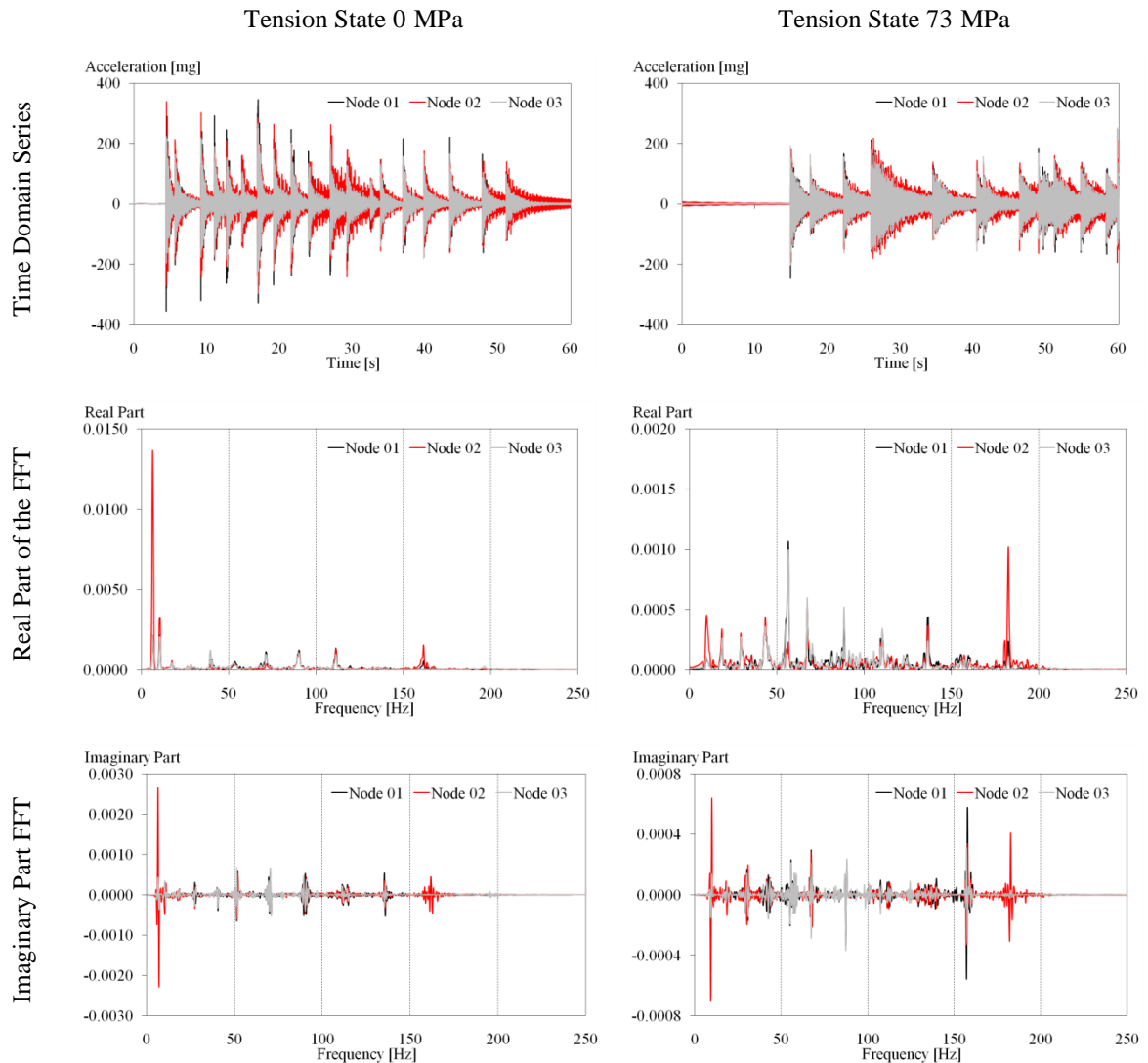


Figure 5.36 – Summary of time domain series and results of the real and imaginary plots for the case of the tie rods tests

From the presented results, the information of the natural frequencies and mode shapes of the structure was extracted. The estimations corresponding to each tension state (0 MPa and 73 MPa) are presented in Table 5.14 and Table 5.15 respectively. For comparison purposes, the results of the application of the FDD method (implemented in the Artemis software) to the same collected information are also included. Considering the outcomes of the FDD method as reference, the results confirmed that with the use of the proposed approach reliable estimations are expectable. In the case of the frequency estimations, smaller errors than 5% were registered, while for the case of the modal coordinates, the high values of MAC obtained (all of them very close to 1) indicate the feasibility of the proposed approach in real field studies.

Table 5.14 – Results of frequencies and mode shapes after the application proposed approach to the collected information in the tie bars tests in 0 MPa of tension state.

Frequencies (Hz)			Normalized Modal Coordinates						MAC
FDD (Artemis)	Prop. App.	Percent Error (%)	FDD (Artemis)			Proposed Approach			
			Node 01	Node 02	Node 03	Node 01	Node 02	Node 03	
6.10	6.36	4.2	0.16	1.00	0.16	0.16	1.00	0.16	1.000
10.01	10.27	2.6	0.69	1.00	-0.67	0.68	1.00	-0.66	0.999
17.58	17.12	2.6	0.91	-1.00	0.91	1.00	-0.99	0.90	0.998
27.10	27.40	1.1	-0.88	1.00	0.88	-0.95	1.00	0.85	0.998
39.31	39.14	0.4	0.99	0.23	1.00	1.00	0.24	0.99	0.999
51.51	51.37	0.3	1.00	0.86	-0.94	0.98	0.80	-0.91	0.999
70.07	69.96	0.2	1.00	0.28	0.90	0.99	0.36	1.00	0.995
89.36	90.02	0.7	-1.00	0.87	0.86	-1.00	0.88	0.85	0.999
111.33	111.10	0.2	1.00	-0.86	0.71	1.00	-0.97	0.66	0.995
135.25	135.50	0.2	-1.00	-0.71	0.55	-1.00	-0.60	0.49	0.994
161.13	161.40	0.2	-0.35	-1.00	-0.03	-0.35	-1.00	-0.01	0.999

Table 5.15 – Results of frequencies and mode shapes after the application proposed approach to the collected information in the tie bars tests in 73 MPa of tension state.

Frequencies (Hz)			Normalized Modal Coordinates						MAC
FDD (Artemis)	Prop. App.	Percent Error (%)	F (Artemis)			Proposed Approach			
			Node 01	Node 02	Node 03	Node 01	Node 02	Node 03	
9.03	9.30	3.0	0.21	1.00	0.20	0.22	1.00	0.20	0.999
18.80	18.59	1.1	-0.80	-1.00	0.76	-0.73	-1.00	0.72	0.998
29.54	29.84	1.0	-0.91	1.00	-0.86	-0.84	1.00	-0.77	0.998
41.50	42.07	1.4	0.95	-1.00	-0.90	0.82	-0.98	-1.00	0.990
55.42	55.77	0.6	1.00	0.29	0.93	1.00	0.24	0.95	0.999
67.38	67.51	0.2	-0.97	-0.92	1.00	-0.90	-0.93	1.00	0.999
87.16	87.57	0.5	0.96	0.07	1.00	0.94	0.07	1.00	0.999
109.13	110.10	0.9	-1.00	0.91	0.92	-1.00	0.86	0.97	0.998
136.23	136.50	0.2	1.00	-0.89	0.58	1.00	-0.81	0.54	0.998
156.98	157.50	0.3	-1.00	-0.59	0.56	-1.00	-0.56	0.55	0.999
181.89	182.00	0.1	-0.23	-1.00	-0.10	-0.24	-1.00	-0.10	0.999

The information presented in Table 5.13 regarding the attained data compression rate (1/15) can be also used for this case study since, even if different acquiring criteria were here used, the same numbers of points were recorded (30000 points per sensing node) and the proposed approach was performed considering the same criteria.

5.6 Conclusions

In the present chapter, the first prototype of a WSN platform specially developed for performing OMA studies in existent structures was presented. This platform is a product of a multidisciplinary work of electronic, communications and civil engineers carried out to fulfill the demanding requirements of these tests.

The measurement transducers in the developed system consisted in two options of triaxial, high sensitivity, and high resolution MEMS accelerometers named in this work as Type A (ASC 5521-002) and Type B (ASC 5631-002) while the network's communication process was performed using TelosB boards. One of the main issues of the WSN_s is the synchronization among sensing nodes which in this case was properly accomplished with the implementation of a beacon based solution using the 802.15.4 communication protocol.

Using the developed platforms, laboratory validation tests were carried out considering the inverted wooden pendulum previously studied in Chapter 4 as testing specimen and the conventional wired based sensors as reference systems. The results of the time domain validation tests showed acceptable similarities in the signals recorded with both systems. In case of the MEMS accelerometers Type A, the results showed the feasibility for their application in scenarios where moderate environmental noises are expected (vibrations amplitude above 1 mg). On the contrary, the MEMS accelerometers Type B have shown a good performance even in low noise scenarios since vibrations higher than 0.1 mg were properly recorded. The results of the frequency domain validations tests evidenced the excellent performance of the developed systems since high quality spectrums in medium (MEMS Type A) and low (MEMS Type B) noise environments were registered. Repeatability evaluation tests were carried out as well, aiming at observing if significant variations in the content of frequencies would be evident in consecutive tests. These results showed that high reliability can be expected when these systems are used, since low deviations from one test to the other were registered. The modal identification stage in these laboratory validation tests was performed using the SSI method. The results of this process showed clear stabilization diagrams obtained through the measurements of the developed systems. In the experiments performed with different pendulum configurations, the stable poles appeared properly aligned coinciding to what was obtained by the conventional sensors confirming the efficacy of the new systems. From this process, it can be concluded that frequencies, damping coefficients and modal shapes can be reliable

estimated from the measurements of the developed solution since results with low dispersions in comparison to the ones obtained from the conventional systems were calculated.

The developed systems were further used for experimentally assessing the service stress state of tie-rods by means of modal identification tests. In this respect, several laboratory tests were carried out considering different levels of applied tensile force. The results of these tests confirmed the efficiency of the developed systems since accurate frequency estimations were achieved. In the case of the identified modal shapes, these also indicated enough precision evidencing the utility of the developed system.

The last part of this chapter presents a theoretical approach for reducing the time duration in the network's communication processes, identified as the main drawback of the developed system. This approach aimed at taking advantage of the remote processing capabilities of the motes for performing simple calculations such as the averaged FFT. These results have shown that, if the process of data transmission only considers the information of one window length resultant from the application of the Welch method, still reliable information can be transmitted and high data compression rates can be attained.

The experimental campaign allowed also the identification of short, medium and long term goals in further developments of the platforms. These are related to: improvement of the signal conditioning process, improvement of the ADC capabilities, improvement of the appearance of the sensor board, implementation of data compression algorithms, deeper characterization of the energy consumption aspects, consideration of the static sensors available in the TelosB boards, and implementation of other network's communication topologies (at the moment the system is working in a single hop configuration).

CHAPTER 6

Automatic System Identification Procedures for Operational Modal Analysis

Abstract

The feasibility of implementing damage detection tools and/or real-time interpretations of the information collected in dynamic monitoring studies relies on the use of automatic feature extraction processes.

This chapter presents two variations of an algorithm for remotely processing the information recorded in Operational Modal Analysis (OMA) tests. The referred algorithm uses the cluster analysis and the rule-based approach for constructing and interpreting the stabilization diagrams resulting from the application of the Stochastic Subspace Identification (SSI-Data) method to raw time series data.

For practical considerations, the proposed algorithm was also implemented into a software tool which was used for automatic processing the information collected in several rounds of numerical and field validation tests (over 8000 events were considered). The results demonstrated the accuracy and reliability of the proposed methodologies indicating that they can be used with confidence in long-term monitoring works.

6.1 Introduction

In recent years the interest of building and infrastructure designers, contractors and owners in system identification techniques for dynamic monitoring of structures has grown significantly. In this process, the implementation of automatic tools for feature extraction of modal parameters is desirable. Such implementation is not a trivial task, since traditional modal identification techniques require constant user interaction and experience.

As discussed in Chapter 3, there are two main groups of methods for Operational Modal Analysis (OMA) that can be implemented in automatic routines. One possibility is to adopt non parametric methods like the Frequency Domain Decomposition (FDD), Enhanced Frequency Domain Decomposition (EFDD) or the Peak Picking (PP) Techniques. Examples of these approaches are presented by Rainieri and Fabroccino (2010), Magalhães et al. (2008) and Zimmerman et al. (2008). Another possibility is to adopt parametric methods like the Stochastic Subspace Identification (SSI-Data) method. Examples of this second approach are given in Magalhães et al. (2009) and Scionti et al. (2003).

An important aspect to consider when implementing an automatic identification algorithm is the selection of the development environment. Currently, the most widespread data processing software is Matlab (Matlab, 2009) which offers fast and powerful tools for this purpose. But Labview (Labview, 2006) should also be considered, as many of the acquisition processes of dynamic and static experimental tests are performed using this tool. Using Labview as the data processing software allows combining data acquisition and data processing routines in the same environment.

This chapter presents the proposal of an automatic modal identification algorithm and its implementation into a Labview routine to complete the dynamic data acquisition process. The proposed algorithm uses the SSI-Data (Peeters and De Roeck, 1999) for the modal identification complemented by a combination of the cluster analysis and the rule-based approach for the automatic analysis. However, as the proposed tool is related to the interpretation of stabilization diagrams of the SSI-Data method, it can also be applied to the results of other parametric processing methods.

6.2 Automatic Feature Extraction Algorithm for Operational Modal Analysis Data

The proposed algorithm uses the SSI-Data method as the main tool for the modal identification process, which is in turn complemented by a combination of the cluster analysis and the rule-based approach for the automatic feature extraction process.

In the present work, non hierarchical clustering techniques are used by means of a simplified version of the K-means clustering algorithm (Macqueen, 1967). The original theory of the K-means algorithm is based on the idea that, for a given set of initial clusters, the data points corresponding to each cluster are (or are not) included in the cluster based on the Euclidian distance to some central point which is in turn iteratively replaced by the clusters' mean point. These two steps are repeated until convergence. This technique is used here for building the initial sets of clusters, taking into account previously defined groups with central values that do not change. The main drawback of the K-means algorithm is the sensitiveness of the results to the selection of the initial clusters (Fung, 2001). Still, it is important to understand that in the experimental modal identification processes, the central values of the initial clusters have minor changes throughout time. Moreover, these changes can be properly determined with the study of the effect of the environmental conditions (temperature, humidity, etc) in the dynamic response of the studied systems. Non-expected changes in the cluster values would cause wrong or null estimations of the proposed methodology. Alternatively, unexpected changes can also be interpreted as an alert, if they represent damage in the structure.

The main assumption for the development of the proposed automatic modal identification algorithm is that there is confidence on the estimations of the natural frequencies and modal shapes, while it is accepted that the damping coefficients exhibit large scatters and their estimations are less reliable. The proposed algorithm considers two consecutive steps: the construction of stabilization diagrams and the selection of the proper model order where the parameters will be estimated.

The first step is performed by creating clusters of data based on the similarity criterion. In the algorithm, the number of clusters is initially defined and corresponds to the number of frequencies of interest. The objects in each level of the cluster of interest are selected considering the similarity between the estimated frequencies and damping coefficients with respect to previously defined control values. The similarities in the frequency estimations

for the iteration level of the model order i and the referred control values CV are calculated according to their Euclidian distance d as stated in Equation 6.1, while an additional criterion is defined in Equation 6.2 for damping, namely:

$$d_{(CV,i)} = |f_{CV} - f_i| \leq \text{Freq. Threshold Value} \quad \text{Equation 6.1}$$

$$\text{Min. Damp. Threshold Value} \leq \zeta_i \leq \text{Max. Damp. Threshold Value} \quad \text{Equation 6.2}$$

where f is the natural frequency and ζ the damping coefficient.

The formed n clusters can contain more than one element in each iteration level of the model order. For each of the considered clusters and for each of the model order levels, the next task is carried out by selecting characteristic values (or poles in the stabilization diagrams) which contain only one set of estimations of frequencies with their corresponding damping coefficients and mode shapes. These characteristics values are calculated according to Equation 6.3 and are defined as the estimations with higher Modal Assurance Criteria (MAC value), proposed by Allemang and Brown (1982), calculated with respect to previously defined control values.

$$\max (\text{MAC}_{CV,i})_k \quad k = [1, 2, \dots, n] \quad \text{Equation 6.3}$$

where, n is the number of clusters of interest (defined in the vector of control frequencies), and MAC the Modal Assurance Criterion.

Once the columns of poles are formed, the next task consists in identifying the stable poles and defining an appropriate level for the selection of the model order. For this purpose, the rule-based approach was used. Stable poles are defined as points whose values have minor changes in successive model orders while the selected model order corresponds to the minimum level where the stable poles appear for all the frequencies of interest. The referred concepts are implemented in an automatic routine using Equation 6.4, 6.5 and 6.6. The equations are repeated in successive iterations until a defined threshold level of the model order is reached. This threshold level should be defined beforehand as the algorithm cannot be repeated indefinitely due to the fact that high model orders include also spurious estimations (Ramos, 2007).

$$FAC = \left| \frac{f_i - f_{i+1}}{f_{i+1}} \right| \tag{Equation 6.4}$$

$$\max (FAC)_k \leq \text{Threshold value} \quad k = [1, 2, \dots, n] \tag{Equation 6.5}$$

$$\min (MAC_{CV,i})_k \geq \text{MAC Threshold value} \quad k = [1, 2, \dots, n] \tag{Equation 6.6}$$

where FAC is the Frequency Assurance Criterion.

The summary of the proposed algorithm is schematically presented in Figure 6.1. The algorithm was implemented in a Labview VI called as Automatic Modal Analyzer version 1.0 (AMA V1.0). Considering that an integral dynamic monitoring tool would also contemplate the incorporation of the data acquisition and data transmission tools, two extra modules for these purposes were implemented in the final software with the dataflow shown in Figure 6.2. It should be noted that these three modules can be used separately according to the specific necessities of each monitoring study. Figure 6.3 presents the front panel of the data acquisition and data processing modules of the developed software. The detailed Block diagram of the Modal Analysis Process module can be found in Annex D.

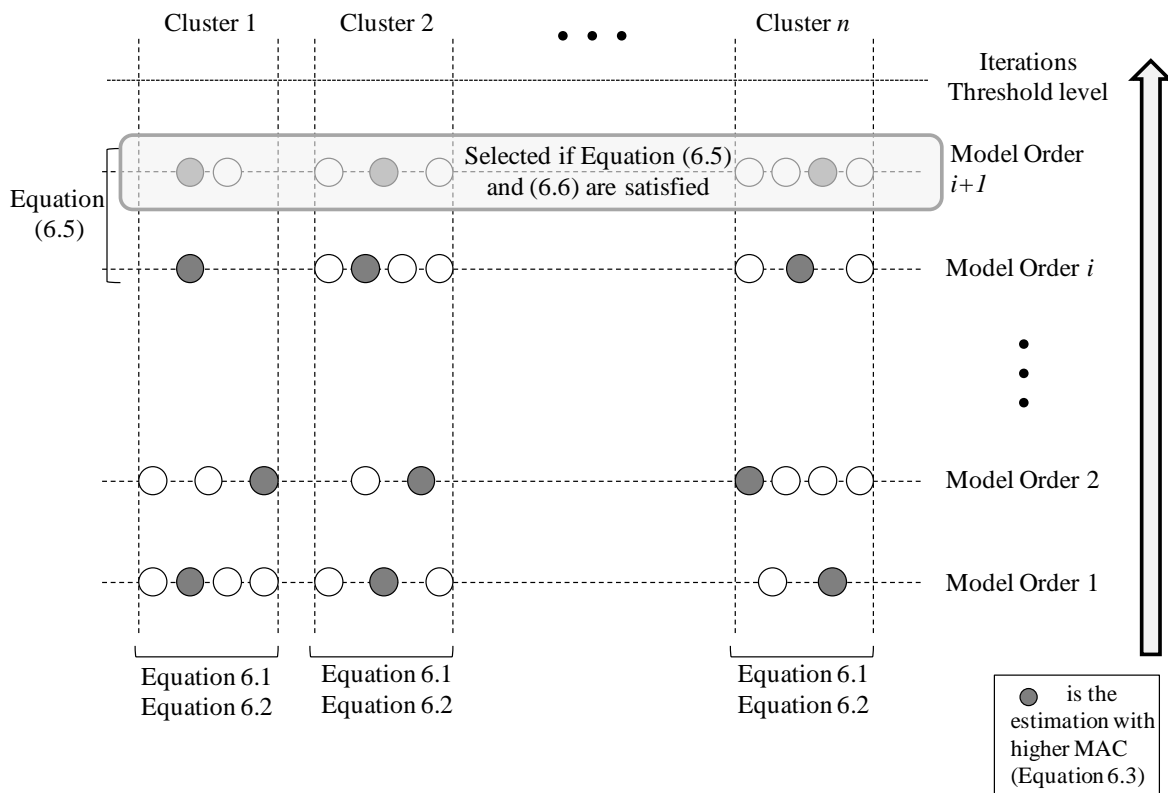


Figure 6.1 – Summary of the proposed automatic modal identification algorithm

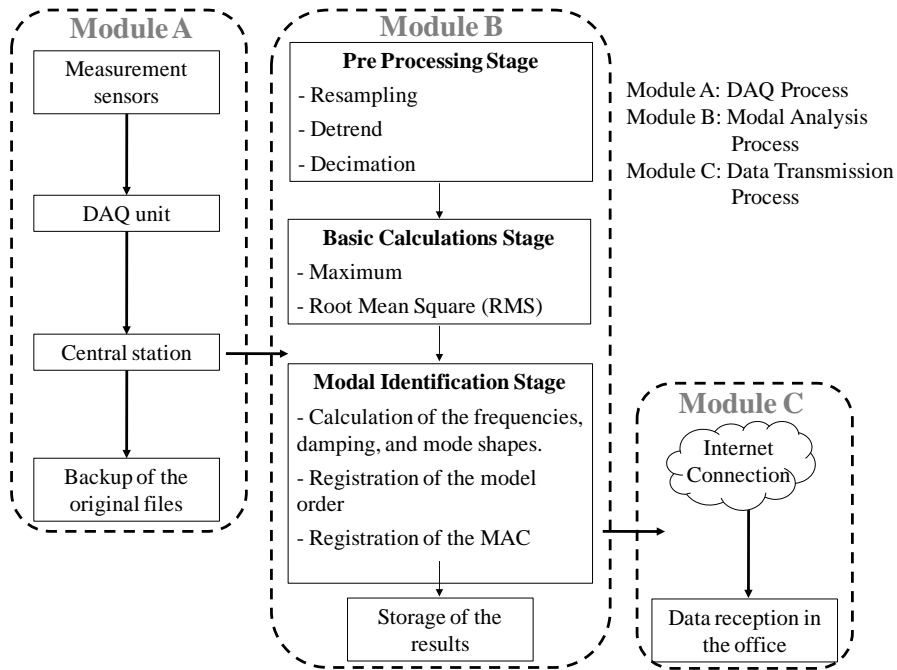
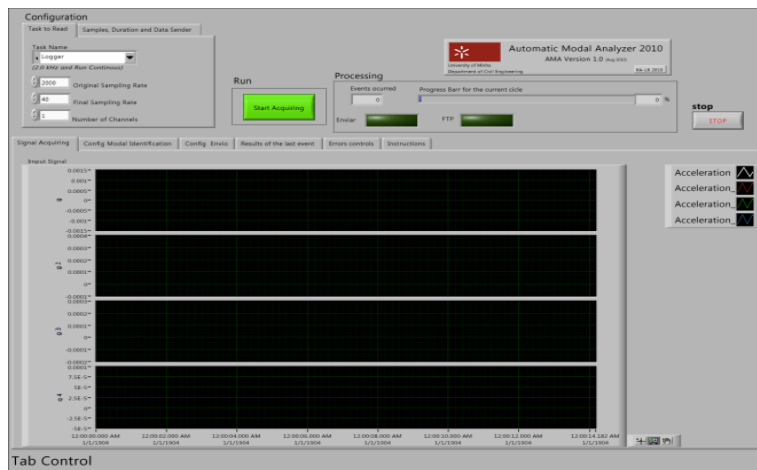
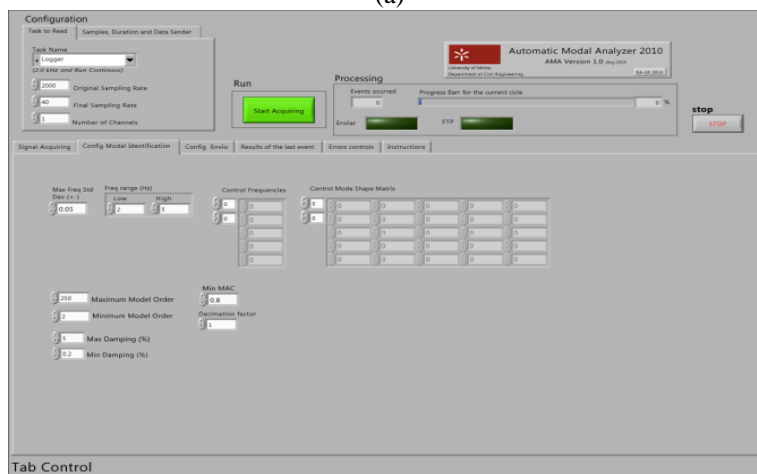


Figure 6.2 – Dataflow of the remote dynamic monitoring system developed in this work



(a)



(b)

Figure 6.3 – Front Panel of the developed Automatic Modal Analyzer tool AMA V1.0: (a) data acquisition tab; and (b) data processing tab

6.3 Numerical Validation Tests

The first tests carried out to validate the proposed automatic modal analysis algorithm considered numerical experiments with artificially signals generated using the basic theory of sinusoidal waves.

The measurements of three nodes acquiring at 100 Hz of sampling rate and 300 seconds of sampling time were simulated as undamped systems in free vibration conditions. Aiming at observing the performance of the proposed algorithm in noisy environments, several tests considering different percentages of this variable (generated as random points in the interval of interest) were studied. Table 6.1 summarizes the variables considered in the referred signals generation process.

Table 6.1 – Variables considered for the signals' generation stage of the numerical validation tests.

Mean Frequencies (Hz)	[2.25 4.25 6.25 8.25 10.25]
Sampling rate (Hz):	100
Number of measurement sensors (nodes)	3
Sampling Time (sec):	300
Noise states (% of the original signal):	0; 25; 50; 100; and 500
Number of generated events:	100 @ each noise state

In order to replicate the typical conditions of OMA tests in civil engineering structures low amplitude signals were generated. Figure 6.4 shows the time domain series of one of the events “registered” with the first sensor in three noise scenarios: 0%; 50%, and an extreme condition with 500% of added noise.

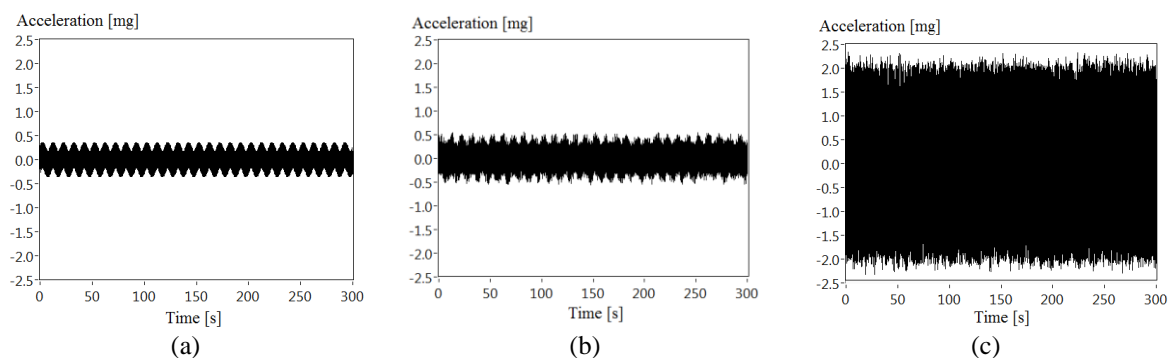


Figure 6.4 – Time domain signals “registered” with the first measurement sensor – Numerical validation tests: (a), (b), (c) signals with 0%, 50% and 500% of added noise respectively

Table 6.2 gives a general idea of the amplitudes of the generated signals in the five considered noise states. It shows the statistical information by means of the maximum peaks and RMS values registered throughout the 500 generated events (100 per noise state).

Table 6.2 – Peak Values and RMS of the time series generated – Numerical validation tests.

Noise Level	Max (mg)					RMS (mg)				
	0%	25%	50%	100%	500%	0%	25%	50%	100%	500%
Node 1	0.360	0.460	0.560	0.760	2.359	0.132	0.145	0.177	0.268	1.169
Node 2	0.209	0.309	0.409	0.609	2.209	0.116	0.131	0.165	0.261	1.168
Node 3	0.224	0.324	0.424	0.624	2.224	0.131	0.143	0.176	0.267	1.171

For simulating the effect of the ambient conditions in field tests the signals were generated in such a way that the natural frequencies had a constant variation along subsequent events. In this way, in each of the generated events and for each of the considered noise states, the signals contained five frequencies which increase in correspondence to a progression of 0.01 until half of the events were reached (50/noise state). After this, the signals' frequencies decrease in the same proportion until the last event (100/ noise state) was achieved.

Figure 6.5 shows the resultant Welch Spectrums (Welch, 1967) from the “registers” of the first sensor in three of the considered noise scenarios (0%, 50% and 500% of added noise). As expected, the quality of the frequency domain spectrum evidenced an inverse relationship to the amount of added noise. In the spectrums corresponding to 0% of added noise (Figure 6.5a) five peaks of natural frequencies were clearly detected while these peaks fade in proportion to the increment of noise until becoming almost undistinguishable in the spectrums resultant from the registers in the extreme condition of 500% of added noise (Figure 6.5c).

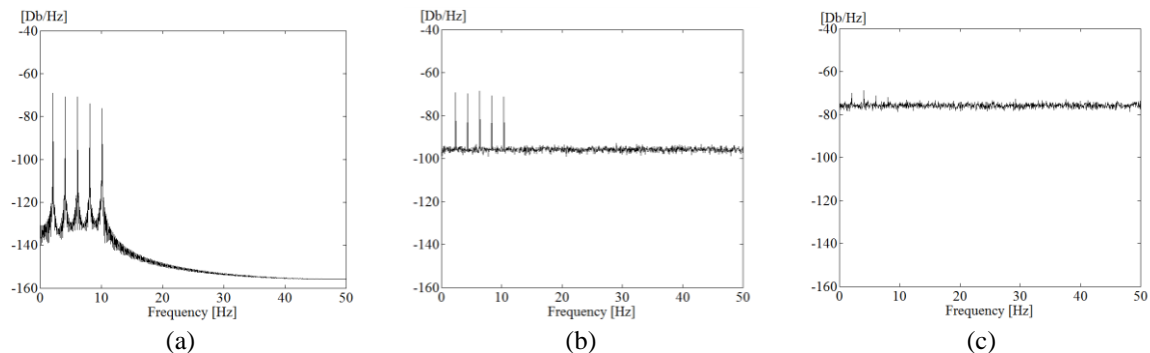


Figure 6.5 – First measurement sensor's frequency domain spectrums – Numerical validation tests: (a), (b), (c) results from the signals with 0%, 50% and 500% of added noise respectively

Since the proposed automatic feature extraction algorithm was here validated considering numerical tests, only the module B (modal analysis process) of the dynamic monitoring scheme presented in Figure 6.2 was activated. As previously mentioned, the proposed methodology for automatic modal identification requires some initial parameters

to which the estimations in each model order level are iteratively compared. The parameters that were considered as control values were the ones related to the expectable natural frequencies (frequency comparison vector, Euclidian distance threshold and FAC value), the expectable damping coefficients (maximum and minimum values) and the expectable mode shapes (mode shape comparison matrix and minimum acceptable MAC threshold value). Table 6.3 summarizes the input parameters required for running the AMA V1.0 in the present numerical validation tests.

Table 6.3 – Processing parameters AMA V1.0 – Numerical validation tests.

Freq. threshold value (\pm Hz):	0.5
Max. Damping (%):	5.0
Min. Damping (%):	1E-6
FAC threshold (Hz):	0.01
MAC threshold:	0.95
Min. model order:	2
Max. model order:	100
Decimation factor:	1
Expected frequency range (Hz):	1.5 – 12
Frequency control vector (Hz):	[2.25 4.25 6.25 8.25 10.25]
Mode shape control matrix:	$\begin{pmatrix} 1.00 & -0.10 & 0.70 & 1.00 & 1.00 \\ -0.67 & 0.50 & 1.00 & 0.10 & 1.00 \\ 0.33 & -1.00 & 0.70 & 0.90 & 1.00 \end{pmatrix}$

In this Table, the values of the frequency threshold, expected frequency range, frequency control vector, maximum and minimum damping coefficients and mode shape control matrix were chosen according to the expected dynamic properties of the studied systems. On the other hand, the FAC and MAC threshold value as well as the minimum and maximum model order were assessed based on the experience developed in the present work.

Using the AMA v1.0 tool, the natural frequencies of the 500 generated events (100/noise state) were automatically estimated. Figure 6.6 shows the results of the estimated frequencies for three of the considered noise states.

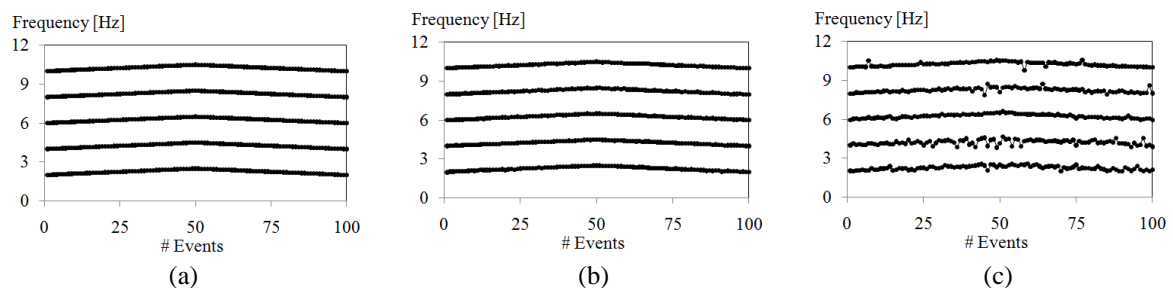


Figure 6.6 – Results of the estimated frequencies – AMA V1.0 Tool: (a), (b) (c) results from the signals with 0%, 50% and 500% of added noise respectively

The results evidenced the high accuracy of the proposed tool for performing the frequency identification task. The simulated ambient conditions (tendency of increasing and decreasing of the natural frequencies throughout the events) were properly traced even in the extremely noisy environments with 500% of noise (Figure 6.6c). Table 6.4 shows the results of the averaged values of natural frequencies and the registered average percent errors (assuming the theoretical values as references) in each of the considered five noise scenarios. The average frequency estimations evidenced a remarkable agreement even in the highest noise scenarios. In case of the maximum errors, these showed an increasing variability in direct proportion to the increase of the background noise. The results showed negligible differences (less than 1%) in the estimated frequencies up to 100% of added noise. In the estimations of the systems with extreme noise conditions (500% of added noise) higher scatter was registered showing that more estimations uncertainties are introduced as the contaminating noise levels increase.

Table 6.4 – Estimated frequencies AMA v1.0 – Numerical validation tests.

Noise Level	Estimated Frequencies Average Values (Hz)					Average Percent Error (%)				
	0%	25%	50%	100%	500%	0%	25%	50%	100%	500%
f_1	2.25	2.25	2.25	2.24	2.26	< 0.01	0.3	0.5	1.1	3.3
f_2	4.25	4.25	4.25	4.26	4.23	< 0.01	0.1	0.2	0.7	2.7
f_3	6.25	6.25	6.25	6.22	6.25	< 0.01	0.1	0.2	0.5	0.6
f_4	8.25	8.24	8.22	8.19	8.25	< 0.01	0.2	0.3	0.8	0.8
f_5	10.25	10.25	10.24	10.24	10.25	< 0.01	0.1	0.1	0.2	0.4

The following stage in the OMA processes consists in the estimation of modal shapes shown in Figure 6.7, for the first natural frequency in three noise scenarios (0%, 50% and 500%). The results corroborated the high precision of the proposed algorithm for estimating modal shapes in scenarios of low added noise. In the extreme noise scenarios, the results must be analyzed in detail since they seem meaningless.

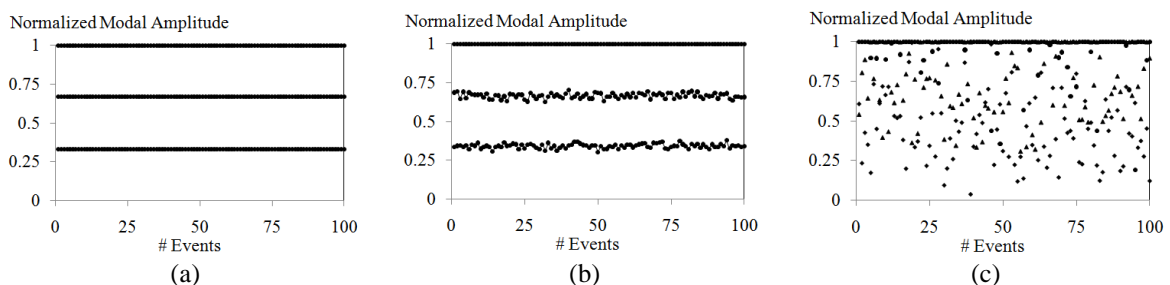


Figure 6.7 – Results of the estimated 1st mode shapes amplitudes – AMA V1.0 Tool: (a), (b), (c) results from the signals with 0%, 50% and 500% of added noise respectively

Table 6.5 confirms the previous results and details the results for five noise scenarios. The average absolute values of the modal shape estimations as well as the 10th percentile of the MAC values (calculated as a function of the values of the theoretical mode shape matrix presented in Table 6.3) are shown. The results the outstanding performance of the proposed algorithm for estimating modal shapes at least in moderate noise conditions. With this respect, the average values of the mode shapes coordinates in the first four noise scenarios (0% - 100%) have high degree of consistence among each other. In these cases, the high values of MAC registered (the lower value obtained was of 0.997) indicated the reliability of the proposed methodology and the feasibility of its application in real situations. In the case of the extremely noise conditions, the MAC value registered indicated less accurate estimations, however it is interesting to observe that MAC values over 0.90 were obtained in the estimations of the last three modes, indicating that the algorithm might be useful even in such an adverse situation.

Table 6.5 – Estimated Mode Shapes AMA v1.0 – Numerical validation tests.

Noise Level	Estimated Mode Shapes Average Absolute Values					10 th Percentile of Registered MAC Values				
	0%	25%	50%	100%	500%	0%	25%	50%	100%	500%
MS ₁₁	1.00	1.00	1.00	1.00	1.00					
MS ₁₂	0.67	0.67	0.64	0.65	0.73	1.000	1.000	1.000	0.999	0.731
MS ₁₃	0.33	0.34	0.34	0.34	0.53					
MS ₂₁	0.10	0.10	0.12	0.12	0.18					
MS ₂₂	0.50	0.50	0.50	0.45	0.83	1.000	1.000	1.000	0.997	0.609
MS ₂₃	1.00	1.00	1.00	1.00	1.00					
MS ₃₁	0.70	0.71	0.72	0.75	0.78					
MS ₃₂	1.00	1.00	1.00	1.00	1.00	1.000	1.000	1.000	0.999	0.960
MS ₃₃	0.70	0.70	0.73	0.73	1.00					
MS ₄₁	1.00	1.00	1.00	1.00	1.00					
MS ₄₂	0.10	0.11	0.13	0.16	0.63	1.000	1.000	0.999	0.998	0.919
MS ₄₃	0.90	0.90	0.89	0.89	0.92					
MS ₅₁	1.00	0.98	0.99	0.92	0.91					
MS ₅₂	1.00	1.00	1.00	1.00	1.00	1.000	1.000	1.000	0.999	0.979
MS ₅₃	1.00	0.99	1.00	1.00	0.82					

Due to the complexity of civil engineering structures, the use of a small number of control parameters seems necessary in the modal identification process. Taking this into account, the proposed methodology was modified for the case of automatic modal identification of unknown scenarios, in which the control parameters might be difficult to determine. The original modal identification methodology was adapted to consider only as control values the ones related to natural frequencies and damping coefficients. To complete the process, a relative mode shape comparison was introduced considering the

estimations i of the mode shapes as control values to which the estimations $i+1$ were compared (i is the iteration level of the model order). With the introduction of this change, the original methodology remains the same with the introduction of Equation 6.7 and 6.8 instead of Equation 6.3 and 6.6 respectively:

$$\max (\text{MAC}_{i,i+1})_k \quad k = [1, 2, \dots, n] \quad \text{Equation 6.7}$$

$$\min (\text{MAC}_{i,i+1})_k \geq \text{MAC Threshold value} \quad k = [1, 2, \dots, n] \quad \text{Equation 6.8}$$

Using the modified methodology, a new version of the tool called Automatic Modal Analyzer version 2.0 (AMA V2.0) was implemented and validated with the analytical information previously presented. As indicated in Table 6.6, in the data processing parameters required to start the modified version of the automatic identification tool, the inputs related to the modal shape control matrix were not required. This is reflected in a simplification for the practical use of the developed tool since in real studies the modal shape estimations are probably the most difficult parameters to assess. Note also that the same parameters adopted in Table 6.3 were used.

Table 6.6 – Processing parameters AMA v2.0 – Numerical validation tests.

Freq. threshold value (\pm Hz):	0.5
Max. Damping (%):	5.0
Min. Damping (%):	1E-6
FAC threshold (Hz):	0.01
MAC threshold:	0.95
Min. model order:	2
Max. model order:	100
Decimation factor:	1
Expected frequency range (Hz):	1.5 – 12
Frequency control vector (Hz):	[2.25 4.25 6.25 8.25 10.25]
Mode shape control matrix:	----

Using the AMA V2.0 tool, the natural frequencies of the time domain signals corresponding to the five noise scenarios were estimated. Figure 6.8 shows the results of this process for three of the considered noise environments (0%, 50% and 500% of added noise), while Table 6.7 summarizes the frequency assessment process by presenting the average estimations and average percent errors detected. The results indicated that precise frequency estimations can be achieved with the use of this second version of the tool since average errors of lower than 5% were evidenced for the five noise scenarios considered. It should be noted that the estimated frequencies showed high similarities to the ones

obtained from the first version of the tool (see Table 6.4) demonstrating the efficacy of the proposed algorithm's modifications.

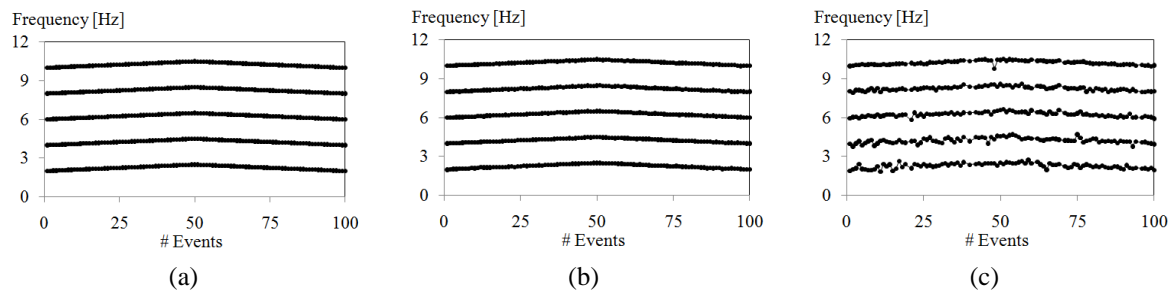


Figure 6.8 – Results of the estimated frequencies – AMA V2.0 Tool: (a), (b), (c) results from the signals with 0%, 50% and 500% of added noise respectively

Table 6.7 – Estimated frequencies AMA v2.0 – Numerical validation tests.

Noise Level	Estimated Frequencies Average Values (Hz)					Average Percent Error (%)				
	0%	25%	50%	100%	500%	0%	25%	50%	100%	500%
f_1	2.25	2.25	2.25	2.24	2.28	< 0.01	0.2	0.4	0.9	4.5
f_2	4.25	4.25	4.25	4.25	4.24	< 0.01	0.1	0.2	0.5	3.3
f_3	6.25	6.25	6.25	6.24	6.25	< 0.01	0.1	0.2	0.3	2.0
f_4	8.25	8.24	8.23	8.20	8.25	< 0.01	0.1	0.3	0.6	1.8
f_5	10.25	10.25	10.24	10.25	10.24	< 0.01	< 0.05	0.1	0.1	1.5

The results of the modal shape coordinates for the first natural frequency of the studied systems in three noise scenarios (0%, 50% and 500%) are presented in Figure 6.9. The statistical results of the modal analysis process by means of the average mode shapes values and the characteristics values of the registered MAC (calculated by taking as reference the values of the control mode shape matrix presented in Table 6.3) are shown in Table 6.8. The results confirmed the high accuracy of the methodology for estimating mode shapes. As observed in the frequency estimation task, the estimations showed also remarkable similarities to the results obtained with the first version of the tool (see Table 6.5) proving the reliability of both proposed algorithms. The high MAC values registered in most of the events (considering the 10th percentile criterion) confirmed that in moderate noise environments (0% - 100% of noise) outstandingly estimations could be attained. However, the results also showed some inaccuracies of the developed methodology when dealing with extreme noise environments which indicate that, in these cases, the results must be carefully interpreted.

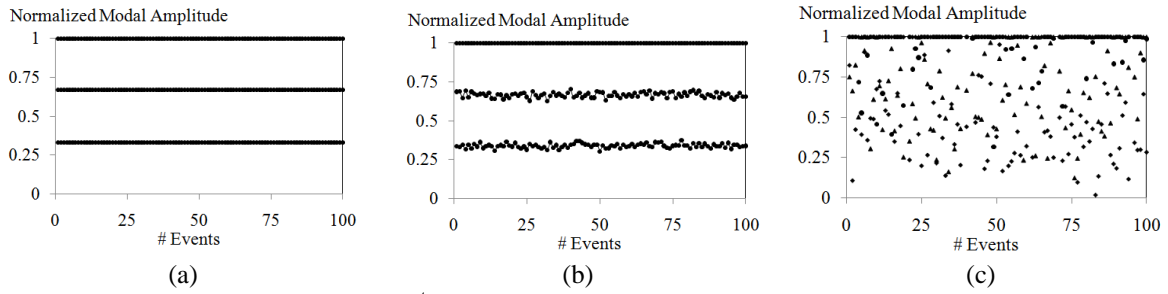


Figure 6.9 – Results of the estimated 1st mode shapes amplitudes – AMA V2.0 Tool: (a), (b), (c) results from the signal with 0%, 50% and 500% of added noise respectively

Table 6.8 – Estimated Mode Shapes AMA v2.0 – Numerical validation tests.

Noise Level	Estimated Mode Shapes Average Values					10% Percentile of Registered MAC Values				
	0%	25%	50%	100%	500%	0%	25%	50%	100%	500%
MS ₁₁	1.00	1.00	1.00	1.00	1.00					
MS ₁₂	0.67	0.67	0.64	0.63	0.73	1.000	1.000	1.000	0.999	0.796
MS ₁₃	0.33	0.34	0.34	0.33	1.00					
MS ₂₁	0.10	0.10	0.12	0.12	0.10					
MS ₂₂	0.50	0.50	0.50	0.48	0.97	1.000	1.000	1.000	0.998	0.708
MS ₂₃	1.00	1.00	1.00	1.00	1.00					
MS ₃₁	0.70	0.71	0.71	0.71	1.00					
MS ₃₂	1.00	1.00	1.00	1.00	0.31	1.000	1.000	1.000	0.999	0.941
MS ₃₃	0.70	0.70	0.73	0.73	0.33					
MS ₄₁	1.00	1.00	1.00	1.00	1.00					
MS ₄₂	0.10	0.11	0.13	0.16	0.29	1.000	1.000	0.999	0.998	0.895
MS ₄₃	0.90	0.90	0.88	0.85	1.00					
MS ₅₁	1.00	0.98	0.98	0.94	0.98					
MS ₅₂	1.00	1.00	1.00	1.00	1.00	1.000	1.000	1.000	0.999	0.965
MS ₅₃	1.00	0.99	0.99	0.99	1.00					

6.4 Structural Health Monitoring of Concrete Specimens since Casting

The evolution of the concrete properties since casting is of interest for many fields of materials science and structural applications. In the civil engineering field, the main parameters associated to this topic are the ones related to the structural setting time and the stiffness evolution over time. As stated in Azenha (2009), the referred parameters can be studied by tracking the evolution of the concrete E-Modulus since the earlier age, just after concrete casting.

The current research efforts of the scientific community in this field are based on the use of non destructive techniques such as the ultrasound or experimental modal identification tests for the determination of the E-modulus in concrete specimens. Ultrasound techniques are based on the continuous evaluation of the propagation's velocity of artificially generated sound waves in small concrete specimens which are related with their E-modulus. Due to the small scale of the specimens, this technique is sensitive to local effects and, thus, is more qualitative than quantitative (Neville, 1995). In case of experimental modal identification based techniques, the theory considers the relation of the E-modulus with the resonant frequencies that are tracked during the hardening process of the concrete. The ASTM standard that regulates this methodology (ASTM, 2002), considers the study of the dynamic response of concrete specimens outside the formwork using Input-Output techniques. The method, as it was originally conceived, does not allow the evaluation of the E-modulus at very early stages, since it can be only applied to specimens out of their casting form. The earliest evaluations of the E-modulus found in the literature using the referred methodology were of 5 hours (Nagy, 1997) and 8 hours after the casting process (Jin and Li, 2001).

Azenha (2009) proposed the improvement of the original methodology for evaluating the E-modulus at very early stages. The changes in the original conception considered the incorporation of the OMA theory and the use of a new structural configuration to skip the form removing process. The original version of the methodology consists of casting concrete into a hollow acrylic beam (100mm external diameter; 92mm internal diameter; 2000mm span). The resulting composite beam is then placed horizontally, under simply supported conditions and its first resonant frequency (which evolves along time due to the stiffening of concrete) is continuously monitored. Through the use of the dynamic equations of motion, it is possible to relate the first resonant frequency of the composite

beam with the evolving E-modulus of the tested concrete. Figure 6.10 shows an overview of the considered experimental setup as well as an example of the results of the referred methodology and their comparison with traditional compression tests.

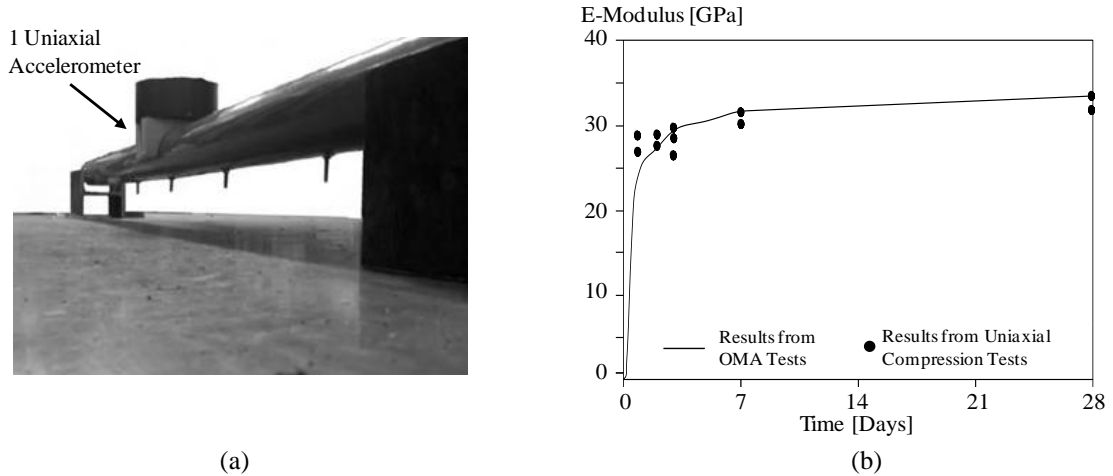


Figure 6.10 – Concrete E-modulus tracking methodology proposed by Azenha (2009): (a) experimental setup; and (b) experimental E-modulus evolution curve

The success and the accuracy of the proposed methodology rely on the “continuous” estimation of the natural frequencies which involve huge quantities of data. With the originally devised version of the method, the acquired acceleration time series were processed using the Welch procedure (Welch, 1967) after the tests were finished and therefore, the real-time information about the resonant frequency (or E-modulus) could not be obtained. The chance of improving the methodology to yield real-time information about the E-modulus evolution of concrete (based on real-time information about the identified resonant frequency of the beam) represents an interesting case study for testing the proposed algorithm for automatic modal identification.

6.4.1 Description of the Testing Specimens

Two beams with the same geometrical characteristics were cast in the laboratory of the Civil Engineering Department of the University of Minho using distinct concrete mixes. For the first specimen – CB 01 – fibre reinforced concrete was used, while for the second specimen – CB 02 – conventional concrete was considered.

Figure 6.11 shows the details of the formwork used for both beams as well as the casting process. The formwork was a steel form 1 mm thick, with cross section of 0.15 m x 0.15 m and span length of 2.4 m. The beams were cast in situ using ready-mix concrete.

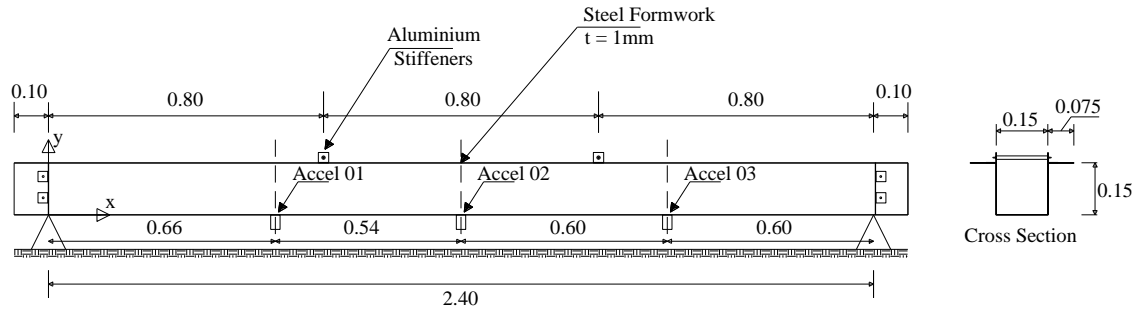


Figure 6.11 – Details of the steel formwork used for the tests of the CB-01 and CB-02 and the concrete casting process

The initial study corresponded to the characterization of the steel plate used in the formwork. With this purpose, uniaxial tensile tests were performed on the formwork’s steel plate for determining the E-modulus of the material. Figure 6.12 shows the experimental setup and the results of the performed tests.

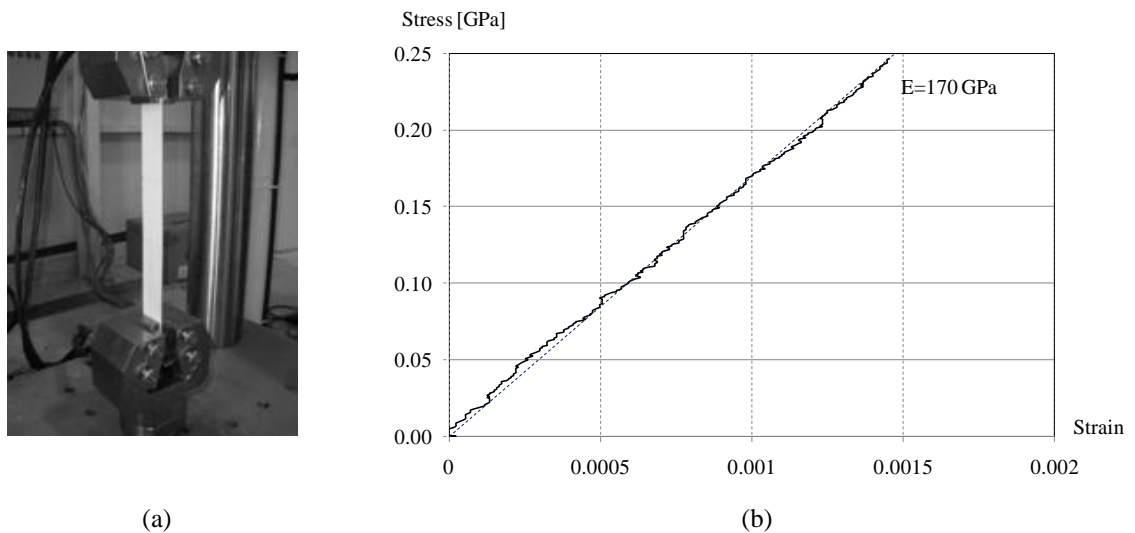


Figure 6.12 – Uniaxial tensile tests of the steel formwork’s plate: (a) experimental setup and; (b) stress-strain curve

6.4.2 Numerical Modal Analysis

When performing experimental modal identification studies it is important to have an initial idea of the expected dynamic behaviour of the studied systems. For the present case, this was achieved considering the analytical solution of a system behaving as a simply supported beam with its mass uniformly distributed (the mass of accelerometers is negligible). The dynamic response of these systems are determined according to Equation 6.9 and Equation 6.10, Chopra (1995):

$$f_n = n^2 \frac{\pi}{2} \sqrt{\frac{EI}{\rho AL^4}} \quad \text{Equation 6.9}$$

$$\psi_n(x) = \sin\left(\frac{n\pi x}{L}\right) \quad \text{Equation 6.10}$$

where n is the mode of interest, f the natural frequency in [Hz], ψ the mode shape coordinate evaluated along the bar elongation given by the coordinate x ($0 \leq x \leq L$), E the Elasticity modulus in [Pa], I the inertia in [m^4], L is the span length in [m], A is area of the cross section in [m^2], and ρ is the material's specific weight in [kg/m^3].

To calculate the analytical solution of the system, it is assumed that at the early stage of the concrete hardening process, its dynamic properties corresponds to the response of the metallic formwork beam with extra mass. In the other extreme, when the concrete is already hardened, the dynamic response corresponds to the sum of the both subsystems, the metallic formwork and the concrete beam. Using these considerations together with Equation 6.9 and 6.10, the dynamic properties of the beams were calculated and are presented in Table 6.9. For the computation of the modal shape coordinates, three measurement points were considered since three measurement sensors were used (see Figure 6.11). For the numerical calculations the following values were considered: 30 GPa and $24 \text{ kN}/\text{m}^3$ for the E-modulus and the specific weight of the concrete respectively, as well as 170 GPa and $78.5 \text{ kN}/\text{m}^3$ for the E-modulus and the specific weight of the steel.

Table 6.9 – Results of the analytical analysis of the dynamic response of the concrete beams at the beginning and the end of the performed tests.

Instant of Time	1 st Natural Frequency [Hz]	1 st Mode Shape Coordinates
t_0	22.2	[0.55 1 0.5]
t_∞	45.8	[0.55 1 0.5]

6.4.3 Dynamic Monitoring System Description

For the present case study, a dynamic monitoring system was deployed using three 10 V/g sensitivity piezoelectric accelerometers, with ± 0.5 g measuring range and one portable USB data acquisition unit model connected to a laptop computer. The dynamic monitoring system is shown in Figure 6.13.

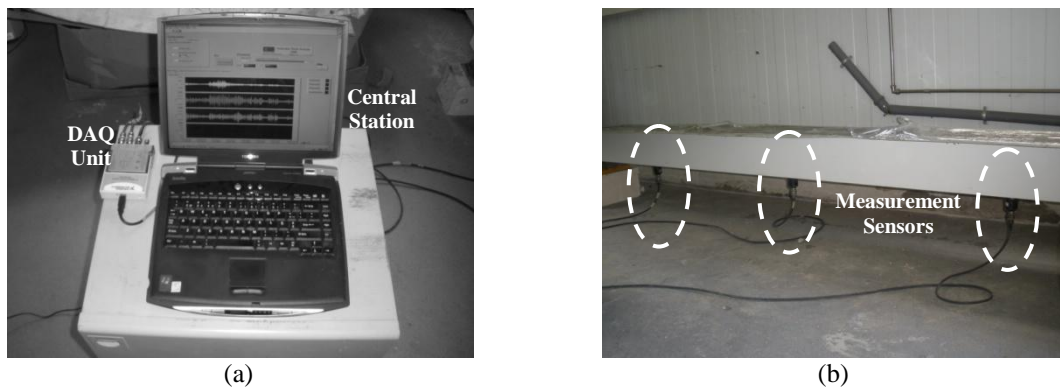


Figure 6.13 – Setup of the dynamic monitoring system used to study the hardening process of concrete specimens: (a) central acquisition unit; and (b) measurement sensors

Since the maximum expectable frequency was below 50 Hz, the data acquisition process was performed at 200 Hz. The continuous monitoring had a total duration of 50 days for CB-01 and 28 days for CB-02.

To accomplish the objective of performing a continuous monitoring process, the system was configured for acquiring short periods of data (240 sec for the CB-01 and 300 sec for the beam CB-02) with increasingly larger intervals between data acquisition periods, as the changes in frequency due to concrete hardening become increasingly smaller along time. Three time intervals between data acquisition periods were considered for the case of the beam CB-01: during the first 7 days, 15 min of interval; during the next 15 days, 30 min of interval; during the last 28 days of measurement, 60 min of interval. In the case of the beam CB-02, 15 min time intervals were considered for the whole acquisition period. In this way, 2068 events and 2381 events were recorded for the CB-01 and CB-02, respectively.

As the experimental tests were carried out in the laboratory at the University of Minho, the remote data transmission process was not needed and thus only the modules A and B (DAQ acquisition and modal analysis process) of the proposed dynamic monitoring tool presented in Figure 6.2 were activated.

The parameters that were considered as control values for running the AMA V1.0 were the ones related to the expectable natural frequencies, the expectable damping coefficients and the expectable mode shapes. The same parameters were considered for the case of the AMA V2.0 with the exception of the mode shape comparison matrix since this tool uses a relative comparison concept for performing this process. Note that the size of the frequency control vector defines the number of clusters to be considered in the analysis, which for the case of the present study, was set to one as only the estimation of the first frequency was of interest Table 6.10 summarizes the acquisition and data processing parameters used for the present case study.

Table 6.10 – Acquisition and processing parameters – Concrete hardening tracking case study.

	Description	CB – 01	CB – 02
Acquisition Parameters	Sampling rate (Hz):	2000	2000
	Decimation until (Hz):	200	400
	Number of measurement sensors	3	3
	Time to read (sec):	240	300
	Sampling interval (sec):	900; 1800; and 3600	900
	Number of recorded events	2068	2381
Processing Parameters	Freq. threshold value (\pm Hz):	17	17
	Max. Damping (%):	5.0	5.0
	Min. Damping (%):	0.1	0.1
	FAC threshold (Hz):	0.01	0.01
	MAC threshold:	0.95	0.99
	Min. model order:	2	2
	Max. model order:	250	250
	Decimation factor:	1	1
	Expected frequency range (Hz):	18 – 50	18 – 50
	Frequency control vector (Hz):	[35]	[35]
Mode shape control matrix (*):	[0.55 1 0.5]	[0.55 1 0.5]	

* Used only in the case of the AMA V1.0 tool

6.4.4 Automatic Modal Identification Results

The original version of the developed tool AMA V1.0 was first used for processing the data acquired in the experimental tests.

Figure 6.14 evidences the accuracy of the proposed algorithm for processing OMA data and presents the evolution of the first natural frequency analyzed for 50 days in the case of the CB-01 and 28 days for the CB-02. An interruption of the electronic power source for a period of four days in the testing period of the CB-02 caused the loss of data (from the 2nd day to the 5th day). Nevertheless, the tracking of the concrete hardening

process by means on the change of the first natural frequency of the system was feasible in both cases.

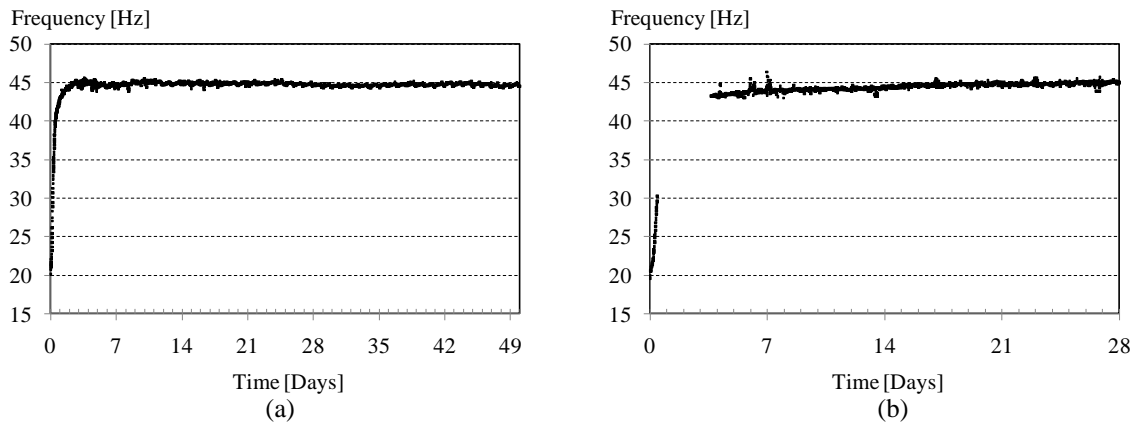


Figure 6.14 – Results of the natural frequencies calculated with the tool AMA V1.0. (a) Evolution of the 1st natural frequency for the CB-01 and; (b) Evolution of the 1st natural frequency for the CB-02

The subsequent analysis consisted in performing the automatic processing of the acquired data using the modified version AMA V2.0. Figure 6.15 presents the new results by means of the identified first natural frequency for the case of the CB-01 and CB-02. As it is possible to observe in Figure 6.14 and Figure 6.15, the results of the proposed original and the new version of the methodology show a very good correlation, with only four clear mistakes on the estimations of the second version for the case of the CB-01 (Figure 6.15a).

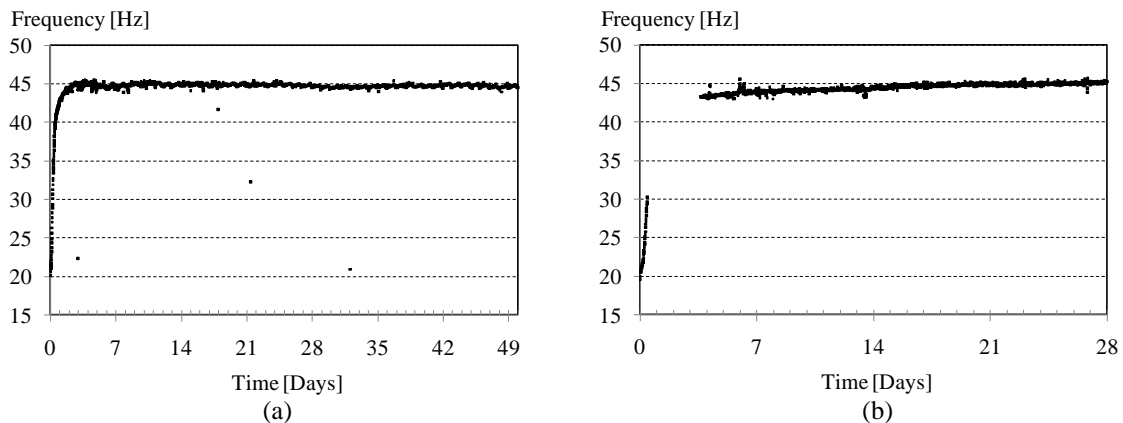


Figure 6.15 – Results of the natural frequencies calculated with the tool AMA V2.0. (a) Evolution of the 1st natural frequency for the CB-01; and (b) evolution of the 1st natural frequency for the CB-02

The identified natural frequencies and damping coefficients of the two developed tools were compared with reference values obtained with a non-automatic data processing tool through the use of the SSI method implemented in the ARTeMIS extractor software (SVS, 2009). Table 6.11 and Table 6.12 show the comparison of 10 randomly chosen points for

the cases of the CB-01 and CB-02 respectively. In these Tables, the percent error was used defined as the relative difference between the estimations of the proposed tools and their counterparts obtained from the SSI method times a factor of 100.

Table 6.11 – Comparison of the results of the proposed algorithms and commercial modal analysis software: Case Study CB-01.

Day	SSI Method (Artemis Extractor 2009)		AMA V1.0 (Freq. and M.S. as control values)				AMA V2.0 (Only Freq. as control values)			
	f	ξ	f	ξ	Error f	Error ξ	f	ξ	Error f	Error ξ
	(Hz)	(%)	(Hz)	(%)	(%)	(%)	(Hz)	(%)	(%)	(%)
0.1	22.84	0.99	22.70	0.59	0.6	40.4	22.75	0.91	0.4	8.1
0.5	39.86	1.84	39.85	1.68	< 0.05	8.7	39.82	1.85	0.1	0.5
0.7	41.48	1.13	41.61	0.95	0.3	15.9	41.51	1.33	0.1	17.7
1.0	42.84	0.94	42.92	0.74	0.2	21.3	42.91	1.11	0.2	18.1
1.5	43.84	1.24	43.98	1.11	0.3	10.5	43.98	1.11	0.3	10.5
2.0	44.31	1.14	44.30	0.81	< 0.05	29.0	44.31	1.34	< 0.01	17.5
7.0	44.70	1.28	44.58	1.04	0.3	18.8	44.62	1.73	0.2	35.2
14.0	44.99	1.39	44.95	1.14	0.1	18.0	44.95	1.14	0.1	18.0
21.0	44.64	1.64	44.76	1.94	0.3	18.3	44.69	1.69	0.1	3.1
28.0	44.54	1.36	44.75	1.87	0.5	37.5	44.77	1.45	0.5	6.6

Table 6.12 – Comparison of the results of the proposed algorithms and commercial modal analysis software: Case Study CB-02.

Day	SSI Method (Artemis Extractor 2009)		AMA V1.0 (Freq. and M.S. as control values)				AMA V2.0 (Only Freq. as control values)			
	f	ξ	f	ξ	Error f	Error ξ	f	ξ	Error f	Error ξ
	(Hz)	(%)	(Hz)	(%)	(%)	(%)	(Hz)	(%)	(%)	(%)
0.1	21.25	0.82	21.28	0.18	0.1	78.1	21.28	0.17	0.1	79.3
0.2	22.45	1.03	22.39	0.31	0.3	69.9	22.40	0.31	0.2	69.9
0.4	29.05	2.50	29.18	0.80	0.5	68.0	29.18	0.80	0.5	68.0
4.0	43.42	1.42	43.09	0.78	0.8	45.1	43.09	0.75	0.8	47.2
5.0	43.53	1.30	43.58	0.45	0.1	65.4	43.58	0.45	0.1	65.4
6.0	43.80	1.11	44.19	0.63	0.9	43.2	44.21	1.01	0.9	9.0
7.0	43.86	1.32	45.74	2.44	4.3	84.9	43.52	0.85	0.8	35.6
14.0	44.59	1.13	44.16	0.67	1.0	40.7	44.50	0.57	0.2	49.6
21.0	44.81	1.22	44.56	0.44	0.6	63.9	44.82	0.53	< 0.05	56.6
28.0	45.11	1.26	44.88	0.47	0.5	62.7	45.14	0.60	0.1	52.4

The results show the accuracy of the proposed methodologies for the estimation of frequencies. Within these 20 randomly selected comparison points, the highest estimation error in the first frequency was lower than 1%, with only one exception. Figure 6.16 and Figure 6.17 present a summary of the results by means of the estimated damping coefficients and registered MAC values.

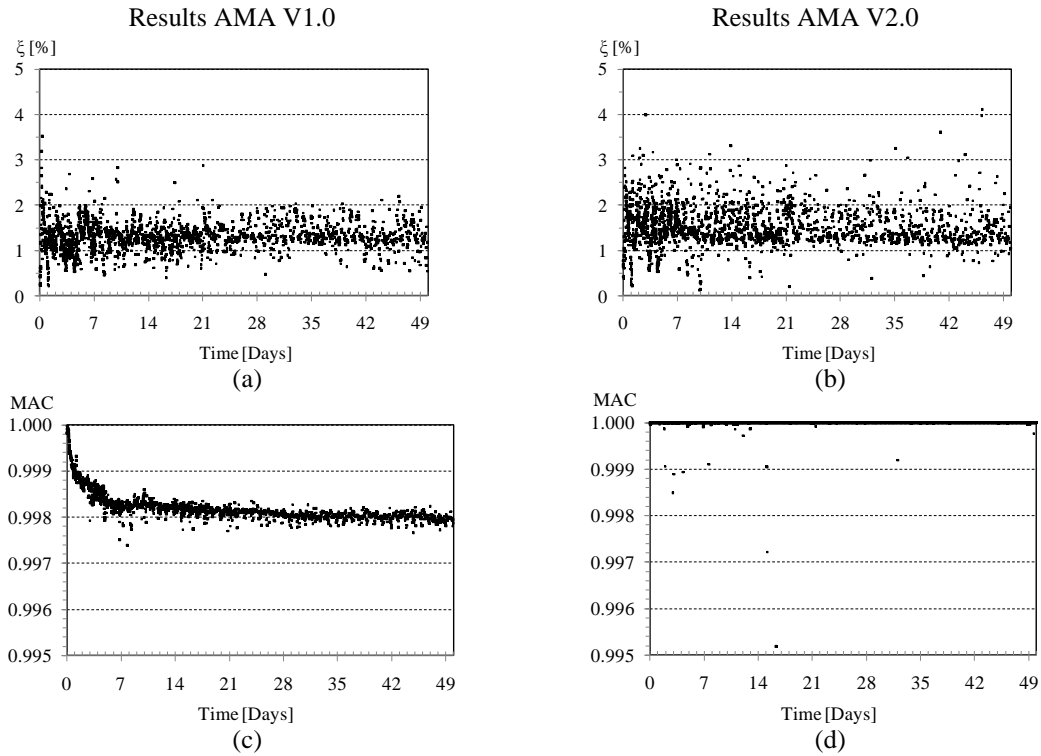


Figure 6.16 – Summary of the results of the automatic modal identification process for the case study CB-01 using the two versions of the developed tool. (a) and (b) Damping coefficients’ estimations, (c) and (d) registered MAC values

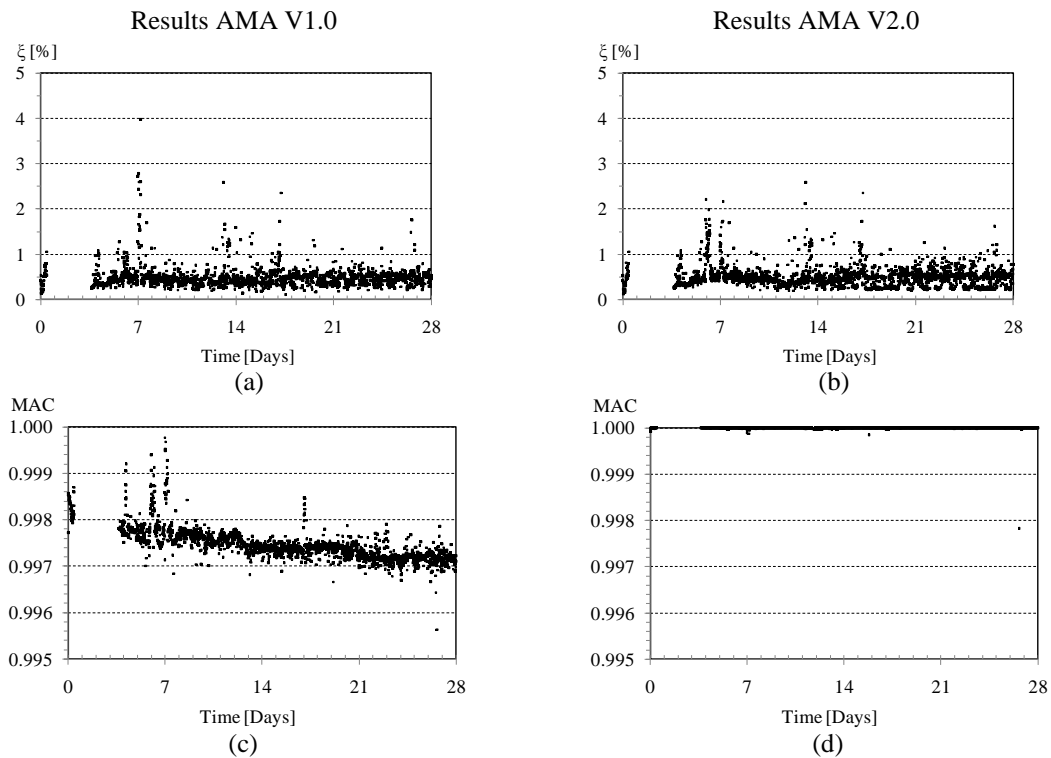


Figure 6.17 – Summary of the results of the automatic modal identification process for the case study CB-02 using the two versions of the developed tool. (a) and (b) Damping coefficients’ estimations, (c) and (d) registered MAC values

With respect to the estimations of damping coefficients shown in Figure 6.16a, 6.16b, 6.17a, and 6.17b, the overall results show a higher dispersion due to the inherent uncertainties in the assessment of this parameter. However, the results evidenced a reasonable coherence on the estimations, as they are mostly located within the range of 1% to 2% in the CB-01 and 0.2% to 1% in the CB-02.

The results of the estimated mode shapes given by the MAC values presented in Figure 6.16c, 6.16d, 6.17c, and 6.17d are very close to 1, confirming the reliability of the proposed tools. The evolution of the MAC values in the first methodology (Figure 6.16c and Figure 6.17c) showed an interesting dynamic behaviour since a slight variation was observed along the time as concrete hardened. However, this behaviour was not evident in the results using the second methodology since this version uses a relative mode shape comparison for performing the automatic modal identification process. With this respect and aiming at observing what had physically happened in the concrete beams, the estimated normalized modal shape amplitudes at the beginning and at the end of the tests are shown in Figure 6.18. The results confirmed the changes in the modal shape of the studied systems associated to the concrete hardening process. Since the study of the performance of the concrete is out of the scope of this work, the registered effect was no longer studied. Nevertheless; the accuracy of the developed tools for estimating the dynamic properties of the structures was established.

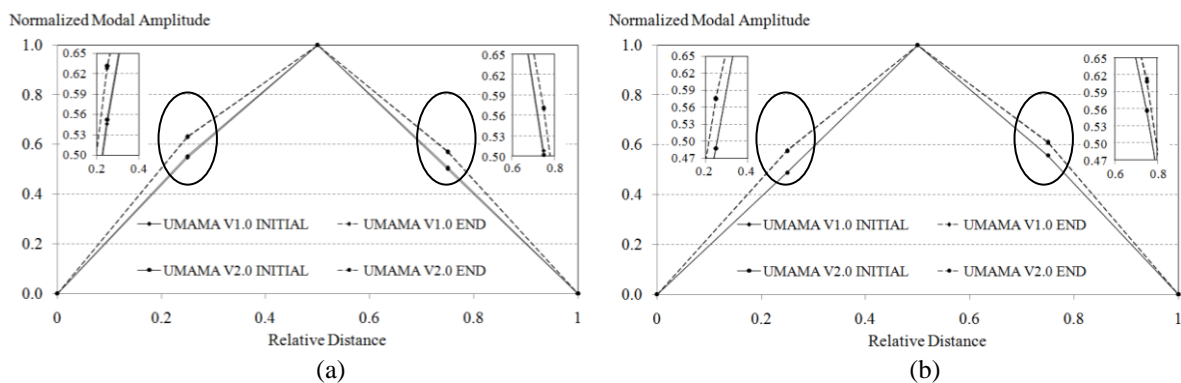


Figure 6.18 – Analysis of the variation of the first modal shape along the experimental tests: (a) CB-01 modal shape's results; and (b) CB-02 modal shape's results

The estimations' model order levels and the required data processing times were then evaluated. These two outcomes are shown in Figure 6.19 and Figure 6.20 for the first and second methodology respectively. The results of the estimations' model orders levels evidence the high reliability of the developed tools since, even if the threshold level was set to 250 (see Table 6.10), the selections were performed at much lower orders, between

the 3rd to the 5th level and the 4th to the 10th level, with the first and the second version of the proposed methodology respectively. On the other hand, the short processing times registered with both versions of the proposed methodologies (maximum of 0.90 sec and 3.7 sec respectively) also evidenced the adequacy of these tools for real case studies, indicating that almost continuous monitoring processes are feasible. It should be noticed that when slower processors are used (in this case a Core2 duo processor was used), higher data processing times should be expectable.

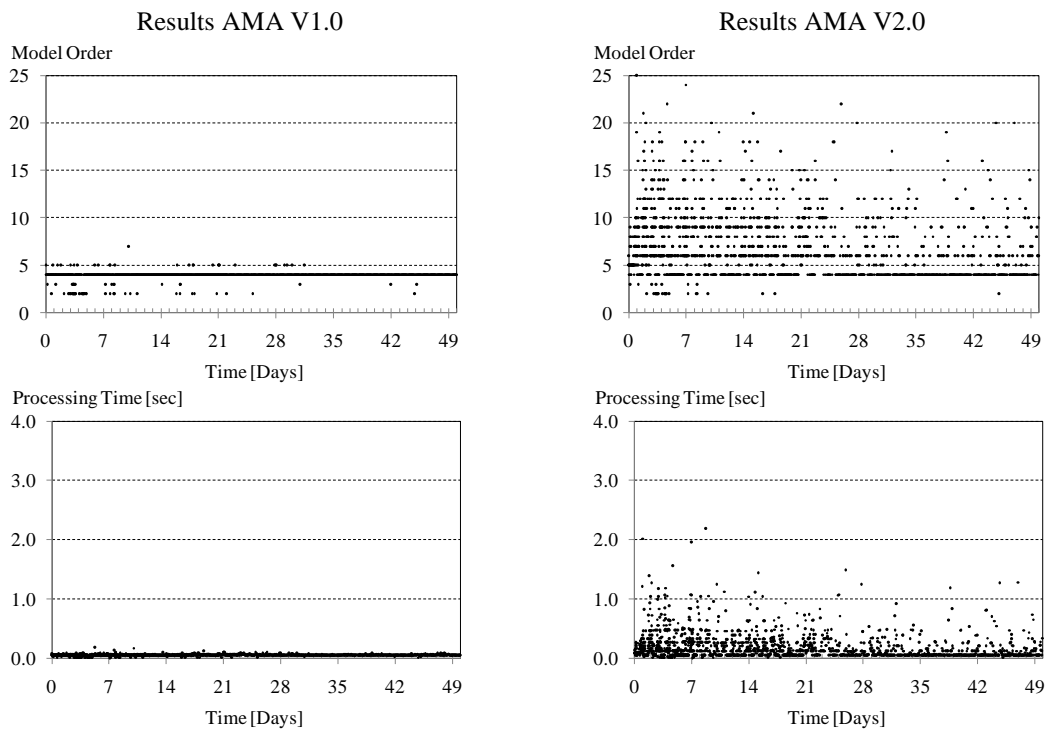


Figure 6.19 – Comparison of the data processing time and the selected model order level where the estimations were performed in both versions of the developed tools: Case study CB-01

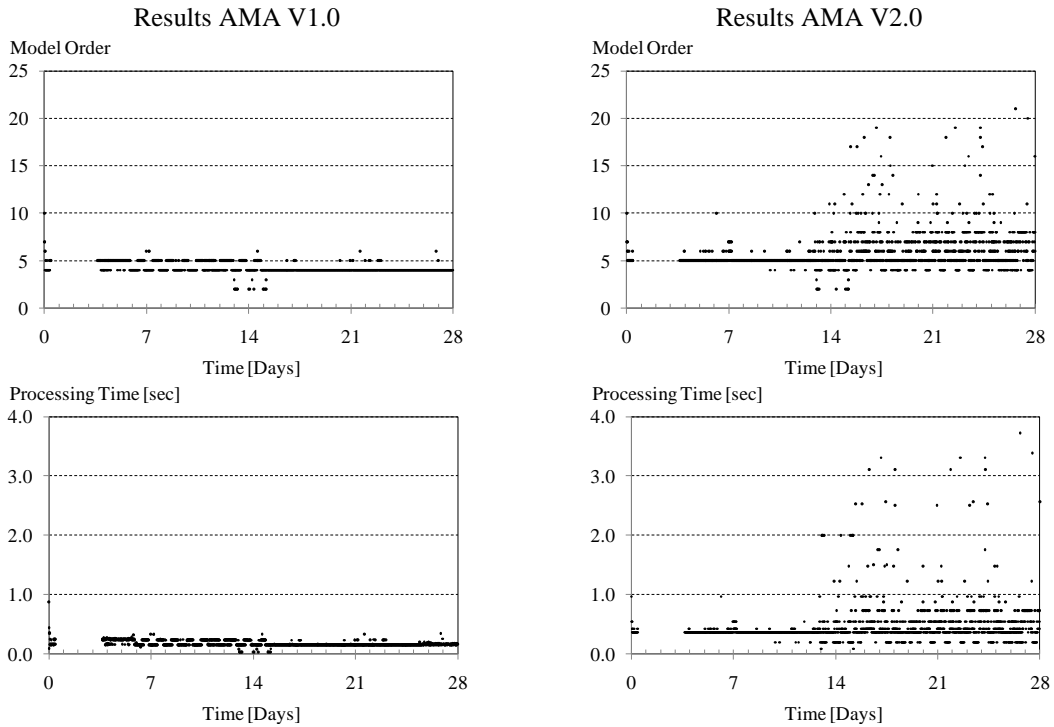


Figure 6.20 – Comparison of the data processing time and the selected model order level where the estimations were performed in both versions of the developed tools: Case study CB-02

Finally, Figure 6.21 presents the relation of the values of the E-modulus determined from the experimental dynamic tests and their counterparts determined from traditional compression tests in concrete samples for the studied beams. The results of the experimentally calculated values of the E-modulus (continuous lines) and the values calculated from the traditional compression tests (isolated dots) evidenced notable similarities. This fact confirmed that the initial goal of tracking the concrete stiffening using OMA tests and a reliable tool for performing automatic and real time modal estimations was achieved.

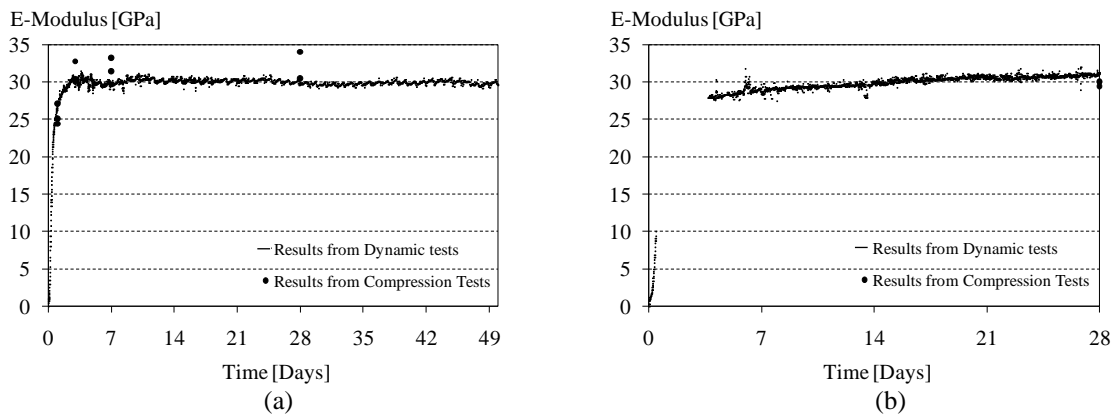


Figure 6.21 – Experimental E-modulus evolution curve: (a) evolution of the concrete E-modulus for the CB-01; and (b) evolution of the concrete E-modulus for the CB-02

6.5 Dynamic Monitoring of the St. Torcato Church

Due to the accuracy and correct estimations attained in the previous laboratory study, the proposed AMA V2.0 tool (version considering only frequency control values) was tested in a field study. For this purpose, the continuous monitoring of a 19th century stone masonry church carried out using the proposed automatic dynamic system will be following detailed.

6.5.1 Description of the Church

The St. Torcato Church is located in the village of the same name near the city of Guimarães, North of Portugal. The construction of the building took more than 130 years starting from 1871 and is being completed only in recent years. Figure 6.22 shows the different stages of the construction until its present situation.

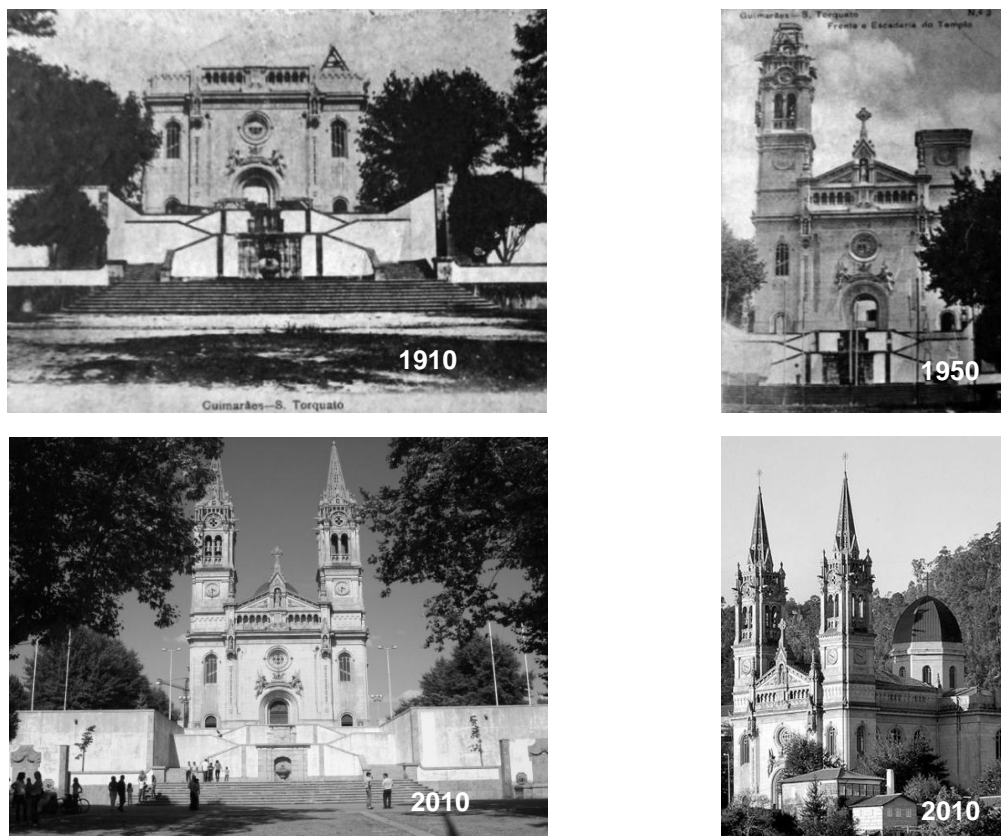


Figure 6.22 – Construction stages of the St. Torcato Church located in Guimarães, Portugal (first two pictures from St. Torcato museum)

The architectural style of the building is a combination of the Classic, Gothic, Renaissance and Romantic styles. The nave of the church has 25 m length and 15 m width, while the stone masonry walls have 1.3 m of thickness. Currently, the church presents

severe damage in the front façade due to soil settlements. This special case represents an interesting possibility for the deployment of continuous monitoring systems. With this purpose, a static monitoring system was implemented in 1998 (Lourenço and Ramos, 1999) and is currently active. The purpose of the present work was to complement the referred study by implementing a continuous dynamic monitoring system.

6.5.2 Preliminary Monitoring System and Numerical Simulation

Before the implementation of the dynamic monitoring system, preliminary studies were carried out considering experimental OMA tests and finite element model updating for the global characterization of the structure (Ramos et al., 2010a). This modal analysis was carried out in May 2009, using 10 high sensitive piezoelectric accelerometers model PCB 393B12 (PCB, 2009) and a DAQ system model NI SCXI-1531 (NI, 2009b). The measurement sensors were located in 35 points with 9 test setups. The reference accelerometers were placed at the top of the towers (two accelerometers in each tower in perpendicular directions) due to the high amplitude and high modal contribution of those points. The schematic layout of the sensors during the tests is shown in Figure 6.23.

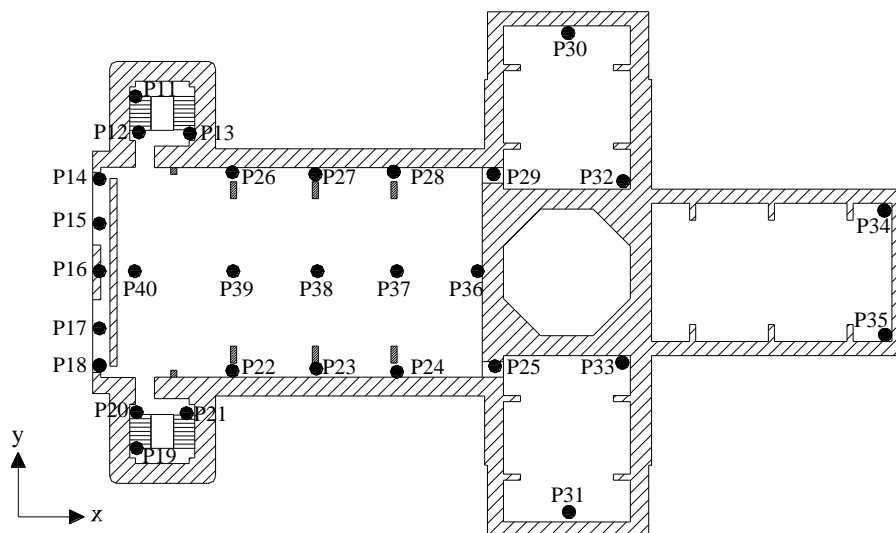


Figure 6.23 – Sensors location; St. Torcato Church case study (adapted from Ramos et al., 2010a)

The experimental modal parameters obtained with the tests were compared with their numerical counterparts. As it is shown in Figure 6.24, the modal parameters obtained by a “tuned” numerical model showed high correspondence with the results obtained from the experimental dynamic tests. More details of the tests can be found in Ramos et al. (2010a).

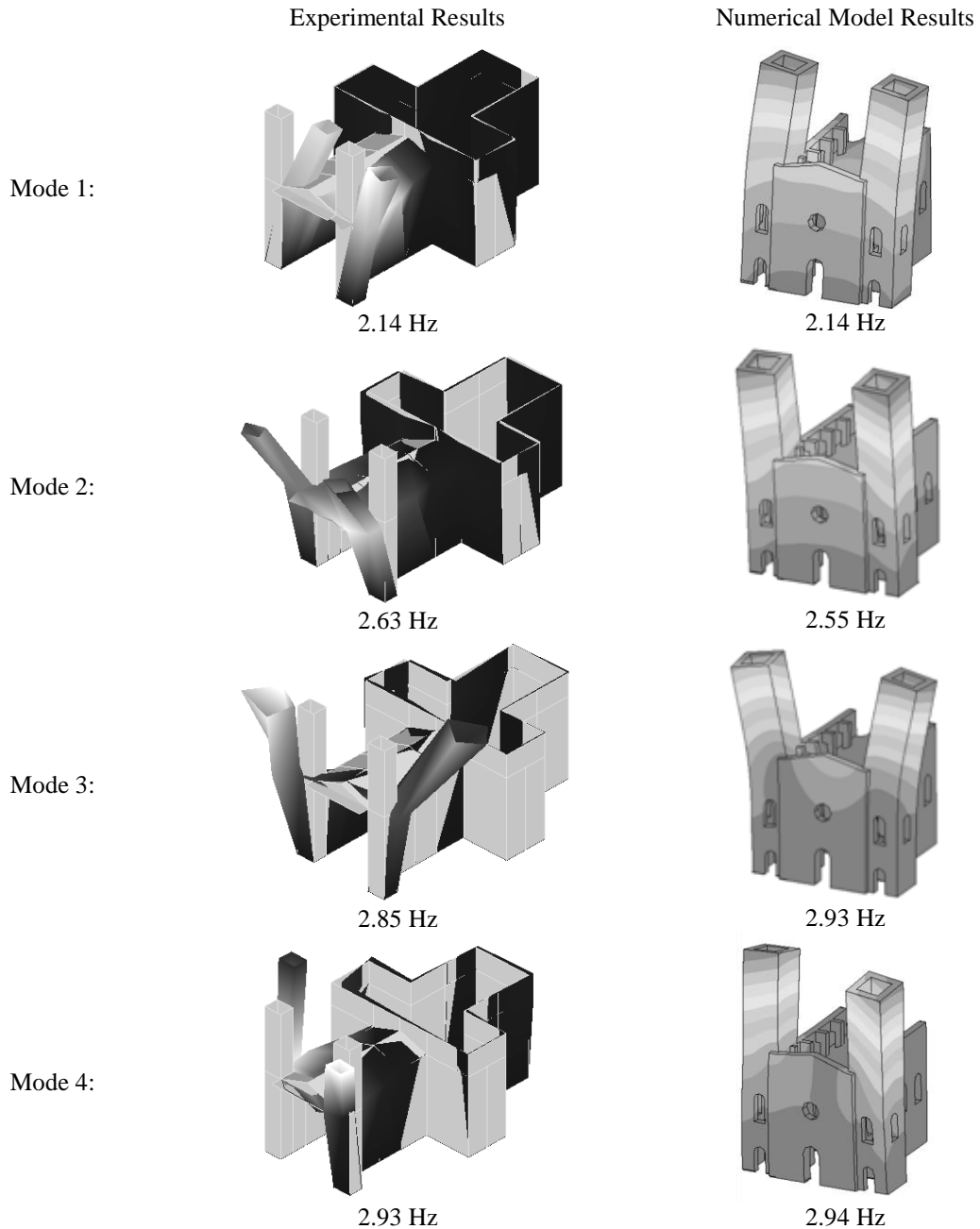


Figure 6.24 – Experimental and numerical modal analysis results; St. Torcato church case study (Ramos et al., 2010a)

6.5.3 Continuous Dynamic Monitoring System Description

The continuous monitoring system is composed by four piezoelectric accelerometers model PCB 393B12 (PCB, 2009), one portable DAQ unit model NI-USB9233 (NI, 2009b), one Uninterruptible Power Supply (UPS), and one computer with embedded processor Pentium IV as remote station. A modem was included in the monitoring system to periodically send the processed data via SMS to a local FTP account.

The four accelerometers were located in two nodes in the towers of the church (one in each tower) for performing measurements in perpendicular directions. The central data acquisition station, one of the measurement nodes, as well as a scheme of the location of the measurement nodes is shown in Figure 6.25.

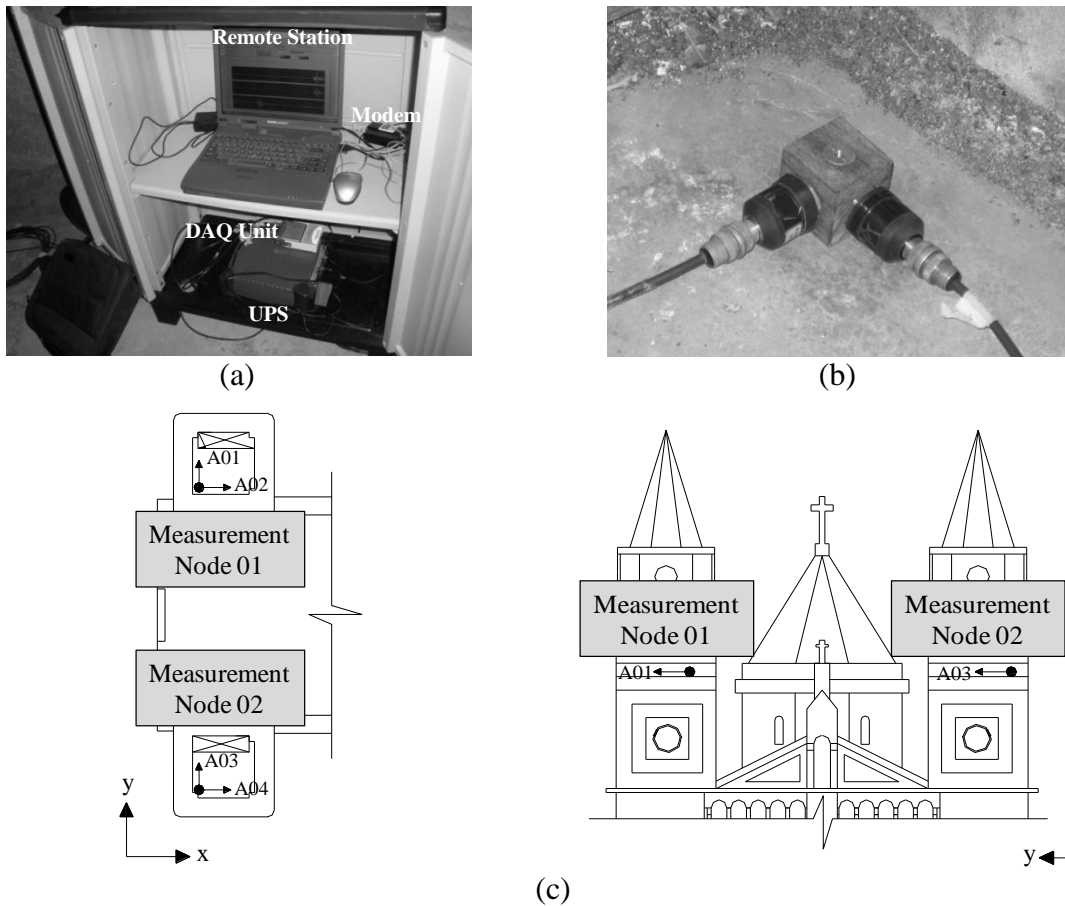


Figure 6.25 – Dynamic monitoring system setup - St. Torcato church case study: (a) data acquisition station; (b) measurement node; and (c) scheme of the location of the measurement sensors

Because the first four frequencies of the church are between 2 Hz and 3 Hz, and in order not to create oversized data files, a conservative sample time of 10 min with a sample frequency of 50 Hz was considered. The acquisition process was repeated using intervals of 60 min. As shown in Table 6.13, five data collecting campaigns were performed in the Church starting from November 2009.

Table 6.13 – Data collection campaigns – St. Torcato church case study.

Description	Corresponding period	Number of recorded events
1 st Campaign	01/11/2009 – 07/12/2009	784
2 nd Campaign	05/01/2010 – 20/02/2010	1089
3 rd Campaign	01/04/2010 – 21/05/2010	1191
4 th Campaign	08/06/2010 – 12/06/2010	93
5 th Campaign	28/06/2010 – 12/07/2010	338
	Total	3495

Since the present study was remotely performed, all modules A, B and C of the proposed dynamic monitoring scheme presented in Figure 6.2 were activated. In this way, the processed information was received in the local central station at the University of Minho. For security reasons a zip file containing the original data was kept in the remote station.

Based on the results of the preliminary experimental and analytical modal identification studies, the control parameters required for processing the collected data were defined. The frequency and damping control parameters were set based on the results of the preliminary monitoring campaigns and taking into consideration that a reasonable variability on the estimated frequencies (frequency threshold value) may exist due to changes in the environmental conditions throughout the monitoring process. The minimum model order and the FAC threshold value were maintained the same than in the previous studies while a maximum model order of 150 was considered for avoiding long data processing times. The summary of the acquisition and data processing parameters used are shown in Table 6.14.

Table 6.14 – Acquisition and processing parameters AMA V2.0 – St. Torcato church case study.

Description		Experimental Tests St. Torcato church
Acquisition Parameters	Sampling rate (Hz):	2000
	Decimation until (Hz):	50
	Number of measurement sensors	4
	Time to read (sec):	600
	Sampling interval (sec):	3600
	Number of recorded events:	1873
Processing Parameters	Freq. threshold value (\pm Hz):	0.095
	Max. Damping (%):	5.0
	Min. Damping (%):	0.1
	FAC threshold (Hz):	0.01
	MAC threshold:	0.80
	Min. model order:	2
	Max. model order:	150
	Decimation factor:	5
	Expected frequency range (Hz):	2 – 3.1
Frequency control vector (Hz):	[2.13 2.57 2.76 2.95]	

6.5.4 Automatic Modal Identification Results

In OMA tests, the quality and confidence on the estimations are directly influenced by the environmental noise level. Therefore, the peak values and the RMS of the time series recordings are of interest and, thus, were remotely calculated in a basic calculation stage of the developed monitoring tool. Table 6.15 show the maximum and minimum values of the peaks and RMS of the collected time series for the considered period of monitoring works.

Table 6.15 – Peak Values and RMS of the time series recordings – St. Torcato church case study.

	Peak Values		RMS	
	Max (mg)	Min (mg)	Max (mg)	Min (mg)
Accelerometer A01	4.980	0.022	0.260	0.003
Accelerometer A02	5.836	0.014	0.157	0.001
Accelerometer A03	2.487	0.014	0.059	0.003
Accelerometer A04	4.526	0.034	0.055	0.003

Figure 6.26a shows the registered RMS of the accelerometer A 04 located at the right tower of the church (node 02 in Figure 6.25c). A close up of the registered values from November 20th to November 30th, 2009 is shown in Figure 6.26b. The structure is subjected to a low level of environmental excitation, especially at night hours. The results indicate that the morning excitations can reach 10 times the excitation at night hours.

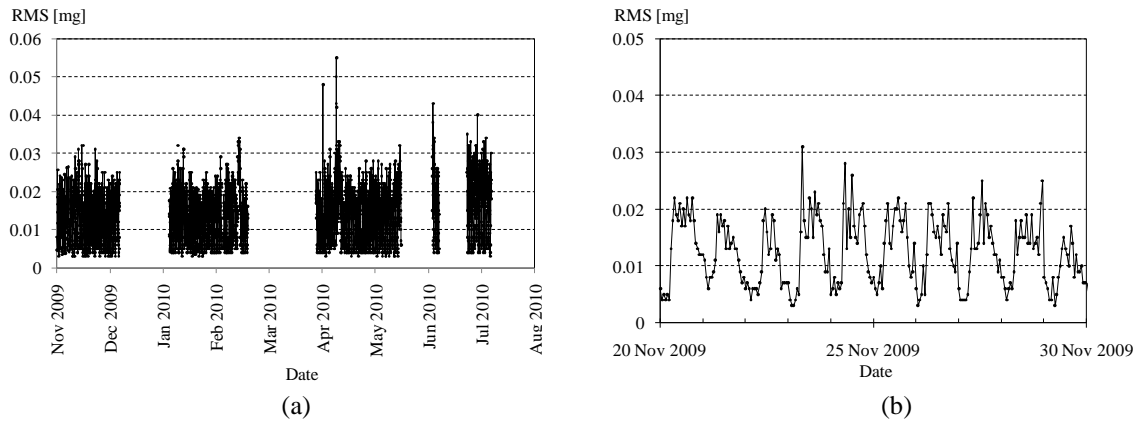


Figure 6.26 – RMS of the time series collected by accelerometer A 04 (node 02) – St. Torcato church case study: (a) variation in the entire monitoring period; and (b) daily variation of the RMS

The time series recordings were remotely processed using the AMA V2.0 tool. The results of the evolution of the first four natural frequencies of the structure as well as their damping coefficients are shown in Figure 6.27 and Figure 6.28. The criterion used to judge a resultant estimation as reliable, was to disregard the values selected at the maximum model order previously specified (150 for this case). Discarding the data not matching the previous data cleaning criterion, the proposed automatic identification algorithm evidenced again its effectiveness with a success identification rate of 89%.

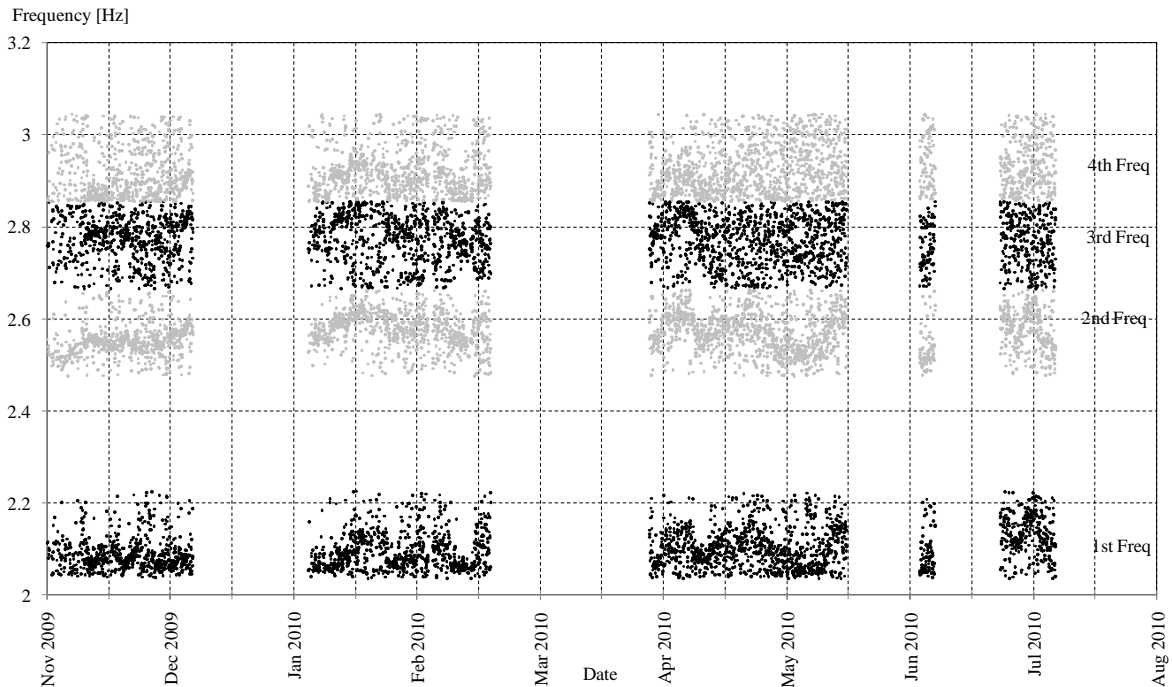


Figure 6.27 – Evolution of the natural frequencies – St. Torcato church case study

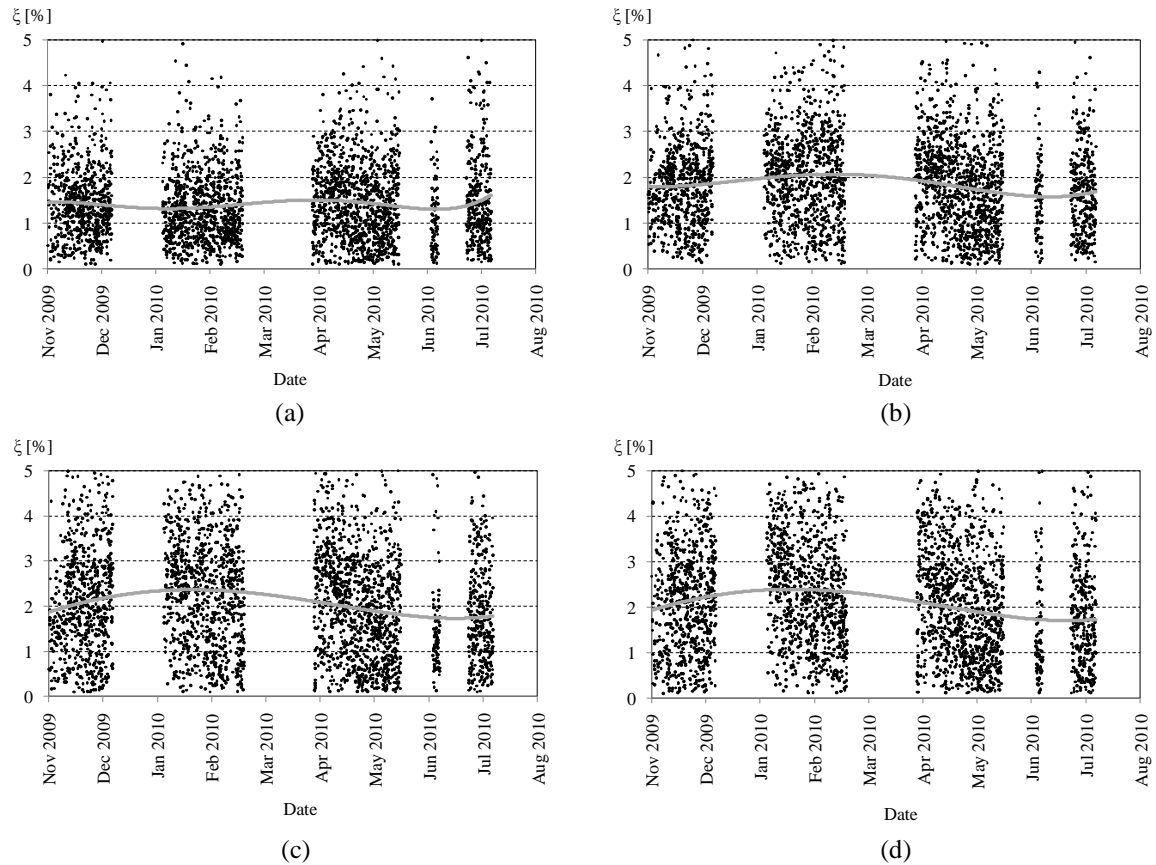


Figure 6.28 – Evolution of the damping coefficients – St. Torcato church case study: (a), (b), (c), and (d) damping estimations of the modes 1, 2, 3 and 4 respectively

The data presented in Table 6.16 shows the mean values and the standard deviation of the estimated natural frequencies and damping coefficients as well as the mean and minimum values registered for the MAC values. The mean values of frequencies showed a low standard deviation varying from 0.041 Hz to 0.052 Hz. These variations might be due to the changes on the environmental conditions (temperature and humidity), as demonstrated in Ramos et al. (2010b). With respect to the estimated damping coefficients, the results show higher dispersions which evidence the difficulties on calculating this factor with OMA tests. However, reasonable mean damping values were calculated, which exhibit a clear trend to increase with higher modes. The results of the MAC values evidenced the adequacy of the proposed algorithm. As shown, high mean MAC values (over 98%) were registered in the processing stage.

Table 6.16 – Automatic modal identification results – St. Torcato church case study.

	f_{mean} (Hz)	$f_{\text{std.dev}}$ (Hz)	ξ_{mean} (%)	$\xi_{\text{std.dev}}$ (%)	MAC_{mean} (%)	MAC_{min} (%)
Mode 1	2.098	0.043	1.414	0.816	99.388	80.169
Mode 2	2.568	0.041	1.848	0.949	99.334	80.081
Mode 3	2.772	0.049	2.071	1.135	98.916	80.123
Mode 4	2.924	0.052	2.085	1.144	98.690	80.101

The results of the median values of the absolute modal shape coordinates were next calculated and compared with the values obtained in the preliminary experimental campaign described at section 6.5.2 (Figure 6.29). These results confirm the precision of the modal shape estimations of the developed tool which evidence high similarities to the experimentally obtained values.

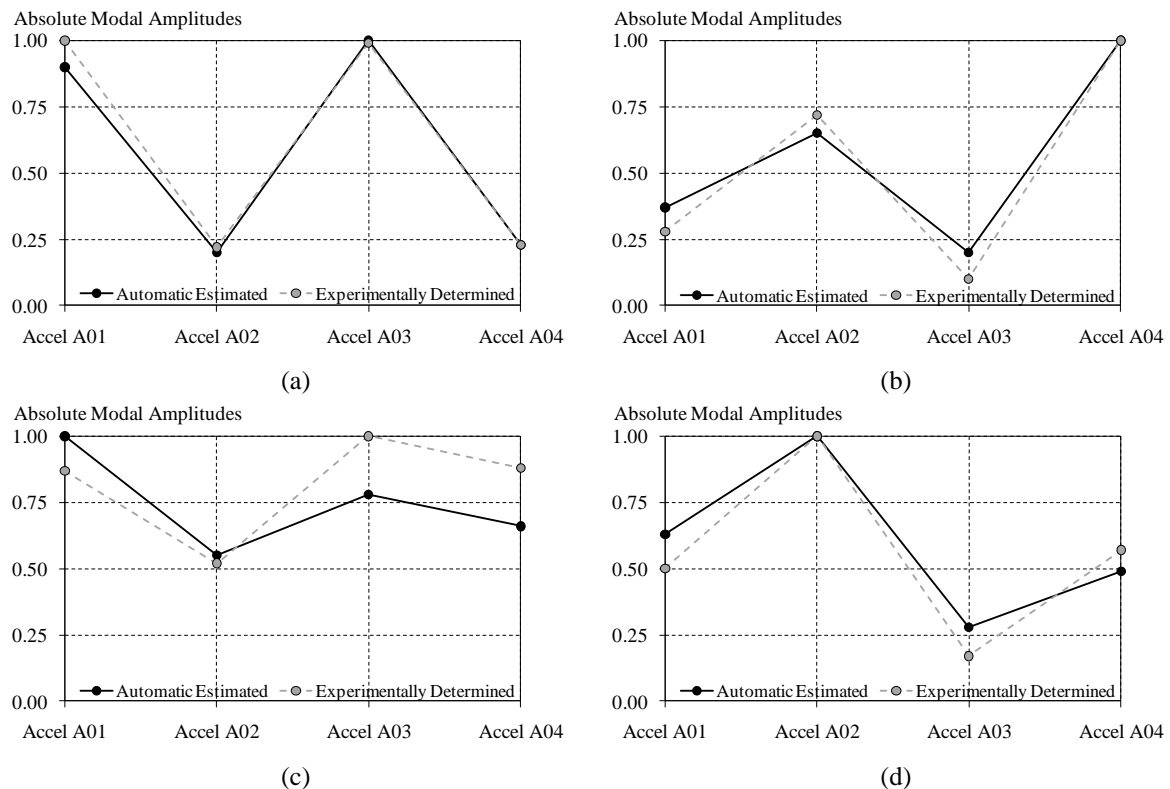


Figure 6.29 – Median values of the absolute modal amplitudes automatically estimated along the dynamic monitoring study: (a) first mode shape; (b) second mode shape; (c) third mode shape; and (d) fourth mode shape

An interesting aspect for confirming the reliability of the proposed methodology is the observation of the model order levels in which the automatic estimations were performed. Figure 6.30 provides the relation between the model order and the RMS of the time domain series, as well as, with the related processing time. A clear trend is found, showing that the feature extraction of higher noise environments is easier (and thus more reliable) since the

estimations are performed at lower level orders. The influence of the processor speed located in the remote station for the automatic feature extraction process provides the following conclusion: A one-order of magnitude speed-up is found with new double core processors. Thus, the processor speed should be taken into account at the stage of choosing the sampling interval and designing the system requirements.

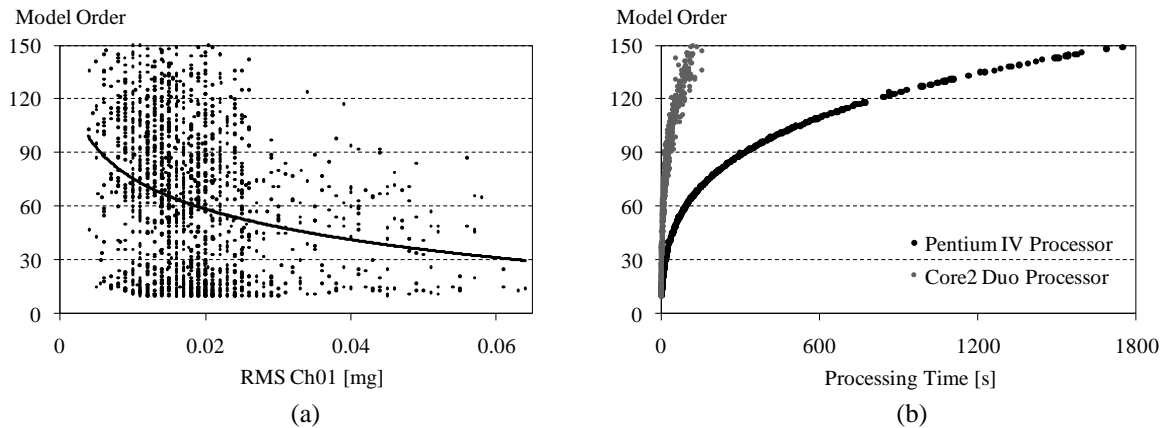


Figure 6.30 – Results of the automatically selected model orders – St. Torcato church case of study: (a) model order vs. RMS of the time domain signals; and (b) model order vs. processing time

6.6 Conclusions

In the present chapter, an automatic feature extraction algorithm to process data from Operational Modal Analysis monitoring was presented. Two versions were proposed, namely a first one, considering frequency and modal parameters as control values (AMA V1.0), and a second one, considering only the frequency information as control parameters (AMA V2.0). The algorithms were validated using analytical, laboratory and field tests.

The first round of calibration tests considered the analysis of computer generated information (500 hundred events were studied) using different percentages of added noise. In these numerical tests, the resultant frequency estimations evidenced excellent precision with less than 5% of average errors even in the extreme noise scenarios with 500% of noise. With respect to the mode shapes estimations, they also evidenced high accuracy. However, it was observed that their reliability decreases in an inverse relationship with the quantity of contaminating noise.

Continuous modal analysis tests were carried out using composite steel/concrete beams in laboratory environment, monitored since the instant of casting. The dynamic monitoring studies recorded over 4000 events. The estimated dynamic parameters were compared against hand calculations and the results of the tests demonstrated the accuracy of the proposed algorithms. As the second version of the algorithm uses less control parameters, its use in practical applications is more feasible.

The last round of experimental validation tests was performed in a 19th Century church located in St. Torcato, North of Portugal. In this case, a continuous dynamic monitoring system was implemented for almost 9 months and the recorded data was analyzed using only the second version of the developed tool. Over 3500 events were studied and the results indicate that the environmental noise is sometimes (especially at night) not strong enough to excite the structure, thus influencing the accuracy of the estimations in such critical hours. Still, the evolution along time of the first four frequencies was appropriately estimated with high rate of successful results (over 89%) confirming the utility of the proposed tools. The results of the field validation tests also confirmed that the study of existent masonry structures by dynamic means is of complex due to the large stiffness of these buildings. It should be noted that in cases where the proposed algorithms may be

used for processing OMA data from more flexible structures, such as bridges or concrete frame buildings, higher quality of estimations should be expected.

The monitoring works on the church are planned to continue and further developments aim at the establishment of correlations between the described dynamic monitoring systems and the currently installed static monitoring systems. Future studies may also contemplate the development of damage detection algorithms and data managing processes for improving the Structural Health Monitoring (SHM) practice. In those studies, other outcomes of the proposed algorithms such as the iteration level where the estimations were performed, the data processing times, as well, as the simple statistic information like the maximum values and RMS of the registered signals may be additional features to take into account.

CHAPTER 7

CONCLUSIONS AND FUTURE WORK

7.1 Conclusions

The conclusions of the present work are addressed next with respect to different aspects, namely monitoring systems, off-the-shelf WSN platforms, the new prototype WSN platform and automatic modal identification.

Dynamic Monitoring Systems and Modal Monitoring Techniques for Studying Existent Structures

In this work, the available techniques for performing modal monitoring were classified according to the excitation source as input-output and output-only methodologies. Due to the difficulties of deployment exciting systems in existent structures, experience has shown that the available options for studying existing buildings rely on the use of output-only methodologies, processes also called Operational Modal Analysis (OMA).

There are known issues of the OMA processes such as the low reliability on the resultant damping estimations or the possibility of not having enough environmental noise for proper excitation of the structures. These aspects should be considered when designing monitoring systems. In this design process, the expected levels of noise and the restrictions of the monitoring environments are fundamental aspects that define the characteristics of the measurement sensors and data acquisition (DAQ) equipments to be used.

In this work, the available systems (sets of sensors and DAQ equipments) for performing dynamic monitoring were divided in two groups: wired and wireless systems. The first main objective of the present work was to explore the use of the last group of systems as reliable alternatives for monitoring existent structures. The main advantages of wireless monitoring systems are their low costs and their possibility for being quickly deployed. Despite the rapid growing of the communications and sensors technologies, the actual application of WSN (combination of microsensors - MEMS and wireless systems) is currently limited to isolated cases in the framework of scientific research. Due to the wide range of scientific areas linked to WSNs and their applications for dynamic monitoring of structures (electronic, communication and civil engineering), in this work it was observed that the most efficient way for performing developments in the field is through interdisciplinary and collaborative researches.

Operational Modal Analysis using Commercial off-the-shelf WSN platforms

Despite the several reasons in favor of using the new technologies on WSNs, there are still some aspects that limit an extensive application of the commercial versions of these platforms. These aspects are related to: 1) resolution of the sensors and DAQ systems; 2) lack of communication protocols implemented in the boards; 3) complexity of the mote's programming environment; and 4) energy consumption considerations. In the present work the study of the last aspect (energy consumption) was not considered. However, this should be taken into account in future development stages where the advances of other scientific groups in energy harvesting systems, solar panels and other solutions, can be used.

The exploration tests carried out in this work considered using one of the best selling models of MEMS accelerometers such as the ADXL202JE embedded in the Crossbow MTS400 sensor's board. The results of these tests indicated that the use of such sensors can be considered in monitoring works where high amplitude vibrations (over 20 mg) are expected. The results of the modal identification tests evidenced that even in those high amplitude excitation environments, only accurate estimations of natural frequencies can be obtained. For what respects the estimations of damping coefficients, modal shape coordinates and also time domain indicators, no consistent results were found. Since in a modal identification process these last parameters are used for verifying the quality of the frequencies estimations (local modes that do not represent the global response of the structures can be discarded), the pros and cons of using these platforms should be carefully considered.

New Prototype WSN platform for Performing Operational Modal Analysis of Structures

From the civil engineering point of view, the main limitations of the existing solutions of MEMS accelerometers are their broad resolution ranges, low sensitivities, and high noise densities. From the available options of triaxial MEMS accelerometers, two of the most appropriate units, the ASC 5521-002 and ASC 5631-002, were selected for being implemented in a first prototype version of a WSN platform. In this prototype platform, the communication throughout the network was carried out using the Crossbow TelosB board. The criterion for selecting this board was the available experience of the project partners (CISTER/HURRAY-ISEP research group) in programming these equipments. An

important advantage of these boards that was also taken into account is the capacity to add future developments on static monitoring solutions since they have already embedded temperature, and humidity microsensors.

The laboratory and field validation tests carried out using the developed platforms indicated that these systems can be positively considered as alternatives to the conventional wired based systems in monitoring works with expected low amplitude vibrations from 0.10 mg. The results of the modal analysis processes also showed the outstanding performance of the developed systems due to the high attained accuracies on the estimations of frequencies, dampings and even mode shapes (the last one with less precision but with fair consistency in all cases).

Automatic Modal Identification Procedure for Operational Modal Analysis Data

A global contribution for Structural Health Monitoring would conjugate the use of up-to-date measurement sensors and the latest developments on data processing techniques. So far, the majority of works carried out represent isolated approaches for developing sensors or pre/post processing methodologies for OMA. Only a few works tried to consider more than one aspect of the monitoring process simultaneously and this was precisely the second main objective of the present work.

This way, the proposed developed solution of WSN was complemented with a proposal for an automatic processing algorithm for OMA data which is obtained from continuous monitoring studies. This algorithm uses a simple combination of clustering techniques and the rule based approach for interpreting the results of parametric data processing methods.

The experimental validation tests carried out, which included analytical, laboratory and field studies, evidenced the excellent performance of the proposed algorithm for extracting reliable information of frequencies, damping coefficients and modal shape coordinates. These results also confirmed that the quality and reliability of the estimations of the proposed algorithm are directly associated with the capacity of the environmental noise to properly excite the structure. This aspect, as mentioned before, is critical when studying existent masonry structures especially at night periods and should be carefully considered.

7.2 Future Work

From the results of the validation tests in the new WSN platform, it can be concluded that three main aspects should be considered as short term developments goals for successful applications:

- The first aspect is the improvement of the ADC capabilities. In this first prototype system the multiplexing process of the acquired signals is not being performed correctly since the measurements of the three accelerometer axes cannot be collected at the same time.
- The second aspect is the improvement of the signal conditioning process. The developed prototype system considered the inclusion of two options of MEMS accelerometers with similar characteristics. However; the acquired signals from both systems have major differences particularly with respect to the minimum vibrations amplitudes that can be recorded (one platform offers the possibility of recording vibrations from 0.1 mg while the other from 1 mg).
- The third aspect to consider is the improvement of the time consuming data transmission process. In this respect, a theoretical approach based on the transmission of small quantities of information, resulting from the remote and decentralized application of the Welch method in each mote, was also proposed. This algorithm, if implemented in the motes, would assure high data compression rates and, thus, shorter data transmission times.

In addition to these aspects, medium and long term research lines should also consider:

- Implementation of WSN systems for static monitoring purposes. This topic may consider the use of humidity, temperature and displacement microsensors in continuous monitoring schemes. Since the acquisition rates of the static procedures are smaller, probably the communication issues would be not as critical as they are for the dynamic monitoring systems. It should be also considered that, in these cases, commercial MEMS static sensors have enough resolution for acquiring environmental indicators.
- Improvement of the performance of the prototype WSN system developed in this work. Here, it is recommended to explore other possibilities of remote data processing procedures, data compression algorithms, energy supplying sources, as well as to implement different network communications topologies.

- Implementation of data management and damage detection procedures. In this respect, tools to manage the large quantity of data resultant from the dynamic monitoring processes (raw time domain series as well as already processed information) should be developed. An important aspect to be considered would be also the development of risk and damage indexes based on the information provided by the continuous monitoring systems.
- The field tests carried out in this work also confirmed the difficulties on studying existent masonry structures by dynamic means. In this respect, the implementation of input-output techniques in continuous monitoring schemes would be of interest. Additionally, further developments on signal processing techniques and their practical inclusion in structural monitoring works must be also explored.

References

A

Allemang, R.J. *The Modal Assurance Criterion - Twenty Years of Use and Abuse*. Sound and Vibration, 37(8): 14-23 pp, (2003).

Allemang, R.J.; and Brown, D.L. *A Correlation Coefficient for Modal Vector Analysis*. International Modal Analysis Conference, IMAC, 110-116 pp, (1982).

Allen, D.W. *Software for Manipulating and Embedding Data Interrogation Algorithms into Integrated Systems*. Master Thesis, Virginia Polytechnic Institute and State University, Blacksburg, VA, (2005).

Analog. Analog devices. www.analog.com. Accessed December, (2009).

Andersen, P.; Brincker, R.; Goursat, M.; and Mevel, L. *Automated Modal Parameter Estimation of Civil Engineering Structures*, International Conference of Experimental Vibration Analysis for Civil Engineering Structures, Porto, Portugal, (2007).

Aoki, S.; Fujino, Y.; and Abe, M. *Intelligent Bridge Maintenance System Using MEMS and Network Technology*. Smart Systems and NDE for Civil Infrastructures - SPIE, San Diego, CA, Vol. 5057, 37-42 pp, (2003).

Arampatzis, T.; Lygeros, J.; and Manesis, S. *A Survey of Applications of Wireless Sensors and Wireless Sensor Networks*. 13th Mediterranean Conference on Control and Automation. IEEE, Limassol, Cyprus, (2005).

ASC. Advanced Sensors Calibration. www.asc-sensors.de. Accessed December, (2009).

ASTM. *C-215 Standard Test Method for Fundamental Transverse, Longitudinal and Torsional Frequencies of Concrete Specimens*. Annual Book of ASTM Standards, American Society for Testing and Materials, (2002).

Azenha, M. *Numerical Simulation of the Structural Behaviour of Concrete since its Early Stages*. PhD Thesis, University of Porto, Engineering Department, Porto, 379 pp, (2009).

Azevedo, A. *Paço dos Duques*. Livraria Lemos, Guimarães, 43 pp, (1964).

B

Baptista, M.A.; Mendes, P.; Afilhado, A.; Agostinho, L.; Lagomarsino, A.; and Victor, L.M. *Ambient Vibration Testing at N. Sra. do Carmo Church, Preliminary Results*. Proc. of

the 4th International Seminar on Structural analysis of Historical Constructions, Padova, Italy, 483-488 pp, (2004).

Basheer, M.R.; Rao, V.; and Derriso, M. *Self-organizing Wireless Sensor Networks for Structural Health Monitoring*. 4th International Workshop on Structural Health Monitoring, Stanford, CA, 1193-1206 pp, (2003).

Bennett, R.; Hayes-Gill, B.; Crowe, J.A.; Armitage, R.; Rodgers, D.; and Hendroff, A. *Wireless Monitoring of Highways*. Proc. of the SPIE Smart Systems for Bridges, Structures, and Highways, Newport Beach, CA, Vol. 3671, 173-182 pp, (1999).

Braun, S.; Ewins, D.J.; and Rao, S.S. *Encyclopedia of Vibration*. 1st ed. Elsevier, Cornwall, UK, (2002).

Brincker, R.; Andersen, P.; and Jacobsen, N.J. *Automated Frequency Domain Decomposition for Operational Modal Analysis*. Proc. of the 25th SEM International Modal Analysis Conference, IMAC, Orlando, FL, USA, (2007).

Brincker, R.; Ventura, C.; and Andersen, P. *Damping Estimation by Frequency Domain Decomposition*. 19th International Seminar on Modal Analysis, IMAC. , Kissimmee, USA, (2001).

Brincker, R.; Zhang, L.; and Andersen, P. *Modal Identification for Ambient Responses using Frequency Domain Decomposition*. 18th International Seminar on Modal Analysis, IMAC. , San Antonio, Texas, USA, (2000a).

Brincker, R.; Zhang, L.; and Andersen, P. *Modal Identification form ambient responses using frequency domain decomposition*. XVIII - International Seminar on Modal Analysis (IMAC). , San Antonio, Texas, USA, (2000b).

Brüel; and Kjaer. User Guide Specifications. www.bksv.com, (2009).

C

Cantieni, R. *Experimental Methods Used in System Identification of Civil Engineering Structures*, 2nd Workshop: Problemi di Vibrazioni Nelle Strutture Civili e Nelle Costruzioni Meccaniche, Perugia, Italy, (2004).

Casarin, F.; and Modena, C. *Dynamic Identification of S. Maria Assunta Cathedral, Reggio Emilia, Italy*. Proc. of the 2nd International Operational Modal Analysis Conference, IOMAC, Copenhagen, Denmark, 637-644 pp, (2007).

Casciati, F.; Casciati, S.; Faravelli, L.; and Rossi, R. *Hybrid Wireless Sensor Network*. Smart Structures and Materials: Sensors and Smart Structures Technologies for Civil,

Mechanical, and Aerospace Systems - SPIE San Diego, CA, Vol. 5391, 308-313 pp, (2004).

Casciati, F.; Faravelli, L.; Borghetti, F.; and Fornasari, A. *Tuning the Frequency Band of a Wireless Sensor Network*. Proc. of the 4th International Workshop on Structural Health Monitoring, Stanford, CA, 1185-1192 pp, (2003).

Cerioti, M.; Mottola, L.; Picco, G.P.; Murphy, A.L.; Guna, S.; Corra, M.; Pozzi, M.; Zonta, D.; and Zanon, P. *Monitoring Heritage Buildings with Wireless Sensor Networks: The Torre Aquila Deployment*. International Conference on Information Processing in Sensor Networks, IPSN09, San Francisco, USA, (2009).

Chopra, A.K. *Dynamics of Structures. Theory and Applications to Earthquake Engineering*. 1st ed. Prentice Hall, Englewood Cliffs, New Jersey, USA., (1995).

Chung, H.C.; Enomoto, T.; Shinozouka, M.; Chou, P.; Park, C.; Yokoi, L.; and Morishita, S. *Real-time Visualization of Structural Response with Wireless MEMS Sensors*. 13th World Conference on Earthquake Engineering, Vancouver, BC, (2004).

Clough, R.; and Penzien, J. *Dynamics of Structures*. 3rd ed. Computers & Structures, Inc., (2003).

Cooley, J.W.; and Tuckey, J.W. *An algorithm for the Machine Calculation of Complex Fourier Series*. 19: 297-301 pp, (1965).

Costa, C.; Arêde, A.; and Costa, A. *Caracterização Dinâmica e Análise da Ponte da Lagocinha*. Proc. of the 6^{to} Congresso de Sismologia e Engenharia Sísmica, Guimarães, Portugal, 931-942 pp, (2004).

Crossbow. Crossbow Wireless Sensors Network. www.xbow.com. Accessed December, (2009).

Cunha, A.; Caetano, E.; Magalhães, F.; and Moutinho, C. *From Input-Output to Output-Only Modal Identification of Civil Engineering Structures*, SAMCO, (2006).

D

De Silva, C.W. *Vibration Monitoring, Testing and Instrumentation*. 1st ed. CRC Press, The University of British Columbia Vancouver, Canada, (2007).

Deraemaeker, A.; Reynders, E.; De Roeck, G.; and Kullaa, J. *Vibration-based Structural Health Monitoring using Output-Only Measurements under Changing Environment*. Mechanical Systems and Signal Processing, 22(1): 34-56 pp, (2008).

Doebbling, S.W.; Farrar, C.R.; and Cornwell, P. *A Statistical Comparison of Impact and Ambient Testing Results from the Alamosa Canyon Bridge*, International Modal Analysis Conference, IMAC, USA, (1997).

E

Eloy, J.C. *Status of the MEMS Industry: Evolution of MEMS Markets and of the Industrial Infrastructure*. *Sensors & Transducers*, 86(12): 1771-1777 pp, (2007).

Ewins, D.J. *Modal Testing : Theory, Practice and Application*. 2nd ed. Research Studies Press, (2000).

F

Farrar, C.R.; Allen, D.; Ball, S.; Masquelier, M.P.; and Park, G. *Coupling Sensing Hardware with Data Interrogation Software for Structural Health Monitoring*. 6th International Symposium on Dynamic Problems of Mechanics - DINAME, Ouro Preto, Brazil, (2005).

Farrar, C.R.; and Worden, K. *An Introduction to Structural Health Monitoring*. *Philosophical Transactions of the Royal Society*, 365: 303-315 pp, (2007).

Felber, A. *Development of a Hybrid Bridge Evaluation System*. PhD Thesis, University of British Columbia (UBC), Vancouver, Canada, (1993).

Fotsch, D.; and Ewins, D.J. *Applications of MAC in the Frequency Domain*. International Modal Analysis Conference, IMAC, 1225-1231 pp, (2000).

Fung, G. *A Comprehensive Overview of Basic Clustering Algorithms*, (2001).

G

Gadre, D.V. *Programming and Customizing the AVR Microcontroller*. McGraw-Hill, New York, (2001).

Galbreath, J.H.; Townsend, C.P.; Mundell, S.W.; Hamel, M.J.; Esser, B.; Huston, D.; and Arms, S.W. *Civil Structure Strain Monitoring with Power-efficient, High-speed Wireless Sensor Networks*. 4th International Workshop on Structural Health Monitoring, Stanford, CA, 1215–1222 pp, (2003).

Gatti, P.; and Ferrari, V. *Applied Structural and Mechanical Vibrations*. 2nd ed. E & FN Spon, USA, (2003).

Gay, D.; Levis, P.; Von Behren, R.; Welsh, M.; Brewer, E.; and Culler, D. *The nesC Language: A Holistic Approach to Networked Embedded Systems*, PLDI '03, San Diego, California, (2003).

Gentile, C.; and Saisi, A. *Dynamic-based F.E. Model Updating to Evaluate Damage in Masonry Towers*. Proc. of the 4th International Seminar on Structural analysis of Historical Constructions, Padova, Italy, 439-449 pp, (2004).

GlobalSpec. MEMS Pressure Sensors Datasheets. <http://sensors-transducers.globalspec.com>. Accessed December, (2009).

Goethals, I.; Vanluyten, B.; and De Moor, B. *Reliable Spurious Mode Rejection Using Self-Learning Algorithms*. ISMA, Leuven, Belgium, (2004).

Gu, H.; Peng, J.; Zhao, Y.; Lloyd, G.M.; and Wang, M.L. *Design and Experimental Validation of a Wireless PVDF Displacement Sensor for Structure Monitoring*. Non-destructive Detection and Measurement for Homeland Security II - SPIE, San Diego, CA, Vol. 5395, 91-99 pp, (2004).

Guan, H.; Karbhari, V.M.; and Sikorski, C.S. *Time-Domain Output Only Modal Parameter Extraction and its Application*. Proceedings of the 1st International Operational Modal Analysis Conference, Copenhagen, Denmark, 577-584 pp, (2005).

H

Hautefeuille, M.; O'Mahony, C.; O'Flynn, B.; and Peters, F. *A Miniaturized MEMS-Based Multi-Parameter Sensing Module*, 31th International Conference of IMAPS Poland Chapter, Rzeszów - Krasiczyn, (2007).

He, J.; and Fu, Z.-F. *Modal Analysis*. 1st ed. Butterworth-Heinemann, Linacre House, Jordan Hill, Oxford, (2001).

Heylen, W.; and Lammens, S. *FRAC: A Consistent Way of Comparing Frequency Response Functions*. International Conference on Identification in Engineering Swansea, 48-57 pp, (1996).

Hunt, D.L. *Application of an Enhanced Coordinate Modal Assurance Criterion (ECOMAC)*. International Modal Analysis Conference, IMAC, 66-71 pp, (1992).

I

Ivorra, S.; and Pallarés, F.J. *A Masonry Bell-Tower Assessment by Modal Testing*. Proc. of the 2nd International Operational Modal Analysis Conference, IOMAC, Copenhagen, Denmark, 269-276 pp, (2007).

J

Jaishi, B.; Ren, W.X.; Zong, Z.H.; and Maskey, P.N. *Dynamic and Seismic Performance of Old Multi-Tiered Temples in Nepal*. Engineering Structures, 25: 1827-1839 pp, (2003).

Jin, X.; and Li, Z. *Dynamic Property Determination for Early-Age Concrete*. ACI - Materials Journal, 98: 365-370 pp, (2001).

K

Kinney, P. *ZigBee Technology: Wireless Control that Simply Works*. In: Z. Alliance (Editor), Communications Design Conference, (2003).

Kintner-Meyer, M.; and Conant, R. *Opportunities of Wireless Sensors and Controls for Building Operation*. ACEEE Summer Study on Energy Efficiency in Buildings, Pacific Grove, CA, 3139 - 3152 pp, (2004).

Kiremijdian, A.S.; Straser, E.G.; Meng, T.H.; Law, K.; and Soon, H. *Structural Damage Monitoring for Civil Structures*. International Workshop - Structural Health Monitoring: 371–382 pp, (1997).

Kling, R.M. *Intel Mote: An Enhanced Sensor Network Node*. International Workshop on Advanced Sensors, Structural Health Monitoring and Smart Structures, Tokyo, Japan, (2003).

Kotapalli, V.A.; Kiremijdian, A.S.; Lynch, J.P.; Carryer, E.; Kenny, T.; Law, K.H.; and Lei, Y. *Two-Tiered Wireless Sensor Network Architecture for Structural Health Monitoring*. Smart Structures and Materials - SPIE San Diego, CA, Vol. 5057, 8-19 pp, (2003).

Krishnamachari, B. *Networking Wireless Sensors*. 1st ed. Cambridge University Press, New York, USA, (2005).

Kullaa, J. *Functions of a Structural Health Monitoring System*, New trends in Vibration Based Structural Health Monitoring. CISM, Udine, Italy, (2008).

L

Labview. *LabVIEW User Manual, Release 8.0*. National Instruments Corporation, USA, (2006).

Lagomarsino, S.; and Calderini, C. *The Dynamical Identification of the Tensile Force in Ancient Tie-Rods*. Engineering Structures, 27(6): 846-856 pp, (2005).

Lieven, N.A.J.; and Ewins, D.J. *Spatial Correlation of Mode Shapes, The Coordinate Modal Assurance Criterion (COMAC)*. International Modal Analysis Conference, IMAC, 690-695 pp, (1988).

Lourenço, P.B.; and Ramos, L.F. *Investigação sobre as Patologias do Santuário de São Torcato. Final Report 99-DEC/E-5*, University of Minho, (1999).

- Luong, M. *Identification of the Tensile Force in Tie-rods using Modal Analysis Tests*. Master Thesis, University of Minho, Guimaraes, (2010).
- Lynch, J.P. *An Overview of Wireless Structural Health Monitoring for Civil Structures*. Philosophical Transactions of the Royal Society of London Series A, Mathematical and Physical Sciences: 345-372 pp, (2007).
- Lynch, J.P.; Law, K.; Kiremijdian, A.S.; Kenny, T.W.; Carryer, E.; and Partridge, A. *The Design of a Wireless Sensing Unit for Structural Health Monitoring*. 3rd International Workshop on Structural Health Monitoring, Stanford, CA, (2001).
- Lynch, J.P.; Law, K.H.; Kiremijdian, A.S.; Carryer, E.; Kenny, T.W.; A., P.; and Sundarajan, A. *Validation of a Wireless Modular Monitoring System for Structures*. Smart Structures and Materials: Smart Systems for Bridges, Structures, and Highways - SPIE, San Diego, CA, Vol. 4696, 17-21 pp, (2002a).
- Lynch, J.P.; Law, K.H.; Kiremijdian, A.S.; Kenny, T.W.; and Carryer, E. *A Wireless Modular Monitoring System for Civil Structures*. 20th International Modal Analysis Conference, IMAC, Los Angeles, CA, 1-6 pp, (2002b).
- Lynch, J.P.; and Loh, K.J. *A Summary Review of Wireless Sensors and Sensor Networks for Structural Health Monitoring*. The shock and vibration digest, 38(2): 91-128 pp, (2006).
- Lynch, J.P.; Parra-Montesinos, G.; Cambolat, B.A.; and Hou, T.C. *Real-time Damage Prognosis of High-performance Fiber Reinforced Cementitious Composite Structures*. Advances in Structural Engineering and Mechanics - ASEM'04, Honolulu, HI, (2004a).
- Lynch, J.P.; Sundararajan, A.; Law, K.H.; Carryer, E.; Farrar, C.R.; Sohn, H.; Allen, D.; Nadler, B.; and Wait, J.R. *Design and Performance Validation of a Wireless Sensing Unit for Structural Health Monitoring Applications*. Structural Engineering and Mechanics, 17(3): 393-408 pp, (2004b).
- Lynch, J.P.; Sundararajan, A.; Law, K.H.; Kiremijdian, A.S.; Carryer, E.; Sohn, H.; and Farrar, C.R. *Field Validation of a Wireless Structural Health Monitoring System on the Alamosa Canyon Bridge*. Smart Structures and Materials: Smart Systems and Nondestructive Evaluation for Civil Infrastructures - SPIE San Diego, CA, Vol. 5057 267-278 pp, (2003).
- Lynch, J.P.; Wang, Y.; Law, K.H.; Yi, J.-H.; Lee, C.G.; and Yun, C.B. *Validation of a Large-scale Wireless Structural Monitoring System on the Geumdang Bridge*. Proc. of the

International Conference on Safety and Structural Reliability (ICOSSAR), Rome, Italy, (2005).

M

Macqueen, J. *Some Methods for Classification and Analysis of Multivariate Observations*. 5th Berkeley symposium on mathematical statistics and probability. University of California, Berkeley, CA, USA, Vol. 1, 281-297 pp, (1967).

Magalhães, F.; Cunha, A.; and Caetano, E. *Dynamic Monitoring of a Long Span Arch Bridge*. *Engineering Structures*, 30(11): 3034-3044 pp, (2008).

Magalhães, F.; Cunha, A.; and Caetano, E. *Online Automatic Identification of the Modal Parameters of a Long Span Arch Bridge*. *Mechanical Systems and Signal Processing*, 23(2): 316-329 pp, (2009).

Maia, N.M.; and Silva, J.M. *Theoretical and Experimental Modal Analysis*. Mechanical Engineering Research Studies. Engineering Control Series, 9, Great Britain, (1997).

Maluf, N.; and Williams, K. *An Introduction to Microelectromechanical Systems Engineering*. 2nd ed. Artech house, Inc, USA, (2004).

Mastroleon, L.; Kiremijdian, A.S.; Carryer, E.; and Law, K.H. *Design of a New Power-efficient Wireless Sensor System for Structural Health Monitoring*. Non-destructive Detection and Measurement for Homeland Security 2nd - SPIE San Diego, CA, Vol. 5395, 51-60 pp, (2004).

Matlab. The Mathworks, Inc. www.mathworks.com. Accessed October, 27th, (2009).

MicroStrain. Microminiature Wireless Sensors. www.microstrain.com. Accessed December, (2009).

Mitchell, K.; Rao, V.S.; and Pottinger, H.J. *Lessons Learned About Wireless Technologies for Data Acquisition*. Smart Structures and Materials – Smart Electronics and MEMS - SPIE, Newport Beach, CA, Vol. 4700, 331-341 pp, (2002).

Moore, J.E. *Cramming More Components onto Integrated Circuits*. Proc. of the IEEE: 82-85 pp, (1968).

N

Nagy, A. *Determination of the E-Modulus of Young Concrete with non Destructive Method*. *Journal of Materials in Civil Engineering*, 9(1): 15-20 pp, (1997).

Neville, A.M. *Properties of Concrete*. 4th ed., (1995).

NI. Overview of Structural Health Monitoring Solutions. <http://zone.ni.com/>. Accessed June, (2009a).

NI. User Guide and Specifications. www.ni.com. Accessed December, (2009b).

O

Olusola, F. *The Evaluation of TinyOS with Wireless Sensor Node Operating System*. Master Thesis, Halmstad University, Sweden, (2007).

Ou, J.; Li, H.; and Yu. *Development and Performance of Wireless Sensor Network for Structural Health Monitoring*. Smart Structures and Materials - SPIE San Diego, CA, Vol. 5391, 765–773 pp, (2004).

Ou, J.P.; Li, H.; Xiao, Y.Q.; and Li, Q.S. *Health Dynamic Measurement of Tall Building Using Wireless Sensor Network*. Proc. of the Smart Structures and Materials, SPIE, San Diego, CA, USA, 205-215 pp, (2005).

P

Pakzad, S.N.; Fenves, G.L.; Kim, S.; and Culler, D. *Design and Implementation of Scalable Wireless Sensor Network for Structural Monitoring*. Journal of Infrastructure Systems, 14(1): 89-101 pp, (2008).

Pascual, R.; Golinval, J.; and Razeto, M. *A Frequency Domain Correlation Technique for Model Correlation and Updating*. Proc. of the International Modal Analysis Conference, IMAC, 587-592 pp, (1997).

PCB. Product Catalog. www.pcb.com. Accessed December, (2009).

Peeters, B.; and De Roeck, G. *Reference-Based Stochastic Subspace Identification for Output-Only Modal Analysis*. Mechanical Systems and Signal Processing, 13(6): 855-878 pp, (1999).

Peeters, B.; and De Roeck, G. *One-Year Monitoring of the Z24-Bridge: Environmental Effects versus Damage Events*. Earthquake Engineering and Structural Dynamics, 30: 149-171 pp, (2001).

Peeters, B.; Van Den Branden, B.; Laquiere, A.; and De Roeck, G. *Output-Only Modal Analysis: Development of a GUI for MATLAB*, 17th International Modal Analysis Conference, IMAC, Kissimmee, FL, USA, (1999).

Pei, J.S.; Kapoor, C.; Graves-Abe, T.L.; Sugeng, Y.; and Lynch, J.P. *Critical Design Parameters and Operating Conditions of Wireless Sensor Units for Structural Health Monitoring*. 23rd International Modal Analysis Conference, IMAC, Orlando, FL, (2005).

R

Rainieri, C.; and Fabroccino, G. *Automated Output-Only Dynamic Identification of Civil Engineering Structures*. Mechanical Systems and Signal Processing, (2009).

Rainieri, C.; and Fabroccino, G. *Automated Output-Only Dynamic Identification of Civil Engineering Structures*. Mechanical Systems and Signal Processing, 24(3): 678-695 pp, (2010).

Ramos, L.F. *Damage Identification on Masonry Structures Based on Vibration Signatures*. PhD Thesis, University of Minho, Guimaraes, Portugal, (2007). Available at www.civil.uminho.pt/masonry

Ramos, L.F.; Alaboz, M.; Aguilar, R.; and Lourenço, P.B. *Dynamic Identification and FE Updating of S. Torcato Church, Portugal*. 28th International Modal Analysis Conference, IMAC. SEM, Jacksonville, Florida, USA, (2010a).

Ramos, L.F.; Casarin, F.; Algeri, C.; Lourenço, P.B.; and Modena, C. *Investigations Techniques Carried out on the Qutub Minar, New Delhi, India*. Proc. of the 5th International Conference of Structural Analysis of Historical Constructions, New Delhi, 633 -640 pp, (2006).

Ramos, L.F.; and Lourenço, P.B. *Investigação sobre as Anomalias das Chaminés do Paço dos Duques de Bragança. Final Report 02-DEC/E-15*, University of Minho, (2002).

Ramos, L.F.; Marques, L.; Lourenço, P.B.; De Roeck, G.; Campos-Costa, A.; and Roque, J. *Monitoring of Historical Masonry Structures with Operational Modal Analysis: Two Case Studies*. Mechanical Systems and Signal Processing, 24(5): 1291-1305 pp, (2010b).

Rebelo, C.; Júlio, E.; and Costa, D. *Modal Identification of the Coimbra University Tower*. Proc. of the 2nd International Operational Modal Analysis Conference, Copenhagen, Denmark, 177-184 pp, (2007).

Rodrigues, J. *Identificação Modal Estocástica – Métodos de Análise e Aplicações em Estruturas de Engenharia Civil*. PhD Thesis, FEUP/LNEC, Lisbon, Portugal, (2004).

Rodrigues, J.; Brincker, R.; and Andersen, P. *Improvement of Frequency Domain Output-Only Modal Identification from the Application of the Random Decrement Technique*, Proc. of the 22nd International Modal Analysis Conference, IMAC, Dearborn, Michigan, USA, (2004).

Ruiz-Sandoval, M.E. *“Smart” Sensors for Civil Infrastructure Systems*. PhD Thesis, University of Notre Dame, Notre Dame, Indiana, (2004).

S

- Sazanov, E.; Janoyan, K.; and Jha, R. *Wireless Intelligent Sensor Network for Autonomous Structural Health Monitoring*. Smart Structures and Materials: Smart Sensor Technology and Measurement Systems San Diego, CA, Vol. 5384, 305-314 pp, (2004).
- Schmidt, T. *Dynamic Behaviour of Twin Bell Towers*. Proc. of the 2nd International Operational Modal Analysis Conference, Copenhagen, Denmark, 261-268 pp, (2007).
- Scionti, M.; Lanslots, J.; Goethals, I.; Vecchio, A.; Van Der Auweraer, H.; Peeters, B.; and De Moor, B. *Tools to Improve Detection of Structural Changes from In-Flight Flutter Data*. 8th International Conference on Recent Advances in Structural Dynamics, Southampton, UK, (2003).
- SD. Silicon Design, Inc. www.silicondesigns.com. Accessed December (2009).
- Sensirion. The Sensor Company. www.sensirion.ch. Accessed December, (2009).
- Severino, R. *On the use of IEEE 802.15.4/ZigBee for Time - Sensitive Wireless Sensor Network Applications*. Master Thesis, Polytechnic Institute of Porto, Porto, (2008).
- Severino, R.; Gomes, R.; Alves, M.; Sousa, P.; Tovar, E.; Ramos, L.F.; Aguilar, R.; and Lourenço, P.B. *A Wireless Sensor Network Platform for Structural Health Monitoring: Enabling Accurate and Synchronized Measurements Through COTS+Custom-Based Design*, 5th IFAC International conference on Management and Control of Production and Logistics - MCPL2010, Coimbra, Portugal, (2010).
- Shannon, C.E. *Communication in the Presence of Noise*. Proc. of the IRE, Vol. 37, no.1, 10-21 pp, (1949).
- Shieh, J.; Huber, J.E.; Fleck, N.A.; and Ashby, M.F. *The Selection of Sensors*. Progress in Materials Science, 46(3-4): 461-504 pp, (2001).
- Shinozuka, M. *Homeland Security and Safety*. International Conference on Structural Health Monitoring and Intelligent Infrastructure, Tokyo, Japan, 1139-1145 pp, (2003).
- Silva, J.H.P. *Paço dos Duques em Guimarães*, (1974).
- Stiharu, I. *MEMS, Applications*. In: Encyclopedia of vibration. 1st ed. Academic Press, 771-779 pp, (2002a).
- Stiharu, I. *MEMS, General Properties*. In: Encyclopedia of Vibration. 1st ed. Academic Press, 794-805 pp, (2002b).
- Straser, E.G.; and Kiremijdian, A.S. *A Modular Visual Approach to Damage Monitoring for Civil Structures*. Proc. of SPIE v2719, Smart Structures and Materials: 112-122 pp, (1996).

Straser, E.G.; and Kiremijidian, A.S. *A Modular, Wireless Damage Monitoring System for Structures*, The John A. Blume Earthquake Engineering Center, Report No.128, (1998).

Straser, E.G.; Kiremijidian, A.S.; Meng, T.H.; and Redlefsen, L. *A Modular Wireless Network Platform for Monitoring Structures*. Proc. of the SPIE The International Society for Optical Engineering: 450-456 pp, (1998).

SVS. *ARTEMIS Extractor Pro User Manual, Release 4.5*. Structural Vibration Solutions, Aalborg, Denmark, (2009).

T

TinyOS. www.tinyos.net. Accessed March, (2009).

Tomazevic, M. *Earthquake Resistant Design of Masonry Buildings*. 1st ed. Imperial College Press, (1999).

V

Van Overschee, P.; and De Moor, B. *Subspace Algorithms for the Stochastic Identification Problem*. Proc. of the 30th Conference on Decision and Control, Brighton, England, (1991).

Verboven, P.; Guillaume, P.; Cauberghe, B.; Parloo, E.; and Vanlanduit, S. *Stabilization Charts and Uncertainty Bounds for Frequency-Domain Linear Least Squares Estimators*. International Modal Analysis Conference, IMAC, Kissimmee, Florida, USA, (2003a).

Verboven, P.; Parloo, E.; Guillaume, P.; and Overmeire, M.V. *Autonomous Structural Health Monitoring. Part I: Modal Parameter Estimation and Tracking*. Mechanical Systems and Signal Processing 16(4): 637-657 pp, (2002).

Verboven, P.; Parloo, E.; Guillaume, P.; and Overmeire, M.V. *An Automatic Frequency Domain Modal Parameter Estimation Algorithm*. Vibration Analysis Techniques and Applications, 265(3): 647-661 pp, (2003b).

Verboven, P.; Parloo, E.; Guillaume, P.; and Van Overmeire, M. *Autonomous Modal Parameter Estimation Based on a Statistical Frequency Domain Maximum Likelihood Approach*. International Modal Analysis Conference, IMAC Kissimmee, FL, USA, (2001).

W

Wang, M.L.; Gu, H.; Lloyd, G.M.; and Zhao, Y. *A Multichannel Wireless PVDF Displacement Sensor for Structural Monitoring*. International Workshop on Advanced Sensors, Structural Health Monitoring and Smart Structures, Tokyo, Japan, (2003).

Wang, X.; Wang, M.L.; Zhao, Y.; Chen, H.; and Zhou, L.L. *Smart Health Monitoring System for a Prestressed Concrete Bridge*. Smart Structures and Materials: Sensors and

Smart Structures Technologies for Civil, Mechanical, and Aerospace System - SPIE San Diego, CA, Vol. 5391, 597-608 pp, (2004).

Wang, Y. *Wireless Sensing and Decentralized Control for Civil Structures: Theory and Implementation* PhD Thesis, Stanford University, (2007).

Wang, Y.; Lynch, J.P.; and Law, K.H. *Wireless Structural Sensors Using Reliable Communication Protocols for Data and Interrogation*. 23rd International Modal Analysis Conference, IMAC, Orlando, FL, (2005).

Welch, P.D. *The Use of the Fast Fourier Transform for the Estimation of Power Spectra: A method Based on Time Averaging over Short Modified Periodograms*. AU-15: 70-73 pp, (1967).

Weng, J.-H.; Loh, C.-H.; Lynch, J.; Lu, K.-C.; Lin, P.-Y.; and Wang, Y. *Output-Only Modal Identification of a Cable-Stayed Bridge using Wireless Monitoring Systems*. Engineering Structures, 30(7): 1820-1830 pp, (2008).

Z

Zimmerman, A.T.; Shiraishi, M.; Swartz, R.A.; and Lynch, J.P. *Automated Modal Parameter Estimation by Parallel Processing within Wireless Monitoring Systems*. Journal of Infrastructure Systems, 14(1): 102-113 pp, (2008).

Annex A

State-of-the-Art of Wireless Technology for Structural Monitoring

Table A.1 – Summary of academic wireless sensing unit prototypes (1998-2003).

	Straser and Kiremidjian, (1998)	Bennet et al., (1999)	Lynch et al., (2001; 2002a; 2002b)	Mitchell et al., (2002)	Kottapalli et al., (2003)	Lynch et al., (2004a; 2004b; 2003)	Aoki et al., (2003)	
Data Acquisition	A/D Channels	8	4	1		5	1	
	Sample Rate	240 Hz		100 kHz	20 MHz	20 MHz	100 kHz	
	A/D Resolution	16 bit	16 bit	16 bit	16 bit	8 bit	16 bit	10 bit
	Digital Inputs	0		2		0	2	
Embedded Computing Specifications	Processor	Motorola 68HC11	Hitachi H8/329	Atmel AVR8515	Cygnal 8051	Microchip PIC16F73	DUAL / Atmel AT90S8515 AVR / MPC555Power Pc	Renesas H8/4069 F
	Bus Size	8 bit	8 bit	8 bit	8 bit	8 bit	8 bit/32 bit	8 bit
	Clock Speed	2.1 MHz	4.9 MHz	4 MHz		20 MHz	4 MHz/20 MHz	20 MHz
	Program Memory	16 kB	32 kB	8 kB	2 kB	4 kB	448 kB	128 kB
	Data Memory	32 kB		32 kB	128 kB	192 kB	512 kB	2 MB
Wireless Channel Specifications	Radio	Proxim ProxLink	Radiometrix	Proxim RangeLan2	Ericsson Bluetooth	BlueChip RBF915	Proxim RangeLan2	Realtek RTL8019AS
	Frequency Band	900 MHz	418 MHz	2.4 GHz	2.4 GHz	900 MHz	2.4 GHz	
	Wireless Standard				IEEE 802.15.1			
	Spread Spectrum	Yes		Yes	Yes	Yes	Yes	
	Outdoor Range	300 m	300 m	300 m	10 m	500 m	300 m	50 m
	Enclosed Range	150 m		150 m	10 m	200 m	150 m	50 m
Data Rate	19.2 kbps	40 kbps	1.6 Mbps		10 kbps	1.6 Mbps		
Final Assembled Attributes	Dimensions	15x13x10 cm	15D x 30 cm	10x10x5 cm	5x3.8x 1.2 cm	10x5x 1.5cm	12x10x2.5 cm	30x6x8 cm
	Power				120 mW	100 mW		
	Power Source	Battery (9V)	Battery (6V)	Battery (9V)	Battery	Battery (9V)	Battery (9V)	
Field Validation (*)	[USA] Alamosa Canyon Bridge	Asphalt Highway Surface	-	-	-	[USA] Alamosa Canyon Bridge	[JAPAN] Tokyo Rainbow Bridge	

(*) Row/Column added by the author to the original proposal made by Lynch and Loh, (2006)

Table A.2 – Summary of academic wireless sensing unit prototypes (2003-2004).

	Basheer et al., (2003)	Casciati et al., (2004; 2003)	Wang et al., (2003; 2004); Gu et al., (2004)	Mastrolo on et al., (2004)	Shinozouk a, (2003); Chung et al., (2004)	Ou et al., (2004)	Sazanov et al., (2004)	
Data Acquisition	A/D Channels	Multiple	8	8	5	4/2	6	
	Sample Rate			> 50 Hz	480 Hz			
	A/D Resolution		12 bit	12 bit	16 bit	12 bit	12 bit	
	Digital Inputs			Multiple	0	16	16	
Embedded Computing Specifications	Processor	ARM7TDMI		Analog Devices ADuC832	Microchip PIC-micro		Atmel AVR ATmega 8L	Texas Instruments MSP430-F1611
	Bus Size	32 bit		8 bit	16 bit/8 bit		8 bit	16 bit
	Clock Speed							
	Program Memory			62 kB			8 kB	16 MB
	Data Memory			2 kB			1 kB	
Wireless Channel Specifications	Radio	Philips Blueberry Bluetooth	Aurel XTR-915	Linx Technologies	BlueChirp RFB915B		Chipcon CC1000	Chipcon CC2420
	Frequency Band	2.4 GHz	914.5 MHz	916 MHz	900 MHz	2.4 GHz	433 MHz	2.4 GHz
	Wireless Standard	IEEE 802.15.1			IEEE 802.15.1	IEEE 802.11b		IEEE 802.15.4
	Spread Spectrum	Yes	No	No	Yes	Yes	Yes (software)	Yes
	Outdoor Range	100 m		152 m	200-300 m	250 m		75 m
	Enclosed Range			61 m				
	Data Rate		100 kbps	33.6 kbps	19.2 kbps		76.8 kbps	250 kbps
Final Assembled Attributes	Dimensions	2.5x2.5x2.5 cm			8x8x 2 cm	6x9x 3.1cm		
	Power							75 mW
	Power Source	Battery		Battery		Battery + Solar	Battery	
Field Validation (*)	-	-	-	-	[USA] 30m steel truss bridge	[CHINA] Di Wang Tower	-	

(*) Row/Column added by the author to the original proposal made by Lynch and Loh, (2006)

Table A.3 – Summary of academic wireless sensing unit prototypes (2005-2008).

		Farrar et al., (2005) Allen, (2005)	Wang et al., (2005)	Pei et al., (2005)
Data Acquisition	A/D Channels	6	4	
	Sample Rate	200 kHz	100 kHz	100/500 Hz
	A/D Resolution	16 bit	16 bit	10/12/16 bit
	Digital Inputs		2	
Embedded Computing Specifications	Processor	Intel Pentium / Motorola	Atmel AVR ATmega 128	Motorola 68HC11
	Bus Size	16 bit	8 bit	8 bit
	Clock Speed	120/233 MHz	8 MHz	
	Program Memory	256 MB	128 kB	32 kB
	Data Memory	Compact Flash	256 kB	32 kB
Wireless Channel Specifications	Radio	Motorola neuRFon	Max-stream 9xCite	Max-Stream Xstream
	Frequency Band	2.4 GHz	900 MHz	900 MHz/ 2.4 GHz
	Wireless Standard	IEEE 802.15.4		
	Spread Spectrum	Yes	Yes	Yes
	Outdoor Range	9.1 m	300 m	
	Enclosed Range	9.1 m	100 m	
	Data Rate	230 kbps	38.4 kbps	
Final Assembled Attributes	Dimensions		10x6x 4 cm	
	Power	6 W		
	Power Source		Battery (7.5V)	Battery (9V)
Field Validation (*)		-	[KOREA] Geumdang Bridge [Taiwan] Gi-Lu bridge (Weng et al., 2008)	

(*) Row/Column added by the author to the original proposal made by Lynch and Loh, (2006)

Table A.4– Summary of commercial wireless sensing unit prototypes (adapted from Lynch and Loh, 2006).

		[1999] UC Berkeley Crossbow WeC	[2000] UC Berkeley Crossbow Rene	[2000] UC Berkeley Crossbow MICA	[2000] UC Berkeley Crossbow MICA2	[2003] Intel iMote (Kling, 2003)	[2003] Microstrain, (Galbreath et al. 2003)
Data Acquisition	A/D Channels	8	8	8	8		8
	Sample Rate	1 kHz	1KHz	1 kHz	1 kHz		1.7 kHz (one channel)
	A/D Resolution	10 bit	10 bit	10 bit	10 bit		12 bit
	Digital Inputs	0					
Embedded Computing Specifications	Processor	Atmel AT90LS8535	Atmel ATmega 163L	Atmel ATmega 103L	Atmel ATmega 128L	Zeevo ARM7TD MI	MicroChip PIC16F877
	Bus Size	8 bit	8 bit	8 bit	8 bit	32 bit	8 bit
	Clock Speed	4 MHz	4 MHz	4 MHz	7.383 MHz	12 MHz	
	Program Memory (Flash)	8 kB	16 kB	128 kB	128 kB	64 kB	
	Data Memory (RAM)	32 kB	32 kB	512 kB	512 kB	512 kB	2 MB
Wireless Channel Specifications	Radio	TR 1000	TR 1000	TR 1000	Chipcon CC1000	Chipcon CC2420	RF Monolithics DR-3000-1
	Frequency Band	868/916 MHz	868/916 MHz	868/916 MHz	315, 433, or 868/916 MHz	2.4 GHz	916.5 MHz
	Wireless Standard					IEEE 802.15.4	
	Spread Spectrum	No	No	No	Yes (Software)	Yes	
	Outdoor Range						
	Enclosed Range						
	Data Rate	10 kbps	10 kbps	40 kbps	38.4 kbps	250 kbps	75 kbps
Final Assembled Attributes	Dimensions	2.5x2.5x 1.3 cm					
	Power	575 mAh	2850 mAh	2850 mAh	1000 mAh		
	Power Source	Coin Cell	Battery (3V)	Battery (3V)	Coin Cell	Battery	Battery (3.6V)

Annex B

Characteristics of the Mica2 Platforms and the Measurement Sensors Embedded in the MTS400 Crossbow Board

Table B.1 – Technical Specifications of the Mica2 platforms.

Processor/Radio	Mica2	Remarks
CPU	ATMega128L	
CPU clock	7.4 MHz	
Program Memory	128 KB	
Data Memory	512 KB	
ADC	7 ports with 10 bit of resolution	
Processor current draw	8mA	Active Mode
	< 15 μ A	Sleep Mode
Radio frequency	315/433/868/916 MHz	
Maximum data rate	38.4 K baud	
Radio current draw	25mA	Transmit
	8 mA	Receive
	< 1 μ A	Sleep
Radio Range	300m	
Power	2AA batteries	
External power	2.7 – 3.3V	

Table B.2 – Characteristics of the Humidity and Temperature Sensor

Sensor Type	Sensirion SHT11	
Channels	Humidity	Temperature
Range	0 to 100%	-40°C to 80°C
Accuracy	$\pm 3.5\%$ RH (typical)	$\pm 2^\circ\text{C}$
Operating Range	3.6 to 2.4 volts	
Interface	Digital Interface	

Table B.3 – Characteristics of the Barometric Pressure and Temperature Sensor

Sensor Type	Intersema MS5534	
Channels	Pressure	Temperature
Range	300 to 110 mbar	-10°C to 60°C
Accuracy	$\pm 3.5\%$	$\pm 2^\circ\text{C}$
Operating Range	3.6 to 2.2 volts	
Interface	Digital Interface	

Table B.4 – Characteristics of the Light Sensor

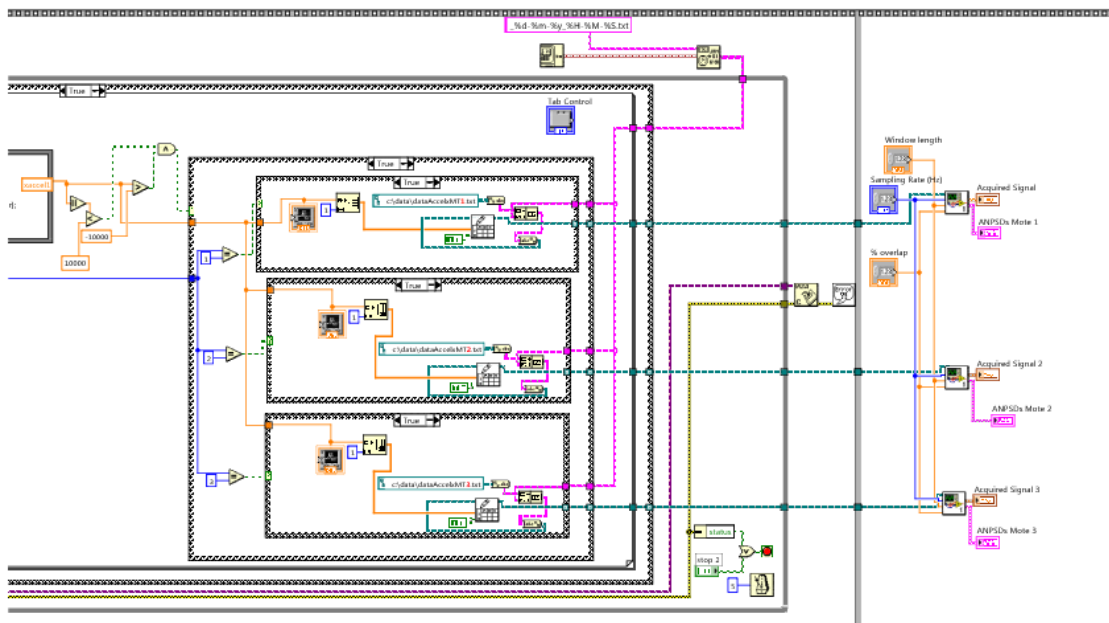
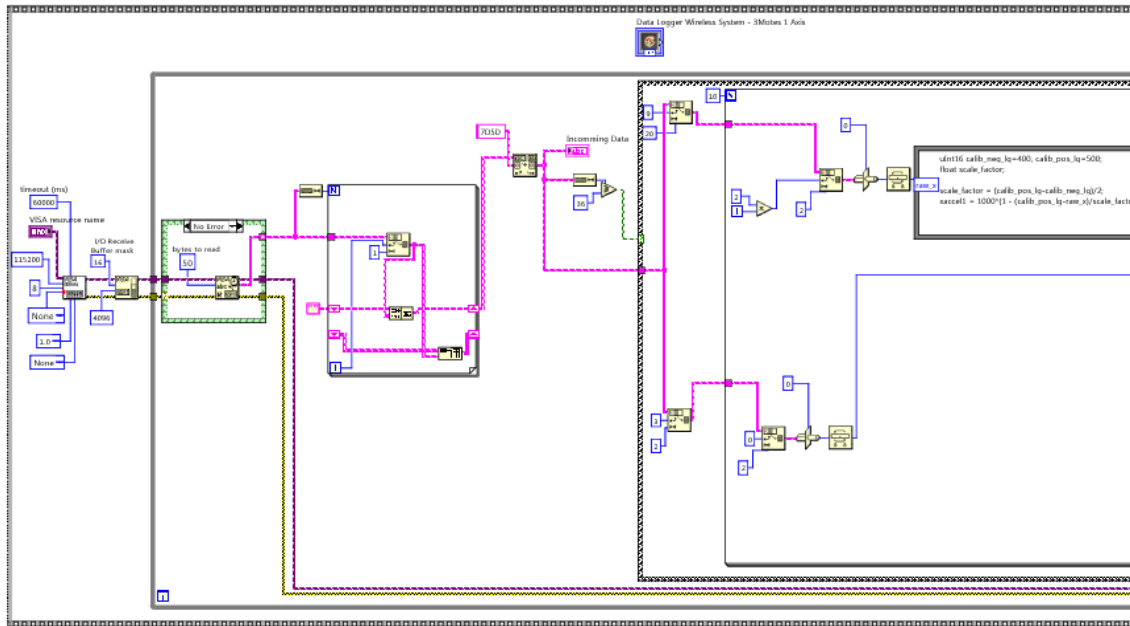
Sensor Type	Taos TSL2550
Channels	Light
Range	400 – 1000 nm
Operating Range	3.6 to 2.7 volts
Interface	Digital Interface

Table B.5 – Characteristics of the Accelerometer Sensor

Sensor Type	Analog Devices ADXL202JE
Channels	X (ADC1), Y (ADC2)
Range	$\pm 2g$
Sensitivity	167 mV/g, $\pm 17\%$
Resolution	2mg (0.002g) RMS
Offset	$V_{Battery}/2 \pm 0.4V$
Operating Range	3.6 to 3.0 volts
Interface	Analog Interface

Annex C

Block Diagram of the Data Acquisition Routine for the Commercial Wireless Platforms



Annex D

Block Diagram of the Data Processing Module of the Automatic Modal Analyzer Routine AMAV1.0

